UNIVERSITÉ DE GENÈVE
Département de biologie moléculaire

FACULTÉ DES SCIENCES
Professeur Robbie Loewith

Département de microbiologie et
médecine moléculaire

FACULTÉ DE MÉDECINE
Professeur Claudio De Virgilio

Structural and Functional Characterization of the Novel Yeast PAS Kinase

Rim15, a Central Regulator of the G_0 Program in Yeast

THESE
présentée à la Faculté des sciences de l'Université de Genève
pour obtenir le grade de Docteur ès sciences, mention biologique

par

Elisabetta CAMERONI
de
Massagno (TI)

Thèse n°3844

GENÈVE
Atelier de reproduction de la Section de physique
2007

La Faculté des sciences, sur le préavis de Messieurs C. de VIRGILIO, professeur et directeur de thèse (Faculté de médecine – Département de microbiologie et médecine moléculaire), R. LOEWITH, professeur adjoint suppléant et co-directeur de thèse (Département de biologie moléculaire), et R. SCHNEITER, professeur (Université de Fribourg – Département de médecine – Fribourg, Suisse), autorise l'impression de la présente thèse, sans exprimer d'opinion sur les propositions qui y sont énoncées.

Genève, le 30 mars 2007

P. Spierer

Thèse - 3844 -

Le Doyen, Pierre SPIERER

La Cigale et la fourmi

La Cigale, ayant chanté
Tout l'été,
Se trouva fort dépourvue
Quand la bise fut venue.
Pas un seul petit morceau
De mouche ou de vermisseau.
Elle alla crier famine
Chez la fourmi sa voisine,
La priant de lui prêter
Quelque grain pour subsister
Jusqu'à la saison nouvelle.
«Je vous paierai, lui dit-elle,
Avant l'oût, foi d'animal,
Intérêt et principal.»
La Fourmi n'est pas prêteuse ;
C'est là son moindre défaut.
«Que faisiez-vous au temps chaud ?
Dit-elle à cette emprunteuse.
«Nuit et jour à tout venant
Je chantais, ne vous déplaise.
«Vous chantiez ? j'en suis fort aise.
Eh bien ! dansez maintenant.»

Jean de LA FONTAINE
Fables, livre I (1668)

Table of contents

Résumé (en français)

Probablement tous les organismes vivants possèdent des cellules avec l'époustouflante capacité de sortir du normal cycle cellulaire et de survivre, pour des très longues périodes, dans un état réversible qui prends le nom de G_0. Une totale compréhension des mécanismes moléculaires qui régulent ce procès presque universel, pourrait avoir des énormes implications cliniques. Par exemple ça permettrait de développer des nouvelles stratégies pour la culture in vitro des cellules staminales, ainsi que des nouvelles thérapies contre le cancer et des immunosuppresseurs. En outre, la connaissance précise de ces mécanismes chez les microbes, permettrait de développer de nouveaux agents antipathogéniques.

Dans la levure, la privation de l'un des éléments nutritifs essentiaux (notamment le charbon, l'azote et le phosphate) provoque l'arrêt de la croissance et induit un programme de différentiation cellulaire. Dans le laboratoire, lorsqu'elles sont cultivés sans remplacer le milieu de croissance, les cellules de levure arrêtent leur croissance après avoir complètement absorbé la source de charbon disponible, habituellement le glucose. L'ensemble des caractéristiques morphologiques, physiologiques et transcriptionelles acquises par ces cellules, définit ce que on appelle l'état de "G_0" ou état "quiescent". Bien que la privation de phosphate et de azote induisent des caractéristiques similaires, il reste à définir si c'est exactement le même programme qui est induit ou s'il s'agit plutôt de programmes similaires mais distingués. En effet c'est connu pour les cellules de mammifère, que les programmes d'arrêt cellulaire acquis en réponse à des signaux différent (par exemple en l'absence de facteurs de croissance, ou une hautes densité de cellules dans la culture) sont tout aussi différents que les signaux qui les ont induites. Malgré ces différences ces programmes partagent aussi des caractéristiques communes, suggérant l'existence de un "programme génétique" spécifique pour la quiescence.

Soit les cellules de mammifère que les levures qui entrent dans la phase G_0 quittent le cycle cellulaire dans un point spécifique, que on l'appelle le point de restriction (chez les cellules de mammifère) ou le point START (chez la levure). Il est très important de mentionner que, à différence de beaucoup d'autres états de non-prolifération (tels que la sénescence ou les différentiations terminales), la quiescence est un état réversible qui est bien différent d'un simple arrêt du cycle cellulaire, notamment caractérisé par l'expression d'un programme génétique spécifique.

La levure est couramment utilisé comme modèle dans l'étude de procès biologiques de base et peut sûrement nous fournir des informations fondamentales qui vont former les bases sur lesquelles on pourra construire la connaissance approfondie des mêmes procès biologiques chez des organismes plus complexes, comme les mammifères.

Parce que l'entré en G_0 a des énormes implications, notamment la morphologie et la physiologie de la cellule changent complètement, cette route n'est entreprise que si les conditions extérieures l'imposent. Au jour qu'il est, nous ne sommes probablement pas encore entièrement à connaissance de la complexité des voies de signalisation impliqués dans la régulation de ce programme. De plus en plus les observations faites nous emmènent à regarder à ces voies non plus comme des cascades parallèles mais comme à un unique et intriqué réseau, qui permet aux cellules d'enregistrer le plus petit changement dans l'environnent et de s'adapter rapidement tout en n'investissant que le minimum indispensable d'énergie. Cette considération m'emmène droit à l'exemple des protéines protagonistes de ce travail, la kinase Rim15 et les facteurs de transcription Msn2 et Msn4, lesquelles illustrent parfaitement ce paradigme, étant contrôlés simultanément par plusieurs voies de signalisation.

La serine/threonine kinase Rim15 est un facteur essentiel pour l'entré correcte dans la phase G_0, elle joue un rôle importante dans l'acquisition de la grand partie des caractéristiques qui définissent la phase G_0. Dans des cellules ou Rim15 est absent or non fonctionnel le programme G_0 ne peut pas être induit en suite à la privation de éléments nutritifs pendant la transition diauxique de la croissance (le passage du métabolisme fermentatif au métabolisme respiratoire), ce qui a pour résultat que ces cellules perdent rapidement leur viabilité dans une culture en phase stationnaire. L'expression de un allèle mutant de Rim15, qui est toujours présent dans le noyau (ou il exerce normalement sa fonction) a un effet inhibitoire sur la croissance, très probablement parce que il induit l'entrée prématurée des cellules en G_0. En raison du rôle clé de cette protéine, sa fonction et sa localisation sont contrôlées de façon très stricte de la part de au moins trois différentes voies de signalisation qui répondent à des éléments nutritifs différents: la voie TORC1 semble répondre à la concentration de la glutamine (qui, étant un produit intermédiaire du cycle de Krebs, représente un très bon indicateur de la disponibilité de nutriments) dans la cellule, la voie PKA (qui répond à la qualité de la source de charbon, en particulier au glucose ou d'autre sucres fermentables), et enfin la voie Pho85 (qui communique le niveau de phosphate). Ces voies de signalisation, ainsi que les

procès cellulaires que elles contrôlent, ont étés décrits de façon détaillée dans l'introduction générale de cette thèse.

La centralité de Rim15, qui, chez la levure, intègre les informations provenant de trois des plus importantes voies de signalisation des nutriments, nous a stimulés à entreprendre des études approfondies de la structure moléculaire et des mécanismes de régulation ainsi que la recherche des cibles possibles de Rim15.

Dans une première partie de cette thèse, présentée dans le Chapitre I, j'ai étudié trois régions particulières, dans la séquence protéique de Rim15 et qui, notamment, pourraient êtres impliqués dans sa régulation.

L'analyse de la séquence de Rim15, nous indique que la région catalytique de Rim15 est encadrée par d'autres régions très conservés, dont la fonction n'avait pas été étudié auparavant. La présence de multiples domaines dans cette grosse protéine est en quelque sorte le reflex de la complexité des ses rôles et de sa régulation.

Deux de ces trois régions conservés, un domaine PER-ARNT-SIM (PAS), situé dans la région amino-terminale, et un domaine receiver (REC), situé dans la partie carboxy-terminale de Rim15, ressemblent à des régions qui sont très souvent retrouvés ensembles dans le contexte de protéines faisant partie de spéciales voies de signalisation appelées « phosphorelay signaling systems ». Malgré le niveau significatif de conservation de la séquence des acides aminés, les deux domaines de Rim15 présentent des différences par apport à leurs cousins plus «classiques», notamment au niveau de résidus importants pour la fonction normale dans les versions classiques des mêmes domaines. Ceci pourrait indiquer que, au cours de l'évolution, les domaines PAS et REC de Rim15 ont perdu leur fonction ou qu'ils ont acquis des nouvelles fonctions. Enfin, le troisième domaine est un nouveau «C_2CH zinc finger», qui n'avait pas été décrit auparavant. Ce domaine montre tout de même une légère ressemblance avec deux domaines connus, notamment le domaine PHD et le domaine FYVE, et, comme ces domaines, il présente la capacité de lier les phosphoinositides.

Des études précédentes ont montré que certains domaines PAS peuvent exercer une activité inhibitrice sur les propriétés enzymatiques de la protéine qui les contient. En particulier, des études sur une protéine appelée hPASK (Kinase PAS humaine) avaient montré que le domaine PAS

pouvait, en se liant à des petites molécules organiques, modifier sa propre structure et de par ces changements inhiber l'activité de la région catalytique (domaine kinase).

Dans le cas de Rim15, le domaine PAS de semble pas avoir un rôle dramatique. Une variante de Rim15 de laquelle le domaine PAS a été retiré, est tout aussi active *in vivo* (mais pas davantage) que la protéine sauvage. L'activité *in vivo* à été mesurée indirectement, en mesurant la quantité du disaccharide trehalose accumulé par les cellules en G_0, un trait qui, notamment, dépends (aussi) de la fonction de Rim15. Il est possible que la mesure d'un trait indirect ne soit pas indiquée pour relever des différences minimes dans l'activité, donc nos observations ne nous permettent pas de affirmer que le domaine PAS de Rim15 n'a aucune fonction dans la régulation de Rim15. Par contre, ces résultats semblent clairement indiquer que le rôle de cette région n'est pas essentiel pour le normal fonctionnement de Rim15.

L'activité in vitro du domaine PAS de Rim15 a aussi été étudié dans ce chapitre. Dans une première expérience nous avons comparé l'activité kinase de la protéine Rim15 sauvage avec celle d'une protéine ou le domaine PAS avait été retiré ($Rim15^{PAS\Delta}$). Dans ce type de expérience (essai kinase), la kinase est purifiée de à partir de la levure et utilisée pour phosphoryler un substrat (dans nôtre cas la caséine α) en présence de ATP radioactif. Le transfert de phosphates radioactifs est facilement visible par autoradiographie après la séparation des protéines par SDS-PAGE. Nous avons remarqué, que alors que le niveau de phosphate radioactif incorporé par le substrat ne montrait pas de différences substantielles, l'autophosphorylation de la kinase $Rim15^{PAS\Delta}$ était légèrement plus élevée que celle de la kinase sauvage Rim15. Ce résultat pourrait indiquer que le domaine PAS a une fonction inhibitoire et que en son absence la protéine est, par conséquence, plus active.

Dans une deuxième expérience, ou le domaine PAS seul a été purifié des bactéries et ensuite rajouté en excès dans un essai kinase, nous n'avons observé aucun effet inhibitoire sur l'activité de la kinase. Il est possible, que lorsque le domaine PAS est purifié des bactéries, comme dans nôtre cas, il perd son activité. Un autre point problématique pourrait être la sensibilité de notre essai: en effet, les études sur la variante humaine de la PAS kinase ont étés conduits en comparant les constantes cinétiques des enzymes, un test beaucoup plus raffiné que celui que nous avons employé. Une autre observation intéressante qui a été faite pendant cet étude, c'est que le domaine PAS de Rim15 peut interagir, aussi bien avec des autres protéines (probablement une kinase régulatrice de Rim15) que avec Rim15 même; de plus, ce domaine semble capables de former des dimères. Ces dernières

informations sont particulièrement intrigantes, vu que la plus part des activateurs de la transcription qui possèdent un domaine PAS sont aussi capables de former des dimères quand le domaine PAS est dans son état «actif».

Au contraire du domaine PAS, un autre domaine, le C_2CH zinc finger, s'est démontré essentiel pour l'activité de Rim15 *in vivo* et *in vitro*. Le remplacement, par des alanines, des résidus qui sont sensés lier le ion de zinc (et de par cela de stabiliser la structure) abolit presque complètement l'activité de la kinase.

Un autre aspect très intéressant de ce domaine est sa capacité de lier spécifiquement certaines phosphoinositides (PtdIns), une propriété qu'il partage avec les très similaires C_2CH zinc fingers des protéines Mgs1 et Rad18. Les mutations décrites der résidus qui sont sensés lier le ion de zinc, dans ce cas, n'éliminent pas l'interaction avec ces lipides mais ils en réduisent plutôt la spécificité. Un lien cause effet entre ces deux fonctions du C_2CH zinc finger dans Rim15 n'a pas pu être établi dans ce travail. Dans la cellule, les phosphoinositides qui sont liés par Rim15, PtdIns(3)P et PtdIns(5)P, ont étés retrouvés aussi dans le noyau, souvent associés avec la chromatine. Ceci pourrait être très intéressant, vu que nous avons aussi trouvé que des fusions de la protéine GFP avec les C_2CH zinc fingers de Rim15, Mgs1 et Rad18 sont accumulés dans le noyau. Comme les trois protéines avaient déjà été impliqués dans des procès liés à la chromatine, les spéculations sont inévitables; il est envisageable que leur association avec des particulières régions de la chromatine soit guidée par les phosphoinositides. Dans le cas de Rim15 on peut imaginer que la kinase puisse être recrutée à des promoteurs spécifiques par l'association avec les phosphoinositides, ou elle régulerait des facteurs de transcription ou des facteurs impliques dans le remodelage de la chromatine. Dans ce contexte, il serait sans doute intéressant de étudier si l'altération de la distribution des phosphoinositides (par exemple suite à la délétion de une enzyme du métabolisme des phosphoinositides) à un effet sur la localisation de Rim15 ou des C_2CH zinc fingers et sur l'activité de Rim15.

Enfin, comme le domaine PAS, le C_2CH zinc finger était aussi capable de interagir avec d'autres protéines, dont plusieurs faisant partie de un complexe décrit récemment et qui contient le facteur de transcription Gis1 (notamment un des cibles de Rim15), ainsi que avec le domaine REC situé dans la partie carboxy-terminale de Rim15.

Nos études préliminaires sur le domaine REC ont démontré une relation entre ce domaine et le domaine C_2CH zinc finger, ainsi que avec plusieurs membres du complexe contenant Gis1. Des études supplémentaires vont être nécessaires pour mieux comprendre la nature de ces interactions. Ces études devraient aussi adresser le rôle possible du domaine REC en tans que module de signalisation. Dans ce domaine l'acide aminé (un aspartate) qui est normalement impliqué dans la transmission du signal n'est pas conservé ; il serait donc intéressant de déterminer si ce domaine est phosphorylé et sur quel résidu.

En conclusion, tandis le C_2CH zinc finger semble être crucial pour la fonction de Rim15, le REC et le PAS semblent de loin être moins importants pour la fonction *in vitro* et *in vivo* de Rim15. Ceci dit, une des limitations principielles dans nôtre analyse était que nous ne disposions pas encore un substrat spécifique pour Rim15. Comme illustré dans le Chapitre III de cette thèse, nous avons enfin identifié un substrat endogène de Rim15, ce qui devrait nous permettre dans le futur de construire des essaies pour l'analyse plus précise et raffinée de l'activité de Rim15 et de sa régulation ainsi que la fonction des différents domaines.

Le deuxième chapitre de cette thèse traite de la fonction de Rim15 comme régulateur de la transcription dans la phase diauxique. Vu le rôle clé de Rim15 pour l'entré en G_0, qui est contrôlée au niveau transcriptionel déjà à partir de la transition diauxique, nous nous somme posés la question dans quelle mesure Rim15 participait à l'induction du programme transcriptionel induit dans la phase diauxique et quel était son rôle en relation de deux facteurs de transcription tout aussi fondamentaux pour l'entré en G_0, Msn2/Msn4 et Gis1. Dans ce but nous avons comparé les profils transcriptionels de une souche sauvage et des souches mutantes *rim15Δ*, *gis1Δ* et *msn2Δmsn4Δ* pendant la transition diauxique avec les profils correspondants en phase exponentielle. Ces études, menés en collaboration avec le groupe du Professeur Joris Winderickx en Belgique, ont montré que, ensemble, Rim15 et les facteurs de transcription Msn2/Msn4 et Gis1 sont responsables de l'induction de la grande partie du programme G_0. La majorité des gènes qui étaient sous le contrôle de Rim15 était comprise dans le plus large ensemble des gènes régulés par Msn2/Msn4 et par Gis1. Nous avons aussi constaté que deux des familles de gènes, qui montraient une très marquée dépendance de Rim15, comprenaient respectivement les gènes nécessaires pour la respiration et les gènes dont les produits aident les cellules à éliminer les radicaux d'oxygène, qui sont produits davantage pendant la respiration. Ceci est particulièrement intéressant si on considère encore une fois l'architecture de Rim15: le domaine PAS, qui se trouve dans la partie amino-terminale, pourrait

servir de senseur pour les radicaux d'oxygène et par cela assurer l'intégration des signaux provenant des nutriments avec un signal indiquant le stress oxydatif. Cette spéculation dérive en partie de l'analogie avec le très similaire domaine PAS de la protéine neuronale 2 (NPAS2) qui lie une molécule de heme comme groupe prosthétique et fonctionne comme senseur pour l'oxygène.

Nous avons ensuite conduit, en collaboration avec le groupe du Professeur James Broach à Princeton, des études très similaires pour mieux comprendre la réponse transcriptionelle à la rapamycine, un inhibiteur de la voie TORC1, qui induit dans la levure un arrêt de croissance et une différentiation très similaires à ceux observés dans la phase G_0 induite par la limitation des nutriments. Nos résultats précédents démontraient que Rim15 était phosphorylé (directement ou indirectement) par TORC1 et que cette phosphorylation ancrait Rim15 dans le cytoplasme. L'inhibition de TORC1 par la rapamycine résultait, au contraire, dans l'accumulation de Rim15 dans le noyau. Nous avons donc analysé l'importance de cette translocation pour l'expression des gènes induits par la rapamycine. Dans ce cas le rôle de Rim15 paraît moins frappant que pendant la transition diauxique. Ceci nous indiquant, entre autres, que les programmes transcriptionels induits par la rapamycine et par l'entré en phase diauxique ne sont pas identiques.

Nous avons ensuite posé la question de comment exactement Rim15 est régulé par TORC1. Beaucoup des fonctions de la voie TORC1, surtout au niveau de la transcription, sont contrôlés par deux différents complexes présentant une activité phosphatase. Nos donnés excluent clairement l'implication du premier de ces deux complexes, le complexe Tap42-Sit4, dans la régulation de Rim15. Par contre le deuxième complexe, formé par l'unité régulatrice Tap42 et les deux unités catalytiques Pph21 et Pph22 (le complexe Tap42-PP2Ac), semblent réguler négativement les gènes qui dépendent de Rim15 pour leur expression suite à un traitement avec la rapamycine. Quand Pph21 et Pph22 sont absents, les gènes contrôlés par Rim15 sont transcrits à des niveaux basaux plus élevés et sont induits davantage après un traitement avec la rapamycine, de façon indépendante de Rim15. Il semblerait que le complexe Tap42-PP2Ac fait partie d'un mécanisme de régulation qui assure la répression du programme G_0 pendant la phase exponentielle de la croissance. Ce résultat est en contradiction apparente avec des travaux précédemment publiés, mais ces résultats peuvent être réconciliés sur la base d'un modèle proposé récemment, selon lequel le complexe Tap42-PP2Ac pourrait avoir des fonctions différentes pendant la phase exponentielle et pensant la réponse à la limitation des nutriments ou à un traitement avec la rapamycine.

Dans le chapitre II, le rôle possible d'une deuxième cible de la voie TORC1, la serine/threonine kinase Sch9, dans la régulation de Rim15 a également été étudié. Nos résultats indiquent en effet que Sch9 pourrait réguler négativement la fonction de Rim15. Dans un mutant sch9Δ, Rim15 est constitutivement accumulé dans le noyau, de plus Sch9 phosphoryle directement Rim15. Ici nous avons démontré que dans un mutant sch9Δ les gènes contrôlés par Rim15 sont plus fortement induits par la rapamycine, tandis que dans un mutant sch92D3E, qui ne peut pas être inhibé par la rapamycine, les gènes contrôlées par Rim15 ne sont pas induits suite à un traitement avec la rapamycine.

La complexité des mécanismes qui régulent Rim15 est bien plus élevée que on ne le croyait: pour comprendre dans le détail les événements en amont et en aval de Rim15 il est impératif de connaître les cibles de Rim15. Pour cette raison, nous avons dédié nos efforts dans le troisième chapitre de cette thèse à l'identification de ces cibles.

En collaboration avec le groupe du Professeur Michael Snyder de Yale, nous avons analysé sur large échelle l'activité kinase de Rim15 et nous avons pu ainsi isoler des substrats possibles pour cette serine/threonine kinase. Une des protéines qui étaient le plus fortement phosphorylés par Rim15 corresponds au produit d'un gène non caractérisé, *YNL157W/IGO1*. Cette protéine représente un de deux homologues, chez la levure, d'une famille de protéines humaines appelés endosulfines. Ces protéines de très petite taille sont très conservées mais leur fonction n'est pas connue précisément; dans les cellules β les endosulfines semblent réguler le canal du potassium (K_{ATP}), tandis que dans les cellules du système nerveux centrales elles semblent êtres impliqués dans la stabilisation de certains mRNAs.

Nous avons confirmé ici que Igo1 ainsi que le produit du gène homologue *YHR132W-A/IGO2* étaient phosphorylés in vitro par Rim15. Des études plus approfondis nous ont permis de identifier exactement l'acide aminé phosphorylé par Rim15, une sérine en position 64 dans Igo1, lequel se trouve dans une région de Igo1 qui est fortement conservée. Nous avons ensuite commandé des anticorps spécifiques contre le site phosphorylé, ce qui nous a permis de démontrer que cette sérine est une cible in vivo pour Rim15. De plus, Igo1 semble être phosphorylé sur cette sérine dans toutes les conditions qui causent l'accumulation de Rim15 dans le noyau, notamment la privation de phosphate, azote et glucose ainsi que l'exposition à la rapamycine.

La délétion des cibles de Rim15, *IGO1* et *IGO2* a un effet très similaire à la délétion de *RIM15*; les mutants *igo1Δigo2Δ* montrent un défauts dans l'induction d'une partie du programme de différentiation G_0 (notamment dans l'accumulation de glycogène et de trehalose, la transcription des genèse spécifiques de la phase G_0, et l'arrêt du cycle cellulaire) suite à un traitement avec la rapamycine ou à l'entré en G_0. De plus, comme les diploïdes *rim15Δ/rim15Δ* aussi les diploïdes homozygotes *igo1Δ/igo1Δ igo2Δ/igo2Δ* présentent des taux de sporulation très bas. L'ensemble de toutes ces observations indique que Igo1 et Igo2 représentent effectivement les cibles de Rim15 qui sont critiques pour l'induction du programme G_0. Les fonctions de Igo1 et Igo2 dans l'induction du programme me G_0 dépends de leur phosphorylation de la part de Rim15: en effet, un allèle de Igo1 qui ne peut pas être phosphorylé, parce que la serine en position 64 a été remplacé par une alanine, ne complémente pas les défaut du mutant *igo1Δigo2Δ*.

L'étude du profil transcriptionel induit par la rapamycine, ainsi que des autres traits caractéristiques de la phase G_0, dans des mutants *igo1Δigo2Δ*, nous montre que le défaut de ces mutants est plus étendu que le défaut des mutants *rim15Δ*. Ceci pourrait indiquer que Igo1 et Igo2 sont impliqués aussi dans le contrôle de procès qui sont indépendants de Rim15. Dans ce contexte, nous avons découvert aussi que Igo1 pourrait être contrôle négativement par un mécanisme dépendant de la PKA. La substitutions dans un site conservé qui représente une site putative pour la phosphorylation dépendante de la PKA, de la sérine en position 105 avec une alanine, rendent Igo1 plus active par apport à l'allèle sauvage mais qui peut toujours être activé davantage par Rim15. Au contraire, si le même résidu est remplacé par un aspartate (qui peut dans beaucoup de cas mimer une phosphorylation) l'allèle résultants semble être inactive. Il est possible que le rôle de la phosphorylation de la sérine 105 par la PKA soit d'empêcher, pendant la phase exponentielle l'activation de Igo1 par Rim15, ou tout simplement la phosphorylation par la PKA pourrait inhiber l'activité de Igo1.

Nous avons clairement établi que Igo1 et Igo2 sont les cibles de Rim15, et que ils sont responsables pour toutes les fonctions connues de cette kinase. Malheureusement, la fonction moléculaire de ces cibles reste encore un mystère. Il y a quelques indications que Igo1/Igo2 pourraient être directement impliqués dans l'expression des gènes, en particulier les interactions qui ont été détectés dans des études sur large échelle montrent un certain numéro de partenaires directement ou indirectement liés à la transcription. Par exemple, Igo1 montre des interactions double hybride avec la protéine Rna15 et avec le facteur de transcription Ace2. De plus Igo1 semble co-purifier avec l'histone H2B,

qui est nécessaire pour l'assemblage de la chromatine, ainsi que avec Cpr1, un possible interacteur du complexe Sin3-Rpd3 (histone deacetylase). Ces dernières interactions sont particulièrement intéressantes en rapport avec le rôle de Rim15 pendant la méiose; Rim15 contribue à l'expression des gènes de la méiose e promeut le détachement du complexe Sin3-Rpd3 des promoteurs de ces gènes. Il est probable que un mécanisme analogue fonctionne aussi pour l'expression des gènes spécifiques de la phase G_0.

Les études futures vont certainement viser à la confirmation ces interactions et observations pour pouvoir mieux comprendre, enfin, les mécanismes qui régulent l'expression des programmes génétiques en réponse à la privation de nutriments.

Comme j'ai mentionné au debout de ce résumé, l'identification des procès qui sont impliques dans la régulation de la prolifération et de la quiescence sont très relevants, aussi d'un point de vue clinique ; il suffise de rappeler les conséquences qui aurai la croissance incontrôlée des cellule dans les tissues, ainsi que l'incapacité des cellules souche de sortir de la phase quiescente pour régénérer un tissu endommagé.

Abstract

Initiation of the G_0 differentiation program is a critical event in the life of a eukaryotic cell and is placed under the control of intricate signaling networks that respond to multiple environmental and intrinsic cues. Complex regulatory mechanisms ensure the correct and timed transition between proliferation and quiescence, which is vital for both unicellular and multicellular organisms.

In *Saccharomyces cerevisiae*, entry into the quiescent G_0 state occurs in response to limitation for essential nutrients, which are mainly monitored by the PKA, the target of rapamycin complex 1 (TORC1) and the phosphate-sensing Pho80/Pho85 cyclin-cyclin dependent kinase (cyclin-CDK) pathways. In the presence of abundant nutrients, all three pathways converge on and negatively regulate the serine/threonine kinase Rim15, which represents a key regulator of the G_0 program. Limitation for essential nutrients or addition of the TORC1 inhibitor rapamycin causes cytoplasmic-to-nuclear translocation followed by activation of Rim15 and induction of the G_0 program.

Cells devoid of Rim15 fail to both arrest growth and acquire G_0 characteristics following nutrient limitation. Consequently, these mutant cells are not adequately equipped for survival in the absence of nutrients and display a reduced life span under these conditions.

Our analysis (presented in Chapter II of this thesis) of the global transcriptional changes occurring during the diauxic transition highlighted a critical contribution of Rim15 and the transcription factors Msn2/Msn4 and Gis1 to the expression of various enzymatic systems that, in anticipation of deteriorating environmental conditions, allow the cells to sustain their metabolic activity and ensure their survival. In particular, we found that Rim15 controls the timely adequate induction of genes required for respiratory metabolism and of genes whose products allow the cells coping with reactive oxygen species that are produced in large amounts during a respiratory life-style. Interestingly, in this context, our analysis of the molecular architecture of Rim15 revealed the presence of an N-terminal PAS domain, which is commonly found in sensor proteins that are involved in sensing oxygen radicals or the redox status of the cell. Another domain in Rim15, which we also characterized, is a novel phosphoinositide-binding C_2CH zinc finger that is essential for the enzymatic activity of Rim15 and may be involved in the recognition of chromatin-associated

phosphoinositide pools. The implications of these newly identified domains in the control of Rim15 function are highlighted in Chapter I.

Finally, a key finding in Chapter III of the present thesis is the identification and molecular description of the *bona fide* Rim15 target proteins Igo1 and Igo2. Like Rim15, Igo1 and Igo2 are essential for the initiation of the G_0 program in response to nutrient depletion. As members of a conserved protein family, *i.e.* the endosulfine family, Igo1 and Igo2 may ultimately lead us the final understanding of the G_0 entry process. More likely, I guess, they will - yet again - be an intriguing starting point for exciting new studies in this field.

General Introduction

Regulation of G_0 in *S. cerevisiae*

Probably all living cells possess the astonishing ability to exit the normal cell cycle and survive for long periods in a reversible, quiescent state termed G_0. Full appreciation of the molecular regulation of this nearly universal process could have enormous clinical implications; for instance for the development of new strategies for *in vitro* stem cell expansion, of new anticancer and immunosuppressant drugs, as well as for the development of novel antipathogenic agents.

In yeast, starvation for any of the essential nutrients (*i.e.* carbon, nitrogen and phosphate) results in growth arrest and the induction of similar differentiation programs. In batch cultures, yeast cells are believed to arrest growth due to carbon (glucose) limitation; they acquire specific physiological and transcriptional characteristics that define what is termed the G_0 (or quiescent) state [1]. Even though nitrogen and phosphate starvation also result in growth arrest and acquisition of a quiescence-like phenotype, it is currently not known whether a common differentiation program is activated in response to starvation for the different nutrients, or whether each signal triggers similar but distinct responses. Mammalian cells enter G_0 in the absence of growth factors (mitogen deprivation), when grown at high cell density in cell cultures (contact inhibition), or upon disruption of cell-substratum adhesions (loss of adhesion); similarly to yeast G_0 cells, they exist in a quiescent, non-proliferating state characterized by a distinctive transcriptional signature [2,3]. Notably, mammalian primary fibroblasts were recently shown to enter distinct quiescent states depending on the initiating signal; although clearly distinct, these different quiescent states comprised a common, signal-independent transcriptional response, implying the existence of a basic genetic program of quiescence [3]. Both, mammalian and yeast cells enter G_0 from a cell-cycle checkpoint in the G_1 phase termed the restriction point (in mammalian cells) or the start point (in yeast cells). Importantly, unlike other non-proliferating states (*e.g.* senescence, terminal differentiation) quiescence is a reversible state that is functionally different from cell-cycle arrest and is characterized by a distinctive pattern of gene expression.

The use of yeast as a model to study the basic regulatory mechanisms underlying cell proliferation and quiescence is likely to provide insightful information about related processes in multicellular eukaryotes.

G_0 entry and nutrient sensing pathways

Under physiological conditions, yeast cells enter G_0 in response to nutrient starvation [4]. In order to understand how signals from different essential nutrients may trigger a common response, it is important to know how these signals are integrated. The next paragraphs describe the main nutrient sensing pathways in *Saccharomyces cerevisiae*; in particular, evidence is presented that these pathways together form a highly interconnected signaling network and that they share common downstream effectors. Some of these act as master regulators, which orchestrate the coordinate entry into G_0, by integrating signals from different nutrients. One such effector is the protein kinase Rim15, which integrates the signals from nitrogen, carbon and phosphate withdrawal and which is essential for the correct initiation of the G_0 program. Here only the response of haploid yeast cells to nutrient starvation is described; it is worthy noting, though, that the G_0-regulatory pathways share some components with the pathways that regulate the processes of dimorphic switch and meiosis, two alternative differentiation programs that occur in diploid yeast cells. Among several others, one important example is the key G_0 regulator Rim15, which is also necessary for the induction of the meiotic program.

The nitrogen signal

Although ammonia, glutamine and glutamate are preferentially used, yeast can use a surprisingly diverse array of compounds as nitrogen sources. As a consequence, no single nitrogen source is essential individually for yeast survival [5]. Genes encoding permeases and enzymes required for catabolism of the various secondary nitrogen sources (low-quality nitrogen sources) are not expressed in the presence of the preferred nitrogen sources (high-quality nitrogen sources). Their regulation is ensured by the nitrogen discrimination pathway (NDP) which regulates a process that has been termed nitrogen catabolite repression (NCR) in analogy to the process of carbon catabolite repression, whereby the presence of glucose inhibits the transcription of genes required for the utilization of alternative (less preferred) carbon sources [5]. Glutamine appears to be the critical metabolite of NCR; although ammonia also leads to strong nitrogen repression, it is probably not itself active, as it does not cause repression in mutants lacking glutamine synthetases [5]. Importantly, the absence of secondary and preferred nitrogen sources altogether activates a distinct response through the nitrogen starvation pathway. This pathway is best known in diploid cells, where nitrogen starvation in the absence of a fermentable carbon source, induces the expression of the phosphatases Yvh1 and Ptp2, that are involved in regulating the process of

meiosis [6,7]. The dual specificity tyrosine phosphatase Yvh1 acts upstream of the protein kinase Mck1p to promote spore development [8]. Interestingly Yvh1 has also been implicated in the regulation of growth and glycogen accumulation [9].

Under nitrogen-rich conditions, phosphorylation of the GATA family transcriptional activators Gln3 and Gat1 prevents them from entering the nucleus by promoting their association with the cytoplasmic protein Ure2, which itself is regulated by phosphorylation (Figure 1) [10]. The transcription of NCR genes is inversely controlled by Gln3 and Gat1 and by the two negative-acting GATA family proteins Dal80 and Deh1. In certain cases, the GATA activators and repressors compete with each other for the occupancy of GATA promoters [10]. Importantly, Dal80 and Deh1 are not responsible for NCR, which is merely due to the absence of transcriptional activation of nitrogen repressed genes in the presence of high-quality nitrogen sources. They are however involved in a reciprocal regulation system, that is necessary to achieve the steady state of this peculiar transcriptional system. Accordingly, nuclear Gln3 activates the expression of GAT1 and Gat1 and Gln3 act together to activate the transcription of *DAL80* and *DEH1*, whose products then decrease the expression of target genes [10].

Nitrogen availability has been proposed by different groups to be transmitted to the NDP via the nutrient responsive TORC1 pathway (described in detail later); the TORC1 pathway is active when nutrients are abundant and stimulates growth by various mechanisms including the positive regulation of general transcription and translation [10]. Although inhibition of TORC1 correlates with reduced levels of Gln3 and Ure2 phosphorylation, and thus with the induction of GATA-mediated transcription, it is currently not clear whether this correlation results from decreased TORC1-dependent phosphorylation of Gln3 and Ure2 (as suggested in [11,12]) or rather from the release of TORC1-regulated phosphatases from inhibition by Tap42 (as suggested in [13,14]). In either case, dephosphorylation of Gln3 and Ure2 promotes the dissociation of the Gln3-Ure2 complex and nuclear import of Gln3 (Figure 1). The nuclear import/export of the different Gln3 phosphoisoforms is controlled by a mechanism involving the nuclear transport proteins Srp1 and Crm1 and which directionality is dictated by the Ran protein Rna1 in its GTP/GDP loading status [10]. In addition, the pleiotropic regulatory factor Mks1 has been suggested to regulate the activity of Ure2 and thereby the NCR (Figure 1) [15], although this result has been debated in a recent work by Tate *et al.* (2002), suggesting that Mks1 indirectly affects the transcription of some nitrogen repressed genes by controlling TCA cycle genes [16].

Rtg1 and Rtg3 transcribe a distinct set of genes whose protein products are involved in carbon metabolism (*e.g.* genes of the TCA cycle and the glyoxylate cycle). Their activity is also induced in response to low-quality nitrogen sources, reflecting the altered metabolic needs of cells (Figure 1). Notably, *de novo* synthesis of amino acids drains important TCA cycle intermediates such as oxaloacetate and α-ketoglutarate, which need to be replenished through anaplerotic reactions in order to maintain the respiratory competency of the cell. These include: the production of succinate via the glyoxylate cycle, the formation of oxaloacetate from pyruvate and aspartate, the formation of α-ketoglutarate from glutamate, and the β-oxidation of fatty acids to succinyl-CoA. In the absence of the preferred nitrogen sources glutamine and glutamate, the cytoplasmic protein Rtg2 stimulates the redistribution of the Rtg1/Rtg3 complex from a predominantly cytoplasmic, to a predominantly nuclear localization [17]. Similarly to what was observed for the GATA family transcription factors Gln3 and Gat1, phosphorylation and cytoplasmic relocalization of the Rtg1/Rtg3 complex is also controlled by the TORC1 pathway [17].

The mechanism by which the NDP pathway receives the signal from nitrogen availability is currently not known. It was speculated that TORC1 may sense the levels of a cytoplasmic or vacuolar amino acid, most likely glutamine. Additionally, signaling by the cell surface amino acid sensor Ssy1–Ptr3–Ssy5 (SPS) is required for the proper transcription of genes encoding proteins associated with amino acid uptake, as well as for the transcription of several nitrogen-regulated genes (Figure 1), including many TORC1-regulated genes. Additionally the SPS sensor is required for the mobilization of a pool of basic amino acids that are stored within the vacuole and is thought to participate in the full repression of NCR genes [18].

Even though, in contrast to nitrogen starvation, a shift from high-quality to low-quality nitrogen sources does not induce growth arrest and entry into G_0. Some of the transcriptional changes induced by the NDP pathway are similar to the changes induced by nutrient depletion or treatment with rapamycin [14,19,20]. In this context, the simultaneous deletion of *GLN3* and of *GAT1* was reported to render the cells partially resistant to the effects of rapamycin, and this effect was increased by mutations resulting in high PKA activity, which by themselves do not produce a rapamycin resistant phenotype [21]. These observations suggest that the NDP may be involved in the induction of a subset of genes that are also important for the expression of the G_0 program.

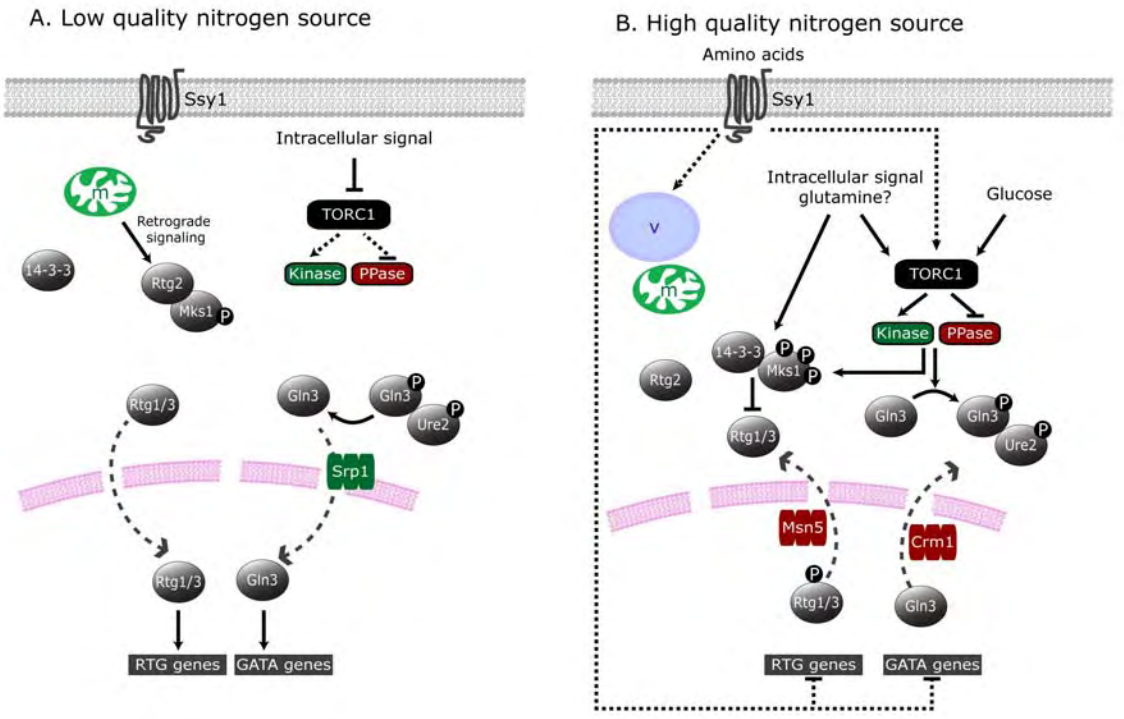

Figure 1

Pathways involved in the transduction of the nitrogen signal. [A.] When only low-quality nitrogen sources are available, the hypophosphorylated forms of the transcriptional activators Rtg1/Rtg3 and Gln3 are transported in the nucleus, where they activate RTG genes (*e.g.* genes of the TCA and glyoxylate cycles) and GATA genes (genes controlled by NCR) respectively. Importantly, Rtg1/3 are also activated in response to impaired mitochondrial activity, through the retrograde signaling. The import of Gln3 is mediated by the karyopherin α homolog Srp1. [B.] In the presence of a high-quality nitrogen source, an intracellular signal, probably glutamine, triggers the phosphorylation of Gln3, which is kept in the cytoplasm via its interaction with phosphorylated Ure2. Hyperphosphorylated Mks1 is thought to promote the association of Rtg1/3 with the 14-3-3 protein Bmh2, resulting in cytoplasmic retention of the transcription activator complex. The export of Rtg1 and Rtg3 from the nucleus requires the karyopherin β homologue Msn5, while Gln3 export depends on the karyopherin Crm1. An additional signal, from extracellular amino acids, is transmitted by the SPS (Ssy1–Ptr3–Ssy5) sensor via still incompletely understood mechanisms (m, mitochondria; v, vacuole).

The carbon (glucose) signal

Yeast cells favor the fermentative life-style over the more efficient respiratory life-style, even in the presence of abundant oxygen; as long as the levels of the fermentable carbon sources are high enough to sustain this life-style, fermentation confers yeast cells a significant selective advantage over other microorganisms, due to the fast growth rates and the production of ethanol. A similar phenomenon is observed in fast-growing tumor cells, where fast fermentative growth is observed even in the presence of oxygen. The predominance of aerobic glycolysis due to the ability to circumvent the Pasteur effect, *i.e.* the inhibitory effect of oxygen on the process of fermentation, is called the "Warburg effect" [22]. Like mammals, yeast cells show a remarkable preference for

glucose as energy and carbon source and in its presence, yeast cells turn down the mechanisms involved in respiration (*e.g.* cytochromes) and in the utilization of alternative carbon sources (galactose, maltose, sucrose) and induce genes for the utilization of glucose, such as genes encoding glycolytic enzymes and glucose transporters. This process, called the carbon catabolite repression, ensures the efficient and exclusive utilization of glucose [23].

Besides being the preferred carbon source, glucose is also the most important energy source and a signaling molecule; thus it is not surprising that eukaryotic cells use several mechanisms to sense this important metabolite. The presence of glucose generates receptor- and transport-mediated signals as well as metabolic signals [24]. Glucose-mediated transcriptional repression (glucose repression or catabolite repression [23]) of genes involved in respiration, gluconeogenesis and in the metabolism of alternative carbon sources, specifically requires glucose phosphorylation by one of three enzymes; the two hexokinases (Hxk1 and Hxk2) and the glucokinase Glk1. While any of the three enzymes can sustain an initial short-term glucose repression, only the most active of them, the hexokinase Hxk2, is essential for long-term maintenance of repression [25]. Interestingly, while the expression of Hxk2 is induced by glucose, the two other enzymes are themselves under the control of the catabolite repression system [26]. The Snf1 kinase counteracts glucose repression by negatively regulating the transcriptional repressor Mig1 (Figure 2). In the absence of glucose, phosphorylation of the transcriptional repressor Mig1 by Snf1 results in its cytoplasmic translocation, conversely, inactivation of Snf1 by glucose allows the hypophosphorylated Mig1 protein to enter the nucleus where it binds to the promoters of glucose-repressed genes and inhibits their transcription by recruiting the general repressor Cyc8-Tup1 [27]. Inactivation of Snf1 in the presence of glucose is thought to depend on the Hxk2-generated signal; alternatively Snf1 may directly sense the low AMP/ATP ratio which reflects high glucose levels (Figure 2). This alternative model for Snf1 activation has been postulated based on the homology with the mammalian AMP kinase (AMPK), which is known to be directly regulated by AMP, and on the observed correlation between Snf1-activation and the AMP/ATP ratios [28]. Additionally, in the presence of glucose, the regulatory subunit Reg1 targets the Glc7 phosphatase to Snf1 and/or Mig1 and thereby promotes glucose repression [23]. The importance of the Snf1-dependent derepression of glucose-repressed genes is underscored by the phenotype of *snf1Δ* mutants: in the absence of *SNF1*, yeast cells are unable to grow on non-fermentable carbon sources and thus *snf1Δ* mutants die quickly after the diauxic shift. Finally the glucose kinase Hxk2, which resides partly also in the nucleus, may further participate in the transduction of the glucose signal by directly interacting with

the transcription machinery and with various transcription regulators including Mig1 (Figure 2) [29].

A second pathway ensures optimal glycolytic capacity by activating many glycolytic enzymes and glucose transporters in the presence of glucose; the glucose receptors Snf3 and Rgt2 generate a signal, the exact nature of which has not yet been identified, that causes the multiprotein ubiquitin-ligase complex SCF-Grr1 to inactivate the transcriptional repressor Rgt1 (Figure 2). The cytoplasmic proteins Std1 and Mth1 may be involved in transmission of this glucose signal; accordingly, both proteins have been shown to interact physically with the putative signaling domains located within the cytoplasmic tails of the Snf3 and Rgt2 sensors [24].

Addition of glucose to glucose-deprived cells triggers the switch to the fermentative life-style by rapidly activating the synthesis of cAMP via adenylate cyclase (Cyr1). This activates the protein kinase A (PKA) pathway, which in turn activates enzymes in glycolysis and inhibits enzymes in gluconeogenesis at a post-translational level (Figure 5) [30]. Initiation of the cascade leading to cAMP synthesis requires two inputs: glucose phosphorylation either by glucokinase 1 (Glk1) or by one of the two hexokinases (Hxk1 and Hxk2), for which only a low level of glucose is required, and activation of a G-protein-coupled receptor (GPCR) system, which requires a higher level of glucose [31]. Upon binding of glucose, the glucose receptor Gpr1 activates the heterotrimeric Gα protein homologue Gpa2 which, in turn, activates Cyr1. Active metabolism of glucose is thought to render Cyr1 responsive to activation by the GPCR system. Importantly, in addition to its role during the transition from respiration to fermentation, the Gpr1-Gpa2 GPCR system is also involved in the response to nitrogen and phosphate starvation in the presence of glucose.

When all the available glucose has been used, cells shortly arrest growth in order to adjust to respiratory metabolism which allows them to metabolize the remaining carbon sources, such as the ethanol that was produced during fermentation [32]. During this short adaptation phase, called the diauxic shift, the glucose-signaling pathways are downregulated and glucose controlled genes are derepressed. Importantly, the G_0 program is initiated during this phase and many genes required for survival during the quiescent phase are already induced.

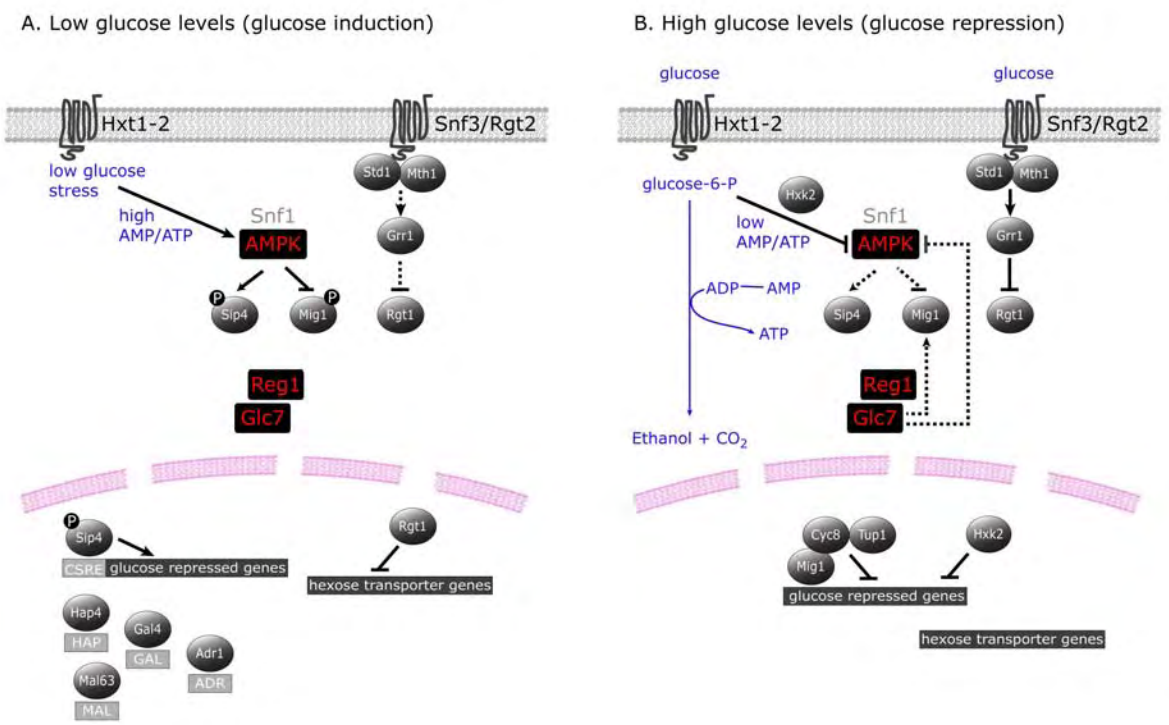

Figure 2

Summary of the mechanisms responsible for glucose-repression and glucose-induction of transcription. [A.] When glucose levels are low, phosphorylation of Mig1 by Snf1 (AMPK) results in cytoplasmic retention of the repressor, allowing the derepression of glucose-controlled genes. In contrast Snf1-dependent phosphorylation allows Sip4 to activate genes harboring carbon-source responsive elements (CSRE) in their promoter regions. Various additional transcription factors are involved in the transcriptional induction of other glucose-repressed gene. [B.] Metabolism of glucose, particularly by Hxk2, results in the downregulation of the yeast AMPK Snf1. The hypophosphorylated target of Snf1, Mig1, resides in the nucleus in the presence of glucose and mediates the carbon catabolite repression. In addition, the glucose receptors Snf3 and Rgt2 associate with Std1 and Mth1, which are thought to transmit the glucose signal to Grr1, ultimately resulting in the degradation of Rgt1, a transcriptional repressor of hexose transporters genes. Importantly, as discussed elsewhere in this work, the presence of glucose activates also the PKA pathway.

The phosphate signal

The phosphate requirements of yeast cells are met by the uptake of inorganic phosphate (P_i) from the medium. Inorganic phosphate is needed in large amounts for the biosynthesis of major cell constituents, such as nucleic acids and phospholipids, as well as for energy metabolism. The intracellular concentration of free phosphate is generally maintained at a very low level and phosphate reserves are stored mainly in the vacuole in the form of linear polymers of orthophosphates in anhydrous linkage, named polyphosphate. Upon transfer of cells to a phosphate-deficient medium, a rapid decrease of the polyphosphate content is observed in whole cells [33]. Polyphosphate is thought to act as a buffer that is continuously mobilized in order to maintain a constant intracellular level of inorganic phosphate particularly during periods of phosphate

limitation [34]. The phosphate signal transduction pathway (PHO pathway) regulates the expression of several phosphate-responsive genes that are involved in scavenging and specific uptake of phosphate from extracellular sources (Figure 3). When the extracellular concentration of phosphate is low, the transcription factor Pho4 is imported into the nucleus by the nuclear import receptor Pse1 where it acts cooperatively with Pho2 to activate the transcription of genes that contain a *PHO* element (5'-CACGTGS-3') in their promoter region [35]. These genes include the acid phosphatase genes (*PHO5*, *PHO10* and *PHO11*) and the genes encoding high-affinity phosphate transporters (*PHO84* and *PHO89*). In addition genes for the uptake and metabolism of inositol phosphate, for the accumulation of polyphosphate in the vacuole (*VTC* genes), as well as genes for the metabolism of various phosphorylated compounds, are specifically induced by phosphate starvation [19]. In contrast, the genes encoding the low-affinity phosphate transporters (*i.e. PHO87*, *PHO90* and *PHO91*) and the acid phosphatase (*PHO3*) are constitutively transcribed under high-phosphate conditions. Under high phosphate conditions, inhibition of the Pho80-Pho85 cyclin-CDK complex by Pho81 is relieved (Figure 3) and Pho80-Pho85 promotes the phosphorylation of Pho4 on several sites, thereby preventing its interaction with Pse1 and Pho2 while favoring its association with the nuclear export receptor Msn5. The PHO pathway is thought to respond to both extracellular phosphate levels and metabolic signals, possibly from intracellular orthophosphate and polyphosphate; accordingly the levels of both molecules have been shown to inversely correlate with the level of *PHO5* expression [36]. Interestingly a novel inhibitory domain in Pho81, which inhibits the Pho80-Pho85 complex when cells are starved for phosphate, may be directly involved in sensing intracellular phosphate levels (Figure 3) [37]. An additional intracellular signal may involve inositol polyphospates, which have been proposed to modulate the expression of *PHO* genes by affecting chromatin remodeling complexes [38]. Sensing of extracellular phosphate is thought to be mediated by the high-affinity phosphate transporters Pho84 and Pho87 (Figure 3); consistently, the expression of the acid phosphatase Pho5 is repressed by the non-metabolizable phosphate analogue methylphosphonate in the presence of Pho84 [34]. Furthermore, addition of phosphate or the phosphate analogue methylphosphonate to cells grown on low-phosphate media triggers internalization and degradation of Pho84, while transcription of *PHO84* and of other *PHO* genes remains unperturbed [34]. Interestingly, the addition of phosphate to phosphate-starved cells was also shown to rapidly activate the PKA, but not cAMP synthesis, by a mechanism that implicates both, the glucose receptor Gpr1 and the high-affinity phosphate transporters Pho84 and Pho87 [39].

Phosphate starvation in the presence of the other essential nutrients results in growth arrest and entry into the resting state G_0, as indicated by the accumulation of G_0 specific transcripts (*e.g. SSA3, GRE1*) and by the downregulation of genes required for transcription and protein synthesis [20]. Activation of both, the PKA pathway and the Pho80-Pho85 cyclin-CDK complex by high phosphate levels in the extracellular medium, may result in the downregulation of the protein kinase Rim15, which plays an essential role in the initiation of the G_0 program. We have previously shown that the activity of Pho80-Pho85 complex affects the induction of Rim15-dependent G_0 traits by a mechanism involving the nuclear export of Rim15 by the nuclear export receptor Msn5 analogously to the regulatory mechanism acting on the transcription factor Pho4 [40]. Furthermore, full length Pho81 has been shown to be required to control trehalose metabolism and the transcriptional induction, during the diauxic shift, of many Rim15 target genes [41]. Besides having a crucial role in the phosphate response, the cyclin-dependent kinase Pho85 performs several other function through its ability to associate with multiple cyclin partners, contributing to the creation of an intricate nutrient signaling network [42].

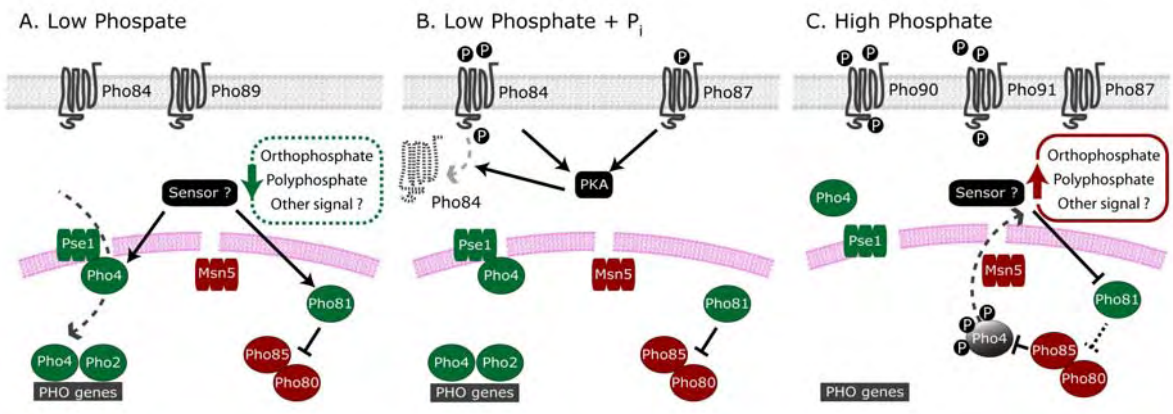

Figure 3

[A.] When extracellular phosphate level is low, an intracellular metabolic signal (presumably the level of orthophosphate or polyphosphate) is transduced by an unknown sensor and results in the inactivation of the Pho80-Pho85 complex thus promoting nuclear localization of the transcription factor Pho4. Pho4 and Pho2 cooperatively activate the transcription of genes required to efficiently scavenge phosphate from the environment (*PHO* genes), such as genes encoding the high-affinity phosphate transporters Pho84 and Pho89 and the secreted acid phosphatases Pho5, Pho10 and Pho11. [B.] Addition of phosphate to cells grown on low phosphate activates the PKA pathway and triggers the internalization and degradation of Pho84 without affecting the transcription of *PHO* genes. [C.] Under high phosphate conditions the low-affinity phosphate transporters are expressed and an intracellular metabolic signal is thought to inhibit Pho81. The active Pho80-Pho85 complex phosphorylates Pho4, and thereby promotes its export from the nuclear compartment. Red proteins, negative regulation of *PHO* genes; green proteins, positive regulation of *PHO* genes.

The TORC1 pathway

Dividing eukaryotic cells treated with rapamycin, an analogue of the macrolide antibiotic FK506, stop proliferating and acquire many characteristics that are reminiscent of the changes associated with the G_0 arrest induced by nutrient starvation [14,43]. In nature, the physiological effect of rapamycin is exploited by the microorganism *Streptomyces hygroscopicus*, which releases this antibiotic into the environment and can thereby successfully compete for nutrient sources by inhibiting the growth of rapamycin-sensitive organisms such as *Saccharomyces cerevisiae* or *Cryptococcus neoformans* [44]. In medical research, rapamycin is appreciated for its immunosuppressive and antitumoral activities. Rapamycin associates with the cytoplasmic peptidyl-prolyl *cis-trans* isomerase FKBP12 (FK506-binding protein) and this drug-receptor complex then binds to the Tor (Target of rapamycin) proteins, within a conserved domain termed the FKBP12-rapamycin-binding domain (FRB). By a still poorly understood mechanism, binding of the FKBP12-rapamycin complex appears to affect the ability of the Tor protein kinases to phosphorylate their targets [45,46].

The Tor proteins are highly conserved among all eukaryotic species and are part of a crucial nutrient signaling network [43]. Due to the sequence homology of the C-terminal portion of the Tor proteins to the catalytic domains of phosphatidylinositol-3 kinase (PI3K), these serine/threonine kinases are ascribed to the phosphatidylinositol 3-kinase related kinase (PIKK) family of protein kinases [43]. Despite the sequence homology to PI3K, PIKK family kinases preferentially phosphorylate serine or threonine residues and have never been shown to possess lipid kinase activity. The Tor proteins can be integrated in two functionally distinct complexes: namely the TOR complex 1 (TORC1) and the TOR complex 2 (TORC2) [47]. Only TORC1 is highly sensitive to rapamycin.

Although the functions of TORC2, *i.e.* the organization of the actin cytoskeleton and the coordination of cell morphogenesis with growth [48], do not appear to be altered after addition of rapamycin, a long-term treatment of yeast cells with rapamycin may, according to a recent study, affect the stability of TORC2 [49]. In contrast, the stability of the rapamycin-sensitive TORC1 is not affected by rapamycin [47], suggesting that the inhibitory effect of this drug may be due to a direct interference with the protein kinase activity of the Tor proteins, or with the ability of the complex to associate with its targets. TORC1 is involved in the regulation of many cellular processes including: protein synthesis, ribosome biogenesis, autophagy, transcriptional activation, meiosis, cell cycle as well as the sorting and turnover of nutrient permeases [50,51].

Unlike all other eukaryotes, which appear to encode only one Tor protein, yeast has two Tor proteins encoded by the *TOR1* and *TOR2* genes respectively; the protein product of *TOR2* can be integrated in both TORC1 and TORC2. In contrast the *TOR1* protein product is only found in TORC1 [47]. TORC1 is thought to be built on a dimeric TOR protein to which the other core components, namely Lst8, Kog1 and Tco89, associate in a rapamycin insensitive manner [47]. Both, Lst8 and Kog1, are essential components of TORC1 and their mammalian counterparts mLST8 and Raptor were suggested to play critical roles for the function of mammalian TORC1 (mTORC1) by interacting physically with downstream components such as the eIF4E-binding protein 1 and the ribosomal S6 kinase, or with regulators of the pathway, thereby bridging the interactions between the kinases and their substrates and/or regulators [52]. The function of Tco89, for which this far no mammalian ortholog has been identified, remains elusive. Importantly, in addition to its function as a component of TORC1, Tco89 may have an additional, TORC1-independent function in maintenance of cellular integrity [53].

Various studies in yeast all acknowledge the association of TORC1 with membranes, however there is no general agreement about the precise subcellular localization of the complex [50]. Although some studies are indicative of TORC1 association with membrane structures different from both, the plasma membrane and the vacuolar membrane [54,55], the association with the vacuolar membrane would support a particularly appealing model that postulates TORC1 regulation by one or several vacuolar nutrients [50,56]. The observed stability of the core TORC1 complex composition and localization (there is no indication that TORC1 composition or localization are affected by rapamycin treatment or nutrient cues) under diverse conditions has lead to the hypothesis that regulation of TORC1 signaling may be achieved through nutrient-dependent modulation of the interactions of TORC1 with its regulators and/or targets.

Most of the current knowledge on the functions of TORC1 results from the study of rapamycin-induced cellular responses. Additionally, TORC1 sensitivity to wortmannin, LY294002 and caffeine has also been reported [45,46,57,58]; however, due to their low affinity to TORC1 and their wide-ranging physiological effects, these drugs have not been largely employed for the study of TORC1 functions. However, although TORC1 binds caffeine with a very low affinity (submillimolar range of concentrations) it appears to be a relevant target of caffeine *in vivo*; notably, treatment of yeast cells with caffeine or rapamycin results in the induction of very similar transcriptional changes [57].

Adverse nutrient conditions or TORC1 inhibition by rapamycin causes both a rapid decline in protein synthesis to preserve cellular energy, and the induction of autophagy to recycle cellular components. In addition, the TORC1 pathway positively regulates growth by antagonizing the activities of a number of stress-responsive transcription factors; thus, similarly to nitrogen- or carbon- withdrawal, exposure to rapamycin causes cell to arrest growth and enter a G_0-like state characterized by the dramatic downregulation of anabolic processes and the upregulation of catabolic and stress-response processes.

Under growth conditions, many of these responses are negatively regulated through TORC1-dependent inhibition of the activity of type 2A protein phosphatase (PP2A) complexes and PP2A-like complexes (Figure 4). In yeast, the catalytic subunits of PP2A (PP2Ac), encoded by *PPH21, PPH22* and *PPH3*, are found predominantly in association with the regulatory subunits Cdc55 and Rts1 and with the scaffolding subunit Tpd3. In contrast, the PP2A-related phosphatase Sit4 associates with members of the Sit4 associated protein (SAP) family [59]. The small subset of PP2A and PP2A-like phosphatase complexes that are controlled by TORC1 contain the regulatory subunit Tap42 and either one of two phosphotyrosyl phosphatase activators (Rrd2 and Rrd1) [60]. There is not yet a uniform view of how these complexes transmit the signal from the TORC1 complex to the downstream effectors; the most recent model (Figure 4) posits that, under conditions of low TORC1 activity, the phosphatases are transiently activated and promote the adaptation to nutrient scarcity by affecting the localization of various transcription factors as well as the sorting of low-specificity permeases [61]. In growing cells, Tap42 is directly phosphorylated by TORC1 [62]; phosphorylated Tap42 forms a complex with the PP2A catalytic subunits and associates with TORC1, tethering the PP2Ac and PP2A-like phosphatase Sit4 to membrane structures [61]. Treatment of yeast cells with rapamycin triggers the release of the Tap42-Rrd2-PP2Ac and Tap42-Rrd1-Sit4 complexes from the interaction with TORC1, resulting in transient activation of their phosphatase activity (Figure 4).

The free, active Tap42-Rrd2-PP2Ac complex may promote transcription of many rapamycin responsive genes by dephosphorylating various transcription factors, including for example Msn2 [63], Rtg1/3 and Gln3 [64], thereby allowing their nuclear translocation/retention (Figure 4). In addition, TORC1 also prevents Rtg1/3-dependent transcription during growth by controlling the phosphorylation state of Mks1 (Figure 4). Upon TORC1 inactivation, the hypophosphorylated Mks1 associates with its inhibitor Rtg2, which allows subsequent nuclear translocation of the Rtg1/3 complex (Figure 1). Although it is currently not known which phosphatase(s) mediate the

dephosphorylation of Mks1, the involvement of Tap42 was suggested based on the observation that rapamycin-sensitive genes, whose regulation depends on Mks1, represent a subset of the Tap42-controlled genes [65]. Dephosphorylation by the Tap42-Rrd1-Sit4 complex positively regulates the activity of the protein kinase Npr1, which is required for the stability and sorting of several aminoacid transporters in response to the quality of the growth conditions (Figure 4) [66,67]. Similarly, the protein kinase Gcn2 is activated by Tap42-Rrd1-Sit4-dependent dephosphorylation. Active Gcn2 promotes Gcn4-translation a key transcription factor of amino acid synthesis genes (Figure 4) [68]. The Tap42-Rrd1-Sit4 complex is also involved in the activation, following rapamycin treatment and during the stationary phase, of Mpk1 (Figure 4), a component of the cell wall integrity (CWI) pathway (or PKC pathway) [69].

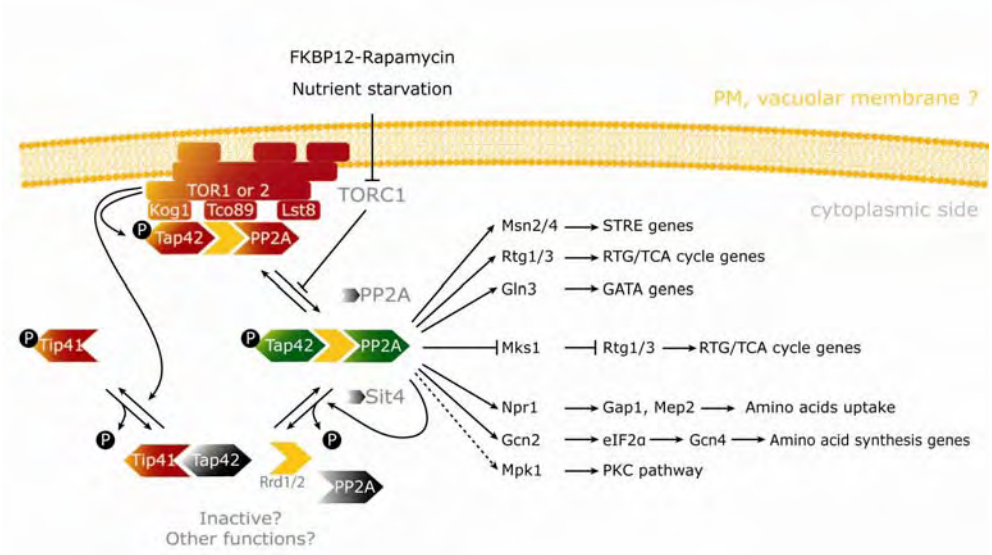

Figure 4

Schematic representation of the Tap42-dependent branch of the TORC1 pathway. During growth, Tap42 associates with both the TORC1 complex and PP2A phosphatases; these TORC1-associated phosphatase complexes may be inactive or direct their activity towards different substrates. Nutrient starvation or rapamycin treatment elicits the release of Tap42 and the associated phosphatases from the TORC1 complex and this correlates with the activation of the complexes. After their release, the Tap42-phosphatase complexes are dismantled following dephosphorylation of Tap42, which then associates with Tip41. It is not known, whether the free phosphatases and the Tap42-Tip41 complexes are inactive or if they rather exhibit an own distinctive activity. Red proteins, negative regulation of quiescence-related processes; green proteins, positive regulation of quiescence-related processes.

After a transient activation, the activity of the cytoplasmic Tap42-Rrd2-PP2Ac and Tap42-Rrd1-Sit4 complexes is thought to decrease due to the dephosphorylation of the Tap42 subunit, possibly by Sit4 or by the cytoplasmic PP2A holoenzyme, and the subsequent disruption of the interaction with the catalytic subunits (Figure 4) [61]. Concomitantly the association of Tap42 with

Tip41, which is also dephosphorylated under conditions of low TORC1 activity, is increased, perhaps preventing the re-association of Tap42 to the phosphatases (Figure 4) [66]. Intriguingly also Tip41 dephosphorylation is dependent on Sit4, suggesting the existence of a possible mechanism of feedback regulation [66].Although Tap42 and the associated phosphatases appear to constitute one of the major routes through which TORC1 exerts its regulatory function on cell growth, some TORC1-dependent processes have been shown to be independent on the presence of Tap42 and/or the PP2Ac and Sit4 phosphatases. In particular, Tap42-independent TORC1-controlled processes may include: autophagy, translation initiation and expression of the translation machinery (transcription of *RP*, *Ribi*, *rRNA* and *tRNA* genes) as well as Ime1-dependent transcription (Table I) [50].

In growing mammalian cells, TORC1-dependent phosphorylation of eIF4E-binding proteins (4E-BPs) favors translation initiation by preventing 4E-BPs from associating with initiator factors which blocks the assembly of the translation initiation machinery. In yeast, eIF4E is encoded by *CDC33,* and *EAP1* encodes a putative ortholog of eIF4E-binding proteins that may be a target of TORC1 (Table I), as suggested by the observation that cells lacking *EAP1* exhibit a rapamycin resistant phenotype [70]. In addition both, rapamycin treatment and nutrient depletion, result in enhanced degradation of another translation initiation factor, eIF4G (Table I). In yeast, TORC1 has also been shown to control translation initiation via eIF2 by negatively regulating the kinase activity of Gcn2 which is believed to be a TORC1 phosphorylation target (Table I) [71]. Conversely Gcn2 is activated during aminoacids starvation or rapamycin treatment through Sit4-dependent dephosphorylation. Phosphorylation of the α subunit of eIF2 (eIF2α) by the hypophosphorylated Gcn2 kinase decreases the rate of general translation initiation, while it specifically promotes the translation of Gcn4 [68].

An additional substrate of TORC1 in mammalian cells is the ribosomal kinase S6K; TORC1-dependent phosphorylation of S6K in the hydrophobic motif triggers its activation. In turn S6K phosphorylates the ribosomal protein (RP) S6, which is thought to positively regulate cell size, as well as several other targets involved in protein synthesis [72]. At present, there is no evidence for the existence of a related ribosome kinase in yeast. Notably, however several transcription factors regulate ribosomal proteins gene (*RPG*) expression in a TORC1-dependent fashion in yeast (Table I). Expression of this suite of genes is coordinately regulated with the *rRNA* gene locus, the *tRNA* genes and a class of accessory genes involved in ribosome biogenesis (*Ribi* genes). The synthesis of ribosomal protein genes is directly controlled by the transcription factor Fhl1, which binds to

ribosomal promoters and associates in a mutually exclusive fashion with either Ifh1, to activate transcription, or with Crf1, to repress transcription. Binding of Fhl1 to promoters is facilitated by the chromatin binding proteins Hmo1 and Rap1. Phosphorylation of both Ifh1 and Crf1 is dictated by the activity of TORC1; Crf1 phosphorylation is regulated by TORC1 indirectly, via the control of Yak1 localization [73], while the Ifh1 kinase has not been identified yet and direct phosphorylation of Ifh1 by TORC1 is not excluded. Surprisingly TORC1-dependent regulation of these genes is still observed in the absence of the whole Fhl1/Ifh1/Crf1 system, suggesting the existence of an additional mechanism by which TORC1 may regulate *RP* expression; this mechanism is likely to involve stimulation of the nuclear accumulation of the transcription factor Sfp1 (Table I) [74]. In addition TORC1 activity promotes the nuclear localization of Rrn3, a transcription factor required for the RNA Polymerase I (PolI)-dependent transcription of *rRNA* genes [75].

By directly or indirectly promoting the hyperphosphorylation of Atg13, and thereby its dissociation from the protein kinase Atg1 (Table I), TORC1 negatively controls the catabolic process of macroautophagy, a membrane trafficking pathway that sequesters bulk cytoplasmic material into nascent autophagosomes for subsequent fusion with and degradation in the vacuole [76]. Nutrient starvation and/or TORC1 inhibition triggers macroautophagy, which serves to recycle surplus cytoplasmic mass and to turn over large structures and organelles such as ribosomes and mitochondria, thereby contributing simultaneously to both reduction of cellular energy consumption and cell-growth arrest.

The AGC-family kinase Sch9 has also been proposed to mediate part of the TORC1 readouts, including the expression of the translation machinery and the inhibition of the Rim15-dependent transcriptional response to nutrient starvation [74,77,78]. In addition Sch9 and the TORC1 pathway have both been proposed to play a role in chronological and replicative life span in yeast, which further reinforces the possibility that Sch9 may act as a component of the TORC1 signaling pathway [79]. Interestingly, during the exponential phase, Sch9 is enriched at the vacuolar membrane and may function downstream of TORC1 to communicate the status of internal nutrient pools to the *RP* and *Ribi* regulons [74]. Moreover, the abundance and electrophoretic mobility of Sch9 depend on TORC1 activity, suggesting that TORC1 is involved directly or indirectly in the phosphorylation of Sch9 [74]. Supporting this hypothesis, recent unpublished data from Dr. Loewith's lab, demonstrate that Sch9 is a direct target of TORC1-dependent phosphorylation. Moreover, the use of a mutated *SCH9* allele that mimics phosphorylation by TORC1, resulted in

loss of rapamycin sensitivity of a subset of the TORC1 readouts, indicating that the function of Sch9 is subject to positive regulation by the rapamycin-sensitive TORC1 (Dr. R.Loewith, personal communication).

In yeast the TORC1 pathway is wired to other nutrient signaling pathways through shared target proteins, resulting in a highly complex signaling network. For instance, TORC1 and PKA independently regulate the transcription factors Msn2/Msn4 and Sfp1 as well as the protein kinase Rim15. The complexity of this network is further highlighted by the observation that the localization of the PKA catalytic subunit Tpk1 is responsive to rapamycin, implying regulation by the TORC1 pathway [21].

The TORC1 pathway shares additional common targets with the AMPK homologue Snf1, namely the transcription factors Gln3 and Msn2. In mammalian and in *Drosophila* cells the AMPK and TORC1 pathways are also interconnected; upon stress or reduction of cellular energy the activity of TORC1 is attenuated by the activated AMP-bound AMPK. The AMPK-dependent phosphorylation activates the tumor suppressor complex TSC1/TSC2 which in turn negatively affects the activity of the small GTPase Rheb (Ras homolog enriched in brain), an activator of TORC1 [72]. In contrast, association of growth factors and hormones with the corresponding receptors ultimately activates mTORC1 by promoting protein kinase B (PKB)-dependent phosphorylation of TSC1/TSC2, resulting in the inactivation of the heterodimeric complex. Thus, in metazoan, Rheb appears to regulate TORC1 by integrating signals from overall organismal growth, nutrient status and stress cues. Budding yeast does not appear to encode the orthologs of the TSC1/TSC2-Rheb system, indicating that the regulation of yeast TORC1 may also involve different mechanisms.

The physiological signal(s) that modulates the activity of TORC1 has not been unequivocally identified. Transcriptional profiling of rapamycin treated yeast cells revealed striking similarities with the transcriptional responses to carbon starvation and to low-quality nitrogen sources, suggesting that the TORC1 pathway responds to the abundance and/or the quality of nutrients [14,65]. Notably, the transcription profile of mammalian cells treated with rapamycin is similar to those elicited by glutamine or leucine starvation [80]. As both, a key intermediate of nitrogen metabolism and an indicator of the cell's general nutrient status, glutamine has been postulated to have a particularly important role in the regulation of TORC1 in both yeast and mammalian cells. In further support of the hypothesis that the physiological signal sensed by the TORC1 pathway may be an indicator of the abundance and quality of nitrogen and carbon sources, mitochondrial and

glycolytic inhibitors were shown to attenuate TORC1 signaling in mammalian cells [72]. As the cell's major nutrient reservoir, the vacuolar compartment is likely to be one origin of the nutrient signals sensed by the TORC1 pathway. Importantly, most amino acids as well as the reserve nutrients allantoin, glycogen and polyphosphate are stored in the vacuole. Moreover, the vacuolar membrane hosts the newly identified EGO complex (EGOC), a GTPase containing complex that is required for the resumption of growth after the rapamycin induced G_0 arrest, and which has been proposed to function upstream of the TORC1 pathway [81].

Target protein	Effect of phosphorylation	Function	Primary Reference
Regulation of translation initiation			
[a] Gcn2	Inhibition of kinase activity	Inihibition of translation initiation	Hinnebusch, 2005
[a] eIF4G	Stabilization, binding to eIF3	Translation initiation	Berset *et al.*, 1998
[c] Eap1 (eIF4E Binding protein)	Inhibition	Inhibitor of eIF4E	Cosentino *et al.*, 2000
Expression of the translation machinery			
[a] Rrn3	Nuclear localization, activation	Transcription of rRNA genes (PolI-dependent)	Claypool *et al.*, 2004
[a] Ifh1	Activation of transcription factor activity	Transcription of ribosome protein (RP) genes	Rudra *et al.*, 2005; Martin *et al.* 2004
[a] Sfp1	Nuclear localization	Transcription of ribosome protein (RP) genes	Jorgensen *et al.*, 2004
[b] Sch9	Activation of kinase activity	Regulation of G1 progression, G0 entry, cell size, ribosome biogenesis and lifespan.	Jorgensen *et al.*, 2004; Urban *et al.*, in press
[a] Tpk1	Cytoplasmic retention	Catalytic subunit of PKA	Schmelzle *et al.*, 2004
[a] Bud27	Positive regulation	Regulation of transcription	Gstaiger *et al.*, 2003
Expression of nutrient- and stress-responsive genes			
[a] Tip41	Dissociation of Tip41-Tip42 complex	Regulator of PP2A phosphatase activity	Jacinto *et al.*, 2001
[b] Tap42	Stabilization of Tap42-PP2A complex	Regulator of PP2A phosphatase activity	Jiang and Broach, 1999
[b] Sch9	Activation of kinase activity	Regulation of G_1 progression, G_0 entry, cell size, ribosome biogenesis and lifespan.	Urban *et al.*, in press
[a] Tpk1	Cytoplasmic retention	Catalytic subunit of PKA	Schmelzle *et al.*, 2004
Autophagy			
[a] Atg13	Inhibition of Atg1 association	Required for the cytoplasm-to-vacuole targeting (Cvt) pathway and autophagy	Kamada *et al.*, 2000
Other functions			
[a] Ime1	Cytoplasmic retention	Master regulator of meiosis	Colomina *et al.*, 2003

[a] A direct phosphorylation by TORC1 has not been demonstrated.
[b] Direct phosphorylation by TORC1 inferred from experimental evidence.
[c] Direct phosphorylation by TORC1 inferred by homology.

Table I

Summary of the known and putative cellular targets of the TORC1 kinase activity in *S. cerevisiae*.

The Pho85 pathway

Although it is best known for its pivotal role in the PHO pathway (described above) the Pho85 cyclin-dependent kinase (CDK), through its association with the different members of the family of Pho85 cyclins (Pcls), is involved in several signaling pathways in *S. cerevisiae*, which generally appear to transduce environmental signals [42]. The multiplicity of the functions associated with Pho85 is mirrored by the pleiotropic phenotype caused by its deletion: cells lacking *PHO85* display a slow growth phenotype with a G_1 delay on rich media, poor growth on non-fermentable carbon sources, hyperaccumulation of glycogen, abnormal morphology, irregular budding, sporulation defects and hypersensitivity to hydroxyurea, hygromycin B and salt.

Importantly, some of the functions of Pho85 are particularly relevant to the establishment of the G_0 program. In complex with Pcl8 and Pcl10, Pho85 counteracts the synthesis of the reserve carbohydrate glycogen by inhibiting the activity of the glycogen synthase; similarly the Pho80-Pho85 cyclin-CDK complex controls the localization of Rim15, a key (positive) regulator of the G_0 program [40,42]. In addition Pho85 has been shown to be involved in the negative regulation of starvation-induced autophagy, although the responsible cyclin remains unknown [82]. In association with Pcl5, Pho85 phosphorylates Gcn4 thereby triggering its degradation; the lower expression of Pcl5 following nutrient starvation results in the stabilization of Gcn4, allowing the transcription of amino acid biosynthesis genes [83].

The PKA pathway

The cyclic AMP (cAMP)-dependent protein kinase A (PKA) pathway is a highly conserved signal transduction pathway operating via the second messenger cAMP (Figure 5). Throughout the eukaryotic kingdom, PKA plays important and diverse roles in signal transduction. In *S. cerevisiae* the PKA pathway responds to the presence of nutrients, in particular of glucose and related fermentable sugars, as well as to various forms of stress and is involved in the control of many processes related to the nutrient status, including cell growth, proliferation and the reprogramming of transcription at the diauxic transition [84]. The activity of this pathway prevents inappropriate initiation of the G_0 differentiation program when the environmental conditions are favorable for growth; axiomatically, inactivating mutations in the PKA pathway result in growth arrest accompanied by the acquisition of most of the hallmarks of quiescence even in the presence of abundant nutrients [30,85]. In its inactive configuration, the PKA kinase is composed of a homodimeric regulatory subunit (Bcy1) that controls three partially redundant catalytic subunits

(Tpk1-3). The regulatory subunits are released from the complex upon binding of cyclic AMP (cAMP) resulting in activation of the enzymatic activity of Tpk1-3 [86]. Importantly, the localization of the PKA holoenzyme is regulated according to the nutritional status of the cells (Figure 5). In rapidly growing cells the catalytically inactive PKA holoenzyme is confined to the nuclear compartment, while the free catalytic subunits are found in the cytoplasm [87]. Inactivation of this cytoplasmic PKA pool following carbon withdrawal, involves partial cytoplasmic relocalization of the regulatory subunit; this requires Yak1-dependent phosphorylation of the N-terminal portion of Bcy1, as well as the presence of the Bcy1-interacting protein Zds1 [88]. Moreover, cAMP withdrawal and treatment with rapamycin both result in the nuclear accumulation of Tpk1, possibly in complex with Bcy1 [21]. As a result, within the nucleus the PKA activity is supposedly kept to minimal levels at all times. In the cytoplasm in contrast, the active holoenzyme is present exclusively during growth. This mode of regulation ensures the precise control of the cytoplasmic targets of PKA, such as glycolytic and gluconeogenetic enzymes, in response to minimal variations in the environmental conditions.

In the presence of glucose and in the absence of stress, PKA is active and promotes growth; the protein substrates of this signaling pathway include enzymes involved in intermediary metabolism and in particular carbon and lipid metabolism. Another function of PKA appears to be coupling nutrient signaling with the cell cycle; in particular, the PKA pathway seems to determine the length of the G_1 phase according to the quality of the carbon source by positively regulating the protein level and the activity of the cyclin Cln3, which in turn regulates the expression of *CLN1* and *CLN2* [89]. The protein products of *CLN1* and *CLN2* are believed to trigger downstream events that ultimately allow passage through START (the yeast equivalent of the restriction point). Control of Cln3 levels by PKA may occur indirectly through transcriptional regulation of genes involved in protein translation, accordingly Cln3 protein levels have been shown to correlate with the protein synthesis rates [89]. As a consequence, after the diauxic shift, yeast cells growing on ethanol divide less frequently and have longer cell cycles than during exponential growth on glucose, due to the reduced kinase activity of the Cln3-Cdc28 cyclin-CDK complex [89]. In addition, PKA activity also causes a strong feedback inhibition on cAMP synthesis, by phosphorylating, and thereby activating, the low-affinity phosphodiesterase Pde1 (Figure 5) [90].

In conjunction to post-translational control, PKA regulates the expression of some of its targets at the transcriptional level by controlling the localization of Msn2/Msn4, two largely albeit not completely functionally redundant transcription factors that translocate into the nucleus in

response to many different stress situations. They regulate the general stress response by promoting the expression of genes whose promoter regions contain stress responsive (STRE) elements (5'-CCCCT-3') [30]. The expression of the *MSN4* gene itself depends on Msn2/Msn4 and is induced by stress, while the expression of *MSN2* expression is constitutive. Adjacent to the zinc-finger domain, Msn2 and Msn4 contain a nuclear localization signal, which is inhibited by PKA-dependent phosphorylation and, which is activated by protein phosphatase 1 (Glc7)-dependent dephosphorylation [91]. Moreover, under non-stress conditions (direct or indirect) phosphorylation within the nuclear export sequences located in the N-terminal halves of Msn2/Msn4 by the TORC1 complex favors their retention in the cytoplasm through the interaction with the 14-3-3 protein Bmh2 [13].

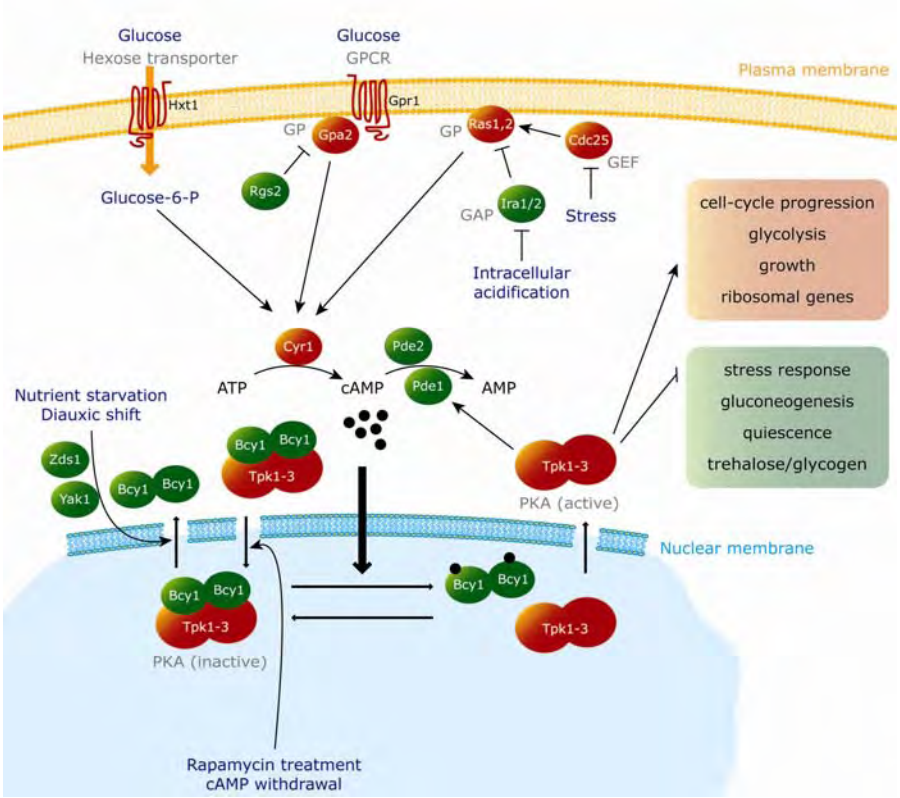

Figure 5

Glucose binds to the G-protein-coupled receptor (GPCR) complex (Gpr1-Gpa2) that, in concert with a glucose phosphorylation dependent mechanism and signaling via the GTP-bound Ras1/2, activates the adenylate cyclase complex Cap2/Cyr1. This leads to the generation of the second messenger cAMP which in turn stimulates the activity of PKA by favoring the dissociation of the cAMP-binding regulatory subunit Bcy1 from the catalytic subunits Tpk1-3. Under nutrient limiting conditions, the GTPase activating proteins (GAP) Ira1 and Ira2 negatively regulate the Ras proteins by converting them from the GTP- to the GDP-bound inactive form; in addition Ira1 mediates the membrane association of adenylate cyclase. The PKA pathway is also known to respond to various stress stimuli, including heat and osmotic shock conditions, which likely destabilize the GDP/GTP exchange factor (GEF) Cdc25. Two cAMP-phosphodiesterases (Pde1, Pde2) catalyze the hydrolysis of cAMP. They downregulate the PKA signaling pathway as part of a regulatory feedback loop [30]. Red proteins, negative regulation of quiescence-related processes; green proteins, positive regulation of quiescence-related processes.

Importantly, PKA stimulates pseudohyphal growth, but prevents the initiation of the G_0 and meiotic programs by inhibiting the nuclear translocation of the transcription factors Msn2/Msn4 as well as the enzymatic activity of the protein kinase Rim15 [92,93]. In addition PKA is thought to control the transcription factor Sok2, which is required for the expression of genes involved in proliferation and metabolism, and for the repression of pseudohyphal growth, glycogen accumulation and STRE-driven transcription [94].

The PKC pathway

Maintenance of viability during G_0 requires the function of another highly-conserved pathway, namely the cell wall integrity (CWI) pathway or protein kinase C (PKC) pathway [95]. Situations such as nitrogen starvation, sporulation, rapamycin treatment and entry into stationary phase, eventually affect remodeling of the cell wall. For instance, cells entering G_0 after rapamycin treatment or during the stationary phase acquire thicker cell walls.

The PKC pathway senses plasma membrane stress through a family of cell surface sensors. The stress signal transmitted through the G-protein Rho1 to the protein kinase Pkc1, ultimately triggers the initiation of a MAP cascade involving the MEK-kinase Bck1, the redundant MEK-kinases Mkk1 and Mkk2, and the MAP kinase Mpk1. The main output of this cascade is the activation of the transcription factors SBF and Rlm1, which control the transcription of genes necessary for the G_1/S transition and for the transcription of cell-wall related genes, respectively. While membrane stress activates the MAP kinase from the top, through surface sensors, other stress signals can initiate the cascade laterally, at different levels by activating one of the kinases [96]. For instance, nutrient limitation or a rapamycin mediated block of TORC1 function leads to the upregulation of Mpk1 via the Tap42-Sit4 complex [69] and activates an upstream element of the PKC pathway distinct from the membrane sensors [95].

Caffeine, which was recently demonstrated to affect the function of the TORC1 complex *in vivo* [57,97], likely activates the PKC pathway through a TORC1-mediated event that depends on the presence of Rom2, the guanine nucleotide exchange factor (GEF) for the GTP-binding protein Rho1 [97]. Although the level of phosphorylation of Mpk1 increases in cells treated with caffeine, the CWI pathway appears to be only partially activated, since only SBF-dependent genes, but not Rlm1-dependent cell-wall remodeling genes, were found to be induced by a caffeine treatment [97].

Importantly, the PKC pathway has also been linked to the TORC2-specific activity and to the PKA pathway. Surprisingly, in contrast to what observed in mammalian cells, the addition of caffeine to yeast cells causes a rapid and transient drop in the levels of cAMP thus inhibiting (rather

than activating) the PKA pathway. Importantly, also this effect of caffeine appears to depend on the GDP/GTP exchange factor Rom2 [97].

Regulation of G_0

Quiescent yeast cells display numerous characteristics that differentiate them from proliferating cells: for one thing, they do not proliferate nor do they accumulate mass or volume, but rather arrest growth and stop dividing. As a consequence they appear as small rounded and unbudded cells, containing unreplicated genomes organized in characteristically condensed chromosomes (termed G_0 chromosomes). The increased rates of autophagy and the decreased rates of transcription and translation are among the principal causes of the reduced size of quiescent cells. The cell wall of these cells is thickened and contributes, together with the accumulation of the storage carbohydrates glycogen and trehalose and the induction of stress-responsive genes, to the increased resistance of these cells to general stress. Importantly, quiescent cells are still metabolically active and maintain the ability to respond to many stress signals like for instance a DNA damage stress signal triggered by MMS [98], or the oxidative stress signal induced by menadione [99], and nutrient signals.

The G_0 state represents a differentiated off-cycle state

Several observations indicate that the G_0 state represents a differentiated state rather than a simple pause of the cell cycle. Cells arrested in G_0 exhibit a distinctive transcription profile and a characteristic morphology. Moreover, entry into this state is reversible and its initiation is regulated by signaling pathways that are distinct from the pathways that are critical for initiation of the cell cycle. In addition, specific mechanisms are required to maintain viability in this state. The existence of a genetic program regulating the entry into G_0 was suggested based on the isolation of mutants that are perfectly viable when supplied with nutrients but are unable to acquire G_0 characteristics when starved for nutrients. But even more importantly, also the exit from the G_0 state appears to be genetically regulated and mutants have been identified that are conditionally defective for exiting G_0; this formally demonstrates that the requirements for resumption of proliferation after G_0 arrest are different from the ones for cell proliferation *per se*.

Regulation of G_0 initiation

Physiologically, yeast cells enter G_0 in response to nutrient starvation; the signaling pathways required for initiation of the G_0 program have been described previously in this introduction. Briefly, G_0 the entry appears to be negatively regulated by the PKA, TORC1 and Pho85 pathways

in response to the presence of essential nutrients. The coordinated downregulation of these pathways may be required to properly induce G_0 differentiation program; this is suggested by the observation that inhibition of TORC1 with rapamycin (in the presence of nutrients) results in a growth arrest that resembles, but not identical to the G_0 program induced by nutrient depletion [100]. Already during the diauxic shift yeast cells sense the vanishing of the carbon source and initiate the expression of a program that continues during post-diauxic growth and ultimately leads the characteristic G_0 state. Numerous changes happen selectively at sequential timepoints, suggesting a stepwise regulation of the G_0 initiation program. Importantly, not all starvation procedures result in G_0 entry: starvation for nitrogen on a poor carbon source for instance results in sporulation in diploids, while starvation for inositols is lethal. There is a close relationship between most described differentiation programs (*i.e.* sporulation, pseudohyphal differentiation, quiescence), which apparently share some signaling components, in particular, but not exclusively, the upstream components required for nutrient sensing.

Maintenance of viability during quiescence and chronological aging

During G_0 the transcription of most genes is repressed, while the expression of a few G_0-specific transcripts is induced and is essential for viability. The changes in transcription result largely from the regulation of transcription factors in response to environmental conditions. In addition, also the activity of the RNA polymerases is altered in post-diauxic and in quiescent cells. For instance, the stoichiometry of the PolII complex is modified during the post-diauxic phase. The Rpb4 subunit, dispensable during normal growth conditions, is preferentially associated with the PolII complex, which requires the PolII complex to be covalently modified. Interestingly, Rpb4 is also required for growth at temperature extremes, suggesting that this particular conformation of the PolII complex may allow transcription under various stressful conditions [101].

The reduced protein synthesis rate in quiescent cells is not simply the result of reduced transcription rates. General translation is also strongly repressed and cap-dependent mRNA recognition (eIF4E-dependent) appears to be dispensable for viability in G_0. Survival during the quiescent phase appears to require an eIF4A-dependent translation mechanism, possibly involving translation from internal ribosomal entry sites (IRES). Importantly IRES-mediated translation has been shown to occur in G_0 yeast cells, but not in exponentially growing cells [102].

When nutrients are depleted from the environment, yeast cells begin to degrade their own cytosolic components and organelles by autophagy; autophagy is a prerequisite for both G_0 and sporulation, as autophagy-deficient yeast mutants die rapidly upon starvation and are not able to

sporulate [103]. Interestingly, all three important TORC1, PKA and Pho85 nutrient signaling pathways are involved in the negative regulation of autophagy [104]. Finally, ubiquitin-dependent protein degradation is also essential for the maintenance of viability in quiescent cells.

The initially abundant levels of storage carbohydrates (*i.e.* glycogen and trehalose) decrease progressively as they are being used to fuel the slow metabolism of quiescent cells. While trehalose may rather fulfill a role as a stress protectant, glycogen mainly serves as a carbon source reserve. Energy may also be derived from mitochondrial respiration and from the slow metabolism of lipids rather than from the utilization of reserve carbohydrates in G_0 cells. Accordingly, peroxisomal and mitochondrial genes are induced during and after the diauxic-shift. Unfortunately, respiration and lipid oxidation produce large amounts of reactive oxygen species, whose toxic effects must be countered if viability is to be maintained. Proper redox homeostasis appears to be of great importance for long term viability of quiescent cells and is an important factor in defining the duration of yeast chronological life span (*i.e.* the length, in time, a stationary phase culture remains viable).

Regulation of G_0 exit

Quiescent cells rapidly respond to the presence of nutrients and the detection of a single key nutrient, such as glucose, is sufficient to trigger the decision to leave the quiescent state. This indicates that the exit mechanism, similarly to the entry mechanism, is responsive to nutrient stimuli. While the induction of the G_0 response by the absence of any of the essential nutrients appears logical, the decision to exit G_0 due to the presence of a single nutrient cue seems counter-intuitive, since it implies the great risk of resuming growth without being able to sustain it. Possibly, this pioneer behavior may provide yeast with an evolutionary advantage.

Besides being required for the process of vesicle formation in the exocytic and endocytic pathways, Gcs1, the GTPase activating protein (GAP) for ADP ribosylation factors (ARFs), is essential for exiting G_0 at low temperatures (15°C) [105]. At the restrictive temperature, G_0 arrested *gcs1Δ* cells are not able to re-enter the mitotic cell cycle and to pass the checkpoint START in response to the re-feeding with nutrients. Nevertheless, they are able to transduce the nutrient cue and to stimulate growth (*i.e.* mass and volume increase), RNA and protein synthesis, degradation of storage carbohydrates, and alter gene expression, all changes which are characteristic of cells exiting G_0. This suggests that remodeling of intracellular vesicular transport may be critical for the transition from the quiescent to the proliferating state. Mutations in the newly identified EGO complex also affect the ability of cells to exit from a rapamycin-induced growth arrest [81]; *ego*

mutants, unlike wild-type cells, were shown to normally acquire G_0 characteristics upon treatment with rapamycin, but they are unable to restart growth, derepress general translation and degrade storage carbohydrates when rapamycin is removed from the medium [81]. Interestingly the EGO complex resides at the vacuolar membrane and was shown to be necessary for the remodeling of the vacuole following a shift from a rapamycin-containing medium to a growth-permissive medium, by stimulating a process of vacuolar membrane recycling known as microautophagy [81]. Moreover, the same complex may be involved in the sorting of low-specificity amino acid permeases to the plasma membrane [106].

The relationship between G_0 exit and vesicular trafficking is currently not understood. In general translation rates need to increase fast to sustain the resumption of cell proliferation and the consequent increase in volume may require an augmented level of membrane recycling. Interestingly a connection between vesicular trafficking and translation initiation was suggested by two recent studies, which point to a role of membrane trafficking in the regulation of translation initiation [107,108]. In this context, it may be important to mention that, in mammalian cells, the phosphatidylinositol 3-kinase hVPS34 is required for both mTORC1 activity [109] and transduction of the insulin-stimulated mitogenic signal [110]. It still remains to be defined whether this is due to the function of hVPS34 in vesicular trafficking, the levels of PIP3, or the hVPS34-dependent regulation of TORC1 [110]. A similar role for the yeast Vps34 protein could not be confirmed so far. Vps34 this protein is involved in vacuolar protein sorting, in vacuole segregation and in endosome-to-Golgi retrograde transport in *S. cerevisiae* [111,112].

Rim15 at the crossroads of important G_0 signaling pathways

Initiation of the G_0 program implies major modifications of the cellular physiology and morphology and this route is only undertaken if the environmental and developmental conditions impose it. The high complexity of the signaling networks involved in the regulation of developmental programs, such as the G_0 differentiation, is probably not fully appreciated. Increasing evidence suggests that the cascades that were previously regarded as distinct pathways are actually highly intertwined thereby enabling the cells to register any minimal change and to respond appropriately by adjusting to any new situation with the minimal energy investment. The protein kinase Rim15 and the transcription factors Msn2/Msn4, which are convergently regulated by several nutrient- and stress-responsive pathways, perfectly illustrate this paradigm.

Rim15 is essential for the correct entry into G_0 it is required for the acquisition of many changes characteristic of G_0 cells. In cells where Rim15 is absent or non-functional the G_0 program is not initiated in response to nutrient depletion during the post-diauxic growth. This results in a rapid loss of viability of stationary phase cells. Conversely, conditions that result in the constitutive localization of an active allele of Rim15 appear to be growth inhibitory, presumably because of the premature induction of G_0 traits, which may counteract cell proliferation (our unpublished observations). Given the pivotal role of Rim15 both, the activity and the subcellular localization of this protein, are exquisitely modulated by at least three nutrient sensing pathways. These include the TORC1 pathway, which is believed to respond to the intracellular levels of glutamine (an indicator of both, the availability of nutrients and the activity of the TCA cycle) the PKA pathway, which responds to the quality of the available carbon source (in particular glucose and comparable fermentable sugars), and Pho85 pathway, which responds to the levels of phosphate. Phosphate, besides being an essential nutrient, is also an indicator of the cellular energy level.

Together, these observations prompted us to undertake detailed studies on the regulation, the molecular structure and the cellular targets of Rim15. The Rim15 protein bears several conserved domains that may be involved in the regulation of Rim15 itself and whose function remains incompletely understood at present. Our work revealed that Rim15 activity, measured by the phosphorylation level of its endogenous substrate (which was identified during this thesis as described in Chapter III) is rapidly regulated by the availability of essential nutrients. It is activated following starvation of carbon, nitrogen and phosphate and is rapidly inactivated when glucose is

added to glucose deprived cells. Active Rim15 induces the expression, during the diauxic shift, of a large set of stress-responsive and metabolic genes that overlaps significantly with the sets of genes controlled by the transcription factors Msn2/Msn4 and Gis1. Despite this observation there is currently no indication that Rim15 directly regulates the activity of these or other transcription factors. Starvation for any of the essential nutrients phosphate, carbon and nitrogen induce similar, but probably not identical, differentiation programs. Moreover all of these signals regulate Rim15 activity or localization indicating that Rim15 may be involved in mediating specific responses to precise nutritional signals.

Chapter I

Analysis of the molecular architecture of Rim15

Analysis of the molecular architecture of Rim15

The Rim15 protein kinase

During proliferation, signals from the essential nutrients phosphate, nitrogen and carbon, transduced by the Pho80-Pho85 cyclin-CDK complex, the TORC1 pathway and the PKA pathway, are integrated at the level of the Rim15 protein kinase [40,78]. In the presence of these essential nutrients, activation of the corresponding pathways results in downregulation of Rim15-dependent signaling by both the retention of Rim15 in the cytoplasmic compartment and the direct inhibition its enzymatic activity (Figure 6). During the adaptation to nutrient deprivation, Rim15 function is necessary for the induction of several G_0-characteristic traits, including the transcription of Msn2/Msn4- and Gis1-dependent genes [93,113]. Notably, cells devoid of Rim15 fail to arrest growth and to acquire G_0 characteristics following nutrient limitation [93]. In addition, in diploid yeast cells, Rim15-dependent phosphorylation of the transcriptional regulator Ume6 is required for the derepression of early meiotic genes in response to sporulation conditions [114]. Accordingly, nitrogen withdrawal in the presence of a non-fermentable carbon source such as acetate, results in Rim15-dependent phosphorylation of the N-terminal region of Ume6 [115]. Concomitantly, the activity of Rim15 stimulates the removal of the silencing complex Sin3-Rpd3 from the promoter region of early meiotic genes [114]. Diploid cells deleted for *RIM15,* or expressing a kinase inactive version of Rim15 (either $Rim15^{K823Y}$ or $Rim15^{D936A}$) show a delayed initiation of meiosis and lower sporulation efficiency compared to wild-type diploid cells [116]. Thus, Rim15 receives several inputs that reflect the nutrient/energy status of the cell and transduce the corresponding signal to specific downstream targets in order to ensure the induction of the appropriate responses.

It is not uncommon to find a protein kinase at the core of a highly complex signal transduction network. Such kinases are usually tightly regulated by various control mechanisms, ranging form the modulation of enzymatic activity to the alteration of intracellular distribution [117,118]. The activity of most protein kinases can be regulated by phosphorylation of a number of specific threonine, serine, or tyrosine residues. For instance many protein kinases, including most members of the AGC group of protein kinases, are stabilized into the active conformation by phosphorylation of one or several residues that are part of a particular segment located in the center of the kinase domain called activation loop. The activation loop can either be involved in recognition of regulatory subunits, in autoinhibition of substrate binding, or in promotion of the correct orientation of the kinase subdomains and of the catalytic-site residues [117,118]. Several other conserved regulatory motifs have been recognized, whose reversible phosphorylation participates in the

modulation of protein kinase activity; for instance, the C-terminal region of most members of the NDR family of protein kinases (a conserved subclass of the AGC group of kinases) encompasses a hydrophobic motif which is targeted by an upstream regulatory kinase and whose phosphorylation triggers structural rearrangements of the molecule ultimately result in the acquisition of the active conformation [119]. The regulated phosphorylation of particular residues of a protein kinase can depend on upstream kinases or, alternatively, on the intrinsic enzymatic activity of the kinase itself (autophosphorylation); whether autophosphorylation may be possible or not is governed by the sequence specificity of the kinase and the sequence in the activation segment that surrounds the phosphorylated residue. Phosphorylation or dephosphorylation of single residues in particular motifs can also alter the localization of the kinase, for instance by modifying its ability to interact with other molecules. A classic and important example is represented by the 14-3-3 proteins; these proteins function as molecular scaffolds that recognize phosphorylated residues in the context of a 14-3-3-specific recognition motif. Through their binding, 14-3-3 proteins may anchor the phosphorylated kinases in a specific subcellular compartment or, alternatively, provide a surface for the association with additional regulatory or effector proteins [120,121]. Many kinases are regulated by additional subunits whose activity depends on the presence/absence of a second messenger (*e.g.* activation of PKA by binding of cyclic AMP to the regulatory subunit [122], activation of CaM kinase I by binding of Ca^{2+}/calmodulin [123]) or whose expression level varies in response to a particular signal (*e.g.* determination of the substrate specificity of cyclin dependent kinases by binding of different cyclin subunits [124]). Finally, another common control mechanism involves the use of additional domains located on the same polypeptide that can interfere with the activity of the kinase, its interactions or its localization [117].

To ensure the integration of several nutrient signals, both enzymatic activity and localization of the protein kinase Rim15 are regulated by at least three nutrient sensory kinases (Figure 6) [40,78]. Furthermore, transcription of *RIM15* is also regulated, which ensures that full expression of Rim15 only occurs under conditions of nutrient deprivation such as those encountered by the cell during the diauxic shift or following the transfer to a sporulation-inducing environment [93,116].

Regulation of Rim15 by nutrient-sensory kinases

During exponential growth and during the adaptation to nutrient starvation, tight regulation of the Rim15 protein kinase is achieved by a complex network of nutrient-sensory kinases that modulate both, the enzymatic activity and the subcellular distribution of Rim15, in response to the nutrient status (Figure 6).

In the presence of the essential nutrients phosphate and nitrogen, nuclear accumulation of Rim15 is antagonized by the TORC1 and the Pho80-Pho85 pathways [40,78], both of which impinge on a common threonine residue (T1075) located in an unusual amino-acid insert between subdomains VII and VIII of the kinase domain of Rim15 (Figure 8). Phosphorylation of Rim15 on T1075 results in its cytoplasmic retention via the association of the domain surrounding the phosphorylated threonine residue with the 14-3-3 protein Bmh2 [40]. In the presence of glucose the cytoplasmic, 14-3-3-bound, Rim15 is kept inactive through PKA-mediated phosphorylation [93]. During the diauxic shift, or when cells are treated with the TORC1 inhibitor rapamycin, as well as upon phosphate withdrawal, the Rim15 protein is transiently relocated into the nucleus [40,78]. Interestingly, concomitantly with its nuclear translocation the Rim15 protein is found to be hyperphosphorylated [12]; this translocation-induced hyperphosphorylation depends on Rim15 kinase activity and therefore likely represents an autoregulatory mechanism (Valeria Wanke, unpublished results). Importantly, autophosphorylation does not appear to be necessary for Rim15 nuclear translocation, as we observed nuclear accumulation of various kinase inactive mutants of Rim15 (*e.g.* $Rim15^{K823Y}$ and $Rim15^{C1176Y}$) [40]. One possibility may be that hyperphosphorylation occurs subsequently to Rim15 nuclear import; notably, the activity of Rim15 is predicted to increase in the nucleus, due to the low activity of the nuclear pool of PKA [125]. Phosphorylation of Rim15 on multiple sites by its own enzymatic activity may be necessary for full activation of the enzyme and/or for its efficient nuclear export [40]. In line with this hypothesis, the wild type Rim15 protein appears to be more efficiently exported from the nucleus following activation; indeed, unlike its kinase inactive counterparts, the wild type Rim15 protein does not accumulate in the nucleus of nutrient-deprived or rapamycin-treated cells and is believed to rapidly shuttle between the cytoplasmic and the nuclear compartments [40]. The nutrient-regulated serine/threonine kinase Sch9 also phosphorylates Rim15 on a serine residue (S1061) located within the kinase insert; our lab is currently studying the significance of this phosphorylation, which is likely to involve the regulation of Rim15 subcellular distribution, since Rim15 was observed to adopt a constitutive nuclear localization in *sch9Δ* mutants [78]. Importantly, Sch9 was recently found to be a direct target of phosphorylation by TORC1 (Robbie Loewith, personal communication). Thus the TORC1 pathway may control the subcellular localization of Rim15 indirectly via the regulation of the activity of the Sch9 kinase. The transiently active, nuclear pool of Rim15 may activate the G_0 response by phosphorylation of one or several nuclear targets before being rapidly transported out of the nucleus by a mechanism involving the exportin Msn5 [78]. The Pho85-dependent phosphorylation on T1075, necessary for the cytoplasmic retention of Rim15 following nuclear export, is likely to occur in the nucleus prior to the export of Rim15, as Pho85 was shown to be a

predominantly nuclear protein [126]. The currently available data on the regulation of the Rim15 protein kinase activity and localization resulted from studies addressing the activation of Rim15-dependent responses during the adaptation to nutrient limitation. No currently published work specifically addresses the regulation of the Rim15 protein kinase under sporulation-inducing conditions. However, it is conceivable that the nutrient signals are impinging on Rim15 may implicate the same signal transduction pathways during both, initiation of meiosis and of quiescence. Additional response-specific signals are likely required to direct the Rim15 kinase function towards appropriate substrates in either case.

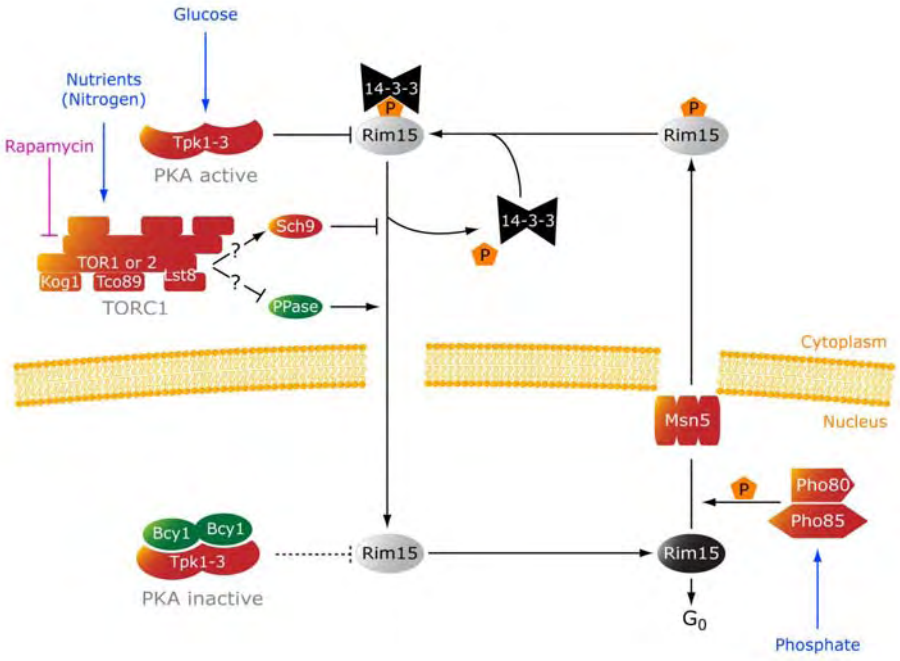

Figure 6

Model for Rim15 regulation during adaptation to nutrient starvation. Cytoplasmic Rim15, anchored through its binding to 14-3-3 proteins, is kept inactive by PKA-mediated phosphorylation on five serine residues. Following the depletion of important growth nutrients (*e.g.* during the diauxic transition) or a treatment with rapamycin, TORC1 inhibition results in the reduced phosphorylation of the threonine residue in a domain recognized by the 14-3-3 proteins (T1075) and, as a consequence, in the nuclear translocation of Rim15. Due to the low activity of PKA in the nuclear environment, the nuclear pool of Rim15 is active and promotes the acquisition of many G_0-characteristic traits, probably by phosphorylation of a nuclear target. The export of Rim15 is mediated by the β-type exportin Msn5 and is believed to require autophosphorylation of the Rim15 kinase on several residues. In addition, nuclear Rim15 is phosphorylated by the Pho80-Pho85 cyclin-CDK complex and this phosphorylation is required for the cytoplasmic retention of Rim15 by 14-3-3 proteins. Red proteins, negative regulation of Rim15; green proteins, positive regulation of Rim15.

Analysis of the amino acid sequence of the Rim15 protein kinase

The serine/threonine kinase Rim15 is a distinct member of the AGC group of kinases, which is distantly related to kinases of the NDR family and to the PAS domain-containing serine/threonine protein kinases Psk1 and Psk2, which belong to the PIM-like family of serine/threonine kinases (Figure 7) [127].

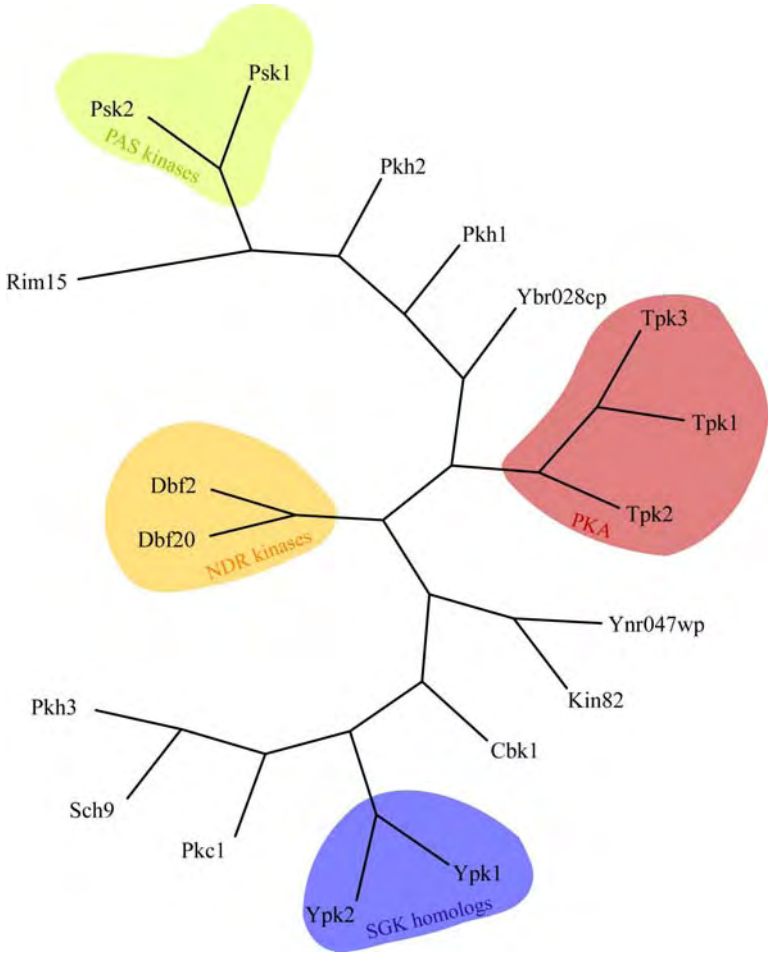

Figure 7

Dendrogramm of the Rim15-related, yeast kinases. The complete amino acid sequence of Rim15 was aligned with the sequences of the two yeast PAS-kinases (Psk1 and Psk2) and with those of the members of the yeast AGC group (*i.e.* Pkh1, Pkh2, Ybr028cp, Tpk1, Tpk2, Tpk3, Ynr047wp, Kin82, Cbk1, Ypk1, Ypk2, Pkc1, Sch9 and Pkh3, as described in Hunter *et al.* [127]) using the clustalW alignment method [128]. The estimation of the phylogeny and the graphical representation of the dendrogramm were obtained using the PHYLIP package [129].

Similarly to the members of the NDR family, Rim15 contains a characteristic, large insert within the kinase domain, between motifs VII and VIII (Figure 8). In addition, kinases of the NDR family harbor a conserved, but poorly characterized, N-terminal regulatory domain and a C-terminal, hydrophobic phosphorylation motif, both of which are missing in the Rim15 sequence [119,130]. The kinase insert of Rim15 contains several potential regulatory sites, these include: a Pho85-consensus phosphorylation site (pTPXL) [131], flanking the residue T1075, and one of the

five consensus sites for PKA-dependent phosphorylation present in the Rim15 polypeptide (RRXpS) [132], encompassing the residue S1094. In addition, our current unpublished studies suggest that Rim15 may be phosphorylated by Sch9 on a serine residue (S1061) that is also located within the kinase insert. Interestingly, in addition of being a consensus site for Pho85 phosphorylation, the motif including T1075 overlaps with a 14-3-3 protein mode I binding motif (RSXpS/pTXP) [120]. Unlike other NDR kinases, the kinase insert of Rim15 does not contain a consensus nuclear localization signal. Nevertheless, phosphorylation of Rim15 on different residues in the kinase insert appears to represent a key mode for the regulation of the intracellular distribution of Rim15 [40,78]. We have shown that the kinase insert is crucial to prevent unscheduled nuclear translocation of Rim15 when nutrients are abundant [40], in contrast the kinase insert is dispensable for Rim15 enzymatic function both during initiation of meiosis and during the diauxic transition [116].

Four additional consensus sites for PKA-dependent phosphorylation (*i.e.* S709, S1416, S1464 and S1621) are located outside of the kinase domain (Figure 8). Rim15 phosphorylation by PKA strongly inhibits Rim15 kinase activity *in vitro* [93]. Moreover *in vivo* studies using a quintuple Rim15 mutant, where the five PKA target serine residues were replaced with alanine residues, indicated that Rim15 is targeted *in vivo* by PKA and that this regulation reduces Rim15 activity [93].

Full activation of most serine/threonine kinases requires prior phosphorylation in the activation loop, the major site implicated in substrate recognition; this phosphorylation promotes the active configuration of the kinase by charge neutralization of a cluster of basic residues, which include the RD sequence at the catalytic aspartate [117]. Kinases that contain a strictly conserved arginine preceding the catalytic aspartate (RD kinases) are usually activated by phosphorylation in the activation loop. Some RD kinases, however are not regulated by phosphorylation; in these kinases, charge neutralization may be achieved by a glutamate residue in the activation loop [117]. Similar regulatory mechanisms may be required to fully activate Rim15 protein kinase activity; however the prediction of such mechanisms is complicated by the absence of a crystal structure for this protein. Analysis of the Rim15 amino acid sequence suggests that Rim15 may require phosphorylation in the activation loop for activation; indeed, the catalytic aspartate (D918) in Rim15 is preceded by two basic histidine residues that, similarly to the conventional aspartate of RD kinases, may require charge neutralization. Surprisingly however, in the Rim15 sequence, the phosphorylated residue within the activation segment residue (a threonine in most AGC kinases and a serine in NDR-family kinases) is not conserved, nor is it replaced by an acidic residue, suggesting that Rim15 may be phosphorylated on a different site, involving a previously uncharacterized

mechanism. Alternatively Rim15 activation may not require phosphorylation on the activation loop, since histidine is only weakly basic when compared to arginine.

Our data indicate that Rim15 is able to phosphorylate itself on multiple sites, both *in vitro* and *in vivo* [40,78,93]. Although the significance of this autophosphorylation for Rim15 enzymatic activity is currently not known, our recent studies suggest that it might promote Rim15 nuclear export [13]. Since a consensus sequence for Rim15-dependent phosphorylation was not known, until recently we have not been able to identify these autophosphorylation sites; the recent identification of a *bona fide* Rim15 phosphorylation target (Chapter III in this work) may allow the elucidation of this possible autoregulatory mechanism. Notably, we should be able do define the consensus sequence for Rim15 and to determine whether the effect of autophosphorylation of Rim15 specifically affects its activity towards the endogenous substrate. Alternatively we may map the differential phosphorylation pattern of the wild-type Rim15 molecule and a kinase inactive version by mass spectrometry (MS).

An additional level of regulation is suggested by the presence, in the large N- and C-terminal extensions of the Rim15 polypeptide, of three conserved motifs which include a receiver domain (or response regulator, REC, Pfam identifier: PF00072), a PAS domain (Pfam identifier: PF00989) and a conserved motif that is predicted to form a zinc-finger like fold (Figure 8). Interestingly the PAS domain and the receiver domain are commonly found associated in bacterial two-component and phosphorelay signal transduction systems [133,134].

The characterization of these domains has been the object of the investigations presented later in this chapter.

Figure 8

Molecular architecture of Rim15. The serine/threonine kinase Rim15 is distantly related to the NDR family of AGC kinases and is sometimes considered a NDR family member [119,127]. Like the other members of this group Rim15 possesses all twelve canonical motifs of the serine/threonine kinase domain [135]; notably, as for the NDR family members, the subdomains VII and VIII are separated by a large insert. A PAS domain and a receiver domain (REC), two domains commonly found in two-component systems of signal transduction, are located near the NH_2- and the COOH-end of the protein, respectively. Finally we identified a highly conserved region, which we propose to be a C_2HC zinc finger, located next to the PAS domain in the N-terminal part of the Rim15 polypeptide.

PAS domain

PAS domains (sometimes referred to as LOV domains; light, oxygen or voltage domains) are important signaling modules of approximately 100 to 120 amino acids that are most commonly found in association with histidine kinase domains in prokaryotic two-component systems. They were recently described in association with various regulatory modules in multidomain proteins from all three kingdoms of life [136]. PAS (PER-ARNT-SIM) is an acronym formed from the names of the proteins in which this domain was first recognized, namely the *Drosophila* period clock protein (PER), the vertebrate aryl hydrocarbon receptor nuclear translocator protein (ARNT) and the *Drosophila* single-minded protein (SIM) [137]. Most known PAS domains are located in the cytosol where they monitor the overall energy level of cells by sensing different parameters, including changes in light, redox potential, oxygen and small ligands [136,138]. Although a few PAS-domain proteins are not thought to require cofactors for sensing, most described PAS domains associate with a cofactor in order to detect particular stimuli that could not be adequately sensed by the protein itself. A considerably dynamic structure allows PAS domains to undergo conformational changes in response to environmental cues or to alterations on the associated cofactor. Through these conformational changes PAS domain modulate the activity of associated signaling modules, usually located within the same molecule.

Definition and structure of PAS domains

Despite the absence of a high level of sequence identity (in the generic PAS sequence there are only nine highly conserved residues), different PAS domains fold into similar three-dimensional structures and are therefore defined by their structural similarity with three prototype PAS domain folds: the PAS domains of the photoactive yellow protein (PYP), the FixL protein and the eukaryotic potassium channel HERG [136,139]. The typical PAS domain fold consists of a five-stranded antiparallel β-sheet, flanked by several α-helices (Figure 9) [136,138]. The PAS core, which includes the first two β strands of the central β-sheet and three α-helices, contains the highest density of residue conservation (principally small residues such as glycines, aspartates, and aspargines) and corresponds approximately to the first reported PAS sequence motif, also termed S1 box [136]. A helical connector diagonally crosses the β-sheet and separates the PAS core from a second conserved motif, sometimes referred to as the PAC motif or S2 box, which folds into a β-scaffold (Figure 9). Notably, although the PAC motif is proposed to contribute to the PAS domain structure, the PAS motif can also occur individually on some proteins [140]. In the literature, the PAS domain may designate both, the conserved PAS motif or the larger domain comprising the PAS and the PAC motifs.

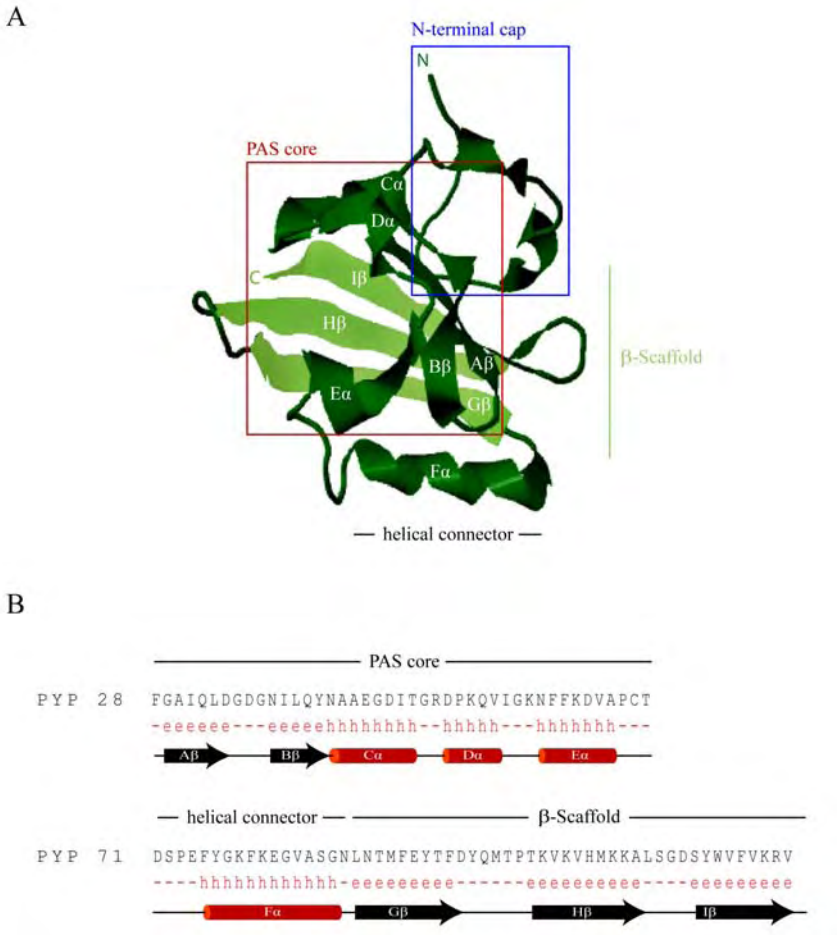

Figure 9.

[A.] Proposed three-dimensional structure of the prototype PAS domain of the 125-residue *Ectothiorhodospira halophila* photoactive yellow protein (PYP) [141]. Structural data were retrieved from the Molecular Structure Database (EMBL) and rendered using the open-source software Jmol (http://www.jmol.org) [142]. [B.] Secondary structure prediction for the PAS domain of PYP adapted from Amezcua CA, *et al.* (2002) [138]. PYP undergoes a self-contained light cycle where the light-induced *trans*-to-*cis* isomerization of the 4-hydroxycinnamic acid chromophore is coupled with structural rearrangements that result in changes in shape, hydrogen bonding and electrostatic potential at the protein surface, allowing transduction of the light signal.

The individual elements of the secondary structure of PYP are conserved throughout the PAS domain superfamily; amazingly, different small molecules are tolerated within similarly folded cores in the various PAS domains, which differ in the residues that surround and interact with the ligand. PAS domains that have no associated cofactor have also retained similar structures [136,143]. In the prototype PAS domain of the *E. halophila* protein PYP, the β-scaffold provides a structure that supports the PAS core, which, in addition to contributing residues to a PAS protein-protein interaction site, forms a hydrophobic pocket that mediates the cofactor attachment (Figure 9.). The central helical connector (Fα) participates in the interaction with the ligand and appears to be the critical regulatory region of the PAS domain family [144]. The ω-loop between segments Gβ and Hβ closes a gap between the PAS core and the β-scaffold and, at least in PYP, participates in

the interaction with the ligand. A poorly conserved N-terminal cap encloses one side of the central β-sheet forming a smaller hydrophobic pocket (Figure 9.). In addition, some PAS domains contain an unusually flexible loop between segment Fα and Gβ in the region that separates the PAS core from the β-scaffold, termed the FG loop, which may serve as functionally relevant binding interface; importantly, the length of this region is largely variable among PAS domains. Finally, in some cases, a C-terminal α helix links the PAS domain with the next protein module.

It is typical to find PAS domains in pairs in eukaryotic transcriptional activators such as SIM. Microbial proteins can contain single, dual or multiple (up to six) PAS domains. While multiple copies of similar PAS domains may be required to amplify sensory signals, evidence is emerging that in some cases divergent PAS domains within a single protein may be functionally divergent and sense distinct stimuli [136].

Signal transduction via **the PAS domain**

Conformational changes within the PAS domain, triggered either by alterations of a bound cofactor (*e.g.* flattening of the heme porphyrin ring associated with the PAS domain of FixL), by the binding state of the PAS core (*e.g.* binding of a small organic molecule within the PAS core of the hPASK PAS domain), or by direct sensing of an intracellular signal by the PAS domain (*e.g.* the human ether-a-go-go potassium channel HERG, which may sense directly changes in the redox state), result in transduction of the signal by modification of intra- or intermolecular protein-protein interactions. A "helix-swap mechanism" (Figure 10) was proposed as a general molecular mechanism for PAS domains; accordingly, in its open, active conformation, the PAS domain interacts with a *Region I* on the same molecule or a second identical molecule (resulting in a PAS-PAS dimerization), whereas in the closed, inactive conformation, it interacts with and inactivates the transmitter module [145].

Interestingly, a similar mechanism was demonstrated for the PAS-dependent regulation of the human PAS kinase (hPASK) and the prokaryotic PAS-containing histidine kinase FixL [138,144]. In the PAS-domain of the human PAS-kinase (hPASK) the FG loop was shown to interact directly with, and thereby inhibit, the serine/threonine-kinase domain within the same molecule, provided that the hydrophobic core of the PAS domain is not occupied by a ligand [138]. Similarly, in *Bradyrhizobium japonicum* and *Rhizobium melioti*, the FixL PAS domain contains a dynamic FG loop region, called the regulatory loop that is thought to be critical for the PAS-mediated O_2 signaling by this protein. The PAS domain of FixL binds heme as a cofactor within the hydrophobic core; upon binding of oxygen or other strong field ligands such as cyanide, the heme molecules

becomes more planar thereby inducing a conformational change in the FG loop and releasing the histidine kinase domain from the inhibitory interaction with the PAS domain [144,146].

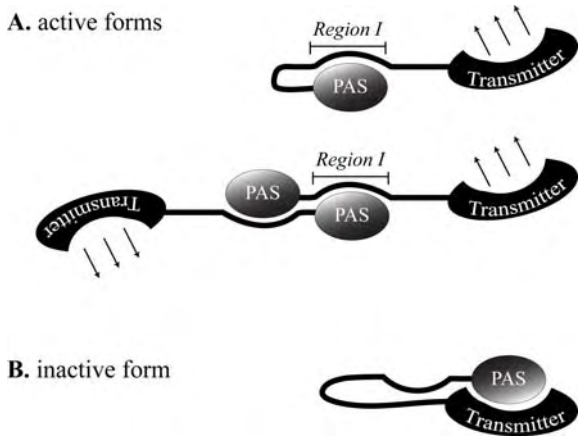

Figure 10

The helix-swap model, according to Gilles-Gonzalez et al., proposes that the external surface of the β-sheet in each PAS domain can engage two mutually exclusive interactions with either a helical region within the transmitter domain or a second helical region termed the *Region I* [145]. These alternative conformations are stabilized by conformational rearrangements within the PAS domain, which are triggered by the absence or presence of a signal. [A.] The association of the PAS domain with *Region I*, within the same or a second molecule, displaces the transmitter which adopts the active conformation. [B.] The association with the PAS domain confines the transmitter to the inactive state.

Different transmitter modules have been found in association with PAS domains, including histidine-kinase domains (*e.g.* sensor kinases of bacterial two-component regulatory systems [144]), serine/threonine-kinase domains (*e.g.* cyanobacterial and plant phytochromes [147]), transcriptional regulators (*e.g.* clock proteins and transcription factors involved in xenobiotic responses [148,149]), and ion channels (*e.g.* the HERG potassium channel [150]). The recently described PAS kinases (PASK or PASKIN) contain both a serine/threonine kinase domain and a PAS domain which exerts allosteric regulation in *cis* on the kinase domain [151,152]. The yeast PAS kinase orthologs, Psk1 and Psk2, are likely implicated in the coordination of metabolism and protein synthesis [153].

The zinc finger fold

The zinc finger protein motif, first discovered in transcriptional regulators, is now known to be extraordinarily widespread in eukaryotic proteins [154]. The typical zinc finger fold is particularly suited to serve as a DNA-binding domain; sequence specific DNA recognition appears to be the most common role of this domain. However, zinc fingers and related zinc-binding modules are used for a variety of other functions ranging from RNA binding (*e.g.* RNA binding of the *Xenopus laevis* zinc finger protein dsRBP-ZFa via a cluster of zinc finger motifs [155]) to protein-protein interaction (*e.g.* the ubiquitin-binding RING domain [156] and probably most C_2HC type domains

[157]), and protein-lipid interaction (*e.g.* the PHD motif found in many chromatin-regulatory proteins [158] and the phosphatidylinositol 3-phosphate binding FYVE domain [159,160]). In higher eukaryotes, zinc fingers mostly occur in clusters of at least two repeats within the same polypeptide and very often different kinds of zinc fingers are found together on the same molecule. Such independent modules can have different functions and show little or no interaction with each other [154]. For example the transcription factor TFIIIA contains a 9-fold repeated zinc finger pattern. In contrast, most zinc finger containing proteins in *S. cerevisiae* contain not more than four zinc-finger like repeats [161].

The usually extremely thermostable zinc finger domains fold autonomously in a zinc-dependent fashion; in each repeat of this motif single divalent zinc ions are tetrahedrally coordinated through the side-chains of cysteine and/or histidine residues thereby stabilizing the entire structure (Figure 11). In the absence of zinc, these domains are highly unstable in the reducing environment within the cell and especially within the nucleus [154]. Interestingly, some zinc fingers have been shown to function as zinc sensors which exploit the altered structural stability in the presence/absence a coordinated zinc ion, to control the expression of zinc-controlled genes [162].

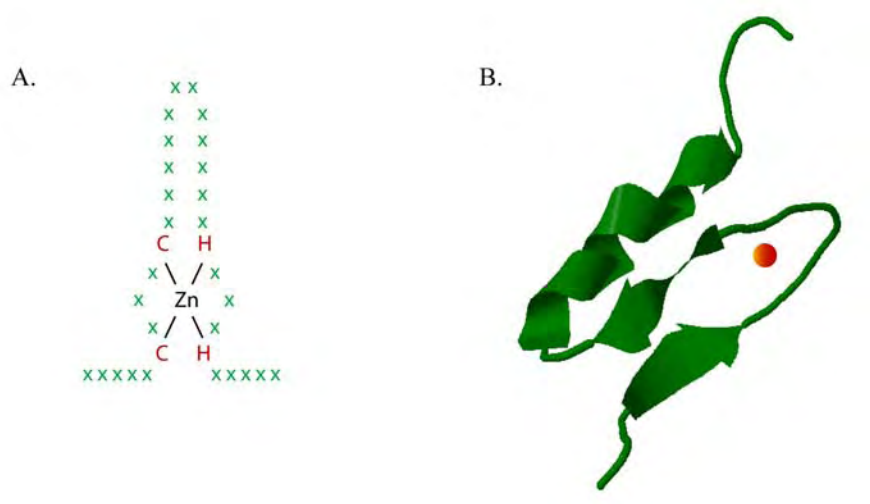

Figure 11

The typical zinc finger fold. [A.] Topology of a typical C_2H_2 type zinc finger. A zinc ion is tetrahedrally coordinated through the sidechains of the cysteine and histidine residues. The cysteine and histidine pairs are separated by 12 amino acids. [B.] Secondary structure of a prototypical DNA binding zinc finger of the C_2H_2 type; structural data for the zinc finger of the yeast Swi5 (Entry name, 1ZFD) protein were retrieved from the Molecular Structure Database (EMBL) and rendered using the open-source software Jmol [142].

Definition and structure of the zinc finger fold

The term "zinc finger" applies to a rather diverse set of protein motifs; at least 70 different zinc finger motif profiles are described in the Prosite database, which share the property of binding zinc ions as a means to stabilize the structure of a small, autonomously folded protein domain [154]. The different zinc finger motifs can be classified according to the type and spacing of the zinc chelating residues [163]. Most, but not all, zinc fingers contain the minimal core structure composed of an irregular, antiparallel, two-stranded β-sheet and a short α-helix, which surrounds a single zinc ion [154]. In certain zinc fingers, this structure may require additional structural elements for stability. Typically, in a zinc finger motif, two pairs of zinc chelating residues, located at each extremity of the motif, are separated by a sequence of variable length and composition that often defines the binding specificity of the zinc finger domain (Figure 11). For instance, in the C_2H_2 zinc fingers, the first characterized zinc fingers; the first pair of zinc coordinating cysteines is separated from a pair of histidines by a stretch of 12 amino acids that are mainly polar and basic. This is a characteristic feature of DNA binding domains (Figure 11). Zinc fingers that bind phosphoinositides usually also contain basic residues that interact with the acidic head group of phosphoinositides.

Two-component signaling systems

The domain composition of Rim15, with both a PAS domain and a receiver domain (REC) on the same polypeptide, is reminiscent of the histidine kinases found in phosphorelay signaling systems. Phosphorelay systems represent a complex variant of the two-component signaling system (Figure 12). A basic stimulus-response mechanism, which relies upon the relatively rapid transfer of a phosphate group between alternating conserved histidine and an aspartate amino-acid residue, to couple signals from a changing environment with the appropriate cellular responses [164]. Two-component systems are found essentially in all kingdoms of life and account for the majority of the signaling pathways in prokaryotes. In contrast, signaling cascades implicating serine, threonine or tyrosine phosphorylation predominate in eukaryotes [165]. Most bacterial two-component systems have a classical domain composition with a sensor kinase upstream of one or more effector proteins, characterized by the presence of a receiver domain (REC). Signal-dependent activation of a dimeric histidine kinase initiates the signaling cascade by ATP-dependent autophosphorylation on a specific histidine residue within the short histidine-containing H-motif (Figure 12). The subsequent phosphate-transfer reaction does not involve a kinase activity, but rather the transfer of a phosphate moiety from the transiently phosphorylated histidine residue to the acceptor, an aspartate residue located within the receiver domain of the effector protein. In this case, a one-step phosphotransfer

occurs between the sensor and the effector protein(s). The more complex phosphorelay systems, which include most of the histidine kinase signaling systems found in eukaryotes, involve additional phosphotransfer steps executed by additional receiver domains and histidine-containing phosphotransfer (HPt) domains (Figure 12). Optional phosphorelay systems are elaborated variations of the phosphorelay signaling mode, where either one of two routes is activated depending on the initiating stimulus: the transmitter module can either transfer the phosphate directly to the receiver domain of the output regulator, or employ intermediate phosphotransfer reactions through additional REC and HPt intermediate domains (*e.g.* the *E. coli* multidomain redox sensor system ArcAB). The additional steps in phosphorelay systems add versatility with respect to signal integration and transmission.

The basic modules of two-component signaling systems

Most sensor histidine kinases include a sensor module, consisting of an extracytoplasmic, periplasmic or, less frequently, membrane-associated domain that is required for ligand binding. Cytosolic sensing modules have also been integrated into histidine kinases; examples include, notably, the versatile PAS domain. These ligand-binding domains are almost as diverse as the signals that can be sensed by the two-component signaling systems. Binding of a ligand to the input module of the sensor histidine kinase causes a conformational change that is propagated along the protein through additional specific modules, namely two transmembrane helices and a cytoplasmic linker domain (termed HAMP, as derived from the names of the protein functions it is found to be associated with; histidine kinases, adenylyl cyclases, methyl-accepting proteins and phosphatases) [166]. This mechanism allows virtually any ligand-binding domain to function as an input module in sensor histidine kinases and accounts for the wide range of environmental stimuli sensed by histidine kinases. Among the most common sensor domains in sensor histidine kinases are: the amino-acid binding FliY-type domains, the small-ligand binding Cache and PAS domains, the metal-binding MHYT domains and the cGMP- and photopigment-binding GAF domains [133]. A few soluble histidine kinases, such as the chemotaxis kinase CheA and the nitrogen regulatory kinase NtrB are regulated by intracellular stimuli [164].

In most transmembrane histidine kinases, a large N-terminal extracytoplasmic domain (100-300 amino acids), which contains the input module, is enclosed between two transmembrane segments and followed by a linker HAMP domain and the cytoplasmic signal-transducing histidine kinase domain (Figure 12). The HAMP domain is a short (50 residues) α-helical, coiled coil-like (CC) motif that is critical for signal transduction. The conformational changes elicited by ligand-binding, propagated through the transmembrane helices and the linker domain, ultimately result in

the alignment of a conserved histidine residue with the ATP-binding pocket, shaping the kinase active site [166]. The subsequent autophosphorylation is a bimolecular reaction, in which one histidine kinase monomer catalyzes the phosphorylation of the conserved histidine residue within the H-motif of the second monomer. Besides directing the forward phosphorylation reaction, many histidine kinases possess a phosphatase activity, enabling them to dephosphorylate their cognate response regulator.

The receiver domain (REC) catalyzes the subsequent step, which consists in the rapid transfer of the high-energy phosphoryl group from the histidine residue to an aspartate group within its own sequence (Figure 12). The lifetime of the resulting phospho-aspartate varies significantly between different response regulators, ranging from seconds to hours. Many response regulators have autoregulatory activities that either stabilize (*e.g.* the yeast Ssk1 response regulator has the longest known phosphorylated lifetime [167]) or decrease (*e.g.* autophosphatase activity [168]) the lifetime of the phospho-aspartate. Phosphorylation of aspartate produces a high-energy acyl phosphate which is believed to drive long-range conformational changes that ultimately alter the transcriptional, enzymatic, or mechanistic activity of the associated output module. This mechanism of "mechanical" activation differs from that observed with serine, threonine and tyrosine phosphorylation, where phosphorylation induces local electrostatic effects [164]. Similarly to the input modules, the downstream signal transduction modules display a great diversity and a wide range of activities. Many response regulators bind DNA through their output domain (*e.g.* the HTH domain) and function as transcriptional regulators; other output domains have RNA-binding activity (*e.g.* the ANTAR domain), protein-binding activity (*e.g.* PAS, GAF, TPR, HPt, and REC domains) or enzymatic activities such as for instance diguanylate cyclase (GGDEF domain) and phosphodiesterase (EAL domain, HD-GYP domain) activity [133,169].

While REC-containing response regulators are the terminal components of the signaling chain in classical two-component systems, in phosphorelay systems, the phosphoryl group is further transferred to a histidine residue within a histidine-containing phosphotransfer (HPt) domain and successively from the HPt domain to another REC domain (Figure 12). The HPt domains, which encompass roughly 120 amino acids, lack overall sequence similarity, except for the small region surrounding the phosphorylated histidine residue. Nevertheless they all share a similar four helix bundle structure [166]. HPt domains can either exist as separate proteins (*e.g.* Ypd1 in *S. cerevisiae*) or as domains of hybrid histidine kinases.

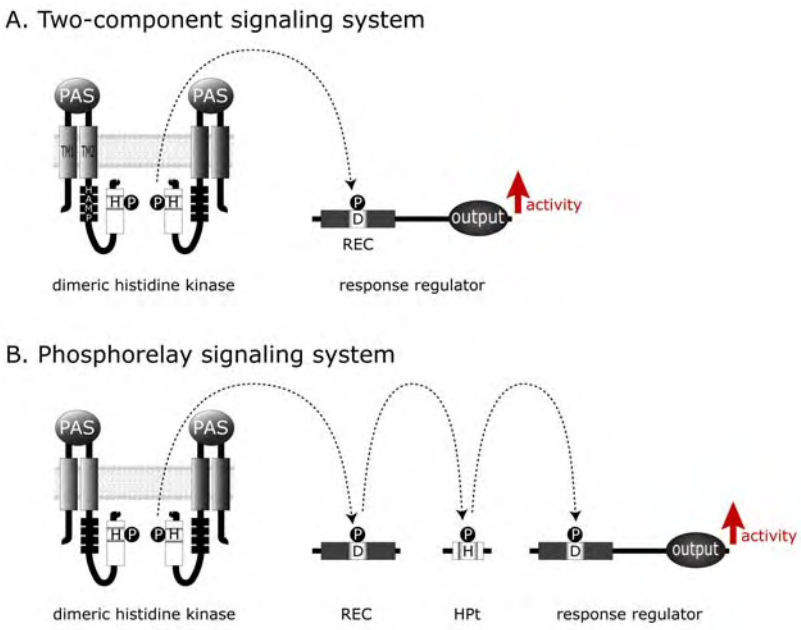

Figure 12

Schematic representation of two-component [A.] and phosphorelay [B.] signaling systems. In both systems a dimeric histidine kinase typically detects an extracellular signal, which is transmitted along the molecule as a series of conformational changes involving the HAMP domain and ultimately activates the kinase of the receptor. This leads to the reciprocal phosphorylation of the two monomers within the corresponding H-motifs. The phosphate group is then transferred to the next component (in both cases a REC domain); in two-component systems the REC-domain containing protein is always the effector of the signaling cascade. Phosphorelay signaling systems involve additional aspartate and histidine residues.

Structure of REC domains and function of the highly conserved residues

The single-domain chemotaxis protein CheY has served as representative model for REC domains. This small protein folds into a doubly wound α/β protein with a central five-stranded β sheet surrounded by five α helices. Phosphorylation of three residues was demonstrated to be critical for CheY activation; the phosphate acceptor, Asp57, is located in a solvent-exposed loop and lies adjacent to other critical acidic residues (Asp12 and Asp13) whose carboxylate side chains are involved in the coordination of $Mg^{2+}$and are required for catalysis. Two other highly conserved residues, Thr81 and Lys109 in CheY, are not absolutely required for phosphorylation/dephosphorylation and are probably involved in the phosphorylation-induced conformational change [170]. The phosphorylation/dephosphorylation of the REC domain is believed to result in the stabilization of either one of two conformational states, the on- and the off-state respectively, which have specific protein-protein or protein-DNA interaction properties. Interestingly, receiver domains can catalyze *in vitro* phosphoryl transfer from small phosphorylated molecules such as acetyl phosphate or carbamoyl phosphate, in a kinase-motif-independent manner. In spite of the promiscuity observed *in vitro*, in particular for HPt domains, cross-reactivity of the motifs involved in different two-component and phosphorelay signaling systems was never detected under physiological conditions.

Results and discussion

The Rim15 PAS domain

The analysis of the amino acid sequence of Rim15 revealed the presence of a single PAS domain in the N-terminal part of the protein, which is conserved among all fungal members of the Rim15 family; to clarify the role of this domain we carried out functional studies of this domain. Notably, the available data on other PAS-containing serine/threonine kinases, indicate that the PAS domain functions as an inhibitor of the enzymatic activity of the associated kinase domain [138] .

Identification of the Rim15 PAS domain

A computerized search for conserved motifs within the amino acid sequences of Cek1 and Cek1-like proteins, the Rim15 homologs in *Saccharomyces pombe*, using SMART and PROSITE revealed the presence of a PAS domain in the N-terminal portion of these proteins [171,172]. Surprisingly, we were not able to detect a PAS domain sequence by subjecting Rim15 the protein sequence to the same kind of analysis. Importantly in some cases PAS domains may escape identification via conventional methods, due to their poor amino acid sequence conservation and to the frequent co-occurrence with other, highly conserved motifs within the same polypeptide [136].

To determine whether Rim15 may also harbor a N-terminal PAS domain, we used a combination of iterative databases searches (initiated with an alignment of the PAS domains found in the *S. pombe* Cek1 and Cek1-like proteins) with generalized profiles and Hidden Markov Models (profile-HMMs) [173,174]. Only sequences that matched a generalized profile or a profile-HMM with a significant score (E-value of <0.01) were used for subsequent iteration cycles. At the second cycle, we identified the *S. cerevisiae* Rim15 PAS domain (with an E-value of 10-3), as well as several other previously characterized PAS domains (Figure 13). These results, published in 2004 [113], indicate that Rim15 may represent a new, distinct member of the PAS kinase family.

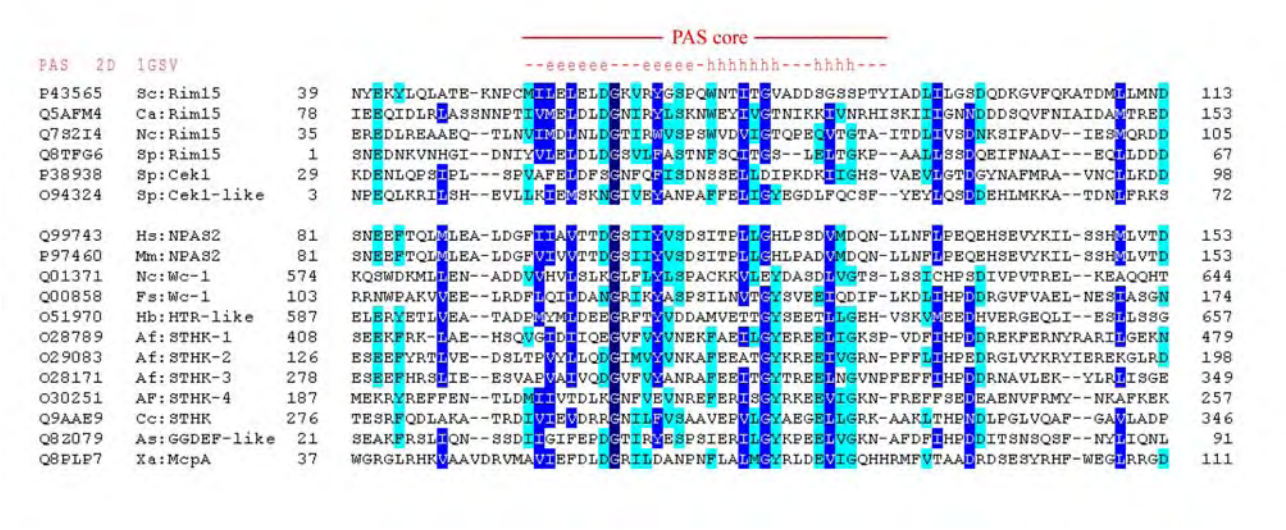

Figure 13

Alignment of the PAS domains found within the Rim15 family of fungal proteins with closely related, well-defined PAS motifs [113]. Amino acids that are conserved in more than 50%, 70% and 90% of the sequences are shown in light blue, blue and dark blue, respectively. The predicted secondary structure of the PAS core, as deduced from the *Ectothiorhodospira halophila* PYP (1GSY) PDB entry, is indicated above the alignment.

The Rim15 PAS domain has only a limited role for the *in vitro* kinase activity of Rim15

The enzymatic activity of the human PAS kinase (hPASK) is subject to regulation *in cis* by a N-terminal PAS domain [151]. A truncated form of hPASK, lacking the N-terminal PAS domain, showed a higher catalytic rate (*k*cat) than full-length hPASK in a kinetic analysis of the kinase activity *in vitro* [151].

To determine whether the N-terminal PAS domain of Rim15 may also act as a regulator of Rim15 kinase activity in vitro we expressed and purified from yeast a truncated version of Rim15 lacking the region comprising the predicted PAS domain sequence. Both, the truncated Rim15$^{PAS\Delta}$ and the full-length Rim15 enzymes phosphorylated the artificial substrate α-casein at a similar rate over the course of a 20-min reaction (Figure 14). Notably in a similar experiment using the recently identified endogenous substrate of Rim15 (expressed and purified from bacteria) we could also not detect any influence of the N-terminal PAS domain on the in vitro activity of Rim15 (data not shown). Nevertheless, we observed increased autophosphorylation of the truncated protein, suggesting that, analogously to what was observed for hPASK, the PAS domain of Rim15 may serve to inhibit Rim15 enzymatic activity (Figure 14).

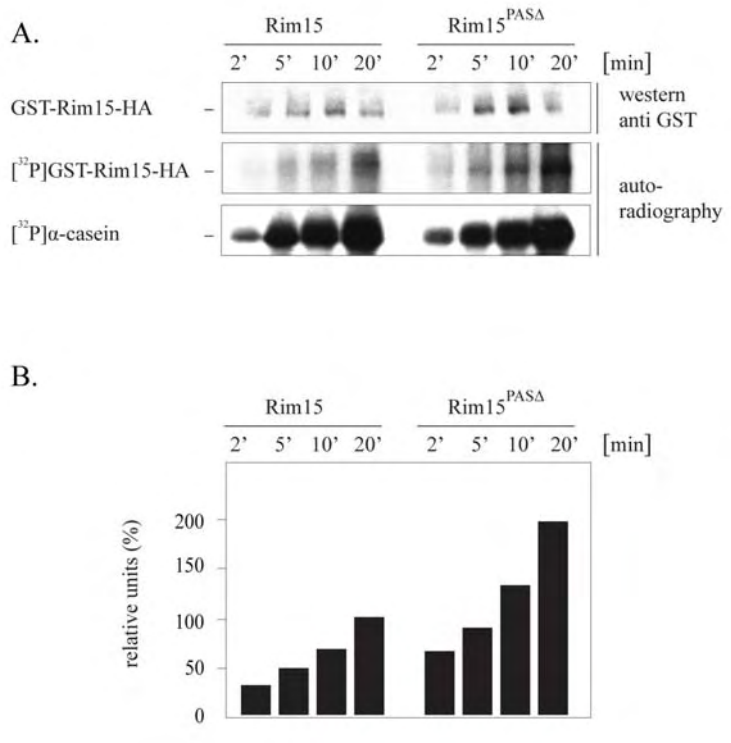

Figure 14

Kinase assay showing the *in vitro* kinase activity of recombinant wild type Rim15 and of a truncated version of Rim15 lacking the N-terminal PAS domain. GST-Rim15-HA and GST-Rim15$^{PAS\ \Delta}$-HA were expressed and purified from yeast and used to phosphorylate the artificial substrate α-casein in a protein kinase assay. Reactions were stopped after the indicated times. Equal amounts of substrate were used in each reaction. [A.] The kinase input bands (top panel) were detected by western blot using antibodies against the HA epitope. The autophosphorylation levels of the Rim15 variants (middle panel) and of the substrate (lower panel) were detected by autoradiography. [B.] The autophosphorylation activity was roughly quantified using the PhotoshopCS2 software. The bars represent the level of incorporation of radioactive phosphate relative to the total level of purified kinase in the assay, expressed as percent of the control (level of phosphorylation of the full-length protein after 20-min incubation in the presence of [γ^{32}P]-ATP).

We next asked whether, in analogy to what was observed for hPASK, addition of the purified PAS domain of Rim15 to protein kinase assays would specifically reduce the enzymatic activity of Rim15. To this end, recombinant MBP-PAS^{Rim15} was purified from bacteria and added it *in trans* to protein kinase assays where the truncated form of Rim15 was used to phosphorylate the artificial substrate α-casein (Figure 15). We observed a slight reduction of the enzymatic activity of Rim15 - as judged by both, the autophosphorylation levels and the incorporation of [γ^{32}P] in the substrate α-casein when MBP-PAS^{Rim15} was added *in trans* (Figure 15). However, since MBP alone had a similar effect, these data allow no conclusive judgment of the effect of the PAS domain in this *in vitro* assay. Future studies, based on the use of the PAS domain solely, are more likely to provide conclusive results.

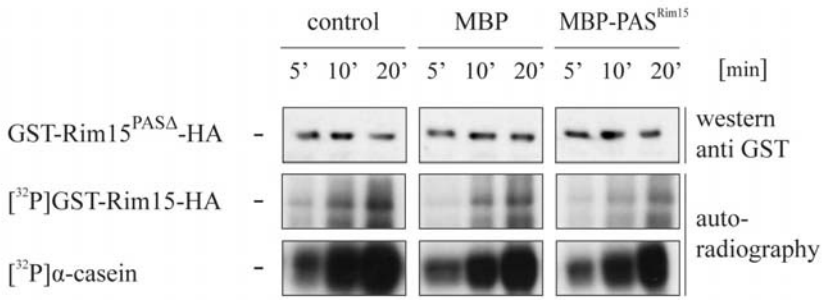

Figure 15

Kinase assay showing the effect of MBP-PAS^{Rim15} on the *in vitro* kinase activity of Rim15. A truncated version of Rim15 (GST-Rim15$^{PAS\,\Delta}$-HA) purified from yeast cells was used to phosphorylate the artificial substrate α-casein in protein kinase assays in the presence or absence of 7.5 µM MBP-PAS^{Rim15} or of 7.5 µM maltose binding protein (MBP). The PAS domain of Rim15 (MBP-PAS^{Rim15}) was expressed and purified from bacteria; MBP was purchased from New England Biolabs. The phosphorylation reactions were stopped after the indicated times. Equal amounts of substrate were used in each reaction. The kinase input bands (top panels) were detected by western blot using antibodies against the HA epitope. The phosphorylation levels of Rim15 (middle panels) and of the substrate (lower panels) were detected by autoradiography.

Notably, work on the human PAS kinase revealed that the deletion of the PAS domain does not affect the affinity of the kinase for the peptide substrate (K_M), but it increases the catalytic rate (*k*cat) of the enzyme [151]. More refined protein kinase assays, using for instance parts of Rim15 as substrate, may allow us in the future to more precisely define a role of the Rim15-PAS domain in autoregulation of Rim15 kinase activity.

Deletion or overexpression of the PAS domain does not affect Rim15 activity *in vivo*

We next asked whether expression of a truncated version of Rim15 as the only copy of Rim15, or overexpression of the isolated PAS domain may result in measurable alterations in any of the known Rim15 readouts (*i.e.* glycogen accumulation, trehalose accumulation, transcriptional induction of G_0-specific genes such as *HSP26* or *HSP12*, and survival in the post-diauxic phase).

If, as suggested by our *in vitro* studies, the PAS domain in Rim15 may have a role as a negative regulator of the enzymatic activity of the kinase, we expect that expression of a Rim15 variant lacking the PAS domain positively affects the expression of Rim15-dependent readouts. Conversely, overexpression of the Rim15-PAS domain is expected to negatively affect the activity of the endogenous Rim15.

Against these expectations, the expression - in a *rim15Δ* mutant - of a truncated version of Rim15 ($Rim15^{PAS\Delta}$) from the endogenous *RIM15* promoter restored a *RIM15* wild-type phenotype to the same level as did the expression of the full-length protein (data not shown). Similarly, expression of the isolated PAS^{Rim15} domain from the constitutively active, strong *TDH3p* promoter, in either wild-type cells or cells deleted for *RIM15,* did not result in any measurable change of the Rim15 readouts when compared to corresponding controls (Figure 16).

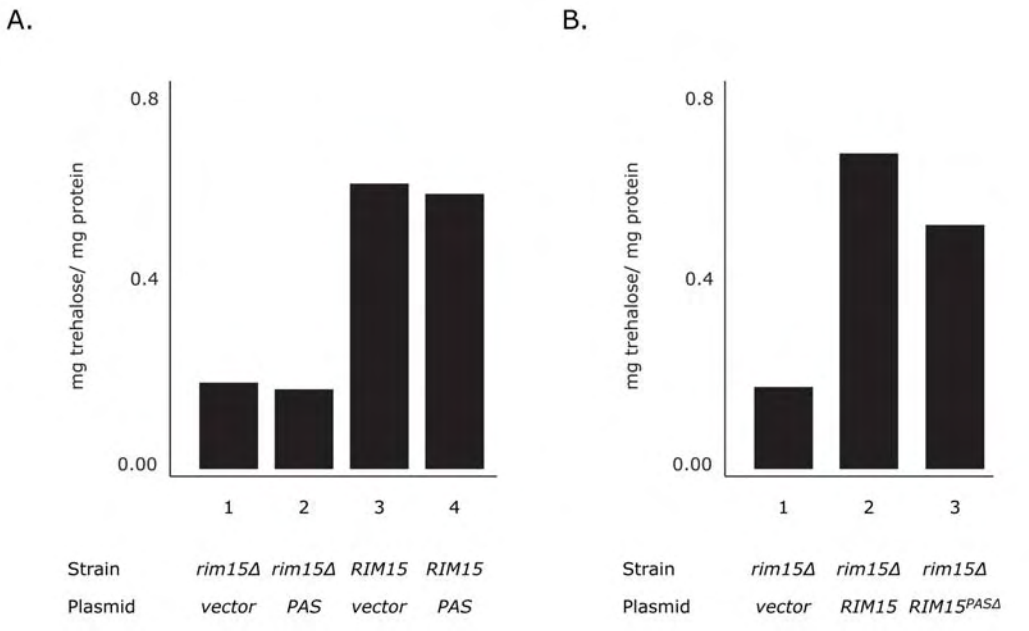

Figure 16

The role of the Rim15-PAS domain *in vivo*, as judged from the trehalose accumulation in the indicated strains [A.] Trehalose levels in *rim15Δ* mutant (1, 2) or wild-type strains (3, 4) overexpressing either PAS^{Rim15} from the strong, constitutive *TDH3* promoter (2, 4), or carrying the empty control vector (1, 3). [B.] Trehalose levels in a *rim15Δ* mutant strain, carrying an empty control vector (1), or expressing the wild-type Rim15 protein (2) or a truncated $Rim15^{PAS\Delta}$ (3) from the endogenous RIM15 promoter.

It is possible that the isolated PAS domain of Rim15 does not acquire the same conformation as in the context of the Rim15 polypeptide and therefore, when provided *in trans*, may not support the same interactions. Alternatively the ability to modulate the activity of Rim15 may depend on the binding of a cofactor. If such a cofactor was present only in limiting amounts within cells the isolated PAS^{Rim15} would not be expected to affect the activity of Rim15. In conclusion, although our results do not rule out a possible role of the PAS domain in regulating Rim15 kinase activity, they clearly demonstrate that the presence of the PAS domain is not essential for the function or the regulation of Rim15.

Rim15 PAS may be phosphorylated *in vitro* by an unknown co-precipitating kinase

During our studies on the effect of Rim15-PAS domain on Rim15 enzymatic activity we noticed that the recombinant GST-PAS^{Rim15}, when purified from yeast, incorporated radioactive phosphate even in the absence of the Rim15 protein kinase (Figure 17).

The most likely interpretation of this data is that an active protein kinase was present in the sample containing the purified GST-PAS^{Rim15}. This kinase, which seems to share with Rim15 the ability to phosphorylate α-casein, may be a specific Rim15-interacting protein, as it co-purified with the Rim15-PAS domain despite the stringent conditions used in the washing steps.

When Rim15 was incubated in the presence of purified GST-PAS^{Rim15} the phosphate-incorporation level of the corresponding SDS-PAGE band, compared to Rim15 alone, was also increased (Figure 17). Notably, even though this may be due to a positive effect of GST-PAS^{Rim15} on the Rim15 kinase activity, it seems more likely that the contaminating kinase that was co-purified with GST-PAS^{Rim15} directly phosphorylated the full length Rim15. This phosphorylation may occur at multiple sites, both within and outside the N-terminal region, since in a similar experiment using a truncated Rim15$^{PAS\Delta}$ protein we also observed an increased incorporation of phosphate in the Rim15 protein (not shown).

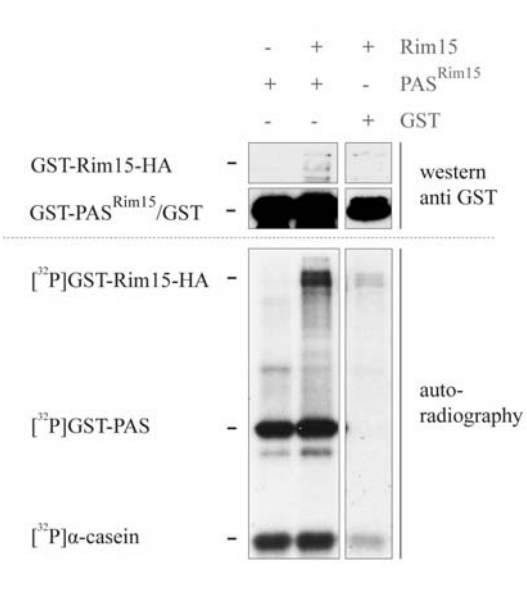

Figure 17

In vitro kinase assay showing the incorporation of [γ^{32}P] into the isolated Rim15-PAS domain (purified from yeast). The full-length GST-Rim15-HA ^{kinase} was used to phosphorylate the artificial substrate α-casein. Assays were carried out in the presence of GST-PAS^{Rim15} or of GST alone, both purified from yeast. As a control the GST-PAS^{Rim15} preparation was incubated with the substrate and [γ^{32}P]-ATP in the absence of Rim15. The kinase input bands (top panels) and the GST-PAS^{Rim15} or GST input bands (middle panels) were detected by western blot against the GST epitope. The incorporation of [γ^{32}P] was detected by autoradiography.

The identification of this Rim15 interacting kinase would be of great interest for the further elucidation of the mechanisms of Rim15 regulation. Unfortunately, a first attempt to identify this kinase by mass spectrometry (MS) was not successful.

Interestingly, analysis of the Rim15-PAS domain sequence using Scansite (http://scansite.mit.edu/motifscan_seq.phtml) predicts a consensus sequence for phosphorylation by casein kinase 1 (CK1). All four yeast CK1-orthologs have been identified as high dosage suppressors of the cold sensitive phenotype of *gcs1Δ* mutants, suggesting their involvement in a process related to the regulation of G_0 exit [175]. Although these interactions have not been confirmed experimentally, Yck1 would be an interesting candidate for the activity that phosphorylates both Rim15 and α-casein. In a very speculative model yeast casein kinases in the termination of G_0, it is tempting to speculate that these kinases could promote exit from G_0 by inhibiting the activity of Rim15 via a mechanism involving phosphorylation, possibly on the PAS domain.

The PAS domain of Rim15 co-immunoprecipitates with full length Rim15

Regulation of PAS containing proteins by an N-terminal PAS domain usually involves an intramolecular interaction between the PAS domain and the transmitter domain on the same protein (Figure 10).

To test whether the PAS domain of Rim15 can interact physically with the full length protein we performed a co-precipitation experiment (Figure 18). We found that GST-Rim15 able to pull down PAS-HA^3, but not Bud14-HA^3 (in a control experiment).

Interestingly, in GST-Rim15 pull down experiments with PAS-HA^3, we detected an additional band, which migrated with an apparent molecular weight corresponding to the size expected from a PAS-HA^3 dimer. Notably, in PAS containing proteins that function as transcriptional activators, the PAS domain is known to offer a surface for both homotypic interactions with other PAS proteins and heterotypic interactions with cellular chaperones [149].

This result further supports the notion that the PAS domain of Rim15 may be implicated in protein-protein interactions, which also seem to include intra-molecular interactions.

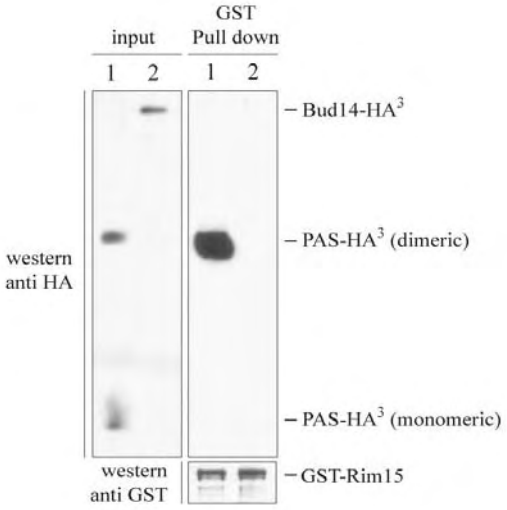

Figure 18

Co-precipitation experiment, showing the interaction between the putative dimeric form of PAS-HA^3 and the full length GST-Rim15 protein. The monomeric PAS domain did not seem to co-purify with GST-Rim15. In a control experiment Bud14-HA^3 did not co-purify with GST-Rim15 (lane 2).

A novel C_2HC zinc finger motif

Identification of a novel C_2HC zinc finger motif in the Rim15 protein sequence:

During our analysis of the Rim15 amino acid sequence we noticed a cysteine rich pattern in the N-terminal part of the protein that was reminiscent of a zinc finger motif, but showed a unique spacing between the putative zinc-coordinating residues. To test whether this sequence corresponds to a conserved motif we used the PROSITE scanning tool to scan the SWISS-PROT Knowledgebase for annotated proteins containing the same cysteine-histidine arrangement, namely [C-x(2)-C-X(11)-H-x(3)-C-x(3)-H], that is found in Rim15 [176-178]. Using this method, we were able to identify 10 proteins, in addition to Rim15, that contained a Rim15-like pattern. These included the human anaplastic lymphoma kinase (ALK), which is mutated in various tumors, the mouse ALK, the human and mouse DNA topoisomerase 3-beta-1, the *S. pombe* cytosolic serine/threonine kinase Ppk18 and the human, mouse and rat orthologs of the Werner helicase-interacting protein 1 (WRIP1). We then subjected the retrieved sequences to a position specific iterative BLAST (PSI-BLAST) using the PSI-BLAST service of MyHits (http://myhits.isb-sib.ch) [179,180]. After two subsequent iteration cycles we identified, although with a low score, the *S. cerevisiae* Rad18 protein and its human, mouse and *S. pombe* orthologs, as well as the *S. cerevisiae* ortholog of the Werner-helicase interacting protein (WRIP) 1, Mgs1 (Figure 19).

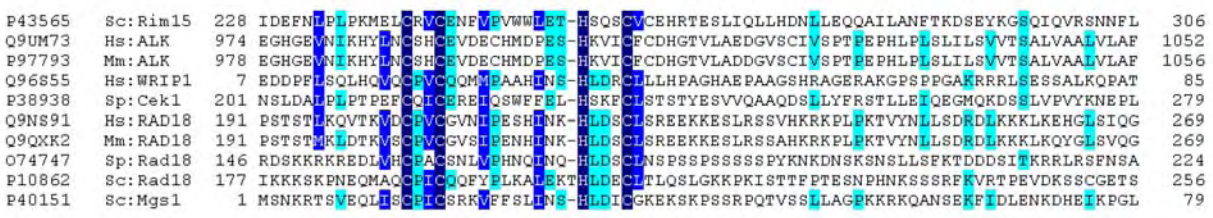

Figure 19

Alignment of the C_2HC zinc finger domains found within the Rim15 and ALK proteins and the previously described Rad18-type zinc finger in WRIP1 and RAD18 proteins [181]. Amino acids that are conserved in more than 50%, 70% and 90% of the sequences are shown in light blue, blue and dark blue, respectively.

Interestingly, a zinc-finger like sequence, that overlaps with the Rim15-type C_2HC zinc finger, had been previously identified in RAD18 and WRIP1 proteins by sequence homology; the role of the Rad18-type C_2HC zinc finger domain has not been investigated, but it was assumed to serve as a protein-protein or a protein-DNA interaction domain [181]. The Rad18-type zinc fingers are also distantly related to the PtdIns(3)P-binding FYVE motif [159]. This prompted us to

investigate whether the zinc finger domain in Rim15 may be involved in the binding of lipids, in particular phosphoinositides.

Rim15-type zinc finger motif binds phosphoinositides *in vitro*

Because Rim15 was found to interact with certain phosphoinositides in a large protein microarray experiment [182], and based on the similarity between the Rim15 zinc finger and the PtdIns(3)P binding FYVE domain, we asked whether the zinc finger motif of Rim15 was sufficient to bind phosphoinositides *in vitro.*

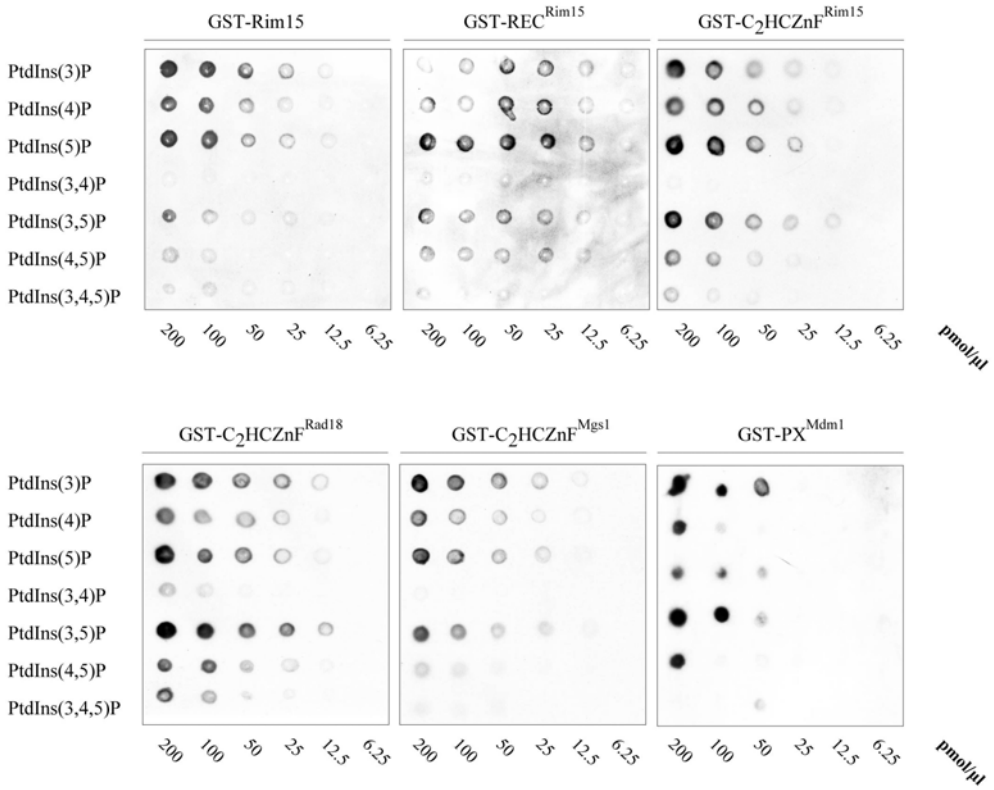

Figure 20

Protein-lipid overlay assay showing the phosphoinositide-binding specificity of the full length Rim15 protein (GST-Rim15) and the isolated C_2HC zinc finger motifs of Rim15 (C_2HCZnF^{Rim15}), Rad18 (C_2HCZnF^{Rad18}) and Mgs1 (C_2HCZnF^{Mgs1}). The proteins were expressed and purified from yeast as GST fusions. Similar amounts of each protein were incubated with nitrocellulose membranes that had previously been spotted with serial dilutions of different PtdIns species (concentrations are indicated under the blots). After extensive washing the membranes were subjected to western blotting using an antibody against the GST epitope to reveal bound protein. The PX motif of Mdm1 (kindly provided by Dr. Michael Knop), which is known to interact specifically with PtdIns(3)P was used as a control.

Our experiments using a protein-lipid overlay assay (materials and methods) confirmed the ability of the purified GST-Rim15 recombinant protein to bind *in vitro* the phosphoinositide species PtdIns(3)P, PtdIns(4)P and PtdIns(5)P. In addition, a weak interaction with the phosphoinositide

PtdIns(3,5)P_2 was also detected (Figure 20). The analysis of different Rim15 fragments, expressed in yeast as GST fusions, revealed that only the region comprising the zinc finger motif was able to bind phosphoinositides with a similar specificity as the full length protein (Figure 20). We then expressed the homologous zinc finger motifs of the yeast Rad18 and Mgs1 proteins as GST fusion and found that the recombinant proteins were able to bind phosphoinositides with a similar specificity as the Rim15 zinc finger domain (Figure 20).

Interaction of the full length GST-Rim15 with PtdIns(3)P and PtdIns(5)P could be confirmed using a different, more sensitive assay. In the liposome binding assay, lipid vesicles containing different phosphoinositides were used to co-precipitate interacting proteins *in vitro*. Using this assay we found that the purified full length GST-Rim15 recombinant protein is enriched in pellets containing PtdIns(3)P and PtdIns(5)P (Figure 21). In contrast the interaction with PtdIns(4)P and PtdIns(3,5)P2 could not be confirmed using this method (Figure 21).

Mutation of the zinc coordinating residues is predicted to weaken the structure of the zinc finger and is thus likely to affect the function of this domain. Surprisingly, mutation of the putative zinc coordinating histidine 256 residue to alanine, did not result in loss of protein-lipid interaction but rather affected its specificity. Accordingly a GST-Rim15^{H256A} mutant protein was found in all phosphoinositides-containing precipitates but not in the pellets containing the "empty" lipid vesicles composed only of phosphatidylserine (PS) and phosphatidylcholine (PC) (Figure 21). A similar result was obtained using the isolated zinc finger motif of Rim15. This observation, together with the slightly higher specificity of the interactions of the full-length Rim15 protein (in the protein-lipid overlay assay, Figure 20) compared to the isolated zinc finger, may indicate that a second region in Rim15 is involved in the recognition of phosphoinositides. Interestingly the Scansite program recognizes a putative PtdIns(3)P interaction motif at a position just adjacent to the C_2HC zinc finger.

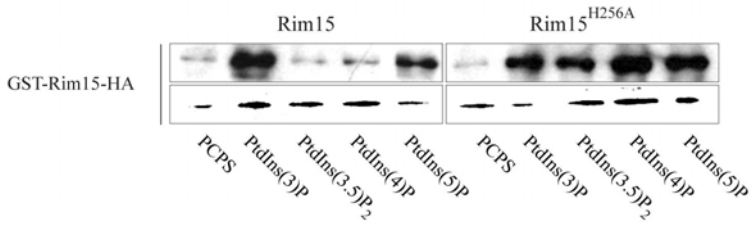

Figure 21

Liposome binding assay, showing the specific interaction of the full length Rim15 protein with PtdIns(3)P and PtdIns(5)P. Liposomes containing the different phosphoinositides, prepared as described in materials and methods, were incubated with either the wild-type Rim15 protein or the Rim15^{H256A} mutant (tagged with both GST and HA). The recombinant proteins were purified from yeast extracts using GST-sepharose.

Importantly, the observation that substitution of histidine at position 256 with alanine altered the lipid binding behavior of the protein indicates that this residue may be structurally important and, although we did not directly assess the zinc content of the purified zinc finger, supports the hypothesis that the zinc finger domain of Rim15 is indeed involved in binding zinc ions.

Phosphoinositides are known to transduce signals essentially via two events: their modification and their interactions with specific proteins [183]. Remodeling of the phosphoinositide profile in response to extracellular signals, by the action of phospholipases, lipid kinases and lipid phosphatases, affects the activity of various downstream targets that control diverse intracellular processes including vesicle trafficking, cell proliferation and survival, gene transcription, and pathogen elimination [183].

Rim15-type zinc finger motifs direct a GFP fusion protein into the nucleus

Phosphoinositides are found in different cellular compartments and are often involved in directing the localization of their interacting proteins. We were therefore interested in studying whether the Rim15-type C_2HC zinc finger was required to direct the localization of Rim15 to a particular cellular compartment.

One intriguing possibility would be that Rim15 is recruited to the vacuolar membrane, which is enriched for PtdIns(3)P. Notably two upstream regulators of Rim15, TORC1 and Sch9, have been proposed to be localized at the vacuolar membrane [50]. Rim15 was shown previously to be localized in both the cytosolic and the nuclear compartments, depending on the nutrient conditions [78]. While nutrient starvation clearly results in its nuclear accumulation, Rim15 is excluded from this compartment in growing cells. Notably, due to the low expression levels of the Rim15 protein during the exponential phase of growth, all these Rim15 localization studies relied on a construct that allowed overproduction of GFP-Rim15. Since this leads to a loading of the cytoplasm with GFP-Rim15 any particular membrane localization may so far have escaped our attention.

Surprisingly, we found that the conserved zinc finger amino acid sequence of Rim15 directed green fluorescent protein (GFP) fused to its N-terminus, predominantly into the nucleus (Figure 22). Similarly GFP fusions with the zinc fingers of Rad18 and Mgs1 were also found predominantly in the nucleus. The sequences of these zinc fingers do not contain nuclear localization signals. Therefore, this finding raises the interesting possibility that the newly identified Rim15-type C2HC zinc finger motifs are retained in the nucleus through their interactions with nuclear phosphoinositide pools.

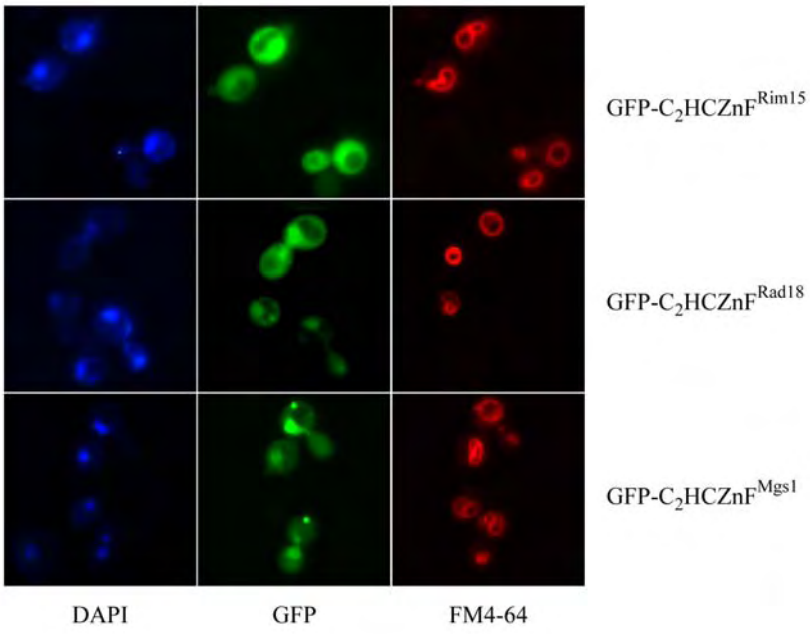

Figure 22

Fluorescence microscopy showing the nuclear localization of GFP fusions with the C_2HC zinc finger motifs of Rim15, Rad18 and Mgs1.

Indeed, it is now well accepted that the nuclear compartment contains a dynamic pool of phosphoinositides that is distinct from the cytoplasmic pool and that is modulated in response to signals that induce processes such as differentiation, cell proliferation and stress adaptation [183]. The nucleus contains its own distinct enzymatic system for the metabolism of phosphoinositides, whose negative charge renders it unlikely that they cross the nuclear membranes. Moreover, an increasing number of nuclear proteins are found to contain phosphoinositide binding domains. For instance, the plant homeodomain (PHD) is a phosphoinositide-binding zinc finger that has been identified in many nuclear proteins. The role of nuclear phosphoinositides is not well understood, but in many cases phosphoinositides appear to be involved in chromatin-related processes [183]. For instance, the interaction of phosphoinositides in the nuclear envelope or matrix with chromatin-associated proteins may provide an ideal mechanism for controlling gene positioning, a process shown to be important in the regulation of gene expression [184]. Notably, all three proteins, Rad18, Mgs1 and Rim15 have been previously implicated in some aspects of chromatin remodeling [114,185,186].

Further experiments are required to assess whether the interaction of the Rim15-type C_2CH zinc fingers with nuclear phosphoinositides is necessary for the nuclear localization of these protein.

Preliminary experiments using a GFP fused to a truncated version of Rim15 that lacks the region encompassing the zinc finger, indicate that this motif is not required for the nuclear import of Rim15 following a rapamycin treatment. Similarly to the wildtype protein the mutant allele remained excluded from the nuclear compartment throughout the exponential phase of growth and accumulated in the nucleus in response to rapamycin (data not shown). It is possible that the nuclear localization of the full length protein is mediated cooperatively by different mechanisms, involving stabilizing interactions with both lipids and proteins. A cooperative mechanism has been shown to mediate the recruitment of FYVE domain containing proteins to specific membranes. Although the FYVE domain is sufficient to recognize the target membranes, protein-protein interactions are required to stabilize membrane binding of these proteins. Alternatively, phosphoinositide binding, although sufficient to direct the small recombinant proteins to the nucleus, may not be required for the localization of the full length Rim15 protein, but rather for the regulation of its nuclear function or to dock the kinase to a particular subnuclear localization.

Taken together our results support a model where Rim15 shuttles across the nuclear membrane via a zinc finger independent mechanism and interacts with phosphoinositides within the nucleus. This protein-lipid interaction may stabilize the nuclear localization of Rim15 or recruit it to a particular sub-nuclear location defined by the presence of a distinct phosphoinositide pattern.

Finally, we can not exclude that the nuclear localization of the small GFP-zinc finger fusions (<50 kD) is due to passive diffusion through the nuclear pores. However, since constructs accumulated in the nucleus significantly better than GFP alone (data not shown), at least some level of active transport or retention may be inferred from our experiment.

Mutations within the zinc finger motif affect Rim15 function both *in vitro* and *in vivo*

We have that mutations predicted to destabilize the structure of the zinc finger motif in Rim15 changed the binding behavior of the protein. We were therefore interested in assessing whether the altered properties conferred by these mutations would also affect the enzymatic activity of Rim15.

Interestingly, the mutations of two conserved residues that are predicted to coordinate zinc ions affect the enzymatic activity of the Rim15 kinase *in vitro* (Figure 23). Substituting the conserved cysteine residue at position 244 or the conserved histidine residue at position 256 resulted in a significant reduction of the *in vitro* catalytic activity of Rim15.

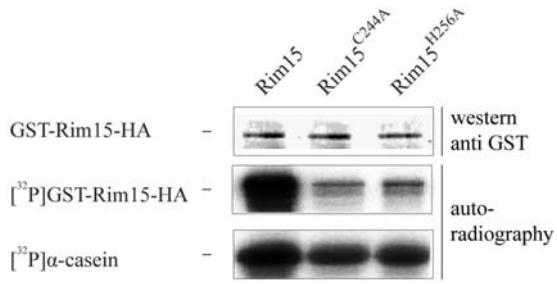

Figure 23

In vitro phosphorylation assay showing the effect of alanine substitutions of the putative zinc coordinating residues in Rim15. Phosphorylation of the artificial substrate α-casein (lower panel) and autophosphorylation (middle panel) are strongly reduced by the C244A and H256A substitutions. The total level of purified kinase in the assay was assessed by western blot using antibodies against the HA epitope (top panel).

This result suggests a connection between the structural stability of the zinc-finger motif and the catalytic activity of the full-length protein. Notably, as the same mutations affect the specificity of the protein-lipid interaction, it is possible that specific interactions with phosphoinositides species are required for the enzymatic activity of Rim15. However, a causal link between lipid binding and kinase activity can not be established based on the current results. Notably, loss of the coordinated zinc ions may affect the folding of the full-length protein and this, rather than the altered lipid-binding behavior may impair the enzymatic activity. Nevertheless, the mutant and wildtype proteins displayed similar stabilities *in vitro*.

To test their impact on Rim15 activity *in vivo*, the same mutations were introduced in an integrative vector expressing *RIM15* from the endogenous promoter. The mutant alleles or the wild-type allele were integrated in a mutant yeast strain carrying a deletion of the endogenous *RIM15* gene. Only the wild-type allele was able to complement the phenotypes of a *rim15Δ* mutant, while a construct expressing a Rim15 version carrying mutations within the zinc finger domain resulted in a similar phenotype as the *rim15Δ* mutant, *i.e.* low trehalose accumulation and shorter chronological lifespan (Figure 24).

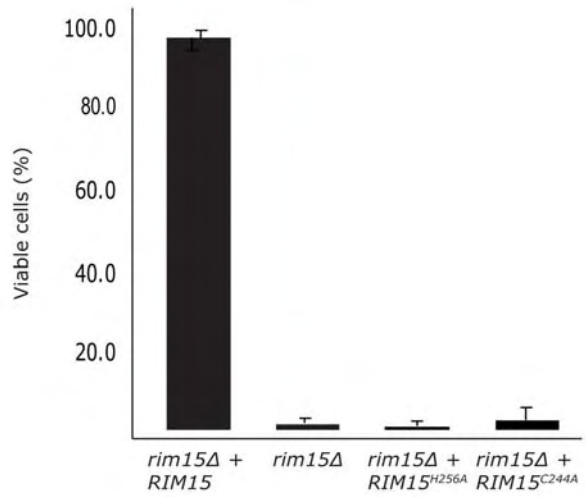

Figure 24

Survival of *rim15Δ* cells expressing wild-type and mutant alleles of *RIM15*. Dead cells after 8 days on full medium containing 1% glucose were detected by trypan blue staining (see Materials and Methods).

Moreover, preliminary experiments with mutant strains deleted for single non-essential PtdIns kinases revealed that Rim15 readouts, such as the level of the *HSP12* and *HSP26* transcripts or the level of trehalose following glucose starvation during the diauxic transition, are altered in stains carrying mutations that supposedly result in altered levels of some PtdIns species. In particular, in the absence of the phosphatidylinositol 3-phosphate 5-kinase Fab1, Rim15 readouts were significantly increased (data not shown).

Exogenous phosphoinositides do not affect the *in vitro* protein kinase activity of Rim15

We reasoned that if phosphoinositide binding was required for the proper functioning of the Rim15 kinase, addition of phosphoinositides to *in vitro* kinase reactions would result in increased kinase activity. Different phosphoinositides were incorporated in lipid vesicles (as described in materials and methods) and added *in trans* to kinase reactions where the purified Rim15 kinase was used to phosphorylate the artificial substrate α-casein. Contrary to our expectations, the presence of the micelles did not alter the *in vitro* kinase activity of Rim15 (Figure 25).

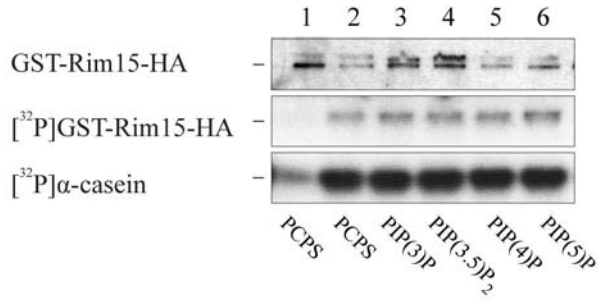

Figure 25

The effect of exogenous phosphoinositides on the kinase activity of Rim15 was assessed in an *in vitro* kinase assay using α-casein as substrate for a wild type GST-Rim15 fusion protein (lanes 2 to 6) or a GST-Rim15 version carrying the amino acid substitution H256A (lane 1); all expressed and purified from yeast.

One possible explanation could be that in our preparations, phosphoinositides co-purified with Rim15 kinase and thus already allow maximal Rim15 activity. Alternatively, only the structure of the zinc finger may be relevant to the enzymatic activity of Rim15, while the binding of phosphoinositides could have a different function. For instance, it could be necessary to direct the activity of Rim15 towards the appropriate sub-nuclear localization and/or the appropriate substrates.

The Rim15 zinc finger domain is involved in protein-protein interactions.

The transcriptional regulator Gis1 was previously identified by our group as a (direct or indirect) downstream target of Rim15. This work demonstrated that Rim15 and Gis1 interact genetically but a physical interaction could never be detected [187]. In a recent publication, Tronnesjö and collaborators (2006) used a two-hybrid screen approach to identify a Gis1-complex, which can act as both a transcriptional activator and repressor [188]. We reasoned that Rim15 may be, under some circumstances, part of a complex involved in the regulation of Gis1 activity.

The use of the full-length Rim15 protein in the classical two-hybrid setup results in high background activation of the reporter, probably due to the intrinsic DNA-binding properties of Rim15. For this reason we cloned different fragments of *RIM15* and used them in a two-hybrid assay with the prey plasmids isolated in the Gis1 two-hybrid screen (kindly provided by Dr. Hans Ronne).

Interestingly, we found that the uncharacteristic prefoldin Bud27, suggested to act as a scaffold protein for the Gis1 complex, interacted specifically also with the Rim15 zinc finger (Table II). This interaction was confirmed by co-immunoprecipitation of the full length Bud27-HA protein

with the full length GST-Rim15 protein (Figure 26). Notably Bud27 has also been suggested to be a target of the TORC1 pathway in yeast [178].

				DBD fusion		
	AD fusion	Insert (Aa)	Full length (Aa)	$C2HCZnF^{Rim15}$	REC^{Skn7}	REC^{Rim15}
a.	Bud27	85-400	796	113.5 ± 4.9	5.0 ± 2.0	4.6 ± 1.3
	REC^{Rim15}	1635-1753	1776	46.5 ± 3.5	13.7 ± 2.4	n.d.
b.	Gds1	268-522	622	1.5 ± 0.7	1.8 ± 1.0	5.1 ± 1.8
	Sir4	1144-1358	1358	7.7 ± 2.1	11.3 ± 2.5	149.4 ± 4.7
	Taf65	386-510	510	2.3 ± 2.3	10.0 ± 0.7	56.2 ± 8.5

Table II

Two hybrid interactions between two regions of the Rim15 protein with components of the Gis1-complex [188]. a. The receiver domain (REC^{Rim15}) as well as a AD-fusion protein encompassing the amino acid residues 85 to 400 of Bud27 interact with the C_2CH zinc finger domain of Rim15 (C_2CH Znf^{Rim15}). b. The regions of the Sir4 and Taf65 proteins that interact with the Jumonji domain of Gis1 can also bind to REC^{Rim15}.

Future studies should be directed towards understanding the role of the zinc finger in mediating the association of Bud27 with Rim15, the conditions under which Rim15 interacts with Bud27 and hence with the Gis1-complex, as well as the role of phosphoinositides in mediating this interactions. It would be interesting for instance to analyze these interactions in PtdIns kinase mutants, where the levels of PtdIns are altered.

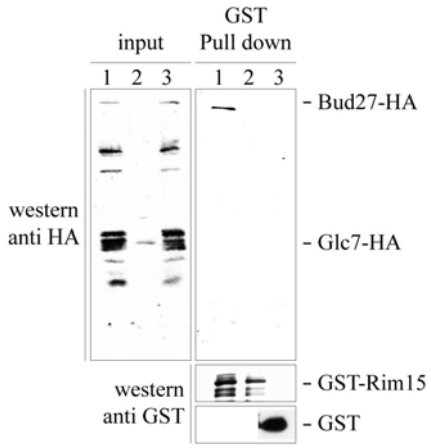

Figure 26

Co-precipitation experiment, showing that Rim15 interacts with Bud27 *in vivo*. Bud27-HA (lanes 1 and 3) or Glc7-HA (lane 2) under the control of the strong *TDH3* promoter, were co-expressed with either GST-Rim15 (lanes 1 and 2) or GST alone (lane 3).

Interestingly, also the receiver (REC) domain of Rim15 interacted with some components of the Gis1-complex, namely the silencing regulator Sir4 and a component of the TFIID complex (Table II). The multiple interactions between the Rim15 domains and components of the dynamic Gis1-complex indicate a possible mechanism by which Rim15 may regulate the functions of this transcriptional activator/repressor.

Notably, the observation that the zinc finger domain was involved in protein-protein interactions is consistent with the published observation that most C_2CH zinc finger have intrinsic protein-protein binding activities as well as with our previous observation that this domain interacted with the C-terminal REC domain in Rim15 an that this interaction required the zinc-coordinating histidine 256.

			DBD fusion			
AD fusion	Insert (Aa)	Full length (Aa)	C2HCZnF^{Rim15}	CAHCZnF^{Rim15}	C2ACZnF^{Rim15}	Msb2
Msb2	85-400	796	12.3 ± 4.2	18.3 ± 9.1	19.0 ± 3.7	n.d.
REC^{Rim15}	1635-1753	1776	71.7 ± 15.6	21.3 ± 5.3	**59.3** ± 10.7	5.1 ± 1.2

Table III

Two-hybrid interactions between the receiver domain of Rim15 (REC^{Rim15}) and the C_2HC zinc finger domain (C_2HCZnF^{Rim15}) or mutant versions where the putative zinc coordinating residues cysteine 244 (CAHCZnF^{Rim15}) and histidine 256 (C_2ACZnF^{Rim15}) were individually replaced with an alanine residue. The plasma membrane protein Msb2 was used as a negative control.

The Rim15 protein kinase contains a non-canonical receiver domain (REC)

The C-terminal region of Rim15 contains a non-canonical receiver domain (REC). Despite the considerable sequence conservation, the receiver domain of Rim15 lacks the critical aspartate residue that has been shown to mediate the phosphotransfer reactions in two-component and phosphorelay systems (Figure 27). It is conceivable that the REC-like domain in Rim15 originated from a canonical REC domain, but has then evolved a separate function. For instance it may have conserved the ability to form dimers, which is well documented for other REC domains [164], or to interact with proteins of canonical two-component systems. Notably, some receiver domains have been shown to undergo protein-protein interactions also in their non-phosphorylated state, although the function of these interactions has not been investigated [164]. Substitution of Asp13 in CheY, or Asp11 in CheB, with a lysine residue was shown to constitutively activate the response regulator even in the absence of phosphorylation of the receiver aspartate, perhaps by stabilizing the domain in its active conformation [170,189]. These observations indicate that non-canonical REC domains may exist that do not depend on aspartate phosphorylation for their function.

Despite the differences with canonical REC domains, the presence of a REC domain in Rim15 is intriguing, in particular since the same molecule also contains another domain that is recurrently found in phosphorelay and two-component systems, namely the PAS domain [133].

Alternatively, the non-canonical receiver domain in Rim15 may be regulated by phosphorylation on a different residue. Interestingly, when the phosphate acceptor Asp57 in CheY is changed to another amino acid, the protein is still phosphorylated at a site that apparently is not an acidic residue [170]. Although it is not known whether this secondary site is phosphorylated in the wild-type protein, or if it has any functional role, this observation indicates that variations of the common REC domain may exist that still support phosphotransfer reactions at sites different from the conserved aspartate residues.

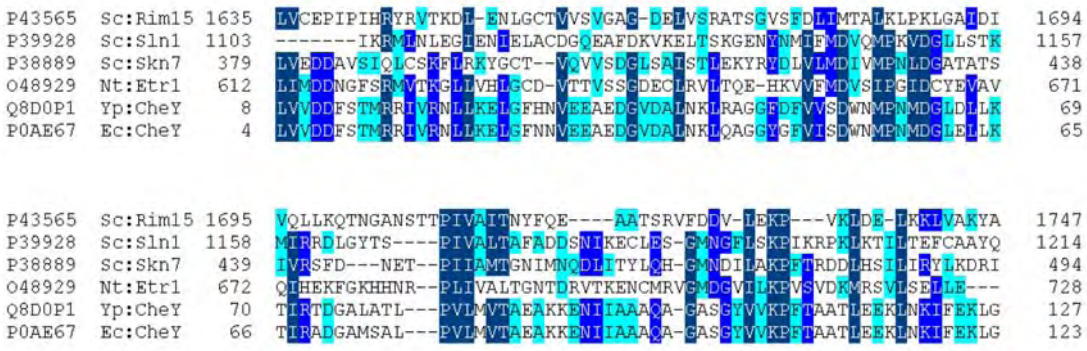

Figure 27

Alignment of the REC domains found in the C-terminal region of Rim15 with well-defined receiver domains. Amino acids that are conserved in more than 50%, 70% and 90% of the sequences are shown in light blue, blue and dark blue, respectively.

Standard phosphorelay reactions are initiated by autophosphorylation on a histidine residue in a sensory histidine kinase. As *S. cerevisiae* encodes only one histidine kinase, namely the osmosensor Sln1 [190], it would be interesting to verify whether Rim15 can directly accept phosphate residues from these protein.

Interestingly, we found that the isolated Rim15 REC domain (REC^{Rim15}) interacts with the C_2HC-type zinc finger domain of Rim15 ($C_2HC\text{-}ZnF^{Rim15}$) and with components of the Gis1-complex in a two-hybrid assay (Table II), suggesting a possible role of REC^{Rim15} in forming an intra- and inter-molecular interactions (see also above).

Conclusions and outlook

The complexity of Rim15 regulation is reflected in its multidomain composition

Analysis of the Rim15 sequence revealed the presence of three conserved regions flanking the catalytic serine/threonine kinase domain. The presence of multiple domains on the Rim15 polypeptide reflects the complexity of the function and regulation of this protein, which is operating at the crossroad between important signaling pathways.

The work presented in this chapter was aimed at the characterization of these domains. Two of these domains, namely the Per-ARNT-Sim (PAS) domain and the receiver (REC) domain, resemble previously described domains acting in phosphorelay signaling systems. Both of these domains, although significantly conserved, appear to functionally deviate from common PAS and REC domains. This may indicate that they represent novel, distinct modules that, even though related to the described PAS and REC domains, may have acquired a new function. Alternatively, these domains could be mere relicts of ancient domains that lost their function during evolution through mutations of the functionally essential residues.

The third domain is a putative zinc finger that had not been described previously. This cysteine-rich module is not only similar to PHD and FYVE domains, but also appears to share with them the property to interact with phosphoinositides.

Possible roles of the conserved motifs in Rim15

Based on our studies, the PAS domain does not appear to have an essential function for the activity of Rim15. The targeted removal of this domain does not alter Rim15 activity *in vivo,* as assessed by measuring the trehalose accumulation during the stationary phase as an indirect readout for Rim15 activity. It is possible that this domain cooperates with other mechanisms to fine tune the enzymatic activity of the Rim15 kinase and that removing it individually is not sufficient to detect significant changes, in particular when using indirect an readout to study the activity of Rim15 *in vivo*. PAS domains are usually part of cytoplasmic sensory proteins and undergo conformational changes upon stimulation by binding a ligand or by modification of an associated cofactor. These conformational changes ultimately affect, positively or negatively, the activity of the protein. The only eukaryotic serine/threonine kinases known to possess a PAS domain are the PAS Kinases (PASK) found in both the human and yeast genomes. As these kinases are known to be negatively regulated *in cis* by a PAS domain located N-terminally to the catalytic domain, we investigated the possibility that the Rim15 PAS domain would also regulate the activity of the kinase domain.

Deletion of the PAS domain of Rim15 resulted in a minor positive effect with respect to the *in vitro* activity of the purified kinase. However, added in excess, a bacterially purified PAS^{Rim15} domain had no significant inhibitory effect on the kinase activity of Rim15 *in vitro*. Notably, the failure of the bacterially purified PAS^{Rim15} domain to efficiently reduce the activity of Rim15 *in vitro* may be simply due to the ligand-status of the purified domain, which may not correspond to its functional configuration. In other words, if the PAS domain functions as an inhibitor exclusively in a configuration that is lost during the purification procedure this domain would be non-functional in our assays. This argument may also apply to our kinase assays using the full length Rim15 and Rim15 without the PAS domain.

It is also important to mention that the reports showing the role of the PAS domain in hPASK, compared the kinetic constants (*k*cat) of the enzymes. In this context, our kinase assays (using the artificial substrate α-casein) were not suited to address minor differences in the *k*cat of Rim15.

Interestingly we found several indications that the PAS domain of Rim15 may be involved in both inter-molecular (probably with an upstream kinase) and inter-molecular protein-protein interactions. The finding that the PAS domain can form dimers and interact with full length Rim15 protein, suggests that, as was shown for some nuclear receptors in higher eukaryotes (*e.g.* the planar aromatic hydrocarbons receptor AHR), Rim15 may undergo PAS-dependent dimerization [191].

In contrast to the PAS domain, the C_2CH zinc finger domain of Rim15 had a strong impact on Rim15 activity *in vivo* as well as *in vitro*. Loss of the residues that are predicted to coordinate the zinc ion, and thus contribute to the structure of the motif, impaired the function of the kinase. Interestingly the zinc finger domain was also able to bind specifically two phosphoinositide species, namely PtdIns(3)P and PtdIns(5)P, that have been found in both cellular membranes and nuclear structures. The mutations described above affected the ability of the protein domain to interact specifically with PtdIns, resulting in non-specific binding to all tested species. Nevertheless, our current data do not allow us to establish a causal link between the ability of the C_2CH zinc finger domain to interact with lipids and its regulatory role. Interestingly, the C_2CH zinc finger domain of Rim15 also interacted with the putative TORC1 target Bud27, which was recently found to be an essential component of a complex containing the transcription factor Gis1, which is likely to be regulated by Rim15 by not yet understood mechanisms. Another interesting aspect was our finding that the zinc finger domain fused to GFP was localized predominantly in the nucleus of yeast cells. This raises the intriguing possibility of a specific interaction with nuclear phosphoinositide pools. Importantly, nuclear phosphoinositide pools are present in the insoluble chromatin fraction as well

as in newly identified subnuclear structures called nuclear speckles [183]. Tethering Rim15 and possibly associated transcriptional regulators to subnuclear regions by the interaction with phosphoinositides may be relevant for their function. In this context, it would be interesting to test in the future whether alterations in the physiological distribution of PtdIns (*i.a.* those caused by deletion of different non-essential PtdIns kinases) affect the subcellular localization of the zinc finger constructs and/or the function of Rim15 *in vivo*.

Our preliminary characterization of the REC^{Rim15} domain indicates that there may be a relationship between this domain and the zinc finger domain. Notably, both motifs interact with each as well as with a number of proteins that were described as components of the Gis1-complex in a two-hybrid assay. Further studies should aim at deciphering the exact nature of the interactions between the Rim15 REC domain and any of the proteins that form the Gis1-complex. Such studies should also address the role of the potential, non-canonical phosphate acceptor residues in the REC^{Rim15} domain for the corresponding interactions. It would be also interesting to determine the phosphorylation status (for example by MS) of the REC^{Rim15} domain under conditions known to influence the activity of Rim15, or to assess its ability to accept phosphate group from a histidine donor.

To conclude, while the C_2CH zinc finger domain is critical to the function of Rim15; both the REC and PAS domains appear to be far less important for the activity of Rim15 both *in vitro* and *in vivo*. Nevertheless, one major constraint of our analysis was the fact that we had not yet a bona fide Rim15 target at hand. As illustrated in chapter III (page 115) we were able to identify such a substrate during the course of this thesis. This tool should be exploited in future experiments to address more subtle questions, such as the role of the Rim15-PAS and -REC domains.

Chapter II

Modulation of the G_0 transcriptional program by Rim15

Modulation of the G_0 transcriptional program by Rim15

The G_0 transcriptional program

The response to starvation involves a relatively rapid cessation of general transcription and translation activities. Concomitantly, genes whose products are required for survival in the post-diauxic phase and in G_0 are specifically induced. The comparison of global transcriptional changes induced by the deprivation for different nutrients, during the diauxic shift, or following a rapamycin treatment has both revealed great similarities, but also the specificities, of each of these responses [14,19,20,192]. Of particular interest for our studies is the subset of nutrient-regulated responses that is controlled via the TORC1 pathway. In this chapter, I present a comparative analysis of the rapamycin- and diauxic shift-induced transcriptional changes. Specifically, I present a study of the relative contributions of the nutrient-sensitive kinase Rim15 and the transcription factors Gis1 and Msn2/Msn4 to both responses.

The work presented here has lead us to appreciate the role of Rim15 in mediating the induction of a significant part of the diauxic shift and G_0 transcriptional programs, which includes transcriptional activation of many genes that are known to be regulated by the TORC1 and the PKA pathways. Our data suggest that Rim15 may control G_0-specific transcription by modulating the transcriptional activity of the transcription factors Msn2/Msn4 and Gis1.

The diauxic shift transcriptome

The transcriptional changes observed during the diauxic shift reflect in part the redirection of the cellular metabolism towards respiration, as well as the reduced protein synthesis rate of slow growing cells. These changes are complex and require the integration of many nutritional and metabolic signals.

During the diauxic shift, there is a massive decrease in the transcription of genes devoted to protein synthesis, including ribosomal protein, tRNA synthetase, and translation initiation factor genes [192]. Control of ribosomal protein biogenesis is mainly exerted at the transcriptional level, through a common upstream-activating element (UAS_{rpg}) recognized by the Rap1 DNA-binding protein (see also general introduction). Rap1 participates in the activation of many RNA polymerase II transcripts (*i.e.* mRNA precursors and most snRNA) in exponentially growing cells [193]. Moreover, it is the primary transcription factor for glycolytic genes and several translation factor

genes and binds different consensus sequences [194]. Notably the levels of Rap1 protein as well as of the *RAP1* mRNA decline during starvation [192].

For the transcription of ribosomal protein genes, Rap1 is required to interact with the two Rap1-cofactors Fhl1 and Ifh1, a process that is controlled by TORC1 [195]. Interestingly, in a mutant strain where the PKA pathway is constitutively active due to the deletion of the high-affinity cAMP-dependent phosphodiesterase (encoded by *PDE2*), almost all ribosomal protein genes (*RPG*s) are upregulated, implicating also the PKA pathway in this process [196].

Similarly, the transcription of rRNA decreases during the diauxic shift due, at least in part, to the reduction of actively transcribed rRNA genes. This reduction depends on one hand on the activity of the silencing factor Rpd3. On the other hand in addition, also the transcription rate of the individual "active" rRNA genes is also decreased [197]. Importantly, treating the cells with rapamycin reduces the initiation of transcription at the rRNA loci [75].

While the cellular translational machinery is coordinately downregulated as a result of entry into the diauxic shift, the increased needs for mitochondrial biogenesis necessitates the general induction of nuclear encoded mitochondrial genes, including those for mitochondrial ribosomal proteins [192].

One of the functions of transcriptional remodeling during the diauxic shift is to adjust the cellular metabolism to respiratory growth. During this adjustment phase, the transcription of glycolytic genes, like the pyruvate decarboxylase encoding gene, is shut down. Concomitantly, genes required for gluconeogenesis, for the TCA cycle, and for the glyoxylate cycles are upregulated. Early TCA cycle genes are under the dual control of HAP2/3/4 and Rtg1/3, while late TCA cycle genes are exclusively under the control of the HAP2/3/4 complex [192,198,199]. The heterotrimeric transcriptional activator complex HAP2/3/4 is also responsible for the induction of several genes important for respiration. Importantly, the transcription of *HAP4* itself was shown to be induced during the diauxic shift [192].

The accumulation of storage carbohydrates, one of the distinctive characteristics of G_0 cells, is also controlled at the transcriptional level [192].

Interestingly, shifting cells from a fermentable (glucose) to a non-fermentable (ethanol) carbon source - a treatment believed to mimic the diauxic shift - results in the induction of some genes that are also under the control of the nitrogen discrimination pathway (NDP) such as genes of the allantoin utilization pathway, a variety of permeases and of vacuolar proteases [65]. However this induction may not involve the "classical" NDP pathway, since the pattern of induction of NDP target genes following the shift from fermentable to non-fermentable carbon differs from the pattern

of induction following the shift from a high- to low-quality nitrogen source. The existence of a carbon discrimination pathway (CDP) has been suggested, which can induce a subset of genes known to be under control of the NDP pathway, by regulating the GATA-tape transcription factors Gat1 and Gln3 [65].

Genes possessing stress responsive promoter elements (STRE) are also expressed during the diauxic shift by the transcription factors Msn2 and Msn4 [192]. Moreover, glucose repressed genes, whose promoters contain a regulatory element known as the carbon source-responsive element (CSRE) are derepressed or even actively induced at late timepoints during the diauxic shift [192].

Another class of genes (the *SNZ* genes) is expressed specifically very late, after entry into quiescence, and has thus been proposed to represent a hallmark of a general core quiescence program [200]. The role of these highly conserved genes during quiescence is not known yet, interestingly the products of *SNZ1, SNZ2* and *SNZ3* are required for vitamin B_6 biosynthesis; a role of vitamin B_6 as a cofactor in stationary-phase specific processes or as an antioxidant has been suggested [201].

The transcriptional response to rapamycin

Rapamycin-treated cells resemble in many aspects glucose-deprived cells. The striking similarity between the transcription profiles of cells shifted to low-quality carbon or nitrogen sources and cells treated with rapamycin, suggests a central role of the TORC1 pathway as a sensor of the quality of both these key nutrients [65]. The TORC1 pathway, initially suggested to be a nitrogen sensor, appears to modulate the starvation-responsive transcription depending on the quality and quantity of the limiting nutrients. Cells treated with rapamycin, like glucose-deprived cells, downregulate hexose transporter gene transcription and induce the transcription of genes involved in respiration. In addition, downregulation of the TORC1 pathway by rapamycin results in increased transcription of genes required for the import and metabolism of low-quality nitrogen sources such as proline or urea [14]. Many, but not all of the rapamycin-induced transcriptional effects are mediated by Tap42 and its associated phosphatases. The transcriptional regulation of translation machinery, TCA cycle, and NDP target genes, as well as genes encoding enzymes implicated in carbohydrate storage and purine biosynthesis depend on Tap42 complexes.

Transcription of a subset of rapamycin-regulated genes, including genes encoding proteins implicated in ATP synthesis, proteasome function, and mRNA export/decay is controlled largely independently of Tap42.

As observed during the diauxic shift, treatment of yeast cells with rapamycin results in a strong transcriptional response aimed at inhibiting translation at multiple levels. Accordingly, ribosomal protein genes, rRNA and tRNA synthesis and processing genes, translation initiation and elongation factors genes, and mRNA export and decay genes are repressed following rapamycin treatment [14]. In contrast, genes encoding mitochondrial ribosomal proteins and tRNA synthetases are upregulated [14].

Genes involved in glyoxylate and TCA cycles and in storage carbohydrate biosynthesis are induced by rapamycin, while glycolytic genes are increasingly repressed with time [14]. The transcription factor Gcr1 controls the transcription of hexose transporter genes as well as of most glycolytic genes; rapamycin, but not the diauxic shift, appears to (negatively) control the expression of this factor at the transcriptional level [14]. Similarly, nearly all of the TCA cycle genes are upregulated in response to rapamycin, albeit less strongly and more transiently that during the diauxic shift [14], suggesting that the TORC1 complex may be upstream of the HAP2/3/4 complex. In addition, the transcription factors Rtg1 and Rtg3 accumulate into the nucleus upon rapamycin treatment [17]. Together, all these data implicate the TORC1 pathway in the regulation of the switch from fermentation to respiration. Notably, the Tor proteins have been shown to regulate the nuclear translocation of the transcription factors Msn2 and Msn4 and of the protein kinase Rim15 by regulating their dissociation from their 14-3-3 anchor proteins [13,78,202].

Rapamycin also activates the nitrogen discrimination pathway (but not the nitrogen starvation response) despite the presence of high quality nitrogen sources in rich media. Accordingly, several permeases are induced by rapamycin, including the membrane permeases *GAP1* and *MEP2*. Genes in the allantoin and in the proline utilization pathways (low quality nitrogen sources) as well as genes encoding enzymes of the glutamine biosynthetic pathway, vacuolar proteases and other proteins required for autophagy are also upregulated [14].

In conclusion inactivation of the TORC1 pathway by rapamycin results in the induction of a transcriptional program that is closely related, but not identical, to the early diauxic shift program. Accordingly genes containing the CSRE in their promoter, which are induced late during the diauxic shift, are not induced by a treatment with rapamycin. This indicates that inhibition of the TORC1 pathways does not mimic a relief of glucose repression. Rapamycin also controls glucose-sensitive signaling pathways that are not regulated during the diauxic shift; involving notably, the transcription factor Rgt1 and its repressor Grr1 [14]. The analysis of the diauxic shift and rapamycin induced changes in the transcriptome support a view where the different nutrient- and stress-

signaling pathways form a network that cooperatively and precisely regulates the adaptive responses depending on the exact nature of the incoming nutrient signals.

Results and discussion

Since Rim15 appears to be a key regulator of G_0 entry, we decided to more precisely define its role by studying the genome-wide transcriptional profiles of wild-type and *rim15Δ* mutant cells at the diauxic transition. We had previously observed that the transcription of some of the genes regulated via stress responsive (STRE) elements (Msn2/Msn4 dependent genes) and post diauxic shift (PDS) elements (Gis1-dependent genes) failed to be induced at the diauxic transition in the absence of Rim15. To further explore whether Rim15 may act through Msn2/Msn4 and/or Gis1, we analyzed the relative contribution of Rim15, Msn2/Msn4 and Gis1 by comparing the global transcription profiles of the different mutants.

The diauxic shift transcriptome

Wild-type yeast strains and the three deletion strains lacking *RIM15*, *GIS1* or *MSN2* and *MSN4* together, were maintained for 24 hours in the exponential phase by repeatedly diluting the cultures with fresh glucose-containing growth medium in order to obtain maximal repression of diauxic shift and stationary phase transcripts. Then, the cells were grown under continuous monitoring of the optical density of the cultures and of the glucose concentration. A first sample was collected during the exponential phase (OD_{600}~1), then a diauxic shift sample was collected 30 minutes after the complete depletion of glucose from the culture medium. To analyze the specific changes that occur during the diauxic transition for each strain, we compared the mRNA levels in the diauxic shift sample with the mRNA levels of the exponential phase sample. We then compared the relative induction/repression in the mutants with the ones in the wild type. This experiment was repeated two times independently and the two datasets were averaged for subsequent analyses. Since the correlation between both datasets was not optimal (with R-squared values lower than 0.5), we discarded genes that displayed high variation between two dataset from further analysis. The remaining 4605 ORFs gave highly reproducible results. As we expected, Rim15 and the transcription factors Msn2/Msn4 and Gis1 to positively regulate the diauxic shift transcriptional response, we were particularly interested in genes that were induced in the wild-type strain (>2 fold induction), and whose induction was affected in the mutants (<1.5 fold induction). Importantly our data for the wild-type strain matched previous reports and are not discussed in detail here [192]. These data were presented in a report from our lab, published in 2004 [113].

Rim15-dependent induction of a distinct set of genes at the diauxic shift

We found six prominent classes of genes that were dependent on Rim15 for their proper induction at the diauxic shift. These classes represent genes whose products are involved in carbohydrate metabolism, general and oxidative stress response, respiration, lipid and fatty acid metabolism and peroxisomal functions (Table IV).

One interesting observation emerging from our genome-wide transcription analysis was that the Rim15 regulon comprises several gene clusters that are implicated in the adaptation to respiratory growth and in the utilization of fatty acids as energy source. Even more interestingly these genes were coordinately regulated with oxidative stress genes, whose products are involved in the antioxidant defense (*e.g. SOD1*, *TRX3* and *CYC1*), regeneration of NADPH (*e.g. ZWF1*, *UGA2* and *GAD1*) and detoxification of metabolic intermediates (*e.g. GLO1*, *GLO2* and *GTT1*). Mitochondrial respiration and fatty acid β-oxidation are recognized as the primary sources of superoxide and hydrogen peroxide in eukaryotic cells. It is therefore not be surprising that the transcription of the enzyme systems required to sustain this metabolic mode and the transcription of genes required to limit the consequent oxidative damage are co-regulated.

Notably, Rim15 was reported to play a key positive role in the determination of the chronological life span, which corresponds to the ability of a stationary culture to maintain viability over time [203,204]. Accordingly, in the absence of Rim15 yeast cells show a reduced chronological lifespan. As oxidative damage by reactive oxygen species (ROS) is thought to be one of the principal causes of chronological aging, the failure to properly induce oxidative stress defenses during the diauxic transition may provide one possible explanation of the reduced longevity of *rim15Δ* mutant cells.

Overlap between the Gis1, the Msn2/Msn4 and the Rim15-dependent genes

Interestingly, most of the genes that depend on Rim15 for their correct induction during the diauxic shift contain STRE or PDS elements in their promoter regions (Table IV). Moreover, when we compared the genome-wide transcriptional profiles of *msn2msn4*, *gis1Δ* and *rim15Δ* mutant cells we found that virtually the entire set of Rim15-dependent genes was included within the combined sets of Gis1 and Msn2/Msn4-dependent genes (Figure 28). Thus, while a fraction of the Gis1- and the Msn2/Msn4-dependent gene sets (27% and 40% respectively) may be controlled independently of Rim15, Gis1 and Msn2/Msn4 appear to mediate the entire Rim15 dependent transcriptional response at the diauxic shift. An attractive model that may explain these findings is that Rim15 regulates the establishment of physiological-context specific interactions of the general

transcription machinery with Gis1, Msn2 and Msn4. This model is further supported by the observation that Rim15 exhibits two-hybrid interactions with three subunits of the general transcription factor TFIID (*i.e.* Taf25, Taf65 and Taf1, this work and our unpublished observations) as well as with several subunit of a newly identified Gis1-complex (See Chapter I, page 77) [188].

Another interesting aspect emerging from our genome-wide analysis was that almost the entire set of Gis1-dependent genes was included within the larger set of Msn2/Msn4-dependent genes (Figure 28). Since 55% of these shared genes harbor either STRE of PDS elements, or both elements combined, our data suggest that, during the diauxic shift, Gis1 and Msn2/Msn4 not only functionally overlap *in vivo*, but also regulate the transcription of a large set of genes in a cooperative manner.

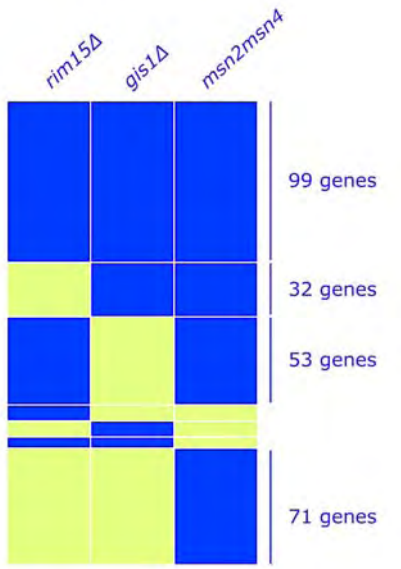

Figure 28

Graphical representation of the relative roles of Rim15, Gis1 and Msn2/Msn4 in the transcriptional changes during the diauxic shift. The number of genes that depend on either protein for their proper induction are represented by the area of the blue rectangles. Almost all of the genes that require Rim15 are transcribed in a Gis1- and/or Msn2/Msn4-dependent manner.

YEAST ORF	Gene	Description	Average fold change				Regulatory elements		
			wt	*rim15Δ*	*msn2/msn4*	*gis1Δ*	STRE	PDS	Other elements
Carbohydrate metabolism									
YGR248W	*SOL4*	6-phosphogluconolactonase	3.84	1.35	2.14	3.91	1	2	
YBR241C		Hexose transporter family member	3.76	1.45	-1.19	1.39	0	1	
YIR036C		Oxidoreductase	3.21	-1.78	1.34	1.21	1	1	HAP2/3/4/5
YOL157C		Alpha-glucosidase	2.84	1.44	1.25	1.60	1	1	
YDL174C	*DLD1*	D-lactate dehydrogenase activity	2.81	1.22	-1.18	-1.01	1	0	YAP1
YNL037C	*IDH1*	Isocitrate dehydrogenase	2.70	1.33	1.33	1.13	2	0	HAP2/3/4/5, HSE
YPL262W	*FUM1*	Fumarate hydratase	2.64	1.12	1.12	1.92	2	0	
YGR193C	*PDX1*	pyruvate dehydrogenase complex	2.31	-1.15	1.00	1.21	2	0	HAP2/3/4/5
YNR072W	*HXT17*	Hexose transporter	2.25	1.18	-1.03	-1.07	1	0	
YDR001C	*NTH1*	Neutral trehalase	2.18	1.27	-1.03	1.71	3	0	
YDR387C		Hexose transporter family member	2.12	1.24	1.48	1.25	0	0	YAP1
YGL104C		Hexose transporter family member	2.11	1.18	-1.04	1.17	1	0	
YIL154C	*IMP2'*	Transcription factor	2.11	1.31	-1.17	1.14	1	0	HAP2/3/4/5, HSE
YPR006C	*ICL2*	Isocitrate lyase	2.07	1.27	1.83	1.58	0	1	HAP2/3/4/5
YBR056W		Glucan 1,3-beta-glucosidase	2.06	1.30	-1.51	1.09	1	0	YAP1
YPR001W	*CIT3*	Citrate synthase	2.02	-1.40	1.41	-1.35	0	1	HAP2/3/4/5, YAP1
YOR393W	*ERR1*	Oxidoreductase	2.01	1.21	1.33	-1.15	4	0	
YBR001C	*NTH2*	Neutral trehalase	2.01	1.25	1.14	1.62	1	0	YAP1, HSE
Stress response									
YBL075C	*SSA3*	Heat shock protein	9.64	1.21	1.99	1.75	0	2	
YPL240C	*HSP82*	Heat shock protein	2.85	1.25	1.05	1.86	2	1	HAP2/3/4/5, YAP1
YER096W	*SHC1*	Sporulation specific protein	2.47	1.14	1.41	1.36	1	2	YAP1
YIL033C	*BCY1*	PKA, regulatory subunit	2.44	1.32	-1.36	1.13	0	0	HAP2/3/4/5
YLR259C	*HSP60*	Heat shock protein	2.42	-1.10	1.49	1.34	0	1	HSE
YPL203W	*TPK2*	PKA, catalytic subunit	2.22	-1.12	-1.18	1.54	1	0	
YBL105C	*PKC1*	ser/thr protein kinase	2.04	1.27	-1.13	-1.06	1	0	
Oxidative stress response									
YIR038C	*GTT1*	Glutathione-S-transferase	3.17	1.02	1.16	1.41	3	0	YAP1
YML004C	*GLO1*	Glyoxalase I	3.16	-1.13	-1.33	1.98	2	2	HSE
YMR250W	*GAD1*	Glutamate decarboxylase	3.11	1.31	-1.07	1.49	1	1	HAP2/3/4/5
YOR031W	*CRS5*	Metallothionein	2.30	1.25	-1.04	2.03	3	2	HAP2/3/4/5
YBR006W	*UGA2*	Succinate-semialdehyde dehydrogenase	2.20	-1.12	-1.42	1.38	0	0	HSE, YAP1, HAP2/3/4/5
YCR083W	*TRX3*	Mitochondrial thioredoxin protein	2.11	1.43	-1.13	1.30	1	0	
YDR272W	*GLO2*	Glyoxalase II	2.10	1.21	-1.18	1.23	0	2	YAP1
YJR048W	*CYC1*	Cytochrome-c isoform	2.05	1.11	1.69	-1.25	0	0	HAP2/3/4/5, HSE
YJR104C	*SOD1*	Superoxide dismutase	1.92	-1.36	-1.34	1.01	2	1	YAP1
YPL202C	*AFT2*	Transcription factor	1.80	-1.17	1.23	1.03	0	0	HAP2/3/4/5
YNL241C	*ZWF1*	Glucose-6-phosphate dehydrogenase	1.78	-1.21	-1.01	-1.38	5	1	
Respiration									
YLR327C		Putative ATPase stabilizing factor	3.35	1.20	2.00	3.43	3	0	
YDR231C	*COX20*	Cytochrome-c oxidase assembly	2.79	1.16	1.07	2.57	1	0	HAP2/3/4/5
YKL016C	*ATP7*	F0-ATPase complex	2.47	1.12	1.31	1.54	0	0	HAP2/3/4/5, YAP1
YLL009C	*COX17*	Cytochrome-c oxidase assembly	2.40	1.14	1.10	1.30	1	0	HSE
YNL052W	*COX5A*	Cytochrome-c oxidase chain	2.28	1.37	-1.07	1.20	0	0	HSE
YMR145C	*NDH1*	NADH dehydrogenase	2.15	1.12	1.37	1.37	4	1	HAP2/3/4/5
YNL073W	*MSK1*	Lysyl-tRNA synthetase	2.13	-1.64	-1.15	1.78	1	0	HSE
YBL045C	*COR1*	Ubiquinol-cytochrome-c reductase	2.12	1.25	1.49	1.79	2	1	HAP2/3/4/5, HSE
YIL136W	*OM45*	Mitochondrial membrane protein	2.05	-1.06	1.49	1.40	3	0	
YIL006W		Mitochondrial carrier family member	2.02	1.11	1.33	1.04	1	1	YAP1
Lipid and fatty acid metabolism									
YDR313C	*PIB1*	PI(3)-phosphate binding protein	2.99	1.01	1.45	1.54	1	0	
YDR497C	*ITR1*	Major myo-inositol permease	2.98	-1.21	1.82	-1.24	0	0	HAP2/3/4/5
YKR067W	*GPT2*	Glycerol-3-phosphate O-acyltransferase	2.63	1.37	-1.02	2.22	2	0	HAP2/3/4/5
YAR035W	*YAT1*	Carnitine acetyltransferase	2.59	1.18	1.14	1.24	2	0	
YGR216C	*GPI1*	GPI anchor biosyntheses	2.58	1.20	1.24	1.36	1	1	HAP2/3/4/5, HSE, YAP1
YDR173C	*ARG82*	Phosphatidylinositol kinase	2.33	1.31	1.59	1.79	0	1	HAP2/3/4/5, HSE
YJR073C	*OPI3*	Phospholipid methyltransferase	2.19	1.25	-1.14	1.93	1	0	HAP2/3/4/5, HSE
YEL020C		Putative oxalyl-CoA decarboxylase	2.04	1.05	1.09	1.20	0	1	
YKL020C	*SPT23*	Transcriptional activator	2.00	1.22	1.19	1.19	0	0	
Peroxisomal functions									
YBR222C	*FAT2*	AMP-binding protein	3.16	-1.05	1.68	1.45	1	0	
YIL160C	*POT1*	Acetyl-CoA C-acyltransferase	2.62	-1.01	1.42	1.22	0	0	YAP1
YDL078C	*MDH3*	Malate dehydrogenase, peroxisomal	2.19	-1.26	1.09	1.55	1	1	
YDR329C	*PAS3*	Peroxisomal assembly protein	2.01	-1.23	1.22	1.22	0	0	HAP2/3/4/5, HSE

Table IV

A change in mRNA levels was deemed significant based on the following criteria: the average fold change was consistent in duplicate experiments, the average fold change was >2 fold in wild type cells entering the diauxic phase, and the corresponding fold change in *rim15Δ* cells was <1.5 fold. Of the selected ORFs, the corresponding average fold changes in *msn2msn4* and *gis1Δ* cells are also shown. The number of STRE (5'-AGGGG-3') and PDS (5'-AGGGAT-3') consensus sites within 1000 base pairs (bp) upstream of the transcription start sites of the corresponding ORFs is indicated, where additional regulatory sequences were identified these are indicated (overlapping matches were allowed).

The rapamycin transcriptome

Previously published results indicated a partial overlap between the transcriptional changes elicited by the macrolide antibiotic rapamycin and those occurring during the diauxic shift (see introduction). These observations suggested that under physiological conditions the TORC1 complex may have a role in sensing and transducing signals from a satisfactory environment and counteracts the induction of a subset of the diauxic shift and G_0-regulated genes [65].

Since Rim15 is both a target of the TORC1 pathway and a key regulator of the transcriptional changes that occurs during the diauxic shift transition, we asked whether Rim15 was also necessary for the transcriptional induction of other rapamycin-controlled genes. To this purpose, in collaboration with Dr. James Broach (Princeton University), we conducted a global transcription study of various strains (*i.e.* the *rim15Δ*, *igo1Δigo2Δ*, *msn2Δmsn4Δ*, *gis1Δ* mutant strains and the corresponding wild-type strain) treated with rapamycin.

We then compared the transcription profiles of wild-type cells exposed to rapamycin for different times with those of exponentially growing cells, again focusing on the transcripts that were induced by the treatment. The rapamycin-induced genes could be divided into three prominent classes, according to the kinetics of their induction: early genes, transiently expressed genes and late genes. The transcripts of the first large group of genes (503 genes) increased early (20 min) during the rapamycin treatment and remained high during the course of the experiment (180 min); these included genes of the nitrogen (*e.g. DAL80, DAL1, DAL2, GLN1, CIT2*) and carbohydrate (*e.g. PIK1, HXK1, GSY2, TPS2*) metabolism, as well as genes required for glutamine metabolism (*e.g. GDH2, GDH3, GLT1*). The 58 transcripts in the second class were induced transiently during the rapamycin treatment and returned (after 90 min) to the levels observed in growing cells. Finally, the 167 genes belonging to the third class were induced after > 40 min and most of these transcripts reached maximal levels after 180 min. To determine the role of Rim15 in these transcriptional responses we compared the level of transcription of a wild type and a *rim15Δ* strain in response to rapamycin. Surprisingly, in contrast to what observed during the diauxic phase, where nearly 80% of all upregulated genes required Rim15 for induction, the transcriptional response induced by rapamycin was largely Rim15-independent. Nevertheless, a small subset of genes was dependent on the presence of Rim15 for their induction by rapamycin. All of these genes belonged to either the first or the third class of genes (both of which are still induced after 180 min rapamycin treatment). This indicates that Rim15 is specifically involved in mediating the long-term effects of rapamycin on transcription (Table V).

Under physiological conditions, such as those experienced by yeast cells during the diauxic shift, Rim15 supposedly integrates signals from various nutrient sensing pathways. In contrast, rapamycin treatment specifically inhibits TORC1 even though all essential nutrient are available, consequently Rim15 may not receive additional inputs from other pathways. Moreover under these conditions the Rim15 protein is likely be expressed at low levels [93].

Importantly, when we compared the genes that were induced during the diauxic shift or by a rapamycin treatment, we found that only bout 53% of the genes are induced under both conditions and are thus likely to be part of a genetic program of quiescence.

Of the genes that were specifically induced by rapamycin, a small fraction (<10%) was controlled in a Rim15 dependent manner. In contrast more than 50% of the genes induced specifically during the diauxic shift depended on Rim15 for their induction. Of the remaining 181 genes that are induced by both, entry in the diauxic shift and a 180-min rapamycin treatment, 85 (47%) depended on Rim15 for their induction during the diauxic shift, while only 12 (< 7%) depended on Rim15 under both conditions. These data indicate that although some common genes are induced under both conditions (*i.e.* rapamycin and diauxic shift) the two responses are clearly distinct. In particular, some genes that are induced under both conditions have different requirements for Rim15-dependent induction.

Interestingly, a relatively small set of all the genes induced following a 180-min rapamycin treatment in the wild type depended on the transcription factors Msn2/Msn4 and Gis1 (this is also at variance with our corresponding results of diauxic-shift cells). Notably, many (>60%) of the genes that depended on Rim15 for transcriptional induction following a 180-min rapamycin treatment also depended on Gis1. Under these conditions Gis1 appeared to have a more important role than Msn2/Msn4 in mediating the Rim15-dependent response. In addition Gis1 also regulated 39 genes independently on Rim15, indicating that this transcription factor may have a previously unrecognized role during the response to rapamycin (Figure 29).

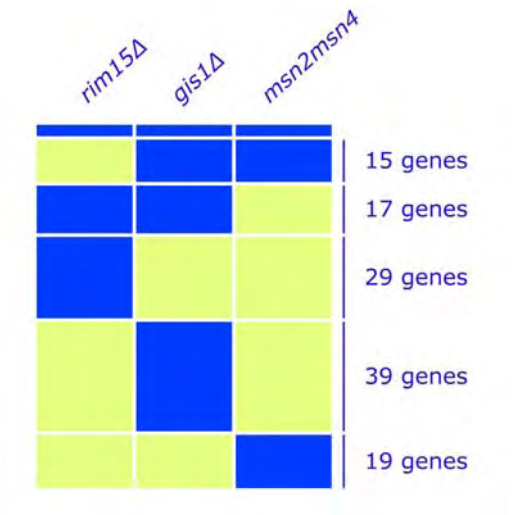

Figure 29

Graphical representation of the relative roles of Rim15, Gis1 and Msn2/Msn4 in the transcriptional changes elicited by rapamycin. The number of genes that depend on either protein for their proper induction are represented by the area of the blue rectangles.

Despite an apparently less important role of Rim15 in the response to rapamycin, when compared to its role during the diauxic shift, transcription of *RIM15* itself was induced in an Msn2/Msn4- and Gis1-independent manner, during the rapamycin time course (Figure 30). This strengthens the hypothesis that, despite the relatively mild transcriptional defect in rapamycin-treated *rim15Δ* cells, Rim15 is specifically required for the induction of a subset of the TORC1-controlled genes during the response to rapamycin.

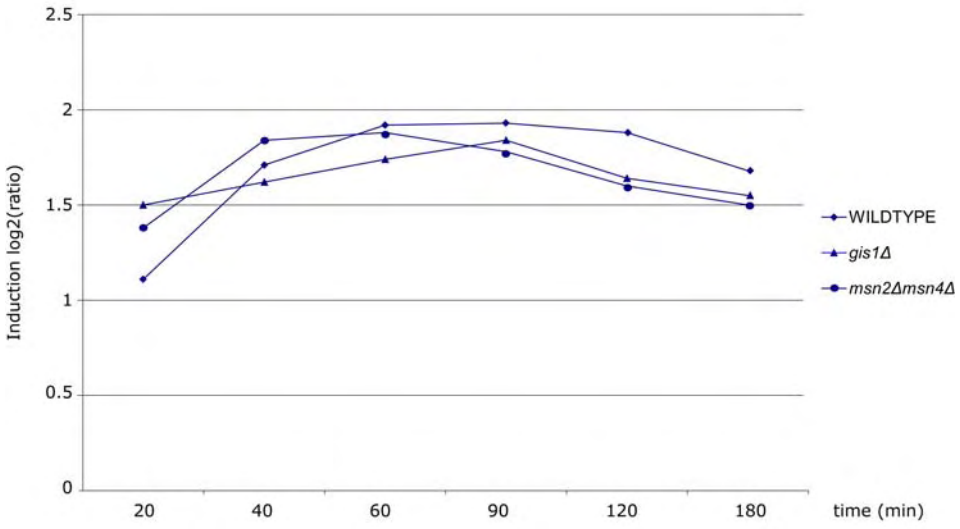

Figure 30

Transcriptional induction (expressed as log2 of the ratios) of *RIM15* during a 180-min treatment with rapamycin in wild type (diamonds) and *gis1Δ* (triangles) or *msn2Δmsn4Δ* (circles) cells.

Yeast ORF	Gene	Description	Fold Change (180-min rapamycin treatment)			
			wt	*rim15Δ*	*msn2Δmsn4Δ*	*gis1Δ*
Carbohydrate metabolism						
[a] YFR053C	*HXK1*	Hexokinase isoenzyme 1, glucose repressed	3.89	-1.72	3.78	1.45
YDR342C	*HXT7*	Hexose transporter	3.23	-2.68	1.79	-1.02
YDR343C	*HXT6*	Hexose transporter	2.91	-2.77	1.71	-1.08
[a] YDR148C	*KGD2*	Alpha-ketoglutarate dehydrogenase	2.64	1.44	2.36	1.62
YOR136W	*IDH2*	NAD-dependent isocitrate dehydrogenase	2.45	1.43	1.72	1.48
[a] YDR277C	*MTH1*	Repression of transcription by Rgt1 in the absence of glucose	2.27	-1.48	3.07	-1.27
[a,b] YJL137C	*GLG2*	Glycogenin glucosyltransferase	2.23	-1.05	1.67	1.55
[a] YKL085W	*MDH1*	Mitochondrial malate dehydrogenase	2.14	1.01	2.11	1.69
[a,b] YDL022W	*GPD1*	NAD-dependent glycerol-3-phosphate dehydrogenase	2.11	-1.27	3.71	1.11
Stress response						
[a,b] YBL075C	*SSA3*	ATPase activity, unfolded protien binding	3.97	1.35	2.60	1.19
YAL005C	*SSA1*	ATPase	2.97	-1.24	4.00	2.41
YPL240C	*HSP82*	Cytoplasmic chaperone	2.75	-1.16	2.83	2.23
YPL203W	*TPK2*	PKA, catalytic subunit	2.51	1.05	2.31	1.55
YML131W		Similarity to oxidoreductases	2.36	1.44	1.54	1.21
YPL004C	*LSP1*	Protein kinase inhibitor activity, induced by heat	2.35	1.20	2.00	1.23
YDL101C	*DUN1*	Protein kinase involved in DNA repair	2.30	1.28	1.61	1.68
YOR007C	*SGT2*	Similarity to chaperons, induced by heat	2.25	1.46	2.33	1.97
YDR513W	*GRX2*	Thioltransferase/glutathione reductase	2.17	1.48	1.72	1.75
YMR152W	*YIM1*	Mutant sensitive to DNA damaging agents	2.17	1.27	1.59	1.59
YNL234W		Heme binding protein	2.03	-1.01	2.91	1.88
[a,b] YIL033C	*BCY1*	PKA, regulatory subunit	2.03	1.24	1.66	1.58
YER095W	*RAD51*	DNA-dependent ATPase involved in DNA repair	2.03	1.45	1.83	1.56
YPR172W		Involved in multidrug resistance	2.01	1.40	1.30	1.39
Respiration, other mitochondrial functions						
YBR054W	*YRO2*	Unknown	3.81	-1.16	4.23	-1.87
YKL150W	*MCR1*	NADH-cytochrome b5 reductase	2.68	1.39	2.08	1.62
YDL181W	*INH1*	F1F0 ATP synthase inhibitor	2.36	1.40	2.53	1.85
[a,b] YJL102W	*MEF2*	Elongation factor, mitochondrial	2.31	1.42	2.38	2.03
YMR031C		Mitochondrial ptotein	2.14	1.34	1.72	1.53
YGR231C	*PHB2*	Subunit of the prohibitin complex, involved in mitochondrial segregation	2.14	1.41	1.82	1.59
[a,b] YBL045C	*COR1*	ubiquinol-cytochrome c oxidoreductase complex subunit	2.13	1.40	1.95	1.47
YCR004C	*YCP4*	electron carrier activity	2.11	-1.13	1.77	1.37
[a,b] YLL001W	*DNM1*	Dynamin-related GTPase, involved in mitochondrial fission	2.07	1.28	1.57	1.33
[a,b] YKL016Ca	*ATP7*	F1F0 ATP synthase subunit d	2.06	1.39	2.14	1.77
Proteolytic degradation						
YKL145W	*RPT1*	ATPase	2.38	1.45	2.03	1.68
YCL057W	*PRD1*	Zinc metalloendopeptidase	2.14	1.43	1.79	1.53
YDR427W	*RPN9*	Structural molecule activity	2.06	-1.07	1.46	1.22
Other functions						
YJL059W	*YHC3*	Vacuolar membrane protein, involved in aminoacid transport	2.66	1.35	2.99	2.10
YJL079C	*PRY1*	Pathogen Related in Yeast	2.62	1.44	3.51	1.64
[a,b] YIR036C	*IRC24*	Similarity with short-chain dehydrogenase/reductase	2.58	1.49	2.23	2.04
YOR230W	*WTM1*	Transcriptional repressor	2.43	1.45	2.39	1.52
[a,b] YOR161C	*PNS1*	Similarity to choline transporters	2.36	-1.29	1.60	1.42
YJL036W	*SNX4*	Phosphatidylinositol 3-phosphate binding	2.23	1.42	1.74	1.48
YGL047W	*ALG13*	UDP-N-acetylglucosamine transferase	2.23	1.29	2.30	1.97
YHL031C	*GOS1*	v-SNARE activity	2.20	1.10	1.13	1.01
YDR202C	*RAV2*	Regulator of (H^+)-ATPase in Vacuolar membrane	2.17	1.16	1.52	1.39
YIL140W	*AXL2*	Required for axial budding	2.14	1.36	2.38	2.43
[a,b] YDR313C	*PIB1*	Phosphatidylinositol 3-phosphate binding, protien ubiquitination	2.14	1.21	1.95	1.67
[a,b] YGR201C		Unknown	2.13	1.22	1.03	1.41
YER053C-A		Unknown	2.08	-1.49	1.60	-1.08
YPR037C	*ERV2*	Thiol oxidase activity	2.00	1.27	2.53	2.45

Table V

Genes induced following a 180-min treatment with rapamycin that depend on Rim15 for their induction. [a] Induced during the diauxic shift; [b] dependent on Rim15 during the diauxic shift.

TORC1 regulation of Rim15 is not mediated by theTap42-Sit4 phosphatase

As demonstrated by the results presented above, Rim15 is clearly involved in the induction of a small subset of the TORC1-controlled genes in response to a rapamycin treatment. Moreover the phosphorylation level and the localization of Rim15 are both known to be regulated by the TORC1 pathway [78]. We were therefore interested in defining the mechanism(s) by which TORC1 controls Rim15-phosphorylation and localization.

Notably, the localization of some TORC1-controlled transcription factors is regulated through TORC1 inhibition of the Tap42-PP2Ac and the Tap42-PP2A-like phosphatase complexes. When TORC1 is inactivated the Tap42-phosphatase complexes are thought to be released into the cytoplasmic compartment, where they transiently dephosphorylate and thereby activate starvation- and stress-responsive transcription factors, such as Msn2/Msn4 and Gln3.

To test whether Rim15 regulation by TORC1 may involve the downregulation of a dephosphorylation mechanism by TORC1, we analyzed the induction of Rim15-dependent transcriptional response to rapamycin in mutants lacking these phosphatases.

Deletion of *SIT4* encoding the catalytic subunit of the Tap42-Sit4 complex did not affect the ability of yeast cells to induce the accumulation of the Rim15-dependent transcripts *SSA3, HSP26* and *HAP12*, indicating that this complex is not required to Rim15 function.

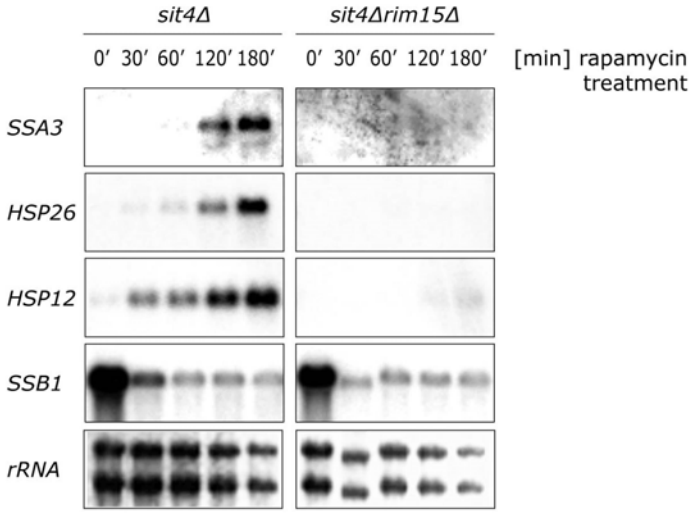

Figure 31

Northern blot analysis of the rapamycin-induced accumulation of Rim15-dependent transcripts in wild-type and *sit4Δ* mutant cells (*i.e. SSA3, HSP26,*and *HSP12*) in the absence of the PP2A-like protein Sit4. The Rim15-independent repression of *SSB1* by rapamycin was used as an internal control; equal amounts of total RNA were loaded in each lane.

Rim15 and PP2Ac inversely control rapamycin-induced transcription of G_0 genes

We next analyzed the effect of the deletion of the PP2A catalytic subunits encoded by *PPH21* and *PPH22*. Surprisingly, we found that deletion of *PPH21* and *PPH22* did not abolish the induction of Rim15-dependent genes (Figure 32), and they caused increased basal levels of the corresponding transcripts both in the presence and in the absence of *RIM15*. Treatment with rapamycin still causer induction of the transcription of these genes, indicating the presence of a rapamycin-response mechanism in these mutants (Figure 32).

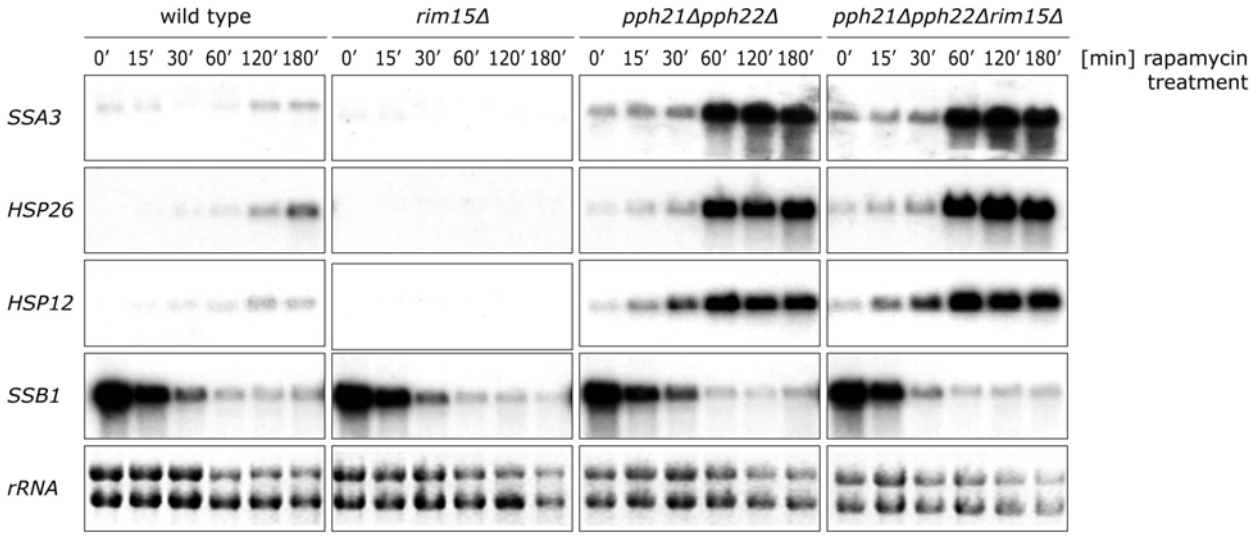

Figure 32

Northern blot analysis of the rapamycin-induced accumulation of Rim15-dependent transcripts (*SSA3, HSP26, HSP12*) in the absence of the PP2A catalytic subunits encoded by *PPH21* and *PPH22*. The rapamycin-repressible gene *SSB1* was used as an internal control for the effect of rapamycin. Equal amounts of total RNA were loaded on each lane.

Interestingly, and in line with our findings, overexpression of *PPH22* has been shown to mimic overactive PKA, which leads to high trehalase activity (and consequently low trehalose levels), constitutive repression of STRE-controlled genes, and heat sensitivity.

One possible explanation for our results is that Rim15 and the PP2Ac phosphatases impinge on a common target. The function of this presumed target may be kept to a basal level during the exponential phase by Pph21 and Pph22 (possibly by the TORC1 associated Tap42-PP2A complex or by the PP2A holoenzyme). Activation of this target may require at least two mechanisms, one of which is not dependent on Rim15. Deletion of *PPH21* and *PPH22* may result in a higher basal phosphorylation level of the presumed target even in the absence of Rim15, and thus to a higher basal level of transcription of Rim15-dependent genes. This high basal activity may then be

sufficient to induce transcription in response to rapamycin even in the absence of Rim15 (Figure 33).

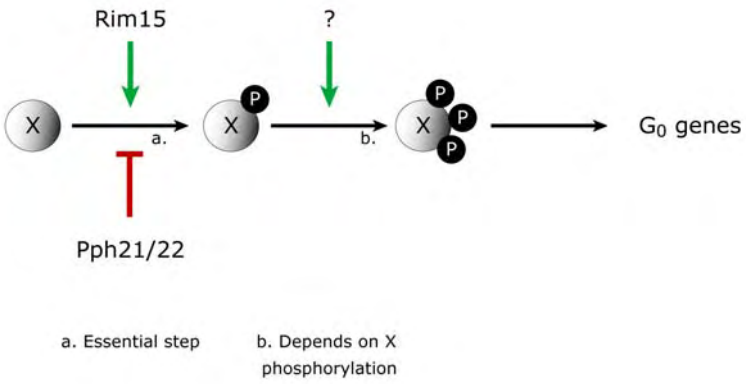

Figure 33

This simple model illustrates a possible regulatory mechanism, where Pph21/22 and Rim15 inversely regulate the phosphorylation state of a common target, which in turn responds to rapamycin or starvation and positively affects the induction of Rim15-dependent genes. The first phosphorylation step [a.] is essential for the activation of this substrate and is greatly reduced in the absence of Rim15, resulting in downregulation of the G_0-responsive genes. When also the phosphatases are absent the remaining level of phosphorylation of substrate X are sufficient to sustain activation by a second Rim15-independent mechanism [b.].

To date, the only known substrates for Rim15-dependent phosphorylation are the two homologous proteins Igo1 and Igo2). Deletion of *IGO1* and *IGO2* simultaneously phenocopies the defect of *rim15Δ* cells in the induction of G_0-characteristics in response to rapamycin (see Chapter III, page 124). Thus, the presumed downstream target that may be shared between Rim15 and Pph21/22 could be Igo1/Igo2. We therefore tested whether the rapamycin-induced expression of the G_0 genes in a *pph21Δpph22Δ* mutant could be suppressed by the deletion of *IGO1* and *IGO2*. Deletion of the PP2A catalytic subunits rendered the induction of G_0 genes also independent of Igo1/2 (data not shown).

We considered the possibility that the transcription factors Msn2/Msn4 and/or Gis1 may be the predicted common targets of Rim15 and Pph21/22. While this would be in line with the finding cited above, that overexpression of PP2Ac results in abrogation Msn2/Msn4-dependent gene expression [205], it would be in overt contradiction with the observation from Santhanam *et. al.* (2004) that Pph21/22 activity is required for Msn2 translocation in response to both rapamycin and nitrogen starvation [63]. Albeit not shown yet, these data predict that loss of *PPH21/PPH22* should prevent Msn2-dependent transcription. It remains interesting therefore, to test the role of these

transcription factors in mediating the *pph21Δpph22Δ* transcriptional phenotype in response to rapamycin.

TORC1 may control Rim15 through the Sch9-branch

The protein kinase Sch9 has been previously suggested to act in parallel or downstream of the TORC1 pathway [74,79]. Interestingly, several observation suggested a relationship between Sch9 and Rim15 activity: the constitutive nuclear accumulation of GFP-Rim15 in the absence of *SCH9* suggests that Sch9 is involved in a mechanism of nuclear export or cytoplasmic retention of Rim15 [78]. Moreover, Sch9 can phosphorylate Rim15 *in vitro* and *in vivo* ([40] and unpublished observations) and, based on the analysis of the transcription profiles of the mutants, was suggested to regulate both the Rim15 kinase and its downstream effectors Msn2/Msn4 and Gis1 [77]. Finally, the chronological life-span extension in *sch9Δ* mutants is mediated by the stress-resistance proteins Msn2/Msn4 and Rim15 [204].

In order to understand whether TORC1 may control Rim15 activity via the kinase Sch9 we decided to analyze the role of Sch9 in the rapamycin-induced transcription of Rim15-dependent genes. The use of two opposing alleles of *SCH9*, the *sch9Δ* allele and the constitutively active $sch9^{2D3E}$ allele (kindly provided by Dr. Robbie Loewith) revealed that Sch9 is indeed a negative regulator of Rim15 (Figure 34). Accordingly, deletion of *SCH9* resulted in slightly increased expression of Rim15-dependent genes and accumulation of glycogen following rapamycin treatment. The amino acid substitutions in the $sch9^{2D3E}$ are thought to mimic phosphorylation of the corresponding residues by TORC1 (Urban *et al.*, unpublished), which is believed to promote the activity of Sch9 towards its substrates, including Rim15. Consistently, the expression of this allele resulted in the constitutive downregulation of Rim15-dependent phenotypes even in the presence of rapamycin (Figure 34).

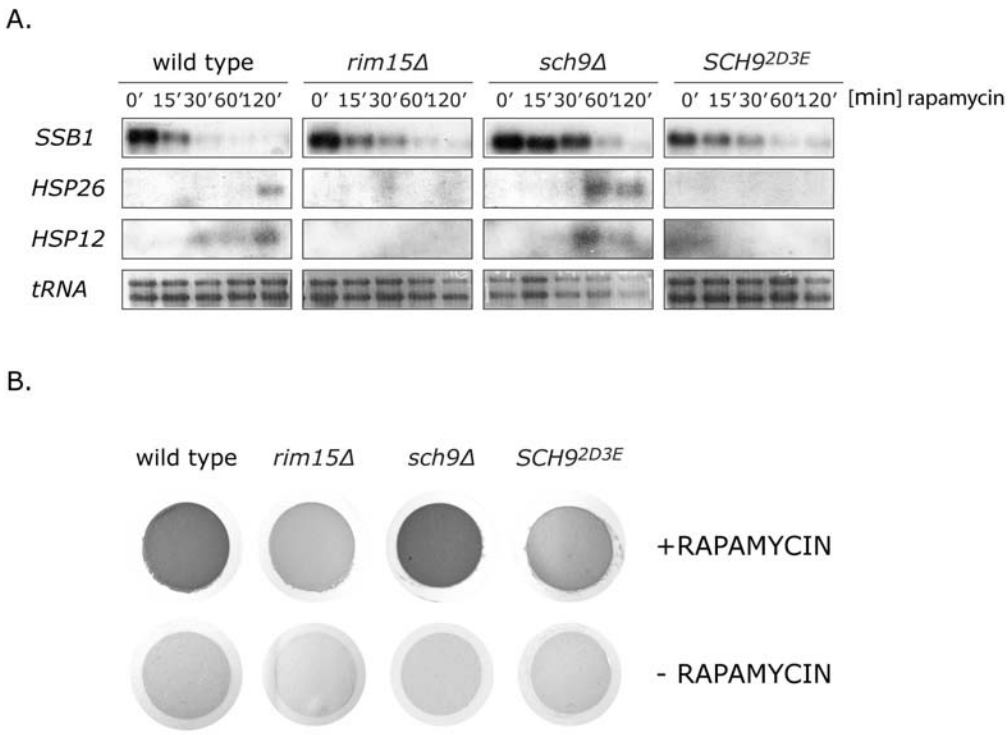

Figure 34

Analysis of the role of Sch9 in mediating rapamycin-induced responses. [A.] Northern blot analysis showing the level of induction of the stress-responsive genes *HSP26* and *HSP12* in wild-type, *rim15Δ*, *sch9Δ* and *sch9*^{2D3} cells treated with rapamycin for the indicated times. [B.] Accumulation of glycogen in wild-type and mutant cells visualized by iodine staining of the filtered cells 6 hours after the addition of 200 ng/ml rapamycin.

Notably, the rapamycin-induced Rim15 dependent responses were normally repressed during the exponential phase, indicating that nuclear accumulation of Rim15 is not sufficient to trigger its activation. Moreover mutants expressing a constitutively active *sch9*^{2D3E} were phenotypically different from a *pph21Δpph22Δ* indicating that TORC1 may regulate Rim15 by two independent mechanisms.

Conclusions and Outlook

Rim15 is a key regulator of transcription during the diauxic shift and responds to different key nutrient-signals. Most of the Rim15 dependent genes are transcribed by Msn2/Msn4 and Gis1, which are thought to act both independently and cooperatively on different promoters. The contribution of Rim15 to the diauxic shift transcriptome is larger than previously suspected and, interestingly, includes the coordinate expression of genes belonging to two interdependent functional groups. The first group includes genes required for respiration and other mitochondrial functions, while the second group represents genes encoding proteins involved in the oxidative stress response. To support growth on the non-fermentable carbon source ethanol, Rim15 induces the transcription of genes required for the respiratory metabolism, in parallel it promotes the transcription of genes whose products counteract the damage induced by this metabolic mode. We were intrigued by this finding, in particular because Rim15 contains a PAS domain in its N-terminal part, which appears to be closely related to the PAS domain in the neuronal PAS domain protein 2 (NPAS2). The latter is known to bind heme as a prosthetic group and to function as a gas-regulated sensor [206]. Thus by analogy, the Rim15-PAS domain may also function as a *cis* regulatory, ligand-activated switch that senses oxidative stress and/or the cellular redox status to properly control the protein kinase activity of Rim15 and thus the Rim15-dependent transcriptional responses.

In the presence of nutrients Rim15 is negatively regulated by the TORC1 pathway; in accordance with this finding Rim15 mediates part of the transcriptional response to rapamycin. Unexpectedly, the contribution of Rim15 to the rapamycin transcriptional response was less important than during the diauxic shift, indicating that inhibition of TORC1 by rapamycin does not perfectly mirror the physiological downregulation of this pathway in response to nutrient starvation. Importantly, some genes required Rim15 for induction during the diauxic shift but were induced independently of Rim15 following rapamycin treatment. Although this may be an artifact of the microarray experiments and certainly requires further testing, it may also indicate that Rim15 can process and integrate signals from different nutrient sensing pathways to fine-tune the expression of genes in response to different metabolic needs.

How exactly Rim15 is regulated by TORC1 is not known. Our data indicate that the Tap42-Sit4 complex is not involved. Interestingly, however the PP2A catalytic subunits Pph21 and Pph22 are involved in negative regulation of Rim15 dependent genes. In their absence, the induction of rapamycin-dependent genes bypasses the requirement for Rim15. It is possible therefore that the

Tap42-PP2A complex is part of a regulatory mechanism that ensures downregulation of the G_0 response to a level that is sufficiently low to allow growth under favorable conditions. This model fits with the extreme slow growth phenotype observed in Tap42-PP2Ac complex mutants (*i.e. pph21Δpph22Δ* mutants or *tap42-11* mutants at restrictive temperature). Possibly, G_0 transcripts are induced to such a high level in these mutants that they cause the slow growth phenotype. Although the disruption of this regulatory mechanism results in higher steady-state transcription rates of G_0-specific genes (also in the absence of Rim15) these cells retain their ability to further increase the transcription of these G_0-specific genes in response to rapamycin and, again, in a manner that is independent of Rim15. This observation adds a level of complexity to our knowledge of Rim15-controlled gene transcription; a possible scenario may be that Tap42-PP2A and Rim15 converge on a common downstream target, which itself is regulated by an additional TORC1-dependent mechanism (Figure 33 page 102, Figure 35 page 107).

The observation, that loss of *PPH21/PPH21* results in increased basal levels as well as increased rapamycin-induced transcription of the G_0 genes, can not easily be reconciled with the models of previous studies, which postulated a role of the PP2Ac in positively regulating the induction of rapamycin-induced responses. A major problem with the interpretation of our and the published data is that the catalytic subunits of PP2A can be integrated in different complexes with distinct, and possibly opposing, functions. By deleting individual subunits, we inevitably affect the function of all of these complexes and it is difficult to predict which one is responsible for the observed phenotypes.

A recently presented model, could account for many of the previous findings that appeared contradictory; this model proposes that, in response to rapamycin, a transiently active Tap42-PP2Ac complex is released from membrane structures, to which it is tethered by its association with TORC1 [61]. It is conceivable that these two forms of the Tap42-PP2Ac complex (*i.e.* the TORC1-associated and the free form) represent distinct complexes with different functions with respect to rapamycin-induced responses (Figure 35) [61]. The TORC1-bound Tap42-PP2Ac complex is formed during normal growth and may compete with the quiescence-promoting mechanisms in order to avoid the unscheduled induction of starvation responses. Such a model may explain why loss of Pph21/22 caused a low, constitutive activation of G_0 transcript expression in our experiments.

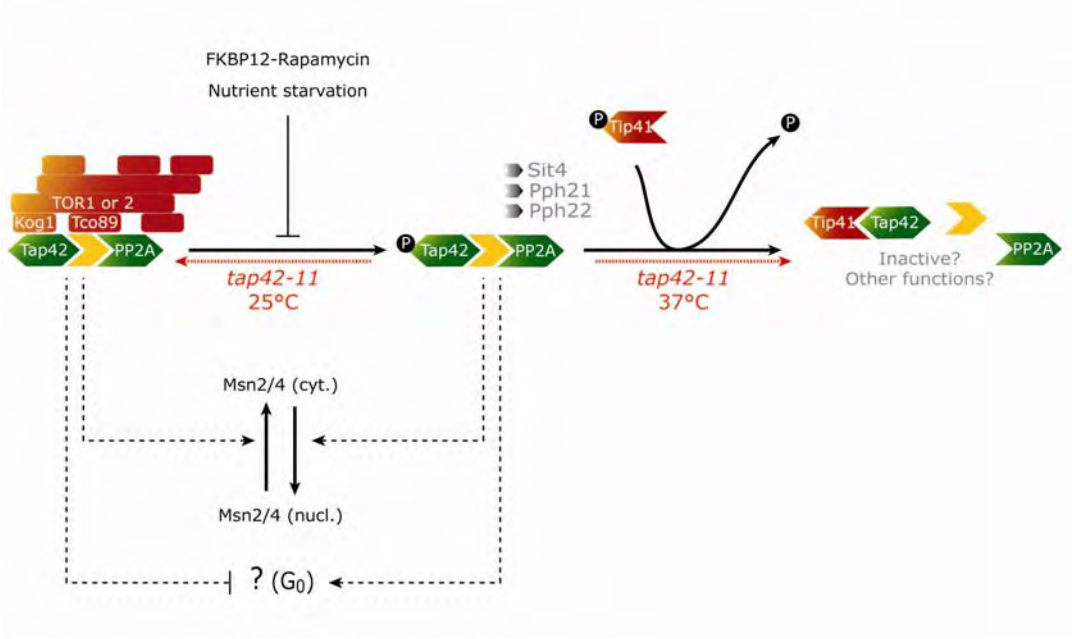

Figure 35

Current model for the function and regulation of the TORC1-associated and the free Tap42-PP2A complexes. The effect of the temperature sensitive *tap42-11* allele at different temperatures is indicated by red arrows. The TORC1-associated and the free Tap42-PP2A complexes may inversely regulate rapamycin/starvation-response mechanisms, including the nuclear localization of Msn2/Msn4 and the induction of G_0 phenotypes.

The use of Tap42 mutants may to help solving this matter since it only associates with two of the three known PP2Ac containing complexes. Mutations in Tap42 are therefore not expected to affect the function of the more abundant PP2A holoenzyme. The TORC1-associated form of the Tap42-PP2Ac complex is thought to be stabilized at 25°C (permissive temperature) in a *tap42-11* mutant strain (Figure 35) [61]. If the phenotypes we observe by deleting *PPH21/PPH22* are indeed due to the loss of a function of this form of the complex, we may expect the opposite phenotype in a *tap42-11* mutant at the permissive temperature. Thus, it would be interesting to study in the future the rapamycin-induced transcription of Rim15-dependent G_0 genes in such a mutant. Notably the *tap42-11* mutant is resistant to rapamycin at permissive temperature [207].

TORC1 may also regulate Rim15 via phosphorylation and activation of the serine/threonine kinase Sch9, which in turn may regulate the localization of Rim15 by phosphorylating a serine residue within the kinase insert, similarly to what has been described for the regulation of Rim15 by Pho85 [40]. The observed phenotypes of the *sch9Δ* and *sch9*^{2D3E} mutant strains support the hypothesis that Sch9 transmit a signal from the TORC1 pathway and negatively regulates the function of Rim15.

The previously unsuspected complexity of the mechanisms regulating and regulated by Rim15 have made us aware of the fact that a more detailed knowledge of the downstream events of the Rim15 signaling pathway is imperative for further progress in this area of research. We therefore decided to dedicate all our efforts (in the next chapter) to elucidate the nature of the Rim15 targets.

Chapter III

Identification of the cellular targets of Rim15

Identification of the cellular targets of Rim15

Introduction

While we now better understand the mechanisms that regulate Rim15, our knowledge of the processes that are regulated by Rim15 is unfortunately quite limited. Ultimately, Rim15 kinase activity is required for the induction of two distinct differentiation programs in response to nutrient starvation. In diploid cells starved for nitrogen (in the presence of a non-fermentable carbon source), Rim15 activates the transcription of early meiotic genes [114]. Similarly, during the response to glucose starvation during the diauxic shift, Rim15 activity is required for the correct transcriptional induction of the G_0 differentiation program [208].

The knowledge of the direct cellular targets for Rim15-dependent phosphorylation would not only allow a better understanding of the molecular mechanisms underlying the Rim15-regulated process, but it would also allow to study more precisely the mechanisms that regulate the function of Rim15. Notably, often the main limitation in our studies of Rim15 function and regulation has been the fact that we studied Rim15 activity indirectly, by reading physiological parameters that are likely to be under the control of multiple mechanisms. This approach is likely to blur the interpretation of results. Moreover, given the high conservation of the pathways regulating quiescence in eukaryotic cells it strikes us that such an important signal transducer as is Rim15 has no sequence homolog in mammalian cells. It is conceivable though, that the same functions are performed in higher eukaryotes by a functional homolog (*i.e.* a protein that is not evolutionary conserved but performs the same function) of Rim15 exists in higher eukaryotes that performs the same functions. Knowledge of the targets of Rim15 is likely to help us to identify the proteins, if they exist, that support the same functions in other organisms.

Possible targets of Rim15

Rim15 targets are likely to be nuclear proteins, as the Rim15 protein accumulates in the nucleus at times where its activity is required. Moreover, they are expected to be directly or indirectly involved in transcription. Accordingly, Rim15 appears to interact with several subunits of the transcription regulator Gis1-complex and of the transcription initiation factor TFIID, although it is not known whether some of these interacting proteins are phosphorylated by Rim15.

Rim15 may not be involved exclusively in nuclear processes as suggested by the fact that it was also identified as a protein interacting with the cytoplasmic trehalose-6-phosphate (Tre6P) synthase subunit Tps1 [93].

The current models of Rim5-dependent regulation of the processes of meiosis and quiescence support a role of Rim15 in transcriptional regulation, probably via the modulation of chromatin-related mechanisms.

Model for the role of Rim15 function during meiosis

The initiation of meiosis requires a specific set of genetic (the cell must be diploid) and nutritional (starvation for both, a fermentable carbon source and nitrogen and presence of a non-fermentable carbon source) conditions. In haploid cells, the expression of *IME1*, encoding a key transcription factor for meiotic genes, is inhibited by the haploid-specific transcriptional repressor Rme1. In contrast, in diploid cells, *IME1* transcription is positively controlled by the diploid-specific transcription factor Ime4 and by the stress-responsive transcription factors Msn2/Msn4, which bind to STRE promoter regions in response to nutrient starvation [209]. Ime1 activates the transcription of early meiotic genes (EMGs) through interaction with Ume6, a DNA binding protein that sits on the URS1 sequences within the promoter regions of EMGs and regulates their transcription both positively and negatively by interacting with either Ime1 or with the silencing complex Sin3-Rpd3 [209]. The binding of Ime1 to Ume6 depends on phosphorylation of both proteins by the serine/threonine kinase Rim11 as well as on the presence of Rim15 [115]. For meiosis Rim15 activity is required to remove the silencing complex Sin3-Rpd3 from EMGs promoters (Figure 36); depletion of both glucose and nitrogen is required for the transient removal of Sin3 and Rpd3 from the promoters of EMGs and both signals appear to be transmitted via Rim15 [114]. Currently, three putative proteins, Sin3, Ume6, and Ime1, are considered as possible targets of Rim15-dependent phosphorylation. Two observations suggest that Rim15 may phosphorylate Ume6 thereby promoting its interaction with Ime1: first, Rim15 is required for the efficient interaction of Ime1 with Ume6, and secondly Rim15 is required for phosphorylation of Ume6. Interestingly, Ume6 has also been implicated in the transcriptional regulation of non-meiotic genes that contain URS1 sequence elements and are involved in arginine catabolism (*e.g. CAR1* and *CAR2*), peroxisomal function (*e.g. FOX3*), and DNA repair (*e.g. PHR1*). Notably these genes are also induced by rapamycin (our microarray data), albeit in a Rim15-independent manner. Interestingly, *ume6Δ* mutant cells display decreased resistance to rapamycin. An additional process, independently regulated by Rim15 may be required to promote the dissociation of Sin3 from Ume6,

as no competition is observed for the binding of Ime1 and Sin3 to Ume6 (both proteins associate with different and distinct regions of Ume6). One possibility would be that Rim15 affects the interaction of the silencing complex with EMGs by affecting the phosphorylation state of Sin3 or an additional domain in Ume6. However the ability of Rim15 to phosphorylate Ume6 and/or Sin3 was never directly assessed neither *in vitro* nor *in vivo*.

Model for the role of Rim15 during the diauxic shift and in the stationary phase

Both Ume6 and the Sin3-Rpd3 complex may be involved in the regulation of the transcription of other classes of Rim15-dependent genes through a similar mechanism as observed for EMGs. However, our study of the diauxic-shift transcription profile indicate that Rim15 is likely to control the transcription of G_0 genes through an additional mechanism involving the transcription factors Gis1 and Msn2/Msn4. Accordingly, none of the genes that were upregulated in a Rim15-dependent manner during the diauxic shift were found to contain URS1 sequences for the binding of Ume6 (*i.e.* TAGCCGCCGA or TAGCCGCCSA). Nevertheless, it can not be excluded that additional Rim15-regulated proteins may function analogously to Ume6 on the promoters of G_0 genes (Figure 36).

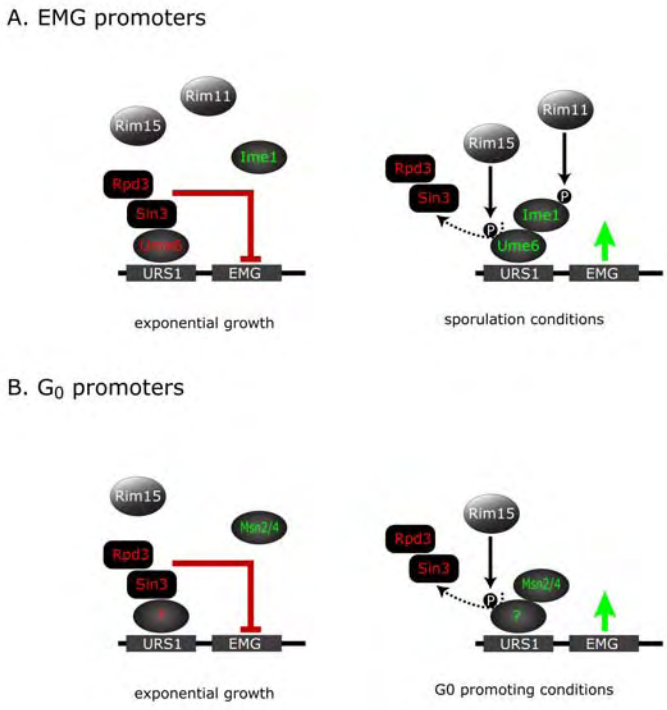

Figure 36

Model for the Rim15-dependent regulation of G_0-specific genes, based on the current knowledge of Rim15 function for the induction of early meiotic genes (*EMGs*).

Noteworthy, some additional observations suggest the possible implication of chromatin remodeling in the regulation of G_0 genes: the ubiquitin-specific protease Ubp10, which is thought to affect silencing by regulating the distribution of silencing protein Sir4 [210], was shown to be involved in the repression of many stress-responsive genes, including genes whose products offer protection from oxidative damage [211]. In the absence of *UBP10* these genes were upregulated and this effect is mitigated by the deletion of *SIR4*, suggesting that the phenotypes observed in *ubp10Δ* mutants are due to promiscuous binding of Sir4 to inappropriate loci. In this context it may be recalled that our results indicated that Sir4 can interact with Rim15 in a two-hybrid assay (Table II). Moreover Rim15-dependent genes and glycogen accumulation are upregulated in both, *ubp10Δ* and *sir4Δ* mutants exposed to rapamycin (data not shown).

Tests of epistasis indicated that Gis1 acts downstream of Rim15 and is positively regulated by its activity, however no direct interaction could be detected [187]. The interaction of Rim15 with several proteins that were recently described to be part of a Gis1-containing complex (Table II) suggest that Rim15 may regulate Gis1 indirectly by phosphorylating another member of the complex and thereby regulating the activity or altering the subunit composition of the complex. In addition of being an activator of transcription from PDS elements and STREs during the diauxic shift, Gis1 was also shown to function as a DNA-damage responsive transcriptional repressor. Accordingly Gis1 possesses a Jumonji domain, which is required for its interaction with the other members of the complex [188]. Jumonji domains are found in many eukaryotic transcription factors and were recently shown to possess histone demethylase activity [212].

Results and discussion

Identification of the first direct target of the Rim15 kinase

Large-scale kinase assay

For all the reasons mentioned above, we decided to invest in the identification of the *bona fide* cellular substrate of Rim15. As a fortunate coincidence, the laboratory of Michael Snyder in Yale was developing a novel protein microarray technology to characterize the activity of protein kinases. This technique consists in the incubation of individual kinases with protein arrays containing 4,400 purified proteins, in the presence of [γ-^{33}P]-ATP [213]. As many proteins display autocatalytic kinase activity or can directly bind ATP, the validation of this technique was dependent on the availability of mutant alleles with impaired kinase activity to serve as negative controls. We purified both the wild type Rim15 protein and the kinase inactive Rim15^{K823Y} allele and shipped them to the renowned university in Connecticut (Materials and Methods).

Of the 14 proteins that were found to be phosphorylated in the presence of Rim15, but not of the kinase inactive Rim15^{K823Y} (Table VI), only one, corresponding to the protein product of *YNL157W*, was confirmed to be strongly phosphorylated *in vitro* by Rim15 in our follow up experiments (Figure 38).

Yeast ORF	Gene Name	Signal (microarray)	Signal (control exp.)
YNL157W	*IGO1*	20312.8	strong
YGL185C	*YGL185C*	18765.9	n.d.
YOR162C	*YRR1*	13185.2	none
YLR263W	*RED1*	12670.4	n.d.
YOR380W	*RDR1*	6752.5	none
YOL147C	*PEX11*	6326.2	n.d.
YGR276C	*RNH70*	4586.7	n.d.
YMR155W	*YMR155W*	4017.5	n.d.
YBR035C	*PDX3*	3958.9	n.d.
YER151C	*UBP3*	3360.3	weak
YIL116W	*HIS5*	3126.1	n.d.
YCR052W	*RSC6*	2746.0	weak
YDL002C	*NHP10*	2637.3	weak
YBL011W	*SCT1*	2410.7	n.d.

Table VI

Rim15 substrates in a large-scale protein kinase assay. The 14 proteins found to be phosphorylated in a large-scale kinase assay in the presence of Rim15 and not of the kinase inactive Rim15^{K823Y} allele. In control experiments, the strongest signal was observed for the unknown ORF *YNL157W* (http://networks.gersteinlab.org/phosphorylome/).

YNL157W encodes a putative protein for which no information had yet been annotated. *YNL157W* is highly homologous (58% identity) to another uncharacterized ORF in *S. cerevisiae*, namely *YHR132W-A*. The protein products of the *S. cerevisiae* genes *YNL157W* and *YHR132W-A* contain a conserved endosulfine motif (Figure 37) that is found in the members of the evolutionary conserved endosulfine family, where it usually occupies the majority of the molecule [214-216]. Within the endosulfine motif, two regions are particularly conserved in all species; the first region contains a 8-residues motif of unknown function (KYFDSGSY) while the second encompasses a consensus site for PKA-dependent phosphorylation, which was shown to be phosphorylated by PKA in the mammalian members of the endosulfine family, ARPP-16 and ARPP-19 [214]. The SDS-PAGE mobility of the members of the endosulfine family is usually significantly higher than the predicted molecular weight, possibly indicating elongated asymmetric structure. Similar biochemical properties are common for small non-enzymatic intracellular regulatory proteins such as calmodulin, the PKA inhibitor PKI, or DARPP-32, all of which are known to influence the activity of enzymes involved in signal transduction.

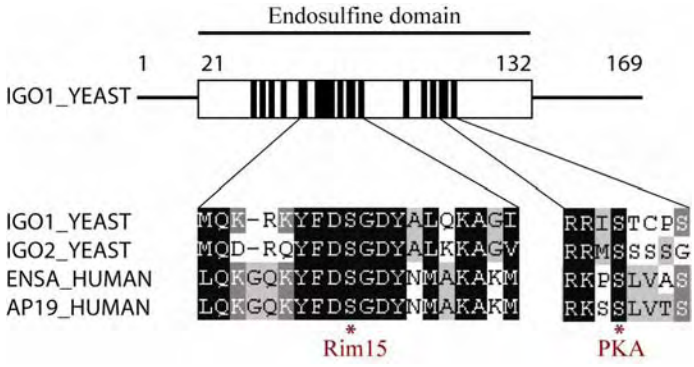

Figure 37

Schematic representation of the sequence conservation between yeast and human endosulfines. The alignments are shown for the two regions with the highest conservation and putative PKA and Rim15 phosphorylation sites are indicated in red.

To date, the molecular function of endosulfines is not known. In mammals α-EDSF has been suggested to be the endogenous ligand of the ATP-sensitive (K_{ATP}) potassium channel, known as sulphonylureas receptor. Sulphonylureas are therapeutic agents employed in the treatment of diabetes. Their action results primarily from their ability to inhibit K_{ATP} channels in the plasma membrane of pancreatic β cells and thereby stimulate insulin release. Similarly to sulphonylureas α-EDSF was shown to block K_{ATP} currents when applied both intracellularly and extracellularly and to stimulate insulin secretion by closing the K_{ATP} channel in β cells when applied extracellularly [216]. Other reports indicated that α-EDSF may not be exclusively an endogenous equivalent for sulphonylureas and not solely a K_{ATP} channel regulator; accordingly, under physiological conditions

α-EDSF was shown to inhibit insulin secretion by blocking the Ca^{2+} influx through the L-type Ca^{2+} channel [217].

The two splicing variants ARPP-16 and ARPP-19 belong to the endosulfine family and were initially discovered as *in vitro* substrates for PKA enriched in mammalian brain [215]. APRR-19 was reported to be involved in the post-transcriptional control of gene expression in human neurons by increasing the half-life of mRNAs in an NGF-dependent manner [218]. Interestingly, mutation of the PKA phosphorylation site affected the ability of APRR-19 to stabilize a reporter mRNA. In addition, recent *in vitro* studies have indicated that ARPP-16 and ARPP-19 are phosphorylated on a common Ser residue by Cdk5, a cyclin-dependent kinase homologous to the *S. cerevisiae* Pho85 [218].

Although these proteins of the endosulfine family are not much larger than their endosulfine domain, they appear to perform various regulatory functions. Currently the mechanisms through which proteins of the endosulfine family regulate different processes have not been elucidated, but may depend on their variable N-terminal extensions.

Here we started the characterization of the yeast endosulfine family members, the proteins Ynl157wp and Yhr132w-a, which we renamed Igo1 (Initiation of G zero 1) and Igo2 respectively.

Igo1 and Igo2 are phosphorylated by Rim15 *in vitro*

The recombinant GST-Igo1 and GST-Igo2 proteins expressed and purified from bacteria, where phosphorylated *in vitro* in the presence of purified Rim15 and [γ-^{32}P]-ATP (Figure 38).

In order to identify the residue in Igo1 that was phosphorylated by Rim15 we repeated a similar experiment, in the presence of non-radioactive ATP and either the wild type Rim15 kinase or the kinase inactive $Rim15^{K823Y}$ allele, followed by SDS-PAGE and mass spectroscopy (MS) analysis of the GST-Igo1 recombinant protein (Materials and Methods). Using this technique we detected a peak with a shift in mass corresponding to about +80 kDa in the sample incubated with the wild-type kinase. The mass of this peptide (1386.565 kDa) ±80 kDa corresponded well to the mass of the theoretical peptide YFDSGDYALQK (1306.595 kDa). We then subjected the same samples to tandem MS and were able to confirm the phosphorylation of this peptide on a serine residue corresponding to serine 64 in Igo1. Substitution of serine 64 with alanine dramatically abolished the phosphorylation signal in a kinase assay using the wild type Rim15 protein (Figure 38).

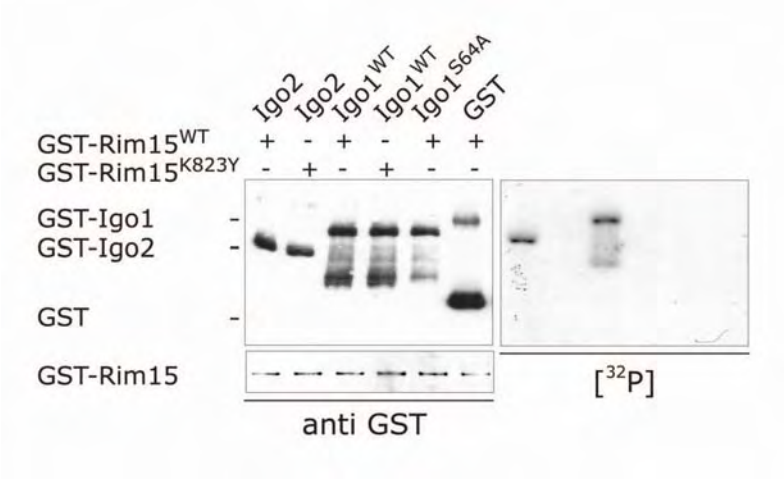

Figure 38

Protein kinase assay showing the Rim15-dependent phosphorylation of Igo1 and Igo2. Top and bottom left panels: western blot using antibodies against the GST epitope showing that similar amounts of substrate and kinase, were used in each reaction. Right panel, autoradiogram showing incorporation of radioactive phosphate into recombinant GST-Igo2 and GST-Igo1 in the presence of Rim15.

Thus Rim15 directly phosphorylates Igo1 and Igo2 on a serine residue located in the conserved region containing the YFDSGDY amino acid motif. Importantly this region is conserved among all members of the endosulfine family. It would be interesting to assess whether the yeast kinase Rim15 can phosphorylate the Igo1 orthologs from other organisms.

To further analyze the Rim15-dependent phosphorylation of serine 64 in the Igo1 protein we ordered polyclonal antibodies against the phosphorylated peptide. The purified phospho-specific antibody (pS64-Igo1) recognized a GST-Igo1 protein, expressed and purified from bacteria, only when it was previously incubated with the wild type Rim15 protein in the presence of ATP (Figure 39).

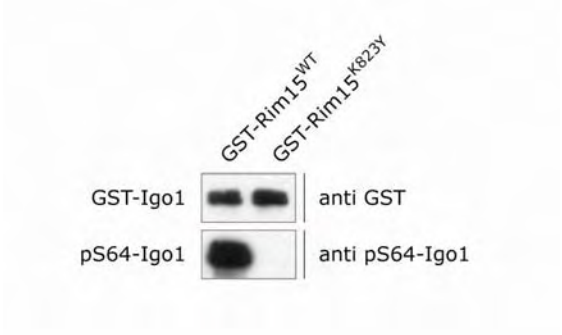

Figure 39

Western blot detection of the purified GST-Igo1 protein using either an antibody against GST (anti GST) to detect the total level of GST-Igo1 or a polyclonal antibody raised against a peptide corresponding to the phosphorylated Igo1 (anti pS64-Igo1) to detect phosphorylated GST-Igo1. Prior to western blot analysis, the GST-Igo1 protein purified from bacteria was incubated either with wild-type Rim15 (first lane) or with the kinase-inactive Rim15 (second lane) in the presence of ATP.

Igo1 and Igo2 characterization

The Igo1 and Igo2 proteins

As already reported for other members of the endosulfine family, both Igo1 and Igo2 proteins migrate on a SDS-PAGE with an apparent mass that is significantly higher than the predicted molecular weight. The endogenous Igo1 migrates with an apparent size of nearly 25 kDa, while the predicted molecular weight is of 18 kDa. Similarly Igo2, whose predicted molecular weight is 14.4 kDa migrates at an apparent size of > 19 kDa (not shown).

To study the levels of Igo1 and Igo2 we integrated 13 consecutive myc tags immediately upstream (3') of the STOP codon at the genomic loci of *IGO1* and *IGO2* respectively; to obtain C-terminal tagged proteins expressed under their endogenous promoters. Both Igo1-myc^{13} and Igo2-myc^{13} were expressed at high levels throughout growth and the protein levels were not significantly affected by a 180-min treatment with rapamycin (Figure 40).

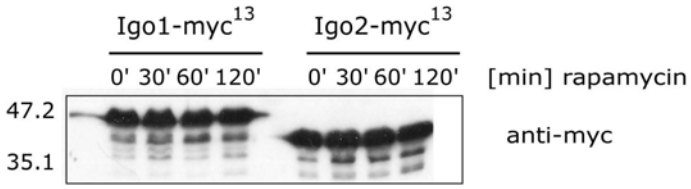

Figure 40

Expression levels of Igo1-myc13 and Igo2-myc13 (top panels) in exponentially growing cells and in cells treated with rapamycin for the indicated times. Total protein extracts were obtained from equal amounts of cells for each strain and time point.

We then used immunofluorescence microscopy to detect the Igo1-myc^{13} and Igo2-myc^{13} proteins *in vivo* and found that the localization of the two proteins was similarly regulated; Igo1-myc^{13} was found both in the nuclei and in the cytoplasm of exponentially growing cells while Igo2-myc^{13} was predominantly cytoplasmic during growth. Addition of rapamycin for 1 and 2 hours triggered the nuclear accumulation of both proteins (Figure 41). Thus the Rim15 targets appear to co-localize with Rim15 throughout growth. Notably, during exponential growth Rim15 is anchored in the cytoplasm via its interaction with the 14-3-3 protein Bmh2, while at least for Igo1 there seem to be no stringent cytoplasmic retention mechanism, as it is found also in the nucleus of growing cells. The protein sequence of Igo1 did not contain any consensus for 14-3-3 binding.

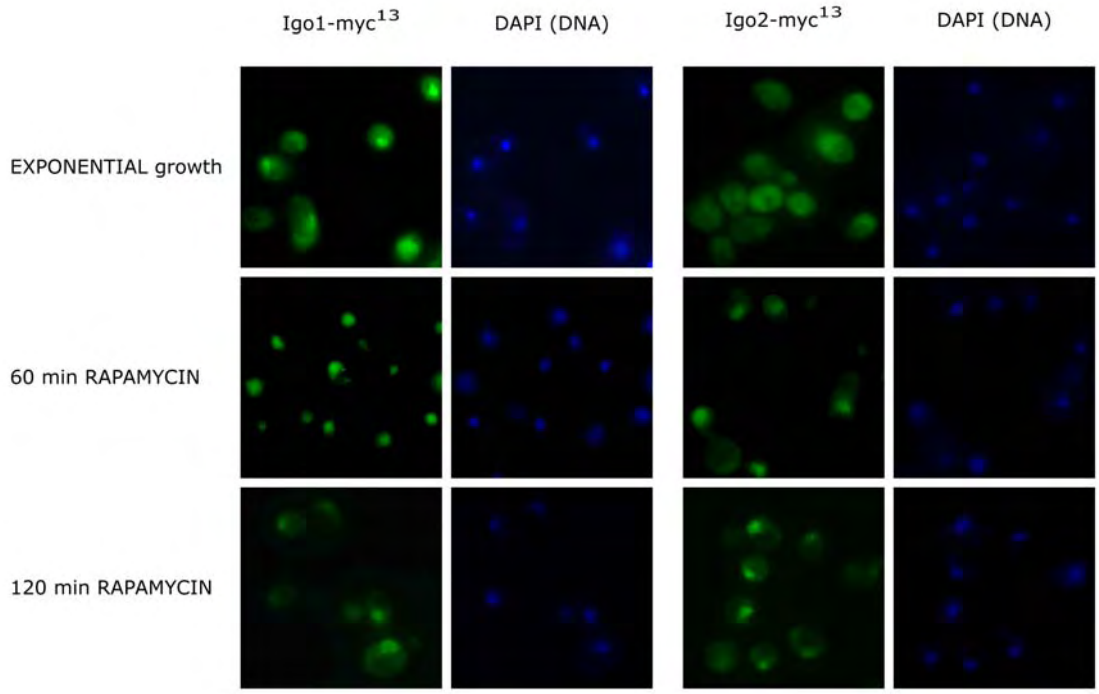

Figure 41

Immunofluorescence microscopy, showing the localization of Igo1-myc[13] and Igo2-myc[13] during the course of a 120-min rapamycin treatment. The nuclei were stained with DAPI.

As treatment with rapamycin causes both Rim15 and its substrates to accumulate in the nucleus, it would be interesting to determine whether their localization are interdependent from each other, for example by studying the localization of Rim15 in a *igoΔ1igo2Δ* strain and *vice versa*.

We next demonstrated, by co-precipitation analysis, that Rim15 and Igo1 forms a complex in yeast cells (Figure 42).

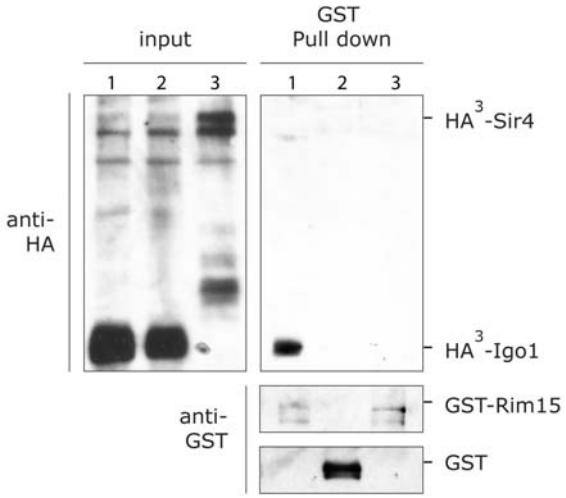

Figure 42

Co-precipitation experiment, showing that Rim15 interacts with Igo1 *in vivo*. Igo1-HA (lanes 1 and 2) or Sir4-HA (lane 3), under the control of the strong *TDH3* promoter, were co-expressed with either GST-Rim15 (lanes 1 and 3) or GST alone (lane 2).

For an initial experiment, aimed to confirm the interaction of Rim15 with Igo1 within cells, we favored efficiency and employed an expression system where both proteins are overexpressed. In particular Rim15 is expressed under the *GAL1* promoter from which reasonable quantities of this protein can be purified. However this system would not allow us to evaluate the possible dynamics of this interaction under physiological conditions. Unfortunately the large size and poor expression of the Rim15 polypeptide strongly reduces our experimental options. Nevertheless should this matter be solved in the future, it would be interesting to study in more detail the nature of this interaction as a function of various physiological conditions.

Igo1 is a target for Rim15-dependent phosphorylation *in vivo*

We next asked whether the endogenous Igo1 protein was the *bona fide* substrate for Rim15-dependent phosphorylation *in vivo*. Using the α-pS64-Igo1 antibody, which recognizes the phosphorylated form of Igo1, we analyzed the phosphorylation of Igo1 *in vivo* under conditions where Rim15 is known to be active.

Phosphorylation *in vivo* of Igo1 depends on Rim15

First, to confirm that the α-pS64-Igo1 antibody only recognizes Igo1 when it is phosphorylated by Rim15, we compared a western blot of the total protein extracts of wild-type cells and of mutant cells lacking *IGO1/IGO2* and *RIM15* using the purified α-pS64-Igo1 antibody (Materials and Methods). A 25-kDa band was detected in the wild type extracts and not in the *igo1Δigo2Δ* extracts, indicating that it corresponded to the Igo1 protein. In the absence of Rim15, the band corresponding to Igo1 phosphorylated on the serine residue at position 64 was not detected, indicating that the antibody only recognizes endogenous Igo1 when it is phosphorylated by Rim15. In addition, this result indicates that no other kinase can phosphorylate Igo1 on serine 64 *in vivo*, in the absence of Rim15 (Figure 43).

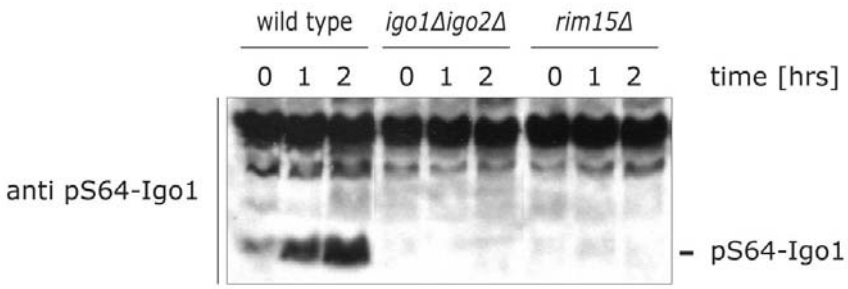

Figure 43

Western blot analysis using antibodies directed against a phosphorylated peptide in Igo1. Cells were treated with rapamycin and proteins were extracted after the indicated times. Equal amounts of protein were loaded in each lane and the blots were probed with anti-p64-Igo1antibodies. A strain deleted for both homologous endosulfines was used as a negative control to test the specificity of the antibody.

Rim15 phosphorylates Igo1 in response to various nutrient-starvation signals

To analyze variations in the phosphorylation state of Igo1, we used a strain that expressed the Igo1-myc[13] protein under the endogenous *IGO1* promoter. We followed the phosphorylation of Igo1-myc[13] under conditions that activate Rim15. We noticed that the insertion of the genomic tag somewhat affected the basal levels of Igo1 phosphorylation on serine 64 (compare Figure 44 with Figure 43).

Remarkably, the phosphorylation level of serine 64 within the Igo1-myc protein increased under all the three conditions known to trigger nuclear accumulation of Rim15, namely rapamycin treatment, phosphate and glucose starvation (Figure 44A and B). Interestingly Igo1 was also rapidly dephosphorylated (within 1 hour) when diauxic shift cells or rapamycin treated cells were allowed to recover in full (YPD) medium (Figure 44 B and C). This rapid downregulation, possibly in response to glucose, may be due to the inactivation/export of Rim15 and/or to the activation of PKA, which is predicted to phosphorylate Igo1 on serine 105. Phosphorylation by PKA and Rim15 are likely to have opposing roles in the regulation of Igo1 and may even be competitive events.

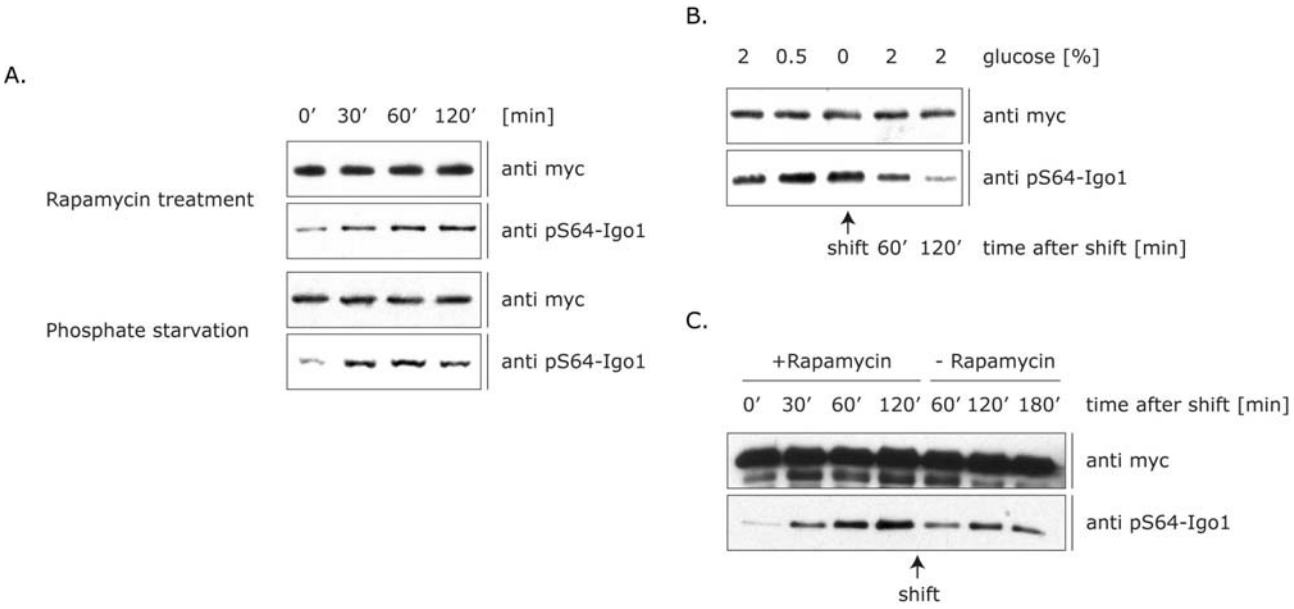

Figure 44

Western blot analysis using antibodies directed against a phosphorylated peptide in Igo1. In all experiments, equal amounts of protein were loaded in each lane of a 16% SDS-PAGE and the blots were probed with anti-p64-Igo1 antibodies to detect the phosphorylated protein or with anti-myc antibodies to detect total levels of Igo1-myc. [A.] Cells were treated with rapamycin or transferred from high-phosphate to low-phosphate medium and proteins were extracted after the indicated times. [B.] Cells were grown for several hours in full medium under continuous monitoring of the glucose levels in the culture medium and collected at the indicated glucose concentrations. After glucose was completely exhausted the cells were shifted to fresh medium containing 2% glucose and collected after the indicated times. [C.] Cells were treated with rapamycin for 120 minutes and after this time they were washed and resuspended in a fresh YPD medium without rapamycin. Samples were collected at the indicated times.

Alternatively, or additionally, phospho-serine 64 in Igo1 may be rapidly dephosphorylated by a yet unknown phosphatase in response to improved environmental conditions. This observation is intriguing, in particular, when considering our previous observation that a Tap42-PP2A complex may be involved in the rapid downregulation of the Rim15- and Msn2/Msn4-dependent stress responses.

Additional modifications are induced during the diauxic shift

In our diauxic shift experiments we observed additional modifications of the Igo1 protein after depletion of glucose. These modifications where even more evident when cells growing on glucose-containing medium where shifted to a medium without glucose, but containing 2% ethanol instead (Figure 45). This medium composition mimics the conditions experienced by cells during the diauxic shift transition; accordingly, shifting exponentially growing cells from rich, glucose-containing medium to an ethanol-based medium results in the Rim15-dependent induction of the G_0 genes *HSP26*, *SSA3* and *HSP12* and the repression of the transcription of the ribosome-associated protein genes *SSB1* (personal observation, not shown).

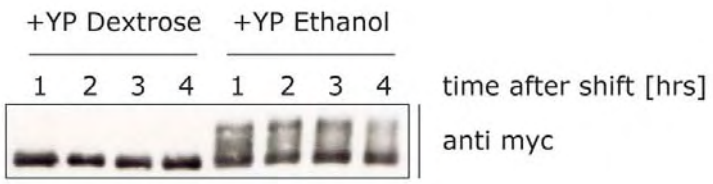

Figure 45

Western blot analysis of Igo1-myc[13] modifications following glucose starvation. Cells were grown overnight on a glucose containing medium and transferred either in a fermentable (YP Dextrose) or non-fermentable (YP Ethanol) medium for the indicated times. Equal amounts of cells were collected and proteins were extracted and loaded on a 7.5% SDS-PAGE. The blots were probed with anti-myc antibody to detect the recombinant Igo1 proteins.

Interestingly, when the cells growing on ethanol were allowed to recover on a full medium containing glucose, the Igo1 band collapsed again to the original size. Further experiments are required to determine the nature of these modifications. In particular, to assess whether the slow migrating isoforms correspond to phosphorylated proteins, we will purify Igo1 under both conditions and analyze the migration of the purified protein on SDS-PAGE both prior and after treatment with phosphatase. Preliminary data indicate that these modifications do not depend on Rim15, as they occur also in the absence of this kinase. Two candidates for Igo1 phosphorylation in response to low glucose levels may be the glucose-responsive kinases Snf1 and Yak1 kinases. Future experiments will include studies of these Igo1 modifications in mutant yeast cells lacking these kinases.

Phenotype of *igoΔigo2Δ* mutants

Igo1 was phosphorylated by Rim15 under all conditions known to trigger Rim15 activation and/or nuclear accumulation, indicating that its function may be regulated by Rim15-dependent phosphorylation. We asked whether Igo1 was involved in the (positive or negative) regulation of the induction of Rim15-dependent responses during the diauxic shift and/or following a treatment with rapamycin. Since *IGO1* and *IGO2* are highly homologous it is possible that they also have redundant functions. For this reason we performed our phenotypical analysis in a strain deleted for both *IGO1* and *IGO2*.

Analysis of Rim15-dependent G_0 characteristics in *igo1Δigo2Δ* mutant cells

Interestingly deletion of *IGO1* and *IGO2* together phenocopied the deletion of *RIM15* with respect to rapamycin-induced readouts like the accumulation of glycogen and the transcription of

the heat shock protein genes *HSP26* and *HSP12* (Figure 46 C and D). In G_0 the phenotype of the double *igo1Δigo2Δ* mutant was even more severe than the phenotype observed for *rim15Δ* mutant cells; the double mutant strain accumulated less trehalose and exhibited an extremely reduced lifespan compared not only to the corresponding wild type but also to a *rim15Δ* mutant strain (Figure 46 A and B).

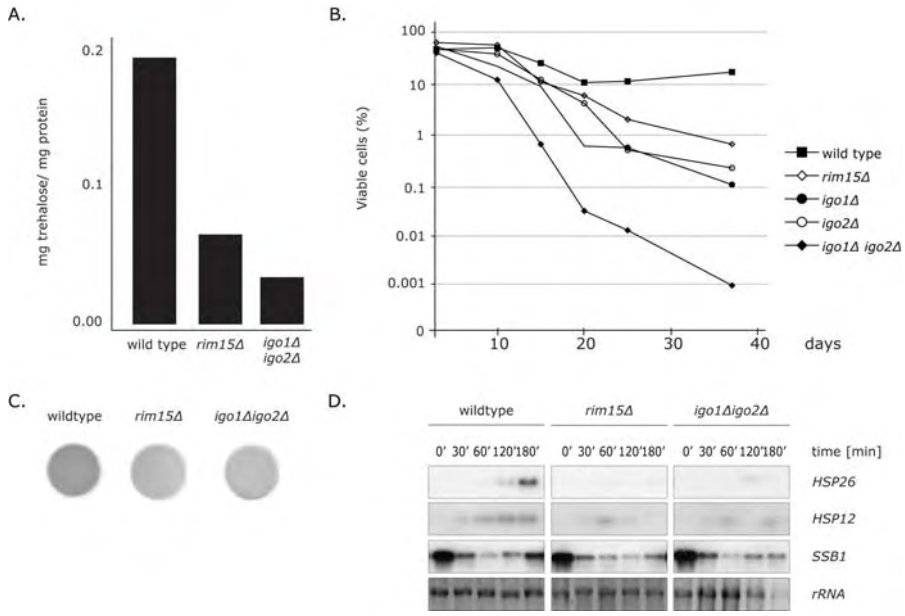

Figure 46

Analysis of the phenotypes induced during the diauxic shift [A, B] or by a rapamycin treatment [C, D] in wild-type strains and in *rim15Δ* and *igo1Δigo2Δ* mutant strains. [A.] Trehalose accumulation during the stationary phase (7 days on 1% glucose-containing YPD). [B.] Assay of the life span in saturated YPD cultures. [C] Accumulation of glycogen following a 6-h treatment with rapamycin. [D.] Northern blot analysis of *HSP26* and *HSP12* transcription. All the assays are described in Materials and Methods.

The more severe phenotype observed in the *igo1Δigo2Δ* double mutants during the diauxic shift suggests that under this condition Igo1 and Igo2 may be regulated by additional Rim15-independent mechanisms. This is in accordance with the observation that Igo1 is modified by both Rim15-dependent phosphorylation and a Rim15-independent mechanism during the response to glucose starvation (Figure 45). Moreover these data indicate that the responses induced by rapamycin and nutrient starvation differentially affect Rim15 and Rim15-dependent readouts.

The transcriptional response to rapamycin in *rim15Δ* and *igo1Δigo2Δ* mutant cells

We next compared the transcription profiles of *rim15Δ* and *igo1Δigo2Δ* mutant strains in response to rapamycin (see also Chapter II, page 89), we found that the induction of 121 genes was affected in *igo1Δigo2Δ* mutants. Surprisingly we found that the set of genes that depended on Rim15 for rapamycin-induced transcription (48 genes) was entirely comprised within the larger set of genes that required Igo1 and Igo2 for their appropriate transcriptional induction. The genes that were specifically affected by the simultaneous deletion of *IGO1* and *IGO2* but independent of *RIM15,* included genes under the control of the nitrogen discrimination pathway (*e.g. DAL80, MEP2, DAL3, GAT2*) and genes encoding high- and low- affinity permeases (*e.g. PUT4, DIP5, GAP1, AGP1*), which were previously shown to be controlled independently on Rim15 [78]. Importantly, many of the Igo1/Igo2-dependent genes are specifically induced by rapamycin and are normally not affected during the diauxic shift (Table VII). Moreover almost 60% of the Igo1/Igo2-dependent genes that were induced in a Rim15-independent manner following a rapamycin treatment were found not to require the transcription factors Gis1 and Msn2/Msn4 for their transcription, despite the fact that most of them contained several STREs and PDS elements (Table VII). These data indicate that Igo1 and Igo2 are important regulators of transcription, which are regulated by TORC1 via both a Rim15-dependent and a Rim15-independent mechanism to induce a subset of the transcriptional response to rapamycin and probably to starvation.

In addition, we observed that the transcription levels of many genes that are downregulated in the wild type remained high even after a 180-min rapamycin treatment in both the *rim15Δ* and *igo1Δigo2Δ* mutant strains, a defect that we had not remarked in our previous analysis. The genes whose repression was affected did not seem to fall in any particular functional class; the deletion of *RIM15* and or of *IGO1* and *IGO2* appears to result in a less pronounced general repression of transcription. This could be a consequence rather than the cause of the inability of the mutant strains to correctly arrest growth in response to quiescence-triggering stimuli like starvation and rapamycin treatment.

Yeast ORF	Gene	Description	Fold Change (180-min rapamycin treatment)					DS	Promoter elements	
			WT	*rim15Δ*	*igo1Δ igo1Δ*	*msn2Δ msn4Δ*	*gis1Δ*		STRE	PDS
Common target genes										
C-compounds and carbohydrate metabolism										
YFR053C	*HXK1*	Hexokinase I	3.89	-1.72	1.45	-3.27	3.78	no	5	0
YDR342C	*HXT7*	High-affinity hexose transporter	3.23	-2.68	-1.02	-4.89	1.79	no	4	0
YDR343C	*HXT6*	High-affinity hexose transporter	2.91	-2.77	-1.08	-5.06	1.71	no	5	0
YDR277C	*MTH1*	Repressor of hexose transport genes	2.27	-1.48	-1.27	-2.99	3.07	**yes**	3	0
YDL022W	*GPD1*	Glycerol-3-phosphate dehydrogenase (NAD+), cytoplasmic	2.11	-1.27	1.11	-1.12	3.71	**yes**	4	0
TCA cycle										
YDR148C	*KGD2*	2-oxoglutarate dehydrogenase complex E2 component	2.64	1.44	1.62	1.19	2.36	**yes**	1	0
YOR136W	*IDH2*	Isocitrate dehydrogenase (NAD+) subunit 2, mitochondrial	2.45	1.43	1.48	1.27	1.72	**yes**	2	0
YKL085W	*MDH1*	Malate dehydrogenase precursor, mitochondrial	2.14	1.01	1.69	-1.06	2.11	**yes**	2	1
Stress response										
YBL075C	*SSA3*	Heat shock protein of HSP70 family, cytosolic	3.97	1.35	1.19	1.23	2.60	**yes**	0	3
YBR054W	*YRO2*	Strong similarity to HSP30 heat shock protein Yro1p	3.81	-1.16	-1.87	1.20	4.23	no	1	2
YAL005C	*SSA1*	Heat shock protein of HSP70 family, cytosolic	2.97	-1.24	2.41	-1.30	4.00	no	2	1
YPL240C	*HSP82*	Heat shock protein	2.75	-1.16	2.23	-1.16	2.83	no	2	1
YJL059W	*YHC3*	May function as a chaperone	2.66	1.35	2.10	1.07	2.99	**yes**	2	1
YPL203W	*TPK2*	cAMP-dependent protein kinase 2, catalytic chain	2.51	1.05	1.55	-1.07	2.31	no	1	0
YPL004C	*LSP1*	Strong similarity to YGR086c	2.35	1.20	1.23	1.12	2.00	no	3	1
YOR007C	*SGT2*	Similarity to protein phosphatases, response to heat	2.25	1.46	1.97	1.39	2.33	no	0	1
YDR513W	*GRX2*	Glutaredoxin	2.17	1.48	1.75	1.45	1.72	**yes**	3	0
YIL033C	*BCY1*	cAMP dependent protein kinase, regulatory subunit	2.03	1.24	1.58	1.13	1.66	**yes**	0	0
Mitochondiral functions, respiration										
YKL150W	*MCR1*	Gytochrome-b5 reductase	2.68	1.39	1.62	1.09	2.08	no	4	1
YJL079C	*PRY1*	Similarity to the plant PR-1 class of pathogen related proteins	2.62	1.44	1.64	1.39	3.51	no	1	1
YDL181W	*INH1*	Inhibitor of mitochondrial ATPase	2.36	1.40	1.85	1.22	2.53	no	2	0
YIL140W	*AXL2*	Required for axial pattern of budding	2.14	1.36	2.43	1.44	2.38	no	0	1
YBL045C	*COR1*	Ubiquinol-cytochrome-c reductase	2.13	1.40	1.47	1.15	1.95	**yes**	2	1
YKL016C	*ATP7*	F_1/F_0-ATPase complex	2.06	1.39	1.77	1.36	2.14	**yes**	0	0
Proteolytic degradation										
YKL145W	*RPT1*	26S proteasome regulatory subunit	2.38	1.45	1.68	1.39	2.03	no	0	0
YJL036W	*SNX4*	Weak similarity to MVP1P	2.23	1.42	1.48	1.14	1.74	no	1	0
YCL057W	*PRD1*	Proteinase	2.14	1.43	1.53	1.32	1.79	no	0	0
YDR427W	*RPN9*	Subunit of the regulatory particle of the proteasome	2.06	-1.07	1.22	-1.01	1.46	no	0	0
DNA processing										
YDL101C	*DUN1*	Protein kinase	2.30	1.28	1.68	1.16	1.61	no	2	1
YMR152W	*YIM1*	Mitochondrial inner membrane protease	2.17	1.27	1.59	1.28	1.59	no	2	1
YGR231C	*PHB2*	Prohibitin	2.14	1.41	1.59	1.35	1.82	no	1	1
YER095W	*RAD51*	DNA repair protein	2.03	1.45	1.56	1.37	1.83	no	2	1
Metabolism of lipids and energy reserves										
YML131W		Similarity to human leukotriene b4 12-hydroxydehydrogenase	2.36	1.44	1.21	1.34	1.54	no	2	0
YJL137C	*GLG2*	Self-glucosylating initiator of glycogen synthesis	2.23	-1.05	1.55	1.04	1.67	**yes**	2	0
YDR313C	*PIB1*	Phosphatidylinositol(3)-phosphate binding protein	2.14	1.21	1.67	1.13	1.95	**yes**	1	0
Protein synthesis										
YJL102W	*MEF2*	translation elongation factor, mitochondrial	2.31	1.42	2.03	1.42	2.38	**yes**	4	0
YGR201C		strong similarity to translation elongation factor eEF1 alpha chain CAM	2.13	1.22	1.41	1.33	1.03	**yes**	2	0
Other or unknown functions										
YHL031C	*GOS1*	SNARE protein of Golgi compartment	2.20	1.10	1.01	-1.04	1.13	no	1	0
YDR202C	*RAV2*	Regulator of (H+)-ATPase in Vacuolar membrane	2.17	1.16	1.39	1.11	1.52	no	3	0
YIR036C		Similarity to E.coli fabD	2.58	1.49	2.04	1.25	2.23	**yes**	1	1
YOR161C	*PNS1*	Similarity to *C.elegans* cosmid F35C8	2.36	-1.29	1.42	1.02	1.60	**yes**	2	0
YGL047W	*ALG13*	Similarity to hypothetical *S. pombe* protein	2.23	1.29	1.97	1.22	2.30	no	1	0
YMR031C		Similarity to YKL050c and human restin	2.14	1.34	1.53	1.13	1.72	no	3	0
YER053C-A		Unknown	2.08	-1.49	-1.08	-1.35	1.60	no	0	0
YLL001W	*DNM1*	Dynamin-related protein	2.07	1.28	1.33	1.09	1.57	**yes**	0	1
YPR172W		Similarity to YLR456w	2.01	1.40	1.39	1.35	1.30	no	0	0
Igo1/2-specific target genes										
C-compounds and carbohydrate metabolism										
YCL040W	*GLK1*	Aldohexose specific glucokinase	5.50	2.43	2.17	1.36	9.06	**yes**	4	0
YJL164C	*TPK1*	cAMP-dependent protein kinase 1, catalytic chain	4.89	2.08	2.01	1.37	3.36	**yes**	3	2
YAL061W		Similarity to alcohol/sorbitol dehydrogenase	3.29	3.05	1.72	1.49	2.08	**yes**	3	1
YJL141C	*YAK1*	ser/thr protein kinase	2.38	2.10	1.72	1.15	2.10	**yes**	3	0
YPL026C	*SKS1*	Suppressor kinase of *SNF3*	2.27	2.45	1.36	-1.05	2.95	no	0	0
YDR043C	*NRG1*	transcriptional repressor for glucose repression of STA1 gene expressi	2.04	2.81	-1.08	1.41	1.40	**yes**	2	0
Mitochondiral functions, respiration										
YER053C	*PIC2*	strong similarity to mitochondrial phosphate carrier protein	3.97	2.04	1.92	1.20	1.88	**yes**	1	0
YML120C	*NDI1*	NADH-ubiquinone-6 oxidoreductase	2.95	2.19	1.77	1.24	2.35	**yes**	1	1
YOR358W	*HAP5*	CCAAT-binding factor subunit	2.27	2.04	1.54	1.39	2.07	no	2	0
NCR controlled genes and amino acid metabolism										
YKR034W	*DAL80*	Transcriptional repressor for allantoin and GABA catabolic genes	11.47	16.00	1.04	-1.04	2.85	no	1	1
YNL142W	*MEP2*	High affinity low capacity ammonia permease	6.45	7.67	1.47	1.16	2.14	no	0	0
YOR348C	*PUT4*	Proline and gamma-aminobutyrate permease	5.86	12.13	1.13	1.40	3.01	no	3	0
YPL265W	*DIP5*	Dicarboxylic amino acid permease	4.20	5.10	1.14	1.21	1.75	no	2	0
YKL124W	*SSH4*	Suppressor of SHR3	3.61	2.39	2.08	1.44	2.89	no	2	0
YIR032C	*DAL3*	Ureidoglycolate hydrolase	3.43	3.46	-1.29	-1.51	1.71	no	1	0
YMR136W	*GAT2*	Weak similarity to YIR013c and YLR013w	3.34	2.46	1.97	1.39	4.35	no	2	0
YKR039W	*GAP1*	General amino acid permease	2.71	2.71	1.38	1.25	1.74	no	3	0
YCL025C	*AGP1*	Asparagine and glutamine permease	2.08	3.27	-1.53	-1.57	1.04	no	2	0
Autophagy										
YDL113C	*ATG20*	similarity to hypothetical protein YDR425w	2.48	2.22	1.47	1.47	1.77	no	1	0
Other or unknown functions										
YDR475C	*JIP4*	Part of a Gis1-complex	2.17	2.17	1.49	1.42	1.78	no	2	0
YHR150W	*PEX28*	Peroxisomal protein	2.10	2.16	1.47	1.25	1.60	no	0	0
YER067W		Unknown	4.66	2.30	1.33	-1.01	1.99	**yes**	4	0
YLR257W		Unknown	2.73	3.20	1.22	1.44	1.75	no	2	0
YKR011C		Unknown	2.68	2.13	1.92	1.34	2.69	no	1	1
YLR108C		Unknown	2.68	2.00	-1.46	-1.84	2.35	no	3	0
YGR243W		Unknown	2.57	2.93	1.01	-1.42	2.31	**yes**	4	1
YIL077C		Unknown	2.16	2.04	1.66	1.36	1.44	**yes**	0	0
YHR159W		Unknown	2.01	2.16	1.47	1.31	1.78	**yes**	0	0

Table VII

Genes induced following a 180-min treatment with rapamycin that depend on Igo1/Igo2 for their induction. DS, induction during the diauxic shift.

The rapamycin-induced G_1 arrest is delayed in *igo1Δigo2Δ* mutants

As we had observed that, similarly to *rim15Δ* mutants, *igo1Δigo2Δ* mutants failed to acquire many characteristics of arrested cells following rapamycin treatment, we decided to closely analyze the ability of these strains to arrest growth as small unbudded cells with a single unreplicated genome following rapamycin treatment. We performed FACS analyses of these mutants and found that, as observed for *rim15Δ* mutants, the rapamycin-induced growth arrest in G_1 was delayed in *igo1Δigo2Δ* mutants (Figure 47).

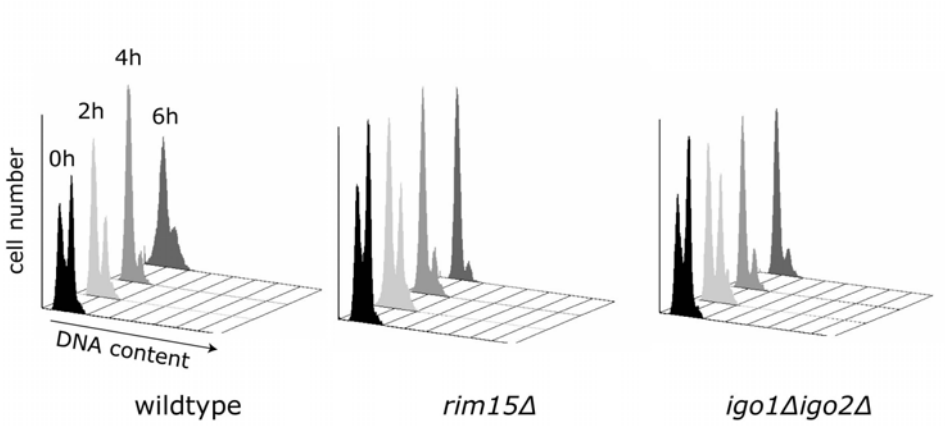

Figure 47

FACS analysis of wild-type strains and of *rim15Δ* and *igo1Δigo2Δ* mutant strains, following treatment with rapamycin for the indicated times.

This difference was more pronounced after 2 hours treatment; notably the same time point where the major differences in gene expression were observed.

Induction of the G_0-program by Rim15 requires phosphorylation of serine 64 in Igo1

We then asked whether Rim15-mediated phosphorylation of serine 64 in Igo1 was required for the function of Igo1 in the induction of Rim15-dependent G_0 traits. To answer this question we introduced in a *igo1Δigo2Δ* deletion strain a centromeric vector expressing, under the endogenous *IGO1* promoter, either a wild-type Igo1 protein or mutated versions where the serine residues at position 64 and 105, phosphorylated by Rim15 and likely PKA, respectively, were replaced with either alanine (which can not be phosphorylated) or aspartate (which may mimic a phosphate group). We then analyzed both the rapamycin-induced accumulation of the Rim15-dependent *HSP26* and *HSP12* transcripts and of glycogen (Figure 48).

We found that, while expression of a wild-type copy of Igo1 complemented the gene expression defect of an *igo1Δigo2Δ* mutant, the expression of two Igo1 versions, which had the Rim15 target serine (serine 64) replaced with either an alanine or an aspartate residue did not

complement this defect (Figure 48A). Curiously the aspartate substitution did not mimic Rim15-dependent activation of Igo1 when expressed at endogenous levels. In contrast, overexpression of this allele was more efficient than the wild-type allele in complementing the defect of a *rim15Δ* strain (Figure 48B).

When the putative PKA target serine was replaced with an alanine, the expression levels of the *HSP26* and *HSP12* genes were slightly higher than with the wild type Igo1 allele. In this case the aspartate substitution resulted in the opposite phenotype (Figure 48A).

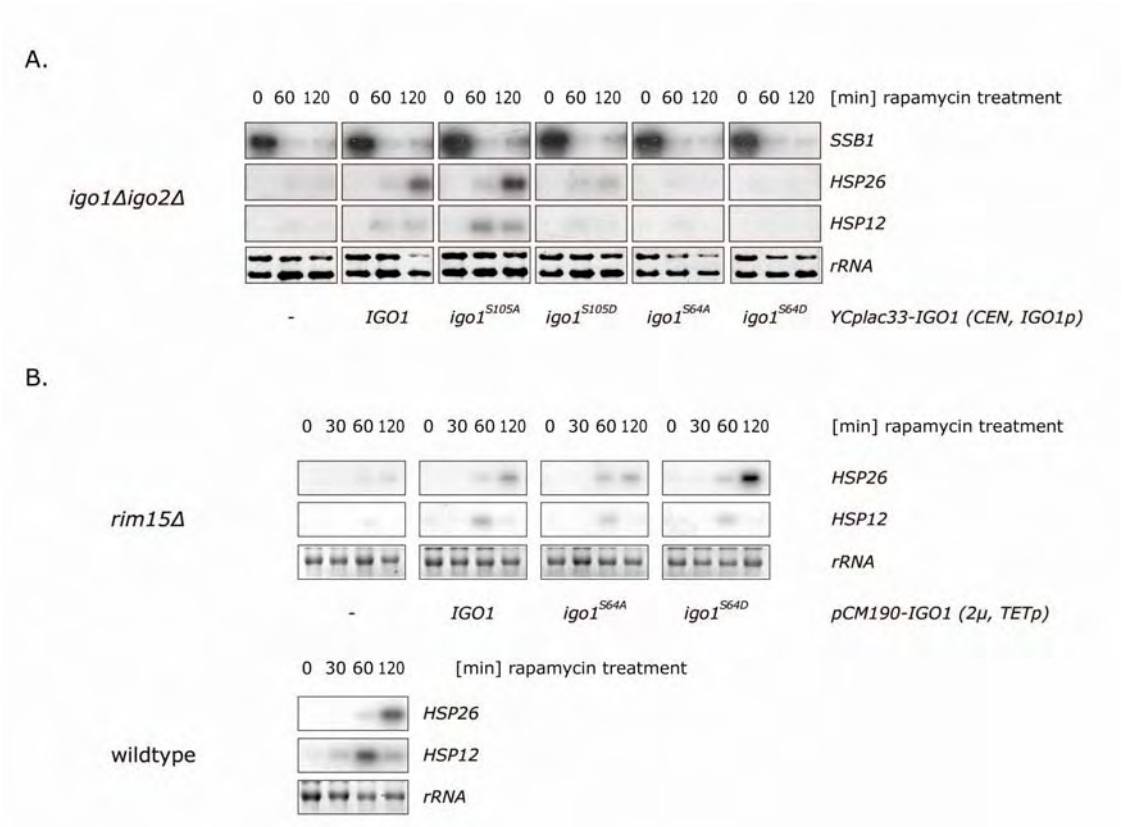

Figure 48

Northern blot analysis of the rapamycin-induced accumulation of Rim15-dependent transcripts (*HSP26, HSP12*) [A.] Gene expression in response to rapamycin in an *igo1Δigo2Δ* strain expressing endogenous levels of either the wild-type *IGO1* or aspartate/alanine substitutions in the conserved putative PKA and Rim15-phosphorylation sites [B.] Gene expression in response to rapamycin in a rim15Δ strain overexpressing either the wild-type *IGO1* or *igo1* variants harboring aspartate/alanine substitutions in the conserved Rim15-phosphorylation site. Bottom panel: wildtype. The rapamycin-repressible gene *SSB1* gene was used as an internal control for the effect of rapamycin; similar amounts of total RNA were loaded in each lane.

These data indicate that phosphorylation of serine 64 in Igo1 is both necessary and sufficient to mediate the Rim15-dependent rapamycin-induced G_0 arrest. Interestingly Rim15 and PKA seem to inversely regulate Igo1 as mimicking a phosphorylation on the presumed PKA target serine at position 105 (by aspartate substitution) prevents the activation of Igo1 by Rim15 in response to

rapamycin. In contrast, an allele which can not be phosphorylated by PKA displays increased activity in response to rapamycin, while the basal activity is not affected by this mutation.

Conclusions and outlook

We have applied a microchip technology to identify possible substrates for the serine/threonine kinase Rim15. Using this technique we were able to isolate a protein product that was efficiently phosphorylated *in vitro* by purified Rim15. The Rim15 substrate corresponded to the product of the uncharacterized open reading frame *YNL157W/IGO1*. Further analysis confirmed that both, this protein and the protein product of the homologous *YHR132W-A/IGO2* gene were phosphorylated *in vitro* by Rim15. Rim15 phosphorylates Ynl157wp (Igo1) on the serine residue at position serine 64, which is located within a highly conserved region. Using antibodies against the phosphorylated serine 64 in Igo1, we confirmed that this residue is a target for Rim15-dependent phosphorylation *in vivo* under all conditions known to trigger nuclear localization/activation of Rim15 including phosphate and nitrogen starvation, diauxic shift and rapamycin treatment.

Deletion of *IGO1* and *IGO2* phenocopies the deletion of *RIM15*; *igo1Δigo2Δ* mutants are defective in the induction of the G_0 differentiation program (including the accumulation of glycogen and trehalose, the transcription of stress-responsive genes, and proper cell-cycle arrest) in response to rapamycin or nutrient starvation (diauxic shift). In addition, similarly to *rim15Δ*/*rim15Δ* diploids *igo1Δ/igo1Δ igo2Δ/igo2Δ* homozygous diploids show dramatically reduced sporulation rates. These observations indicate that the products of these genes are essential downstream effectors of Rim15 and are critical for the induction of the G_0 program.

Notably the absence of *IGO1* and *IGO2* appears to affect some phenotypes more severely than the absence of *RIM15* suggesting that Igo1 and Igo2 may be involved also in the control of some Rim15-independent responses.

Interestingly, in addition to being positively controlled by Rim15, Igo1 may also be negatively regulated by a PKA-dependent mechanism. Mutations that presented the phosphorylation of the conserved PKA consensus site at position 105 in Igo1 resulted in an overactive, yet still Rim15-regulated, Igo1 allele. Conversely, a phosphomimetic substitution at the corresponding position resulted in a Rim15-resistant allele which could not be activated by phosphorylation on serine 64 following a rapamycin treatment. Phosphorylation of serine 105 by PKA under growth-permissive conditions may affect the activity of Igo1 or its ability to be activated by Rim15; on the other hand, dephosphorylation of the PKA site at serine 105 and (subsequent) phosphorylation of the Rim15 site at serine 64 may ensure maximal activation of Igo1 and of the Igo1-dependent G_0-characteristic phenotypes. Interestingly, mutation of the PKA site to

either alanine or aspartate was also reported to affect the ability of the human homologue ARPP-19 to stabilize a reporter mRNA of a neuronal gene in response to nerve growth factor (NGF) [218].

We have established that Igo1 and Igo2 are the targets of Rim15, which are responsible for all the known functions of this kinase. Unfortunately, the function of these Rim15 targets remains still a mystery. There are a few indications that Igo1/Igo2 may be involved directly in the regulation of gene expression; in particular, the reported (two hybrid and affinity purification) interactions for these proteins support a role that is closely related to the transcriptional machinery.

Igo1 was identified as an interactor of *RNA15*, a component of the cleavage and polyadenylation factor I (CF I) that is involved in the recognition of the A-rich element in mRNA, an essential step in mRNA 3'-end formation. Importantly, processing of the 3'ends is an event that ultimately affects the efficiency of transcriptional termination, nuclear export and translation and contributes to the longevity of mRNA in the cytoplasm and is thus considered an additional mechanism for the control of gene expression. In this context it is important to mention that in human cell lines the Igo1 homolog ARPP-19 binds directly to mRNA and is involved in the post-translational regulation of gene expression by promoting the stabilization of particular mRNAs in response to NGF, thereby contributing to the development and plasticity of the nervous system [218].

Igo1 was also reported to interact in a two-hybrid assay with the transcription factor Ace2, which, in its dephosphorylated form, is found in the nucleus where it activates the expression of early G_1-specific genes. Another protein with which Igo1 was found to exhibit a two-hybrid interaction was Yer064cp, which is likely to be involved in transcription. Finally, Igo1 co-purifies with Htb2, one of two nearly identical histone 2 B (H2B) subtypes, which are required for chromatin assembly, and with Cpr1, the target of the immunosuppressive agent FK506 and a possible component of the Sin3-Rpd3 histone deacetylase complex. These interactions are particularly intriguing since the Rim15-dependent regulation of meiosis in known to involve remodeling of chromatin by removal of the Sin3-Rpd3 histone deacetylase complex from EMGs promoters [114]. It is conceivable that Rim15 regulates the transcription of both EMGs and G_0 genes by affecting the acetylation/deacetylation of histones indirectly via regulation of chromatin remodeling factors such as the Sin3-Rpd3 deacetylase or the silencing protein Sir4. The interactions involving Igo1, together with our observation that Igo1 and Igo2 mediate the Rim15-dependent responses support a model where Igo1 and Igo2 directly bind to chromatin elements to mediate their modification in response to the activity of the protein kinase Rim15. Interestingly, preliminary data

indicate that Igo1 and Igo2 may associate with the unsoluble fraction of chromatin; moreover our chromatin immunoprecipitation (ChIP) experiments also suggest that the promoter region of *HSP26* may be enriched in Igo1-myc^{13} immunoprecipitates (Not shown).

Future efforts will certainly be directed in confirming these interactions and observations in order to define the mechanism through which Rim15 and Igo1/Igo2 modulate the expression of genes that critically affect the cell differentiation program in response to nutrient starvation.

Concluding Remarks

Concluding Remarks

Understanding the complex signaling networks that are involved in the regulation of proliferation and quiescence in eukaryotic cells is clinically extremely relevant, as many serious pathological conditions implicate the regulation or the misregulation of these processes. Suffice to recall at this point the consequences of the failure of cells in tissues to arrest growth, or of stem cells to exit from quiescence and to regenerate damaged tissues.

In the general context of the efforts aimed at elucidating the regulatory mechanisms of G_0 entry/exit in eukaryotic cells, we specifically studied the molecular structure, the regulation and the function of the *S. cerevisiae* protein Rim15, which represents a key regulator of G_0 in yeast.

During the diauxic transition, signals from key nutrients induce metabolic, morphological and transcriptional modifications that are required for the survival during the subsequent post-diauxic phase, which is characterized by respiratory metabolism. Most genes required for the initiation of (and survival in) the G_0 state also need to be induced during the diauxic phase. In the absence of Rim15, yeast cells do not respond correctly to nutrient signals during the diauxic shift and are not able to induce the transcriptional changes required for the initiation of the quiescent program. In particular, here I describe that Rim15, through its cellular targets Igo1 and Igo2, mediates the transcriptional induction of a subset of the genes that require the transcription factors Msn2/Msn4 and Gis1 for their expression during the diauxic shift. The genes that depend on Rim15 include notably genes required for respiratory metabolism, as well as for detoxification of reactive oxygen species, which are increasingly produced during respiration. As a consequence *rim15Δ* mutants as well as *igo1Δ igo2ΔI* mutants fail to acquire many G_0 characteristics such as the accumulation of stress-protective reserve carbohydrates. Instead they continue proliferating despite the lack of nutrients and eventually perish, probably under the weight of the damage produced by their own metabolism or due to the complete depletion of extracellular nutrients and their failure to accumulate intracellular nutrient storages.

Notably the role of Rim15 appears to be essential under physiological conditions, when the nutrients are actually absent. Accordingly, the absence of Rim15 severely reduces the time a culture remains viable in stationary phase, indicating a positive role of this protein in a process required for the determination of the chronological life span. As observed for the induction of the quiescence program, the function of Rim15 in controlling longevity is negatively regulated by the nutrient

sensing pathways TORC1, Sch9 and PKA. Accordingly mutations affecting these pathways significantly prolong the yeast's life span [79,203,204].

By addressing the molecular structure of Rim15 the fist part of this study revealed an unsuspected level of complexity that requires further analysis. Rim15 is a multidomain protein and contains a PAS and a REC domain that are both conserved and unique. While, the domains in Rim15 resemble previously described domains, they differ significantly from the "classical" domains in catalytically important residues, indicating that provided that they are functional, they may operate via novel molecular mechanisms. In addition, Rim15 contains a previously unidentified zinc finger motif that shows phosphoinositide-binding activity and that is essential for the kinase activity of Rim15 both *in vitro* and *in vivo*.

The molecular complexity of Rim15 is mirrored by an equally complex regulation by the pathways that transduce signals from key nutrients. These form an intricate signaling network of which Rim15 appears to be an essential node. While the regulation of Rim15 by PKA had been elucidated previously, it was not clear how Rim15 was controlled by the TORC1 pathway. The observations from this study, together with other studies from our laboratory lead us to the conclusion that TORC1 may affect the intracellular localization of Rim15 via independent phosphorylation by both the TORC1-controlled Sch9 kinase and the cyclin-CDK Pho80-Pho85 complex. The corresponding two residues represent, when phosphorylated, the docking sites for the cytoplasmic 14-3-3 anchor proteins Bmh1 and Bmh2. TORC1 by regulating a yet unknown Rim15 downstream effector, a process that also involved the catalytic subunits of PP2A and their regulatory Tap42 protein.

We identified the cellular targets and found that their Rim15-dependent phosphorylation is necessary to the initiation of G_0 (hence the names Igo1 and Igo2 for initiation of G_0) in response to nutrient depletion during the diauxic shift and to the TORC1 inhibitor rapamycin. The Rim15 targets are the yeast homologues of a family of small mammalian proteins of unknown functions, the endosulfine family. In addition of mediating the Rim15-dependent G_0 response, Igo1 and Igo2 are also involved in the integration of additional, Rim15-independent signals.

Finally, a key finding of the present thesis is the identification and molecular description of the *bona fide* Rim15 target proteins Igo1 and Igo2. Like Rim15, Igo1 and Igo2 are essential for the initiation of the G_0 program in response to nutrient depletion. As members of a conserved protein family, *i.e.* the endosulfines family, Igo1 and Igo2 may ultimately lead us to the "holy grail" in this field of research, namely the understanding of the mechanism that ultimately controls entry into G_0.

Materials and Methods

Methods

Growth conditions, media, microbiological and recombinant DNA methods

Yeast and *Escherichia coli* media were prepared according to standard recipes [219,220] unless otherwise stated. Yeast cells were grown at 30°C either in (full) YPD medium (1% w/v yeast extract, 2% w/v bacto-peptone, 2% w/v glucose) or in selective medium (0,67% w/v yeast nitrogen base without amino acids, 2% w/v glucose) supplemented with the appropriate auxotrophic requirements. Solid media were prepared like the liquid media but contained 2% w/v agar in addition. For Kan^R selection, geneticin (Brunshwig, Cat.No. BRP25-011) was added to a final concentration of 100 μg/ml. For Nat^R selection, nourseothricin (WERNER BioAgents, Cat.No. 50000) was added to a final concentration of 100 μg/ml. For experiments with post-diauxic phase cells, cell cultures were grown on full YPD media and glucose consumption was monitored using the Glucose Liquicolor reagent (Human GmbH, Cat.No. 10260). For experiments with rapamycin, cell cultures maintained in the exponential phase of growth were treated with 200 ng/ml rapamycin. The rapamycin stock solution was prepared dissolving powdered rapamycin (LC Labs, Cat.No. R-5000) in an Ethanol:Tween20 (90:10) solution to a final concentration of 1 mg/ml.

Bacterial cultures were grown at 37°C on LB medium (1% w/v NaCl, 1% w/v Bacto-tryptone, 0.5% w/v yeast extract). Solid medium contained 2 % w/v agar in addition. For Amp^R selection, ampicillin was added to a final concentration of 100 μg/ml.

Plasmid manipulations were performed in *E. coli* strain DH5α (Gibco BRL) using standard procedures [219]. The *E. coli* strain BL21 (Stratagene, Cat.No. 230280) was used for bacterial expression of yeast proteins. Standard procedures of yeast genetics and molecular biology were used [219-221]. Yeast transformations were performed using a modification of the Li^+-ion method [222].

Viability and determination of the chronological life span

To determine the percentage of viable cells in a culture cells were collected by centrifugation and the pellets resuspended directly in a trypan blue solution (Sigma-Aldrich, Cat.No. T8154). After 5-min incubation cells were observed under a light microscope; blue-colored cells which incorporated the dye were scored as dead, white-colored cells which actively excrete the dye were scored as viable. For each strain and condition >100 cells were counted.

To determine the chronological life span, cells cultures were incubated at 30°C without replacing the growth medium for several weeks. Culture aliquots were collected regularly and serial dilutions were plated on rich media (YPD) containing 2% glucose. The colony forming units per ml (CFU/ml) culture were determined by visually scoring the plates (number of colonies x dilution factor) and expressed as a percent of the initial value (CFU/ml of the same culture at the beginning of the experiment). The results were plotted on a logarithmic scale.

Enzyme assays and determination of metabolite levels

Glucose concentrations in the culture media were determined using the enzymatic Glucose Liquicolor assay (Human GmbH, Cat. No. 10260) according to the manufacturer's instructions. For determination of trehalose concentrations, 1 ml stationary-phase cells was filtered (Whatman GF/C, Cat. No. 1822021), washed four times with distilled H_2O, resuspended in 1 ml distilled H_2O and transferred to a boiling water bath for 5 min. After centrifugation (5 min at 13'000 rpm), 50 µl of the supernatant were incubated with 0.01 units of trehalase EC 3.2.1.28 (Sigma, Cat. No. T8778) in 50 µl 0.2 M Na-acetate, 30 mM $CaCl_2$, pH 5.7 at 37°C for at least 2 hours. Trehalase cleaves one trehalose moiety into 2 glucose moieties; after the reaction the glucose level was determined as described above and control values were obtained from control samples without trehalase.

To assay the β-Galactosidase activity, *o*-nitrophenyl-β-galactoside (ONPG) was used as a substrate (Fluka, Cat. No. 73660), the product of ONPG cleavage by β-Galactosidase can be readily detected at $\lambda = 420$ nm. The galactosidase activity was expressed in Miller Units, an arbitrary value depending on the OD_{420} and on the cell density in the assay (OD_{420} / OD_{600} x volume of cells in assay [l] x time [min]).

To determine the glycogen levels in the cells, liquid yeast cultures were vacuum filtered over a nitrocellulose 0.45 µm MF-Membrane Filters (Millipore, Cat. No. HAWP02500); the filters, placed on an agarose layer in a Petri dish, were exposed to iodine vapor.

Analysis of two-hybrid interactions

Protein interactions were analyzed by two-hybrid analysis using the LexA system described in detail elsewhere [223]. Strain EGY48 (Invitrogen, Cat. No. C83500) containing the LexAop-lacZ reporter plasmid pSH18-34 (Invitrogen, Cat. No. V61120) was co-transformed with pEG202 or a pEG202-derived plasmid expressing a LexA-DBD fusion protein under the constitutive *ADH1* promoter and a pJG4-5 or a pJG4-5-derived plasmid expressing an AD fusion protein under the inducible *GAL1* promoter. Plasmids were constructed as described above, the β-galactosidase

activity was then assessed in at least 3 independent clones of each strain grown for 16 h at 30°C in minimal medium containing 2% w/v galactose, 1% w/v raffinose and 20 µg/ml leucine.

Purification, quantification and analysis of proteins

For protein purification from yeast, cells were harvested by 5-min centrifugation at 4°C (4000 rpm) and washed with 1½ volume cold water. Total cellular proteins were extracted in lysis buffer (50 mM Tris-HCl pH 7.5, 100 mM NaCl, 1 mM EDTA, 1 % NonidetP40) containing 1 mM (final concentration) PMSF, 1 tablet of the protease cocktail inhibitor Complete® (Roche Applied Science, Cat. No. 11697498001) and a phosphatase inhibitor mix (10 mM Sodium Fluoride, 10 mM 4-nitrophenyl phosphate Bis [tris-(hydrixymethyl) aminomethane] salt, 10 mM tetra-Sodium pyrophosphate, 10 mM β-glycerophosphate disodiumsalt, 10 mM Sodium Orthovanadate) using a FastPrep FP120 cell distruptor (BIO101/Q-biogene) and 0.4 mm acid-washed glass-beads (Verrerie De Carouge, 22901-050).

For protein purification from bacteria, cells were harvested by centrifugation, resuspended in 10 ml PBS 1x and sonicated by at least 8 cycles of 30 seconds each with pauses on ice. Cell debris were separated by 10-min centrifugation at 10 rcf. For GST fusion proteins the protein extracts were treated as described for yeast, except that all the buffers were PBS based, MBP fusion proteins (pMAL Protein Fusion and Purification System, New England Biolas, Cat. No. E8000S) were purified according to the manufacturer's instructions.

Protein concentrations were either measured using a bradford protein assay (Bio-Rad, Cat.No. 500-0006) according to the manufacturer's instructions or by a modified Lowry assay, using bovine serum albumine (BSA) as standard. For the pull down of epitope-tagged proteins, 10-30 mg protein extract were incubated with the proper amount of antibody for 1 h followed by incubation with ProteinG Agarose (Roche, Cat. No. 11243233001). For the pull down of GST-tagged proteins 50 µl GST-Sepharose beads were incubated with 10 to 30 mg protein extract. The beads were washed extensively with lysis buffer containing the phosphatase and protease inhibitors and 100 to 500 mM NaCl. Samples for loading were boiled for 5 min in the presence of SDS loading buffer. Usually 5 to 10 µl of the immunoprecipidated protein were loaded on SDS-polyacrylamide gels (SDS-PAGE) and transferred to nitrocellulose membranes for western-blot analysis. Blots were stained with Ponceau S to assess equal protein loading. The membranes were incubated with the indicated primary antibodies followed by (H+L)HRP Conjugate, human IgG anti-mouse/rabbit IgG secondary antibodies (Bio-rad, Cat. No. 170-6516/170-6515) and detected using the ECL Western blotting reagents (Amersham pharmacia, Cat. No. RPN2106) according to the manufactorer's instructions.

The bands were visualized by autoradiography on a BioMax MR film (Kodak, Cat. No. 8952855) developed using and automated film processor (M35 X-OMAT, Kodak).

Urea extraction of proteins for analysis

For analysis of protein levels and modifications *in vivo*, total proteins were extracted from equal amounts of cells (corresponding to 14 OD) by lysing the cells with an urea-based buffer. Basically the cells were collected by centrifugation and the culture medium was discarded; the cell pellet was respuspended in 300 µl SUME buffer (8 M urea, 1 % SDS, 10 mM MOPS pH 6.8, 10 mM EDTA, 0.01 % Bromphenol blue and 10 mM PMSF) and 0.3 g acid-washed glass-beads (0.4 mm). The cells were broken by subjecting these suspension to 5-min vortexing at room temperature after which 300 µl 2x-UREA sample buffer (8 M Urea, 4 % SDS, 10 % β-Mercaptoethanol, 0.125 M Tris pH 6.8) were added. The proteins were denaturated by a 10-min incubation at 65°C and the supernatant containing the proteins was transferred in a fresh tube and cleared from remaining cell debris by repeated centrifugation. The extracts were used immediately for loading on a SDS-PAGE or stored at -20°C.

Protein kinase assays

The GST-tagged wild-type or mutant Rim15 kinase proteins were purified using GST-Sepharose as described above and eluted from the beads using 15 mM reduced glutathione(Sigma-Aldrich, Cat.No. G4251). Equal amounts of the eluted protein were used to phosphorylate the indicated substrate in the presence of [γ^{32}P]-ATP in kinase buffer (50 mM Tris-HCl at pH 7.5, 20 mM $MgCl_2$, 1 mM DTT and 1 mM ATP). The reactions were stopped after the indicated times by adding 5 µl SDS-gel loading buffer and subsequent boiling for 5 min. Samples were subjected to SDS-PAGE and the gels were dried and exposed to X-ray film or transferred to nitrocellulose membranes for western-blot analysis.

Large scale kinase assay

The GST-tagged wild type or mutant Rim15 kinase proteins were purified using GST-Sepharose as described above and eluted from the beads using 15 mM reduced glutathione. The eluted kinases were used to phosphorylate a protein microarray containing virtually all yeast proteins, as described elsewhere [213].

Liposome assay for protein-lipid binding

Liposomes were prepared essentially as described before [224]. Phosphoinositide lipids were purchased from Echelon Biosciences Inc. and lipid stock solution were prepared by dissolving the lyophilized lipids in a Metanol:Chloroform (2:1) solution. A mixture containing 320 µg phosphatidylcholine (PC), 80 µg phosphatidylserine (PS) and 100 µg of the indicated phosphoinositide were dried using a speed vacuum concentrator. The lipid film was resuspended in 0.5 ml of liposome buffer (25 mM Hepes-NaOH, pH 7.0 and 1 mM dithiothreitol) and sonicated for 30' in a water bath sonicator. The suspension was centrifuged for 15 min at 14,000 rpm in a microcentrifuge and resuspended in liposome buffer containing 0.5 mg/ml bovine serum albumine (BSA). For protein-lipid binding assays 50 µl of these suspensions were incubated with 2 µg of the purified protein diluted in 20 µl liposome buffer containing 0.5 mg/ml BSA. These mixtures were incubated for 15 min at room temperature or for 1 h at 4°C. The liposomes were then collected by 15-minutes centrifugation at 14'000 rpm in a microcentrifuge and the supernatant (SUP) was saved for further analysis. After washing twice with liposome buffer the liposome-containing pellet (PEL) was resuspended in 70 µl liposome buffer. Equal amounts of SUP and PEL were subjected to SDS-PAGE and western blotting to detect pellet-associated proteins.

For protein kinase assays in the presence of liposomes, a modified protocol was used; the procedure was essentially as described except that liposomes were resuspended in a Tris-HCl buffer (50 mM Tris-HCl pH 7.5, 20 mM $MgCl_2$, 1 mM DTT).

Protein-lipid overlay assays

Lipid stock solution were prepared by dissolving the lyophilized lipids in a Metanol:Chloroform:Water (2:1:0.8) solution to a final concentration of 1 mM (1000 pmol/µl). Serial dilutions of the indicated phosphoinositides were spotted onto Hybond-c extra membranes (Amersham Life Science, Cat. No. RPN203E) and the filters were allowed to dry at least 1 hour before use. The membranes were blocked overnight at 4°C in 3% fatty acid free BSA (Sigma-Aldrich, Cat.No. A8806) in TBS-Tween 20, then 0.25 to 1.0 µg/ml of the protein of interest (diluted in 10 ml TBS-Tween 20 containing 3% BSA) were incubated with the membranes for 1 to 4 hours. After extensive washing with TBS-Tween 20 the membranes were subjected to western blotting to detect lipid-bound proteins.

Preparation of mRNA for microarray analysis

For mRNA preparation and synthesis of cDNA, yeast strains were grown at 30°C in YPD medium. Overnight cultures of 5 ml were diluted to an OD_{600} of 0.2 and maintained in exponential

growth phase (OD_{600} < 1.0) for a period of 12 h by repeated dilution in fresh YPD medium to ensure complete depletion of stationary phase-specific transcripts. At this point exponential-phase samples were harvested. Subsequently, the cultures were grown until glucose was exhausted in the medium, and diauxic-shift samples were harvested 30 min after glucose exhaustion. Total RNA was then extracted using the RNApure kit (GeneHunter Corporation) according to the manufacturer's instructions. Radiolabeled cDNA probes were generated from 1 μg of total RNA by reverse transcription of mRNA using Superscript II reverse transcriptase (Invitrogen, Cat. No. 18064-022), an oligo(dT) primer (10- to 20-mer mixture; Research Genetics), and [γ^{33}P]-dCTP. Labeled probes were purified by passage through Bio-Spin 6 Chromatography Columns (Bio-Rad, Cat. No. 7326221) and denatured for 5 min at 95°C.

GeneFilter hybridization and data analysis

Yeast Index GeneFilters (Research Genetics-Invitrogen) were hybridized with the labeled probes according to the manufacturer's protocol. The filters were scanned by use of a PhosphorImager (Fuji BAS-1000) to obtain digital images. The images were then converted to TIFFs and imported into the Pathways version 4.0 software (Research Genetics) for analysis and quantification of spot intensities. The intensities were normalized against all data points. The average ratio was calculated from log2 expression ratios during the diauxic-shift transition relative to the exponential phase of growth from two independent experiments. Non-interpretable spots were manually flagged and excluded. Descriptions of gene products were derived from the Saccharomyces Genome Database and/or the Comprehensive Yeast Genome Database (MIPS).

Agilent microarrays and data analysis

Analysis of global transcription changes in response to rapamycin were performed in collaboration of Dr. James Broach, in his laboratory.

Strains were grown in full medium (YEPD) overnight, diluted to OD_{600} of 0.1 and treated with rapamycin when they reached OD_{600} of 0.5. Samples were collected in the exponential phase and after 20, 40, 60, 90, 120 and 180 min from the addition of rapamycin. Standard protocol for Agilent microarrays were used. The normalized data, expressed as log2 expression ratios relative to the exponential phase, were analyzed as described in the text.

Preparation of mRNA for Northern blot analysis

Samples were collected at the indicated times. Cells were harvested by centrifugation and washed twice in DEPC-H_2O. Total RNA was extracted using the Hot Phenol method and prepared as described [223], 5 µg RNA were loaded for Northern blot analysis. DNA probes were labeled with [α^{32}P]-CTP using the PRIME-IT II Random Primer labeling kit (Stratagene, Cat. No. 300385). The labeled probes were purified through a spin column by size separation (Bio-Rad, Cat. No. 7326221).

Mass Spectrometry

To identify the phosphorylation site in Igo1, the recombinant GST-Igo1 protein purified from bacteria was incubated with either the wild type GST-Rim15 kinase or a kinase inactive GST-Rim15^{K823Y} purified from yeast in the presence of ATP. The reaction mixtures were then separated on a SDS-PAGE and the bands corresponding to GST-Igo1 were excised and digested with trypsin. The protein digest was loaded onto a microcapillary liquid chromatography system (OD-SAQ, C18, 5um 300 A, 75µm i.d. x 10cm) and eluted directly into a tandem mass spectrometer (Voyager Super STR) with electrospray ionisation.

Igo1 phosphorylation

Antibodies against the phosphorylated peptide H_2N-KRKYFDpSGDYALQC-$CONH_2$ were raised in rabbits and purified by double-affinity purification in order to separate phosphospecific antibodies from sequence specific (Eurogentech).

Immunolocalization

For immunolocalization studies cells were fixed by adding 1:10 formaldehyde (final formaldehyde concentration 3.7 % directly to the culture sample. After 1 h incubation at RT cells were harvested by centrifugation at 4000 rpm, resuspended in 2 ml fixative solution (3.7 % Formaldehyde, 0.1 M KPO_4, 1 mM $MgCl_2$) and incubated overnight at room temperature. The fixed cells were resuspended in 1 ml TEB buffer (200 mM Tris.HCl pH 8.0, 20 mM EDTA, 1 % β-mercaptoethanol) and incubated for 10 min at 30°C. Cells were collected and resuspended in 1 ml SPM buffer (1.2 M Sorbitol, 50 mM KPO_4 pH 7.4, 1 mM $MgCl_2$) and spheroblasted by addition of 10 µl 15 mg/ml zymolyase 20T for 30 min at 30°C. The spheroblasts were washed twice with 1.2 M sorbitol and 5-10 µl of the spheroblasts suspension were transferred to each well of slides, pretreated with 10 µl polylysine (10 mg/ml) for 1 min, rinsed with H_2O and dried completely. After 30 min at RT, the droplets were aspirated and the deposited cells were washed in PBS (10x: 80 g

NaCl, 2 g KCl ,11.5 Na_2HPO_4:7H_2O, 2 g KH_2PO_4), the slides were blocked by addition of 10 mg/ml BSA (dissolved in 1x PBS) to each well. After 10-15 minutes the droplets were aspirated again and the appropriate (in 10 mg/ml BSA in 1x PBS) antibody was added to each well. After 2h the slides were washed in PBS, secondary antibody (anti-mouse-alexafluor) was added (in 10 mg/ml BSA in 1x PBS). To stain the nuclei of the fixed cells, 10 μl DAPI (1 μg/ ml in 1x PBS) were added to each well. The slides were washed again and sealed.

Flow cytofluorimetric analysis

For the analysis of the cell-cycle arrest promoted by rapamycin, cultures in the exponential phase of growth were treated with 200 ng/ml rapamycin for several hours. Samples, corresponding to a total of $2x10^7$ cells, were collected during the exponential phase and at various times during the treatment. The cells were fixed by addition of 70% ethanol and subsequently processed for FACS analysis. A propidium iodide solution (Propidium Iodide 0.046 mM Tris.HCl pH 7.7 0.05 M; MgCl2 15 mM pH 7.7) was used to stain DNA, basically the cells were washed extensively and incubated for 3 h at 37°C in the presence of RNAse (1 mg/ml). After digestion of RNA the cells were washed again, the propidium iodide solution was added and cells were incubated on ice and in the dark for at least 30 min. Before FACS analysis with a FACScan instrument (Becton Dickinson) equipped with blue laser (488-nm laser emission) the cell suspensions were sonicated for 10 seconds.

Materials

Plasmids

Plasmid Name	ORI	Marker	Promoter	Description (purpose)	Source	Figure(s)
Plasmids used in Chapter I						
pLC803	2 µ	*URA3*	*GAL1*	Cloning of N-terminal GST-HA^3 fusions	LC	17, 18, 20, 27
pLC820	2 µ	*URA3*	*GAL1*	Yeast expression of GST-Rim15-HA^3	LC	14, 17, 20, 21, 23, 25
pLC821	2 µ	*URA3*	*GAL1*	Yeast expression of GST-$Rim15^{PAS\Delta}$-HA^3	LC	14, 15, 17
pMALc2	pBR322	*AmpR*	*T7*	Bacterial expression of MBP	NEB Biolabs	15
pLC985	pBR322	*AmpR*	*T7*	Bacterial expression of MAL-PAS	LC	15
p755	2 µ	*LEU2*	*TDH3*	Cloning of C-terminal HA fusions	T. Schmelzle	16A
pLC1062	2 µ	*LEU2*	*TDH3*	Yeast expression of PAS^{Rim15}-HA^3	LC	16A, 18
pLC1060	integrative	*URA3*	*endogenous*	Rim15 expression endogenous level	LC	16B
pLC1352	integrative	*URA3*	*endogenous*	$Rim15^{PAS\Delta}$ expression endogenous level	LC	16B
pLC804	2 µ	*URA3*	*GAL1*	Yeast expression of GST-PAS^{Rim15}	LC	17, 27
pNB566	2 µ	*URA3*	*GAL1*	Yeast expression of GST-RIM15	NB	18
pFD662	2 µ	*LEU2*	*endogenous*	Yeast expression of Bud14-HA^3	FD	18
pLC807	2 µ	*URA3*	*GAL1*	Yeast expression of GST-REC^{Rim15}-HA^3	LC	20
pLC808	2 µ	*URA3*	*GAL1*	Yeast expression of GST-C_2CHZnF^{Rim15}-HA^3	LC	20
pLC809	2 µ	*URA3*	*GAL1*	Yeast expression of GST-C_2CAZnF^{Rim15}-HA^3	LC	20
pLC1028	2 µ	*URA3*	*GAL1*	Yeast expression of GST-C_2CHZnF^{Mgs1}-HA^3	LC	20
pLC1027	2 µ	*URA3*	*GAL1*	Yeast expression of GST-C_2CHZnF^{Rad18}-HA^3	LC	20
pLC731	2 µ	*URA3*	*GAL1*	Yeast expression of GST-$Rim15^{H256A}$-HA^3	LC	21, 23
pLC1022	CEN/ARS	*LEU2*	*GPD1*	Yeast expression of GFP-C_2CHZnF-REC^{Mgs1}	LC	22
pLC1019	CEN/ARS	*LEU2*	*GPD1*	Yeast expression of GFP-C_2CHZnF-REC^{Rim15}	LC	22
pLC1021	CEN/ARS	*LEU2*	*GPD1*	Yeast expression of GFP-C_2CHZnF-REC^{Rad18}	LC	22
pLC729	2 µ	*URA3*	*GAL1*	Yeast expression of GST-$Rim15^{C244A}$-HA^3	LC	23
pRS306	integrative	*URA3*		Integrative vector	P. Hieter	24
pLC1060	integrative	*URA3*	*endogenous*	Rim15 expression endogenous level	CDV	24
pRS306-RIM15*4	integrative	*URA3*	*endogenous*	$Rim15^{H256A}$ expression endogenous level	CDV	24
pRS306-RIM15*5	integrative	*URA3*	*endogenous*	$Rim15^{C244A}$ expression endogenous level	CDV	24
pJG4-5+PL	2 µ	*TRP1*	*GAL1*	Two-hybrid system (AD)	R. Brent	II, III
pEG202	2 µ	*HIS3*	*ADH1*	Two-hybrid system (DBD)	R. Brent	II, III
pLC702	2 µ	*TRP1*	*GAL1*	pJG4-5-REC^{Rim15}	LC	II, III
pCDV31	2 µ	*TRP1*	*GAL1*	pJG4-5-MSB2	CDV	II, III
pCDV86	2 µ	*HIS3*	*ADH1*	pEG202-MSB2	CDV	II, III
pLC701	2 µ	*HIS3*	*ADH1*	pEG202-REC^{Rim15}	LC	II, III
pLC703	2 µ	*HIS3*	*ADH1*	pEG202-C_2CHZnF-REC^{Rim15}-HA^3	LC	II, III
pLC711	2 µ	*HIS3*	*ADH1*	pEG202-CACHZnF-REC^{Rim15}-HA^3	LC	II, III
pLC713	2 µ	*HIS3*	*ADH1*	pEG202-C_2CAZnF-REC^{Rim15}-HA^3	LC	II, III
pLC732	2 µ	*HIS3*	*ADH1*	pEG202-SKN7-RD	LC	II, III
pLC1051	2 µ	*LEU2*	*TDH3*	Yeast expression of Bud27-HA^3	LC	26
pFD666	2 µ	*LEU2*	*endogenous*	Yeast expression of Bud14-HA^3	FD	26
Plasmids used in Chapter III						
pLC1092		*AmpR*	*T7*	Bacterial expression of GST-Igo1	LC	38, 39
pLC1226		*AmpR*	*T7*	Bacterial expression of GST-Igo1S105A	LC	
pLC1217		*AmpR*	*T7*	Bacterial expression of GST-Igo1S105D	LC	
pLC1134		*AmpR*	*T7*	Bacterial expression of GST-Igo1S64A	LC	38
pLC1196		*AmpR*	*T7*	Bacterial expression of GST-Igo1S64D	LC	
pVW1109		*AmpR*	*T7*	Bacterial expression of GST-Igo2	VW	38
pCDV487	2 µ	*URA3*	*GAL1*	Yeast expression of GST-Rim15-HA^3	CDV	38, 39
pIP779	2 µ	*URA3*	*GAL1*	Yeast expression of GST-$Rim15^{K823Y}$-HA^3	IP	38, 39
pCDV1159	2 µ	*LEU2*	*TDH3*	Yeast expression of Sir4-HA^3	CDV	42
pCDV1157	2 µ	*LEU2*	*TDH3*	Yeast expression of Igo1-HA^3	CDV	42
pNB566	2 µ	*URA3*	*GAL1*	Yeast expression of GST-RIM15	NB	42
pLC803	2 µ	*URA3*	*GAL1*	Cloning of N-terminal GST-HA^3 fusions	LC	42
p873	2 µ	*URA3*	*tetO7*			48
pCDV1155	2 µ	*URA3*	*tetO7*	pCM190-IGO1	CDV	48
pLC1200	2 µ	*URA3*	*tetO7*	pCM190-IGO1 S105A	LC	48
pLC1199	2 µ	*URA3*	*tetO7*	pCM190-IGO1 S105D	LC	48
pLC1202	2 µ	*URA3*	*tetO7*	pCM190-IGO1 S64A	LC	48
pLC1201	2 µ	*URA3*	*tetO7*	pCM190-IGO1 S64D	LC	48
p101	CEN/ARS	*URA3*		YCplac33	R. Gietz	48
pCDV1149	CEN/ARS	*URA3*	*endogenous*	Igo1 expression endogenous level	CDV	48
pLC1218	CEN/ARS	*URA3*	*endogenous*	$IgO1^{S105A}$ expression endogenous level	LC	48
pLC1229	CEN/ARS	*URA3*	*endogenous*	$IgO1^{S105D}$ expression endogenous level	LC	48
pLC1216	CEN/ARS	*URA3*	*endogenous*	$IgO1^{S64A}$ expression endogenous level	LC	48
pLC1215	CEN/ARS	*URA3*	*endogenous*	$IgO1^{S64D}$ expression endogenous level	LC	48

Yeast strains

Strain Name	Background	MAT	Genotype	Reference	Figure
Strains used in Chapter I					
EGY48		*a*	*his3 trp1 ura3 LEU2::pLexAop6-LEU2* (+ pSH18-34)	Zervos et al., 1993, Cell 72: 223-232.	II, III
IP31	KT1960	*a*	*ura3-52 leu2 his3 trp1 rim15Δ::kanMX2*	Pedruzzi et al., 2003, Mol. Cell 12: 1607-1613.	16, 22, 23, 24
IP37	KT1960/1	*a/α*	*ura3-52/ura3-52 leu2/leu2 his3/his3 trp1/trp1 rim15$_{Δ}$::kanMX2/rim15Δ::kanMX2*	Pedruzzi et al., 2003, Mol. Cell 12: 1607-1613.	14, 15, 17, 18, 20,
KT1960	KT1960/1	*α*	*ura3-52 leu2 his3 trp1*	Pedruzzi et al., 2003, Mol. Cell 12: 1607-1613.	16
Strains used in Chapter II					
W303-1A	W303	*a*	*ade2-1 trp1-1 can1-100 leu2-3,112 his3-11,15 ura3-1*	Thomas and Rothstein, 1989, Cell 56:619-630.	IV
PEY78	W303	*a*	*ade2-1 trp1-1 can1-100 leu2-3,112 his3-11,15 ura3-1 msn2::HIS3 msn4::TRP1*	Martinez-Pastor et al., 1996, EMBO J. 15: 2227-2235.	IV
CDV115	W303	*a*	*ade2-1 trp1-1 can1-100 leu2-3,112 his3-11,15 ura3-1 rim15Δ::kanMX2*	Pedruzzi et al., 2003, Mol. Cell 12: 1607-1613.	IV
CDV116	W303	*a*	*ade2-1 trp1-1 can1-100 leu2-3,112 his3-11,15 ura3-1 gis1Δ::kanMX2*	Cameroni et al., Cell Cycle 3: 461-468.	IV
CDV308-1B	Y2864/5	*α*	*gal1Δ::HIS3 ade2-1 his3-11,15 leu2-3,112 trp1-1 ura3-1 can1-100, igo1Δ::kanMX4,igo2Δ::kanMX4*		V
VW15-14D	Y2864/5	*α*	*gal1Δ::HIS3 ade2-1 his3-11,15 leu2-3,112 trp1-1 ura3-1 can1-100, msn2Δ::kanMX4, msn4Δ::kanMX4*		V
CDV314	Y2864/5	*α*	*gal1Δ::HIS3 ade2-1 his3-11,15 leu2-3,112 trp1-1 ura3-1 can1-100 rim15Δ::kanMX4*		V
CDV315	Y2864/5	*α*	*gal1Δ::HIS3 ade2-1 his3-11,15 leu2-3,112 trp1-1 ura3-1 can1-100 gis1Δ::natMX4*		V
CDV318	Y2864/5	*α*	*1 can1-100, msn2Δ::kanMX4, msn4Δ::kanMX4 gis1Δ::natMX4*		V
Y2864	W303	*α*	*gal1Δ::HIS3 ade2-1 his3-11,15 leu2-3,112 trp1-1 ura3-1 can1-100*		V
W303-1A	W303-1A	*a*	*ade2-1 trp1-1 can1-100 leu2-3,112 his3-11,15 ura3-1*	Thomas and Rothstein, 1989, Cell 56:619-630.	31, 32
CDV202	W303-1A	*a*	*ade2-1 trp1-1 can1-100 leu2-3,112 his3-11,15 ura3-1 rim15Δ::kanMX2*		31, 32
YPA5H	W303-1A	*a*	*ade2-1 trp1-1 can1-100 leu2-3,112 his3-11,15 ura3-1 sit4$_{Δ}$::HIS3*	Sakumoto et al., Yeast 19: 587-599.	31
CDV206	W303-1A	*a*	*ade2-1 trp1-1 can1-100 leu2-3,112 his3-11,15 ura3-1 sit4::HIS3 rim15Δ::kanMX2*		31
CDV203	W303-1A	*a*	*ade2-1 trp1-1 can1-100 leu2-3,112 his3-11,15 ura3-1 pph21Δ::TRP1 pph22Δ::HIS3 rim15Δ::kanMX2*		32
YP0607WH	W303-1A	*a*	*ade2-1 trp1-1 can1-100 leu2-3,112 his3-11,15 ura3-1 pph21Δ::TRP1 pph22Δ::HIS3*	Sakumoto et al., Yeast 19: 587-599.	32
Strains used in Chapter III					
IP37	KT1960/1	*a/α*	*ura3-52/ura3-52 leu2/leu2 his3/his3 trp1/trp1 rim15$_{Δ}$::kanMX2/rim15Δ::kanMX2*	Pedruzzi et al., 2003, Mol. Cell 12: 1607-1613.	38, 39
LC54	BY4741/2	*a*	*his3Δ1 leu2Δ0 met15Δ0 ura3Δ0 igo1::IGO1-myc13-KanMX2*		40, 41, 44, 45
LC55	BY4741/2	*a*	*his3Δ1 leu2Δ0 met15Δ0 ura3Δ0 igo2::IGO2-myc13-KanMX2*		40, 41, 44, 45
BY4741	BY4741/2	*a*	*his3Δ1 leu2Δ0 met15Δ0 ura3Δ0*		42, 43, 46, 47, 48
BY4742	BY4741/2	*α*	*his3Δ1; leu2Δ0; lys2Δ0; ura3Δ0*		46
CDV288-12A	BY4741/2	*MATa*	*his3Δ1 leu2Δ0 MET15 LYS2 ura3Δ0 igo1Δ::kanMX4 igo2Δ::kanMX2*		46, 47, 48
YFL033C	BY4741/2	*MATa*	*his3Δ1 leu2Δ0 met15Δ0 ura3Δ0 rim15Δ::kanMX4*		46, 47, 48
Y12055	BY4742	*MATa*	*his3Δ1 leu2Δ0 lys2Δ0 ura3Δ0 igo1Δ::kanMX4*		46
Y17298	BY4742	*MATa*	*his3Δ1 leu2Δ0 lys2Δ0 ura3Δ0 igo2Δ::kanMX4*		46
JK9-3D	JK9-3D	*a*	*leu2 his4 trp1 ura3 rme1 GAL HMLa*		36
IP11	JK9-3D	*a*	*leu2 his4 trp1 ura3 rme1 GAL HMLa rim15Δ::kanMX2*		36
TS120-2D a	TB50	*MATa*	*leu2 his4 trp1 ura3 rme1 GAL HMLa sch9Δ::KanMX*		36
TS120-2D a	TB50	*MATa*	*leu2 his4 trp1 ura3 rme1 GAL HMLa sch9Δ::KanMX* (+ pRL841 = *SCH9^{2D3E}*)		36

Oligonucleotides

Oligo Name	Gene	Sequence	Direction	Purpose
HSP12-F	HSP12	ATG TCT GAC CGA GGT AGA AAA GGA TTC	F	DNA/RNA probe
HSP12-R	HSP12	TTA CTT CTT GGT TGG GTC TTC TTC ACC	R	DNA/RNA probe
SSB1-F	SSB1	ATG GCT GAA GGT GTT TTC CAA GGT GC	F	DNA/RNA probe
SSB1-R	SSB1	TTA ACG AGA AGA CAT GGC CTT GGT GAC	R	DNA/RNA probe
HSP26-F	HSP26	ATG TCA TTT AAC AGT CCA TTT TTT GAT TTC	F	DNA/RNA probe
HSP26-R	HSP26	TTA GTT ACC CCA CGA TTC TTG AGA ACA AAC	R	DNA/RNA probe
SSA3-F	SSA3	ATG TCT AGA GCA GTT GGT	F	DNA/RNA probe
SSA3-R	SSA3	ATC AAC CTC TTC CAC TGT	R	DNA/RNA probe
GRE1-F	GRE1	ATG TCC AAT CTA TTA AAC AAG TTT GCT G	F	DNA/RNA probe
GRE1-R	GRE1	CTA CCA GAC GCC TTG GTT CCC ACT ATC	R	DNA/RNA probe
MgsFN1-2	MGS1	GGA TCG CAC AGT CTC AAG CGG CCG CAA GAG GAC ATC TGT A	F	Cloning of Mgs1 ZnF
MgsRS2-1	MGS1	GGT CCT TAT TTT CAA GGT CGA CGA ATT TCT CTG AGT T	R	Cloning of Mgs1 ZnF
RadFN1-1	RAD18	GCA AAT TGT TGC AAG CGG CCG CAG AAA ACT TGC CAA AAG AT	F	Cloning of Rad18 ZnF subclone 1-1
RadRX2-1	RAD18	GCT TTT GTC GAC TTC TGG AGT CTC GAG CTT GAA TCT GGA TGA A	R	Cloning of Rad18 ZnF subclones 1-1 and 1-2
FN1	RIM15	AAC GAA GAC GGC GGC CGC GAC ATG GTC ATC CAG TTA TCC GAT AAT TGC	F	Rim15 subclones
RS1	RIM15	GAC CAT GTC GTC GAC AGC GTC TTC GTT GGC ATA AAA GTC TGA CC	R	Rim15 subclones
FN2	RIM15	TGT CAG GAC GGC GGC CGC ATC AAC CCG AGT GAA ATG GTT CCT GAT C	F	Rim15 subclones
RS2	RIM15	CGG GTT GAT GTC GAC GGC GTC CTG ACA CAG CTC TCT TAA GGA G	R	Rim15 subclones
FN3	RIM15	CTC TCG GCA GGC GGC CGC GAC CGA CTA CAG GCT ATA TCA AGA GTT AAC	F	Rim15 subclones
RS3	RIM15	TAG TCG GTC GTC GAC CTC TGC CGA GAG ATC ACT GGA ATT GGT CC	R	Rim15 subclones
RS4	RIM15	TCT TAA AAT GTC GAC GTG CGT TTC ATC AGA ATC GCT CAA TAT AG	R	Rim15 subclones
PAS-XbaI-cF	RIM15	CCC AGT AGA TCT AGA CAG ATG TTC AAT AGA A	F	Cloning of PAS domain in p414(ADH) and GPD vectors
PAS-XbaI-cF2	RIM15	CCC AGT AGA GGA AGA TCT AGA TTC AAT AGA A	F	Cloning of PAS domain in pMAL vectors for expression in bacteria
SKN7-RDF	SKN7	GTC ACG CTA GAA TTC GGT TTC CAT GTA CTG TTG GTG GAA GAT GAC	F	Cloning of Skn7-receiver domain into pJG4-5/pEG202
SKN7-RDR	SKN7	CTG TTC GCA CTC GAG AAT ACG GTC CTT TAG ATA ACG TAT TAA AAT TG	R	Cloning of Skn7-receiver domain into pJG4-5/pEG202
IGO1-BamHI-F	IGO1	ATC TAA CTC GCC GGG ATC CTG TCG AAT G	F	Cloning of Ynl157w in pGEX-3x
IGO1-EcoRI-R	IGO1	TAC AGG GAA TTC CTA TTA TCT AAT GG	R	Cloning of Ynl157w in pGEX-3x
IGO1-F-XBAI	IGO1	GCA TAA TAC TCT AGA TAT TGA ACT GGC GGA CTT ACA GCG AG	F	Cloning of IGO1 into YCplac33 and pRS306
IGO1-R-SACI	IGO1	GAT CAG GAA GAG CTC GTG GAA CTC CTC TTT GCA GGC GGC AG	R	Cloning of IGO1 into YCplac33 and pRS306
IGO1-F-NOTI	IGO1	AAT ATC TAA CGC GGC CGC ATG TCG AAT GAA AAC TTA TCT CCC AAT AG	F	Cloning of IGO1 into pCM190
IGO1-R-PSTI	IGO1	GTG ATC AGG AAC TGC AGG TGG AAC TCC TCT TTG CAG GCG GCA G	R	Cloning of IGO1 into pCM190
IGO1-F2	IGO1	GGA ACC ACA GCT CTT CGT CGT CCA GTT TGT ATA CTG AAT CAC CCA TTA GAC GGA TCC CCG GGT TAA TTA A	F	Genomic C-terminal tagging of Igo1
IGO1-R1	IGO1	GAG ACC CTT CTC TTT CCC TAA AAA AAT ATA AAA AAG TAC AGG TTG TCT ATG AAT TCG AGC TCG TTT AAA C	R	Genomic C-terminal tagging of Igo1
S64A-F	IGO1	GCA GAA AAG AAA ATA TTT CGA CGC TGG TGA TTA CGC TTT GCA GAA	F	Point mutation in IGO1 S64A
S64A-R	IGO1	TTC TGC AAA GCG TAA TCA CCA GCG TCG AAA TAT TTT CTT TTC TGC	R	Point mutation in IGO1 S64A
S64D-R	IGO1	GCC AGC TTT CTG CAA AGC GTA ATC ACC ATC GTC GAA ATA TTT TCT TTT CTG CAT GGT AT	R	Mutation of S64 of IGO1 to a D
S105A-F	IGO1	AGA AGA TAT AAT AAA AAG AAG GAT AGC CAC TTG TCC GTC AAC TGC CTC AAC CGC TGG	F	Mutation of S105 in IGO1 to an Alanine
S105A-R	IGO1	CCA GCG GTT GAG GCA GTT GAC GGA CAA GTG GCT ATC CTT CTT TTT ATT ATA TCT TCT	R	Mutation of S105 in IGO1 to an Alanine
S105D-F	IGO1	AGA AGA TAT AAT AAA AAG AAG GAT AGA CAC TTG TCC GTC AAC TGC CTC AAC CGC TGG	F	Mutation of S105 in IGO1 to an Asp
S105D-R	IGO1	CCA GCG GTT GAG GCA GTT GAC GGA CAA GTG TCT ATC CTT CTT TTT ATT ATA TCT TCT	R	Mutation of S105 in IGO1 to an Asp
IGO2-BamHI-F	YHR132W	CGCGGATCCCCTCAGAGGATCTTTCACCTAC	F	Cloning of IGO2 in pGEX3X as GST fusion for E.coli expression
IGO2-EcoRI-R	YHR132W	CCGGAATTCTTATCATTTATTTGGAGATCTTGGTGG	R	Cloning of IGO2 in pGEX3X for E.coli expression
IGO2-BamHI-F	IGO2	GTG TTA TAA AAG TGG ATC CAC TAT GTC AGA GGA T	F	Cloning of IGO2 in pAS334
IGO2-SphI-R	IGO2	CAT TAG GCA TGC ATT TGG AGA TCT TGG TGG AGG TCC ACT TG	R	Cloning of IGO2 in pAS334
IGO2-F-XBAI	IGO2	AAG CTT CTT TCT AGA AGA TCC AAC CAC ATA TAA ATA GTA TCC	F	Cloning of IGO2 into YCplac33 and pRS306
IGO2-R-SACI	IGO2	GAG CTT ATT GAG CTC TGT TCT GTG GTT GTT CTT TGA TGG CAC	R	Cloning of IGO2 into YCplac33 and pRS306
IGO2-F-NOTI	IGO2	TAT AAA AGT GGC GGC CGC ATG TCA GAG GAT CTT TCA CCT ACA AGC	F	Cloning of IGO2 into pCM190
IGO2-R-PSTI	IGO2	GAG CTT ATT CTG CAG TGT TCT GTG GTT GTT CTT TGA TGG CAC	R	Cloning of IGO2 into pCM190
IGO2-F2	IGO2	CGA GAC AAG GAA GTA TCT CAA GTG GAC CTC CAC CAA GAT CTC CAA ATA AAC GGA TCC CCG GGT TAA TTA A	F	Genomic C-terminal tagging of Igo2
IGO2-R1	IGO2	GCT AGT GAT GAT AAA AAA AAA GTA ATA CCA CAT AAT ATC ATT CCT TCA TTA GGA ATT CGA GCT CGT TTA AAC	R	Genomic C-terminal tagging of Igo2

Appendix

Rim15 protein sequence

List of Abbreviations

4E-BPs	eIF-4E binding proteins
AMPK	AMP-dependent Kinase
cAMP	Cyclic AMP
CDK	Cyclin-dependent kinase
CSRE	Carbon source repressible
CWI	Cell Wall Integrity
EGO	Exit from rapamycin-induced G_0 arrest
FKBP12	FK506-binding protein 12
FRB	FKBP12-rapamycin binding
GAP	GTPase activating protein
GEF	Guanine nucleotide exchange factor
GFP	Green fluorescent protein
GPCR	G-Protein coupled receptor
HMM	Hidden Markow Model
IGO	Initiation of G_0
IRES	Internal Ribosome entry sites
MS	Mass spectrometry
NCR	Nitrogen catabolite repression
NDP	Nitrogen discrimination pathway
ORF	Open reading frame
PAGE	Polyacrylaminde gel electrophoresis
PAS	PER, ARNT, SIM
PDS	Post diauxic shift
PKA	Protein Kinase A
TORC1	TOR Complex 1
PKC	Protein Kinase C
PolII	RNA Polymerase II
PP2A	Protein Phosphatase 2 A
PtdIns	Phosphatityl inositol (non phosphorylated)

PtdIns(3)P	Phosphatidty inostitol 3-phosphate (Phosphoinositide)
PtdIns(3,5)P_2	Phosphatidty inostitol 3,5-bis-phosphate (Phosphoinositide)
REC	Receiver Domain
Ribi	Ribosome biogenesis (genes)
RPG	Ribosomal protein genes
RPGs	Ribosome protein genes
STRE	Stress-responsive element
TCA	Tricarboxylic acid cycle
TOR	Target of Rapamycin
UAS	Upstream activating sequence
ZnF	Zinc Finger

References

[1] Gray JV, Petsko GA, Johnston GC, Ringe D, Singer RA, Werner-Washburne M. "Sleeping beauty": quiescence in Saccharomyces cerevisiae. Microbiol Mol Biol Rev 2004;68 (2):187-206.

[2] Venezia TA, Merchant AA, Ramos CA, Whitehouse NL, Young AS, Shaw CA, Goodell MA. Molecular signatures of proliferation and quiescence in hematopoietic stem cells. PLoS Biol 2004;2 (10):e301.

[3] Coller HA, Sang L, Roberts JM. A new description of cellular quiescence. PLoS Biol 2006;4 (3):e83.

[4] Hirimburegama K, Durnez P, Keleman J, Oris E, Vergauwen R, Mergelsberg H, Thevelein JM. Nutrient-induced activation of trehalase in nutrient-starved cells of the yeast Saccharomyces cerevisiae: cAMP is not involved as second messenger. J Gen Microbiol 1992;138 (10):2035-43.

[5] Marzluf GA. Genetic regulation of nitrogen metabolism in the fungi. Microbiol Mol Biol Rev 1997;61 (1):17-32.

[6] Park HD, Beeser AE, Clancy MJ, Cooper TG. The S. cerevisiae nitrogen starvation-induced Yvh1p and Ptp2p phosphatases play a role in control of sporulation. Yeast 1996;12 (11):1135-51.

[7] Guan K, Hakes DJ, Wang Y, Park HD, Cooper TG, Dixon JE. A yeast protein phosphatase related to the vaccinia virus VH1 phosphatase is induced by nitrogen starvation. Proc Natl Acad Sci U S A 1992;89 (24):12175-9.

[8] Beeser AE, Cooper TG. The dual-specificity protein phosphatase Yvh1p acts upstream of the protein kinase mck1p in promoting spore development in Saccharomyces cerevisiae. J Bacteriol 1999;181 (17):5219-24.

[9] Beeser AE, Cooper TG. The dual-specificity protein phosphatase Yvh1p regulates sporulation, growth, and glycogen accumulation independently of catalytic activity in Saccharomyces cerevisiae via the cyclic AMP-dependent protein kinase cascade. J Bacteriol 2000;182 (12):3517-28.

[10] Cooper TG. Transmitting the signal of excess nitrogen in Saccharomyces cerevisiae from the Tor proteins to the GATA factors: connecting the dots. FEMS Microbiol Rev 2002;26 (3):223-38.

[11] Bertram PG, Choi JH, Carvalho J, Ai W, Zeng C, Chan TF, Zheng XF. Tripartite regulation of Gln3p by TOR, Ure2p, and phosphatases. J Biol Chem 2000;275 (46):35727-33.

[12] Cardenas ME, Cutler NS, Lorenz MC, Di Como CJ, Heitman J. The TOR signaling cascade regulates gene expression in response to nutrients. Genes Dev 1999;13 (24):3271-9.

[13] Beck T, Hall MN. The TOR signalling pathway controls nuclear localization of nutrient-regulated transcription factors. Nature 1999;402 (6762):689-92.

[14] Hardwick JS, Kuruvilla FG, Tong JK, Shamji AF, Schreiber SL. Rapamycin-modulated transcription defines the subset of nutrient-sensitive signaling pathways directly controlled by the Tor proteins. Proc Natl Acad Sci U S A 1999;96 (26):14866-70.

[15] Edskes HK, Hanover JA, Wickner RB. Mks1p is a regulator of nitrogen catabolism upstream of Ure2p in Saccharomyces cerevisiae. Genetics 1999;153 (2):585-94.

[16] Tate JJ, Cox KH, Rai R, Cooper TG. Mks1p is required for negative regulation of retrograde gene expression in Saccharomyces cerevisiae but does not affect nitrogen catabolite repression-sensitive gene expression. J Biol Chem 2002;277 (23):20477-82.

[17] Komeili A, Wedaman KP, O'Shea EK, Powers T. Mechanism of metabolic control. Target of rapamycin signaling links nitrogen quality to the activity of the Rtg1 and Rtg3 transcription factors. J Cell Biol 2000;151 (4):863-78.

[18] Forsberg H, Gilstring CF, Zargari A, Martinez P, Ljungdahl PO. The role of the yeast plasma membrane SPS nutrient sensor in the metabolic response to extracellular amino acids. Mol Microbiol 2001;42 (1):215-28.

[19] Boer VM, de Winde JH, Pronk JT, Piper MD. The genome-wide transcriptional responses of Saccharomyces cerevisiae grown on glucose in aerobic chemostat cultures limited for carbon, nitrogen, phosphorus, or sulfur. J Biol Chem 2003;278 (5):3265-74.

[20] Wu J, Zhang N, Hayes A, Panoutsopoulou K, Oliver SG. Global analysis of nutrient control of gene expression in Saccharomyces cerevisiae during growth and starvation. Proc Natl Acad Sci U S A 2004;101 (9):3148-53.

[21] Schmelzle T, Beck T, Martin DE, Hall MN. Activation of the RAS/cyclic AMP pathway suppresses a TOR deficiency in yeast. Mol Cell Biol 2004;24 (1):338-51.

[22] Warburg O. The Metabolism of Tumors. London: Arnold Constable, 1930.

[23] Gancedo JM. Yeast carbon catabolite repression. Microbiol Mol Biol Rev 1998;62 (2):334-61.

[24] Rolland F, Winderickx J, Thevelein JM. Glucose-sensing mechanisms in eukaryotic cells. Trends Biochem Sci 2001;26 (5):310-7.

[25] De Winde JH, Crauwels M, Hohmann S, Thevelein JM, Winderickx J. Differential requirement of the yeast sugar kinases for sugar sensing in establishing the catabolite-repressed state. Eur J Biochem 1996;241 (2):633-43.

[26] Rodriguez A, De La Cera T, Herrero P, Moreno F. The hexokinase 2 protein regulates the expression of the GLK1, HXK1 and HXK2 genes of Saccharomyces cerevisiae. Biochem J 2001;355 (Pt 3):625-31.
[27] Treitel MA, Carlson M. Repression by SSN6-TUP1 is directed by MIG1, a repressor/activator protein. Proc Natl Acad Sci U S A 1995;92 (8):3132-6.
[28] Wilson WA, Hawley SA, Hardie DG. Glucose repression/derepression in budding yeast: SNF1 protein kinase is activated by phosphorylation under derepressing conditions, and this correlates with a high AMP:ATP ratio. Curr Biol 1996;6 (11):1426-34.
[29] Herrero P, Martinez-Campa C, Moreno F. The hexokinase 2 protein participates in regulatory DNA-protein complexes necessary for glucose repression of the SUC2 gene in Saccharomyces cerevisiae. FEBS Lett 1998;434 (1-2):71-6.
[30] Thevelein JM, de Winde JH. Novel sensing mechanisms and targets for the cAMP-protein kinase A pathway in the yeast Saccharomyces cerevisiae. Mol Microbiol 1999;33 (5):904-18.
[31] Rolland F, De Winde JH, Lemaire K, Boles E, Thevelein JM, Winderickx J. Glucose-induced cAMP signalling in yeast requires both a G-protein coupled receptor system for extracellular glucose detection and a separable hexose kinase-dependent sensing process. Mol Microbiol 2000;38 (2):348-58.
[32] Johnston M. Feasting, fasting and fermenting. Glucose sensing in yeast and other cells. Trends Genet 1999;15 (1):29-33.
[33] Trilisenko LV, Vagabov VM, Kulaev IS. The content and chain length of polyphosphates from vacuoles of Saccharomyces cerevisiae VKM Y-1173. Biochemistry (Mosc) 2002;67 (5):592-6.
[34] Pratt JR, Mouillon JM, Lagerstedt JO, Pattison-Granberg J, Lundh KI, Persson BL. Effects of methylphosphonate, a phosphate analogue, on the expression and degradation of the high-affinity phosphate transporter Pho84, in Saccharomyces cerevisiae. Biochemistry 2004;43 (45):14444-53.
[35] Harbison CT, Gordon DB, Lee TI, Rinaldi NJ, Macisaac KD, Danford TW, Hannett NM, Tagne JB, Reynolds DB, Yoo J, Jennings EG, Zeitlinger J, Pokholok DK, Kellis M, Rolfe PA, Takusagawa KT, Lander ES, Gifford DK, Fraenkel E, Young RA. Transcriptional regulatory code of a eukaryotic genome. Nature 2004;431 (7004):99-104.
[36] Auesukaree C, Homma T, Tochio H, Shirakawa M, Kaneko Y, Harashima S. Intracellular phosphate serves as a signal for the regulation of the PHO pathway in Saccharomyces cerevisiae. J Biol Chem 2004;279 (17):17289-94.
[37] Huang S, Jeffery DA, Anthony MD, O'Shea EK. Functional analysis of the cyclin-dependent kinase inhibitor Pho81 identifies a novel inhibitory domain. Mol Cell Biol 2001;21 (19):6695-705.
[38] Auesukaree C, Tochio H, Shirakawa M, Kaneko Y, Harashima S. Plc1p, Arg82p, and Kcs1p, enzymes involved in inositol pyrophosphate synthesis, are essential for phosphate regulation and polyphosphate accumulation in Saccharomyces cerevisiae. J Biol Chem 2005;280 (26):25127-33.
[39] Giots F, Donaton MC, Thevelein JM. Inorganic phosphate is sensed by specific phosphate carriers and acts in concert with glucose as a nutrient signal for activation of the protein kinase A pathway in the yeast Saccharomyces cerevisiae. Mol Microbiol 2003;47 (4):1163-81.
[40] Wanke V, Pedruzzi I, Cameroni E, Dubouloz F, De Virgilio C. Regulation of G0 entry by the Pho80-Pho85 cyclin-CDK complex. Embo J 2005;24 (24):4271-8.
[41] Swinnen E, Rosseels J, Winderickx J. The minimum domain of Pho81 is not sufficient to control the Pho85-Rim15 effector branch involved in phosphate starvation-induced stress responses. Curr Genet 2005;48 (1):18-33.
[42] Carroll AS, O'Shea EK. Pho85 and signaling environmental conditions. Trends Biochem Sci 2002;27 (2):87-93.
[43] Heitman J, Movva NR, Hall MN. Targets for cell cycle arrest by the immunosuppressant rapamycin in yeast. Science 1991;253 (5022):905-9.
[44] Arndt C, Cruz MC, Cardenas ME, Heitman J. Secretion of FK506/FK520 and rapamycin by Streptomyces inhibits the growth of competing Saccharomyces cerevisiae and Cryptococcus neoformans. Microbiology 1999;145 (Pt 8):1989-2000.
[45] McMahon LP, Choi KM, Lin TA, Abraham RT, Lawrence JC, Jr. The rapamycin-binding domain governs substrate selectivity by the mammalian target of rapamycin. Mol Cell Biol 2002;22 (21):7428-38.
[46] McMahon LP, Yue W, Santen RJ, Lawrence JC, Jr. Farnesylthiosalicylic acid inhibits mammalian target of rapamycin (mTOR) activity both in cells and in vitro by promoting dissociation of the mTOR-raptor complex. Mol Endocrinol 2005;19 (1):175-83.
[47] Loewith R, Jacinto E, Wullschleger S, Lorberg A, Crespo JL, Bonenfant D, Oppliger W, Jenoe P, Hall MN. Two TOR complexes, only one of which is rapamycin sensitive, have distinct roles in cell growth control. Mol Cell 2002;10 (3):457-68.
[48] Schmidt A, Kunz J, Hall MN. TOR2 is required for organization of the actin cytoskeleton in yeast. Proc Natl Acad Sci U S A 1996;93 (24):13780-5.

[49] Sarbassov DD, Ali SM, Sengupta S, Sheen JH, Hsu PP, Bagley AF, Markhard AL, Sabatini DM. Prolonged rapamycin treatment inhibits mTORC2 assembly and Akt/PKB. Mol Cell 2006;22 (2):159-68.
[50] De Virgilio C, Loewith R. Cell growth control: little eukaryotes make big contributions. Oncogene 2006;25 (48):6392-415.
[51] De Virgilio C, Loewith R. The TOR signalling network from yeast to man. Int J Biochem Cell Biol 2006;38 (9):1476-81.
[52] Inoki K, Ouyang H, Li Y, Guan KL. Signaling by target of rapamycin proteins in cell growth control. Microbiol Mol Biol Rev 2005;69 (1):79-100.
[53] Reinke A, Anderson S, McCaffery JM, Yates J, 3rd, Aronova S, Chu S, Fairclough S, Iverson C, Wedaman KP, Powers T. TOR complex 1 includes a novel component, Tco89p (YPL180w), and cooperates with Ssd1p to maintain cellular integrity in Saccharomyces cerevisiae. J Biol Chem 2004;279 (15):14752-62.
[54] Araki T, Uesono Y, Oguchi T, Toh EA. LAS24/KOG1, a component of the TOR complex 1 (TORC1), is needed for resistance to local anesthetic tetracaine and normal distribution of actin cytoskeleton in yeast. Genes Genet Syst 2005;80 (5):325-43.
[55] Wedaman KP, Reinke A, Anderson S, Yates J, 3rd, McCaffery JM, Powers T. Tor kinases are in distinct membrane-associated protein complexes in Saccharomyces cerevisiae. Mol Biol Cell 2003;14 (3):1204-20.
[56] Cardenas ME, Heitman J. FKBP12-rapamycin target TOR2 is a vacuolar protein with an associated phosphatidylinositol-4 kinase activity. Embo J 1995;14 (23):5892-907.
[57] Reinke A, Chen JC, Aronova S, Powers T. Caffeine targets TOR complex I and provides evidence for a regulatory link between the FRB and kinase domains of Tor1p. J Biol Chem 2006;281 (42):31616-26.
[58] Sarkaria JN, Busby EC, Tibbetts RS, Roos P, Taya Y, Karnitz LM, Abraham RT. Inhibition of ATM and ATR kinase activities by the radiosensitizing agent, caffeine. Cancer Res 1999;59 (17):4375-82.
[59] Luke MM, Della Seta F, Di Como CJ, Sugimoto H, Kobayashi R, Arndt KT. The SAP, a new family of proteins, associate and function positively with the SIT4 phosphatase. Mol Cell Biol 1996;16 (6):2744-55.
[60] Zheng Y, Jiang Y. The yeast phosphotyrosyl phosphatase activator is part of the Tap42-phosphatase complexes. Mol Biol Cell 2005;16 (4):2119-27.
[61] Yan G, Shen X, Jiang Y. Rapamycin activates Tap42-associated phosphatases by abrogating their association with Tor complex 1. Embo J 2006;25 (15):3546-55.
[62] Jiang Y, Broach JR. Tor proteins and protein phosphatase 2A reciprocally regulate Tap42 in controlling cell growth in yeast. Embo J 1999;18 (10):2782-92.
[63] Santhanam A, Hartley A, Duvel K, Broach JR, Garrett S. PP2A phosphatase activity is required for stress and Tor kinase regulation of yeast stress response factor Msn2p. Eukaryot Cell 2004;3 (5):1261-71.
[64] Duvel K, Broach JR. The role of phosphatases in TOR signaling in yeast. Curr Top Microbiol Immunol 2004;279:19-38.
[65] Shamji AF, Kuruvilla FG, Schreiber SL. Partitioning the transcriptional program induced by rapamycin among the effectors of the Tor proteins. Curr Biol 2000;10 (24):1574-81.
[66] Jacinto E, Guo B, Arndt KT, Schmelzle T, Hall MN. TIP41 interacts with TAP42 and negatively regulates the TOR signaling pathway. Mol Cell 2001;8 (5):1017-26.
[67] De Craene JO, Soetens O, Andre B. The Npr1 kinase controls biosynthetic and endocytic sorting of the yeast Gap1 permease. J Biol Chem 2001;276 (47):43939-48.
[68] Hinnebusch AG. Translational regulation of GCN4 and the general amino acid control of yeast. Annu Rev Microbiol 2005;59:407-50.
[69] Torres J, Di Como CJ, Herrero E, De La Torre-Ruiz MA. Regulation of the cell integrity pathway by rapamycin-sensitive TOR function in budding yeast. J Biol Chem 2002;277 (45):43495-504.
[70] Cosentino GP, Schmelzle T, Haghighat A, Helliwell SB, Hall MN, Sonenberg N. Eap1p, a novel eukaryotic translation initiation factor 4E-associated protein in Saccharomyces cerevisiae. Mol Cell Biol 2000;20 (13):4604-13.
[71] Cherkasova VA, Hinnebusch AG. Translational control by TOR and TAP42 through dephosphorylation of eIF2alpha kinase GCN2. Genes Dev 2003;17 (7):859-72.
[72] Reiling JH, Sabatini DM. Stress and mTORture signaling. Oncogene 2006;25 (48):6373-83.
[73] Martin DE, Soulard A, Hall MN. TOR regulates ribosomal protein gene expression via PKA and the Forkhead transcription factor FHL1. Cell 2004;119 (7):969-79.
[74] Jorgensen P, Rupes I, Sharom JR, Schneper L, Broach JR, Tyers M. A dynamic transcriptional network communicates growth potential to ribosome synthesis and critical cell size. Genes Dev 2004;18 (20):2491-505.
[75] Claypool JA, French SL, Johzuka K, Eliason K, Vu L, Dodd JA, Beyer AL, Nomura M. Tor pathway regulates Rrn3p-dependent recruitment of yeast RNA polymerase I to the promoter but does not participate in alteration of the number of active genes. Mol Biol Cell 2004;15 (2):946-56.
[76] Kamada Y, Funakoshi T, Shintani T, Nagano K, Ohsumi M, Ohsumi Y. Tor-mediated induction of autophagy via an Apg1 protein kinase complex. J Cell Biol 2000;150 (6):1507-13.

[77] Roosen J, Engelen K, Marchal K, Mathys J, Griffioen G, Cameroni E, Thevelein JM, De Virgilio C, De Moor B, Winderickx J. PKA and Sch9 control a molecular switch important for the proper adaptation to nutrient availability. Mol Microbiol 2005;55 (3):862-80.
[78] Pedruzzi I, Dubouloz F, Cameroni E, Wanke V, Roosen J, Winderickx J, De Virgilio C. TOR and PKA signaling pathways converge on the protein kinase Rim15 to control entry into G0. Mol Cell 2003;12 (6):1607-13.
[79] Kaeberlein M, Powers RW, 3rd, Steffen KK, Westman EA, Hu D, Dang N, Kerr EO, Kirkland KT, Fields S, Kennedy BK. Regulation of yeast replicative life span by TOR and Sch9 in response to nutrients. Science 2005;310 (5751):1193-6.
[80] Peng T, Golub TR, Sabatini DM. The immunosuppressant rapamycin mimics a starvation-like signal distinct from amino acid and glucose deprivation. Mol Cell Biol 2002;22 (15):5575-84.
[81] Dubouloz F, Deloche O, Wanke V, Cameroni E, De Virgilio C. The TOR and EGO protein complexes orchestrate microautophagy in yeast. Mol Cell 2005;19 (1):15-26.
[82] Wang Z, Wilson WA, Fujino MA, Roach PJ. Antagonistic controls of autophagy and glycogen accumulation by Snf1p, the yeast homolog of AMP-activated protein kinase, and the cyclin-dependent kinase Pho85p. Mol Cell Biol 2001;21 (17):5742-52.
[83] Shemer R, Meimoun A, Holtzman T, Kornitzer D. Regulation of the transcription factor Gcn4 by Pho85 cyclin PCL5. Mol Cell Biol 2002;22 (15):5395-404.
[84] Boy-Marcotte E, Tadi D, Perrot M, Boucherie H, Jacquet M. High cAMP levels antagonize the reprogramming of gene expression that occurs at the diauxic shift in Saccharomyces cerevisiae. Microbiology 1996;142 (Pt 3):459-67.
[85] Thevelein JM, Cauwenberg L, Colombo S, De Winde JH, Donation M, Dumortier F, Kraakman L, Lemaire K, Ma P, Nauwelaers D, Rolland F, Teunissen A, Van Dijck P, Versele M, Wera S, Winderickx J. Nutrient-induced signal transduction through the protein kinase A pathway and its role in the control of metabolism, stress resistance, and growth in yeast. Enzyme Microb Technol 2000;26 (9-10):819-25.
[86] Taylor SS, Buechler JA, Yonemoto W. cAMP-dependent protein kinase: framework for a diverse family of regulatory enzymes. Annu Rev Biochem 1990;59:971-1005.
[87] Griffioen G, Anghileri P, Imre E, Baroni MD, Ruis H. Nutritional control of nucleocytoplasmic localization of cAMP-dependent protein kinase catalytic and regulatory subunits in Saccharomyces cerevisiae. J Biol Chem 2000;275 (2):1449-56.
[88] Griffioen G, Branduardi P, Ballarini A, Anghileri P, Norbeck J, Baroni MD, Ruis H. Nucleocytoplasmic distribution of budding yeast protein kinase A regulatory subunit Bcy1 requires Zds1 and is regulated by Yak1-dependent phosphorylation of its targeting domain. Mol Cell Biol 2001;21 (2):511-23.
[89] Hall DD, Markwardt DD, Parviz F, Heideman W. Regulation of the Cln3-Cdc28 kinase by cAMP in Saccharomyces cerevisiae. Embo J 1998;17 (15):4370-8.
[90] Ma P, Wera S, Van Dijck P, Thevelein JM. The PDE1-encoded low-affinity phosphodiesterase in the yeast Saccharomyces cerevisiae has a specific function in controlling agonist-induced cAMP signaling. Mol Biol Cell 1999;10 (1):91-104.
[91] Gorner W, Durchschlag E, Martinez-Pastor MT, Estruch F, Ammerer G, Hamilton B, Ruis H, Schuller C. Nuclear localization of the C2H2 zinc finger protein Msn2p is regulated by stress and protein kinase A activity. Genes Dev 1998;12 (4):586-97.
[92] Sagee S, Sherman A, Shenhar G, Robzyk K, Ben-Doy N, Simchen G, Kassir Y. Multiple and distinct activation and repression sequences mediate the regulated transcription of IME1, a transcriptional activator of meiosis-specific genes in Saccharomyces cerevisiae. Mol Cell Biol 1998;18 (4):1985-95.
[93] Reinders A, Burckert N, Boller T, Wiemken A, De Virgilio C. Saccharomyces cerevisiae cAMP-dependent protein kinase controls entry into stationary phase through the Rim15p protein kinase. Genes Dev 1998;12 (18):2943-55.
[94] Ward MP, Gimeno CJ, Fink GR, Garrett S. SOK2 may regulate cyclic AMP-dependent protein kinase-stimulated growth and pseudohyphal development by repressing transcription. Mol Cell Biol 1995;15 (12):6854-63.
[95] Krause SA, Gray JV. The protein kinase C pathway is required for viability in quiescence in Saccharomyces cerevisiae. Curr Biol 2002;12 (7):588-93.
[96] Harrison JC, Zyla TR, Bardes ES, Lew DJ. Stress-specific activation mechanisms for the "cell integrity" MAPK pathway. J Biol Chem 2004;279 (4):2616-22.
[97] Kuranda K, Leberre V, Sokol S, Palamarczyk G, Francois J. Investigating the caffeine effects in the yeast Saccharomyces cerevisiae brings new insights into the connection between TOR, PKC and Ras/cAMP signalling pathways. Mol Microbiol 2006;61 (5):1147-66.
[98] Jelinsky SA, Estep P, Church GM, Samson LD. Regulatory networks revealed by transcriptional profiling of damaged Saccharomyces cerevisiae cells: Rpn4 links base excision repair with proteasomes. Mol Cell Biol 2000;20 (21):8157-67.

[99] Cyrne L, Martins L, Fernandes L, Marinho HS. Regulation of antioxidant enzymes gene expression in the yeast Saccharomyces cerevisiae during stationary phase. Free Radic Biol Med 2003;34 (3):385-93.
[100] Barbet NC, Schneider U, Helliwell SB, Stansfield I, Tuite MF, Hall MN. TOR controls translation initiation and early G1 progression in yeast. Mol Biol Cell 1996;7 (1):25-42.
[101] Rosenheck S, Choder M. Rpb4, a subunit of RNA polymerase II, enables the enzyme to transcribe at temperature extremes in vitro. J Bacteriol 1998;180 (23):6187-92.
[102] Paz I, Choder M. Eukaryotic translation initiation factor 4E-dependent translation is not essential for survival of starved yeast cells. J Bacteriol 2001;183 (15):4477-83.
[103] Tsukada M, Ohsumi Y. Isolation and characterization of autophagy-defective mutants of Saccharomyces cerevisiae. FEBS Lett 1993;333 (1-2):169-74.
[104] Noda T, Ohsumi Y. Tor, a phosphatidylinositol kinase homologue, controls autophagy in yeast. J Biol Chem 1998;273 (7):3963-6.
[105] Drebot MA, Johnston GC, Singer RA. A yeast mutant conditionally defective only for reentry into the mitotic cell cycle from stationary phase. Proc Natl Acad Sci U S A 1987;84 (22):7948-52.
[106] Gao M, Kaiser CA. A conserved GTPase-containing complex is required for intracellular sorting of the general amino-acid permease in yeast. Nat Cell Biol 2006;8 (7):657-67.
[107] Cameroni E, De Virgilio C, Deloche O. Phosphatidylinositol 4-phosphate is required for translation initiation in Saccharomyces cerevisiae. J Biol Chem 2006;281 (50):38139-49.
[108] Deloche O, de la Cruz J, Kressler D, Doere M, Linder P. A membrane transport defect leads to a rapid attenuation of translation initiation in Saccharomyces cerevisiae. Mol Cell 2004;13 (3):357-66.
[109] Nobukuni T, Joaquin M, Roccio M, Dann SG, Kim SY, Gulati P, Byfield MP, Backer JM, Natt F, Bos JL, Zwartkruis FJ, Thomas G. Amino acids mediate mTOR/raptor signaling through activation of class 3 phosphatidylinositol 3OH-kinase. Proc Natl Acad Sci U S A 2005;102 (40):14238-43.
[110] Siddhanta U, McIlroy J, Shah A, Zhang Y, Backer JM. Distinct roles for the p110alpha and hVPS34 phosphatidylinositol 3'-kinases in vesicular trafficking, regulation of the actin cytoskeleton, and mitogenesis. J Cell Biol 1998;143 (6):1647-59.
[111] Herman PK, Emr SD. Characterization of VPS34, a gene required for vacuolar protein sorting and vacuole segregation in Saccharomyces cerevisiae. Mol Cell Biol 1990;10 (12):6742-54.
[112] Burda P, Padilla SM, Sarkar S, Emr SD. Retromer function in endosome-to-Golgi retrograde transport is regulated by the yeast Vps34 PtdIns 3-kinase. J Cell Sci 2002;115 (Pt 20):3889-900.
[113] Cameroni E, Hulo N, Roosen J, Winderickx J, De Virgilio C. The novel yeast PAS kinase Rim 15 orchestrates G0-associated antioxidant defense mechanisms. Cell Cycle 2004;3 (4):462-8.
[114] Pnueli L, Edry I, Cohen M, Kassir Y. Glucose and nitrogen regulate the switch from histone deacetylation to acetylation for expression of early meiosis-specific genes in budding yeast. Mol Cell Biol 2004;24 (12):5197-208.
[115] Xiao Y, Mitchell AP. Shared roles of yeast glycogen synthase kinase 3 family members in nitrogen-responsive phosphorylation of meiotic regulator Ume6p. Mol Cell Biol 2000;20 (15):5447-53.
[116] Vidan S, Mitchell AP. Stimulation of yeast meiotic gene expression by the glucose-repressible protein kinase Rim15p. Mol Cell Biol 1997;17 (5):2688-97.
[117] Johnson LN, Noble ME, Owen DJ. Active and inactive protein kinases: structural basis for regulation. Cell 1996;85 (2):149-58.
[118] Huse M, Kuriyan J. The conformational plasticity of protein kinases. Cell 2002;109 (3):275-82.
[119] Tamaskovic R, Bichsel SJ, Hemmings BA. NDR family of AGC kinases--essential regulators of the cell cycle and morphogenesis. FEBS Lett 2003;546 (1):73-80.
[120] Aitken A. 14-3-3 proteins: a historic overview. Semin Cancer Biol 2006;16 (3):162-72.
[121] Yaffe MB, Elia AE. Phosphoserine/threonine-binding domains. Curr Opin Cell Biol 2001;13 (2):131-8.
[122] Walsh DA, Perkins JP, Krebs EG. An adenosine 3',5'-monophosphate-dependant protein kinase from rabbit skeletal muscle. J Biol Chem 1968;243 (13):3763-5.
[123] Meyer T, Hanson PI, Stryer L, Schulman H. Calmodulin trapping by calcium-calmodulin-dependent protein kinase. Science 1992;256 (5060):1199-202.
[124] Hunt T. Cyclins and their partners: from a simple idea to complicated reality. Semin Cell Biol 1991;2 (4):213-22.
[125] Griffioen G, Thevelein JM. Molecular mechanisms controlling the localisation of protein kinase A. Curr Genet 2002;41 (4):199-207.
[126] Kaffman A, Rank NM, O'Neill EM, Huang LS, O'Shea EK. The receptor Msn5 exports the phosphorylated transcription factor Pho4 out of the nucleus. Nature 1998;396 (6710):482-6.
[127] Hunter T, Plowman GD. The protein kinases of budding yeast: six score and more. Trends Biochem Sci 1997;22 (1):18-22.

[128] Thompson JD, Higgins DG, Gibson TJ. CLUSTAL W: improving the sensitivity of progressive multiple sequence alignment through sequence weighting, position-specific gap penalties and weight matrix choice. Nucleic Acids Res 1994;22 (22):4673-80.
[129] Felsenstein J. PHYLIP -Phylogeny Inference Package (Version 3.2). Cladistics 1989;5:164-6.
[130] Hergovich A, Stegert MR, Schmitz D, Hemmings BA. NDR kinases regulate essential cell processes from yeast to humans. Nat Rev Mol Cell Biol 2006;7 (4):253-64.
[131] O'Neill EM, Kaffman A, Jolly ER, O'Shea EK. Regulation of PHO4 nuclear localization by the PHO80-PHO85 cyclin-CDK complex. Science 1996;271 (5246):209-12.
[132] Edelman AM, Blumenthal DK, Krebs EG. Protein serine/threonine kinases. Annu Rev Biochem 1987;56:567-613.
[133] Galperin MY, Nikolskaya AN, Koonin EV. Novel domains of the prokaryotic two-component signal transduction systems. FEMS Microbiol Lett 2001;203 (1):11-21.
[134] Perraud AL, Weiss V, Gross R. Signalling pathways in two-component phosphorelay systems. Trends Microbiol 1999;7 (3):115-20.
[135] Hanks SK, Hunter T. Protein kinases 6. The eukaryotic protein kinase superfamily: kinase (catalytic) domain structure and classification. Faseb J 1995;9 (8):576-96.
[136] Taylor BL, Zhulin IB. PAS domains: internal sensors of oxygen, redox potential, and light. Microbiol Mol Biol Rev 1999;63 (2):479-506.
[137] Nambu JR, Lewis JO, Wharton KA, Jr., Crews ST. The Drosophila single-minded gene encodes a helix-loop-helix protein that acts as a master regulator of CNS midline development. Cell 1991;67 (6):1157-67.
[138] Amezcua CA, Harper SM, Rutter J, Gardner KH. Structure and interactions of PAS kinase N-terminal PAS domain: model for intramolecular kinase regulation. Structure 2002;10 (10):1349-61.
[139] Pellequer JL, Wager-Smith KA, Kay SA, Getzoff ED. Photoactive yellow protein: a structural prototype for the three-dimensional fold of the PAS domain superfamily. Proc Natl Acad Sci U S A 1998;95 (11):5884-90.
[140] Hefti MH, Francoijs KJ, de Vries SC, Dixon R, Vervoort J. The PAS fold. A redefinition of the PAS domain based upon structural prediction. Eur J Biochem 2004;271 (6):1198-208.
[141] Genick UK, Borgstahl GE, Ng K, Ren Z, Pradervand C, Burke PM, Srajer V, Teng TY, Schildkamp W, McRee DE, Moffat K, Getzoff ED. Structure of a protein photocycle intermediate by millisecond time-resolved crystallography. Science 1997;275 (5305):1471-5.
[142] Herráez A. Biomolecules in the Computer: Jmol to the rescue. Biochem. Educ 2006;34:255–61.
[143] Pandini A, Bonati L. Conservation and specialization in PAS domain dynamics. Protein Eng Des Sel 2005;18 (3):127-37.
[144] Gong W, Hao B, Mansy SS, Gonzalez G, Gilles-Gonzalez MA, Chan MK. Structure of a biological oxygen sensor: a new mechanism for heme-driven signal transduction. Proc Natl Acad Sci U S A 1998;95 (26):15177-82.
[145] Gilles-Gonzalez MA, Gonzalez G. Heme-based sensors: defining characteristics, recent developments, and regulatory hypotheses. J Inorg Biochem 2005;99 (1):1-22.
[146] Miyatake H, Mukai M, Park SY, Adachi S, Tamura K, Nakamura H, Nakamura K, Tsuchiya T, Iizuka T, Shiro Y. Sensory mechanism of oxygen sensor FixL from Rhizobium meliloti: crystallographic, mutagenesis and resonance Raman spectroscopic studies. J Mol Biol 2000;301 (2):415-31.
[147] Yeh KC, Lagarias JC. Eukaryotic phytochromes: light-regulated serine/threonine protein kinases with histidine kinase ancestry. Proc Natl Acad Sci U S A 1998;95 (23):13976-81.
[148] Kay SA. PAS, present, and future: clues to the origins of circadian clocks. Science 1997;276 (5313):753-4.
[149] Gu YZ, Hogenesch JB, Bradfield CA. The PAS superfamily: sensors of environmental and developmental signals. Annu Rev Pharmacol Toxicol 2000;40:519-61.
[150] Wang J, Trudeau MC, Zappia AM, Robertson GA. Regulation of deactivation by an amino terminal domain in human ether-a-go-go-related gene potassium channels. J Gen Physiol 1998;112 (5):637-47.
[151] Rutter J, Michnoff CH, Harper SM, Gardner KH, McKnight SL. PAS kinase: an evolutionarily conserved PAS domain-regulated serine/threonine kinase. Proc Natl Acad Sci U S A 2001;98 (16):8991-6.
[152] Hofer T, Spielmann P, Stengel P, Stier B, Katschinski DM, Desbaillets I, Gassmann M, Wenger RH. Mammalian PASKIN, a PAS-serine/threonine kinase related to bacterial oxygen sensors. Biochem Biophys Res Commun 2001;288 (4):757-64.
[153] Rutter J, Probst BL, McKnight SL. Coordinate regulation of sugar flux and translation by PAS kinase. Cell 2002;111 (1):17-28.
[154] Klug A, Schwabe JW. Protein motifs 5. Zinc fingers. Faseb J 1995;9 (8):597-604.
[155] Finerty PJ, Jr., Bass BL. Subsets of the zinc finger motifs in dsRBP-ZFa can bind double-stranded RNA. Biochemistry 1999;38 (13):4001-7.
[156] Freemont PS. The RING finger. A novel protein sequence motif related to the zinc finger. Ann N Y Acad Sci 1993;684:174-92.

[157] Matthews JM, Kowalski K, Liew CK, Sharpe BK, Fox AH, Crossley M, MacKay JP. A class of zinc fingers involved in protein-protein interactions biophysical characterization of CCHC fingers from fog and U-shaped. Eur J Biochem 2000;267 (4):1030-8.
[158] Gozani O, Karuman P, Jones DR, Ivanov D, Cha J, Lugovskoy AA, Baird CL, Zhu H, Field SJ, Lessnick SL, Villasenor J, Mehrotra B, Chen J, Rao VR, Brugge JS, Ferguson CG, Payrastre B, Myszka DG, Cantley LC, Wagner G, Divecha N, Prestwich GD, Yuan J. The PHD finger of the chromatin-associated protein ING2 functions as a nuclear phosphoinositide receptor. Cell 2003;114 (1):99-111.
[159] Stenmark H, Aasland R, Toh BH, D'Arrigo A. Endosomal localization of the autoantigen EEA1 is mediated by a zinc-binding FYVE finger. J Biol Chem 1996;271 (39):24048-54.
[160] Gaullier JM, Simonsen A, D'Arrigo A, Bremnes B, Stenmark H, Aasland R. FYVE fingers bind PtdIns(3)P. Nature 1998;394 (6692):432-3.
[161] Bohm S, Frishman D, Mewes HW. Variations of the C2H2 zinc finger motif in the yeast genome and classification of yeast zinc finger proteins. Nucleic Acids Res 1997;25 (12):2464-9.
[162] Bird AJ, McCall K, Kramer M, Blankman E, Winge DR, Eide DJ. Zinc fingers can act as Zn2+ sensors to regulate transcriptional activation domain function. Embo J 2003;22 (19):5137-46.
[163] Schwabe JW, Klug A. Zinc mining for protein domains. Nat Struct Biol 1994;1 (6):345-9.
[164] Stock AM, Robinson VL, Goudreau PN. Two-component signal transduction. Annu Rev Biochem 2000;69:183-215.
[165] Koretke KK, Lupas AN, Warren PV, Rosenberg M, Brown JR. Evolution of two-component signal transduction. Mol Biol Evol 2000;17 (12):1956-70.
[166] Khorchid A, Ikura M. Bacterial histidine kinase as signal sensor and transducer. Int J Biochem Cell Biol 2006;38 (3):307-12.
[167] Janiak-Spens F, Sparling JM, Gurfinkel M, West AH. Differential stabilities of phosphorylated response regulator domains reflect functional roles of the yeast osmoregulatory SLN1 and SSK1 proteins. J Bacteriol 1999;181 (2):411-7.
[168] Hess JF, Oosawa K, Kaplan N, Simon MI. Phosphorylation of three proteins in the signaling pathway of bacterial chemotaxis. Cell 1988;53 (1):79-87.
[169] Galperin MY. Structural classification of bacterial response regulators: diversity of output domains and domain combinations. J Bacteriol 2006;188 (12):4169-82.
[170] Bourret RB, Hess JF, Simon MI. Conserved aspartate residues and phosphorylation in signal transduction by the chemotaxis protein CheY. Proc Natl Acad Sci U S A 1990;87 (1):41-5.
[171] Letunic I, Copley RR, Schmidt S, Ciccarelli FD, Doerks T, Schultz J, Ponting CP, Bork P. SMART 4.0: towards genomic data integration. Nucleic Acids Res 2004;32 (Database issue):D142-4.
[172] Hulo N, Sigrist CJ, Le Saux V, Langendijk-Genevaux PS, Bordoli L, Gattiker A, De Castro E, Bucher P, Bairoch A. Recent improvements to the PROSITE database. Nucleic Acids Res 2004;32 (Database issue):D134-7.
[173] Eddy SR. Profile hidden Markov models. Bioinformatics 1998;14 (9):755-63.
[174] Bucher P, Karplus K, Moeri N, Hofmann K. A flexible motif search technique based on generalized profiles. Comput Chem 1996;20 (1):3-23.
[175] Wang X, Hoekstra MF, DeMaggio AJ, Dhillon N, Vancura A, Kuret J, Johnston GC, Singer RA. Prenylated isoforms of yeast casein kinase I, including the novel Yck3p, suppress the gcs1 blockage of cell proliferation from stationary phase. Mol Cell Biol 1996;16 (10):5375-85.
[176] Sigrist CJ, Cerutti L, Hulo N, Gattiker A, Falquet L, Pagni M, Bairoch A, Bucher P. PROSITE: a documented database using patterns and profiles as motif descriptors. Brief Bioinform 2002;3 (3):265-74.
[177] Gattiker A, Gasteiger E, Bairoch A. ScanProsite: a reference implementation of a PROSITE scanning tool. Appl Bioinformatics 2002;1 (2):107-8.
[178] Gasteiger E, Jung E, Bairoch A. SWISS-PROT: connecting biomolecular knowledge via a protein database. Curr Issues Mol Biol 2001;3 (3):47-55.
[179] Altschul SF, Madden TL, Schaffer AA, Zhang J, Zhang Z, Miller W, Lipman DJ. Gapped BLAST and PSI-BLAST: a new generation of protein database search programs. Nucleic Acids Res 1997;25 (17):3389-402.
[180] Pagni M, Ioannidis V, Cerutti L, Zahn-Zabal M, Jongeneel CV, Falquet L. MyHits: a new interactive resource for protein annotation and domain identification. Nucleic Acids Res 2004;32 (Web Server issue):W332-5.
[181] Jones JS, Weber S, Prakash L. The Saccharomyces cerevisiae RAD18 gene encodes a protein that contains potential zinc finger domains for nucleic acid binding and a putative nucleotide binding sequence. Nucleic Acids Res 1988;16 (14B):7119-31.
[182] Zhu H, Bilgin M, Bangham R, Hall D, Casamayor A, Bertone P, Lan N, Jansen R, Bidlingmaier S, Houfek T, Mitchell T, Miller P, Dean RA, Gerstein M, Snyder M. Global analysis of protein activities using proteome chips. Science 2001;293 (5537):2101-5.
[183] Jones DR, Divecha N. Linking lipids to chromatin. Curr Opin Genet Dev 2004;14 (2):196-202.

[184] Feuerbach F, Galy V, Trelles-Sticken E, Fromont-Racine M, Jacquier A, Gilson E, Olivo-Marin JC, Scherthan H, Nehrbass U. Nuclear architecture and spatial positioning help establish transcriptional states of telomeres in yeast. Nat Cell Biol 2002;4 (3):214-21.
[185] Ulrich HD, Jentsch S. Two RING finger proteins mediate cooperation between ubiquitin-conjugating enzymes in DNA repair. Embo J 2000;19 (13):3388-97.
[186] Hishida T, Ohno T, Iwasaki H, Shinagawa H. Saccharomyces cerevisiae MGS1 is essential in strains deficient in the RAD6-dependent DNA damage tolerance pathway. Embo J 2002;21 (8):2019-29.
[187] Pedruzzi I, Burckert N, Egger P, De Virgilio C. Saccharomyces cerevisiae Ras/cAMP pathway controls post-diauxic shift element-dependent transcription through the zinc finger protein Gis1. Embo J 2000;19 (11):2569-79.
[188] Tronnersjo S, Hanefalk C, Balciunas D, Hu GZ, Nordberg N, Muren E, Ronne H. The jmjN and jmjC domains of the yeast zinc finger protein Gis1 interact with 19 proteins involved in transcription, sumoylation and DNA repair. Mol Genet Genomics 2006.
[189] Stewart RC. Activating and inhibitory mutations in the regulatory domain of CheB, the methylesterase in bacterial chemotaxis. J Biol Chem 1993;268 (3):1921-30.
[190] Posas F, Wurgler-Murphy SM, Maeda T, Witten EA, Thai TC, Saito H. Yeast HOG1 MAP kinase cascade is regulated by a multistep phosphorelay mechanism in the SLN1-YPD1-SSK1 "two-component" osmosensor. Cell 1996;86 (6):865-75.
[191] Ponting CP, Aravind L. PAS: a multifunctional domain family comes to light. Curr Biol 1997;7 (11):R674-7.
[192] DeRisi JL, Iyer VR, Brown PO. Exploring the metabolic and genetic control of gene expression on a genomic scale. Science 1997;278 (5338):680-6.
[193] Lieb JD, Liu X, Botstein D, Brown PO. Promoter-specific binding of Rap1 revealed by genome-wide maps of protein-DNA association. Nat Genet 2001;28 (4):327-34.
[194] Pina B, Fernandez-Larrea J, Garcia-Reyero N, Idrissi FZ. The different (sur)faces of Rap1p. Mol Genet Genomics 2003;268 (6):791-8.
[195] Zhao Y, McIntosh KB, Rudra D, Schawalder S, Shore D, Warner JR. Fine-structure analysis of ribosomal protein gene transcription. Mol Cell Biol 2006;26 (13):4853-62.
[196] Jones DL, Petty J, Hoyle DC, Hayes A, Ragni E, Popolo L, Oliver SG, Stateva LI. Transcriptome profiling of a Saccharomyces cerevisiae mutant with a constitutively activated Ras/cAMP pathway. Physiol Genomics 2003;16 (1):107-18.
[197] Sandmeier JJ, French S, Osheim Y, Cheung WL, Gallo CM, Beyer AL, Smith JS. RPD3 is required for the inactivation of yeast ribosomal DNA genes in stationary phase. Embo J 2002;21 (18):4959-68.
[198] Liu Z, Butow RA. A transcriptional switch in the expression of yeast tricarboxylic acid cycle genes in response to a reduction or loss of respiratory function. Mol Cell Biol 1999;19 (10):6720-8.
[199] Drazinic CM, Smerage JB, Lopez MC, Baker HV. Activation mechanism of the multifunctional transcription factor repressor-activator protein 1 (Rap1p). Mol Cell Biol 1996;16 (6):3187-96.
[200] Fuge EK, Braun EL, Werner-Washburne M. Protein synthesis in long-term stationary-phase cultures of Saccharomyces cerevisiae. J Bacteriol 1994;176 (18):5802-13.
[201] Osmani AH, May GS, Osmani SA. The extremely conserved pyroA gene of Aspergillus nidulans is required for pyridoxine synthesis and is required indirectly for resistance to photosensitizers. J Biol Chem 1999;274 (33):23565-9.
[202] Bertram PG, Zeng C, Thorson J, Shaw AS, Zheng XF. The 14-3-3 proteins positively regulate rapamycin-sensitive signaling. Curr Biol 1998;8 (23):1259-67.
[203] Fabrizio P, Liou LL, Moy VN, Diaspro A, SelverstoneValentine J, Gralla EB, Longo VD. SOD2 functions downstream of Sch9 to extend longevity in yeast. Genetics 2003;163 (1):35-46.
[204] Fabrizio P, Pozza F, Pletcher SD, Gendron CM, Longo VD. Regulation of longevity and stress resistance by Sch9 in yeast. Science 2001;292 (5515):288-90.
[205] Sugajska E, Swiatek W, Zabrocki P, Geyskens I, Thevelein JM, Zolnierowicz S, Wera S. Multiple effects of protein phosphatase 2A on nutrient-induced signalling in the yeast Saccharomyces cerevisiae. Mol Microbiol 2001;40 (4):1020-6.
[206] Dioum EM, Rutter J, Tuckerman JR, Gonzalez G, Gilles-Gonzalez MA, McKnight SL. NPAS2: a gas-responsive transcription factor. Science 2002;298 (5602):2385-7.
[207] Di Como CJ, Arndt KT. Nutrients, via the Tor proteins, stimulate the association of Tap42 with type 2A phosphatases. Genes Dev 1996;10 (15):1904-16.
[208] Swinnen E, Wanke V, Roosen J, Smets B, Dubouloz F, Pedruzzi I, Cameroni E, De Virgilio C, Winderickx J. Rim15 and the crossroads of nutrient signalling pathways in Saccharomyces cerevisiae. Cell Div 2006;1:3.
[209] Vershon AK, Pierce M. Transcriptional regulation of meiosis in yeast. Curr Opin Cell Biol 2000;12 (3):334-9.
[210] Kahana A, Gottschling DE. DOT4 links silencing and cell growth in Saccharomyces cerevisiae. Mol Cell Biol 1999;19 (10):6608-20.

[211] Orlandi I, Bettiga M, Alberghina L, Vai M. Transcriptional profiling of ubp10 null mutant reveals altered subtelomeric gene expression and insurgence of oxidative stress response. J Biol Chem 2004;279 (8):6414-25.
[212] Chen Z, Zang J, Whetstine J, Hong X, Davrazou F, Kutateladze TG, Simpson M, Mao Q, Pan CH, Dai S, Hagman J, Hansen K, Shi Y, Zhang G. Structural insights into histone demethylation by JMJD2 family members. Cell 2006;125 (4):691-702.
[213] Ptacek J, Devgan G, Michaud G, Zhu H, Zhu X, Fasolo J, Guo H, Jona G, Breitkreutz A, Sopko R, McCartney RR, Schmidt MC, Rachidi N, Lee SJ, Mah AS, Meng L, Stark MJ, Stern DF, De Virgilio C, Tyers M, Andrews B, Gerstein M, Schweitzer B, Predki PF, Snyder M. Global analysis of protein phosphorylation in yeast. Nature 2005;438 (7068):679-84.
[214] Dulubova I, Horiuchi A, Snyder GL, Girault JA, Czernik AJ, Shao L, Ramabhadran R, Greengard P, Nairn AC. ARPP-16/ARPP-19: a highly conserved family of cAMP-regulated phosphoproteins. J Neurochem 2001;77 (1):229-38.
[215] Horiuchi A, Williams KR, Kurihara T, Nairn AC, Greengard P. Purification and cDNA cloning of ARPP-16, a cAMP-regulated phosphoprotein enriched in basal ganglia, and of a related phosphoprotein, ARPP-19. J Biol Chem 1990;265 (16):9476-84.
[216] Heron L, Virsolvy A, Peyrollier K, Gribble FM, Le Cam A, Ashcroft FM, Bataille D. Human alpha-endosulfine, a possible regulator of sulfonylurea-sensitive KATP channel: molecular cloning, expression and biological properties. Proc Natl Acad Sci U S A 1998;95 (14):8387-91.
[217] Virsolvy A, Smith P, Bertrand G, Gros L, Heron L, Salazar G, Puech R, Bataille D. Block of Ca(2+)-channels by alpha-endosulphine inhibits insulin release. Br J Pharmacol 2002;135 (7):1810-8.
[218] Irwin N, Chao S, Goritchenko L, Horiuchi A, Greengard P, Nairn AC, Benowitz LI. Nerve growth factor controls GAP-43 mRNA stability via the phosphoprotein ARPP-19. Proc Natl Acad Sci U S A 2002;99 (19):12427-31.
[219] Sambrook J, Russel, D.W. Molecular cloning : a laboratory manual: Cold Spring Harbor, NY, Cold Spring Harbor Laboratory Press, 2001.
[220] Rose MD, Winston, F. and Hieter, P. Methods in Yeast Genetics: Cold Spring Harbor, NY, Cold Spring Harbor Laboratory Press, 1990.
[221] Guthrie CaF, G.R. Guide to yeast genetics and molecular biology. Methods Enzymol. 1991;194.
[222] Gietz RD, Woods RA. Transformation of yeast by lithium acetate/single-stranded carrier DNA/polyethylene glycol method. Methods Enzymol 2002;350:87-96.
[223] Ausubel Fe. Current protocols in molecular biology. New York, N.Y., 1999.
[224] Zhao R, Fu X, Li Q, Krantz SB, Zhao ZJ. Specific interaction of protein tyrosine phosphatase-MEG2 with phosphatidylserine. J Biol Chem 2003;278 (25):22609-14.

Acknowledgements

I would like to thank to…

Claudio De Virgilio, who guided this thesis with much enthusiasm and creativity. Working in his lab has been a great experience and I am really grateful to him for this opportunity.

The members of my thesis jury board, Roger Schneiter and Robbie Loewith..

Jean-Claude Martinou and Patrick Linder for being my “parrains”. I particularly appreciated Patrick’s substantial contribution to create a pleasant working environment.

Martine Collard and Robbie Loewith for reading my “hors these” and for the occasional, edifying, collaborations.

Matthias Peter and Joris Windericks, who welcomed me in their labs, where I had the opportunity to fruitfully carry out some crucial experiments for this thesis, the acknowledgment is extended to the members of their labs, in particular Nicolas Page and Jonny Roosen.

Ruth Bisig and Valeria Wanke, for their incredible support and invaluable friendship, as well as the others, current and former members of Claudio’s group in Geneva: Ivo Pedruzzi (the amazing Ivo), Yvonne Gloor, Frédérique Dubouloz and Matteo Binda.

All the people from “outside the lab”, friends and family, who were always supportive and reminded me, when necessary, that “outside the lab” actually exists.

And finally of course Tiziano, who was so brave to be on my side during this period and to listen to my endless monologues about my experiments and so patient to wait for me all this time.

Remerciements

J’aimerais remercier…

Claudio De Virgilio, qui a supervisé et cette thèse avec beaucoup de enthousiasme et de créativité. Travailler dans son laboratoire a été pour moi une grande expérience et je lui suis sincèrement reconnaissante pour tout ce que j’ai appris pendant ces années ou j’ai eu l’honneur de travailler à ses cotés.

Je remercie aussi vivement les jurés : les Professeurs Roger Schneiter et Robbie Loewith.

Je tiens aussi à remercier mes parrains Jean-Claude Martinou et Patrick Linder. En particulier j’ai beaucoup apprécié la gaieté de Patrick qui à contribué et contribue toujours à créer l’ambiance très plaisante du département Mimol.

Je remercie Martine Collard et Robbie Loewith pour avoir lu et évalué mon travail “hors these” et pour les occasionnelles et édifiantes collaborations avec leur groupes.

Matthias Peter et Joris Windericks m’ont accueillie dans leurs laboratoires ou j’ai eu l’opportunité de travailler à l’obtention de importants résultats qui ont étés cruciaux pour cette thèse. Ces remerciements vont bien entendu aussi aux membres de ces laboratoires, en particulier Nicolas Page and Jonny Roosen.

Ruth Bisig and Valeria Wanke, m’ont soutenue et encouragée et je les remercie très fort pour ça ainsi que pour leur precieuse amitié. Je remercie tous les membres, présents et anciens, du group De Virgilio a Genève: Ivo Pedruzzi (the amazing Ivo), Yvonne Gloor, Frédérique Dubouloz and Matteo Binda.

Un gros merci va aussi à toutes les personnes «au dehors du laboratoire», ma famille et mes amis, toujours prêts à me rappeler qu’il existe vraiement une vie «au dehors du laboratoire».

Pour finir je remercie Tiziano, toujours patiemment et courageusement à l’écoute de mes monologues infinis sur mon travail, pour m’avoir « attendue » si longtemps.